# MODAL ANALYSIS AND CONTROL OF FLEXIBLE MANIPULATOR ARMS

**Octavio Maizza Neto**

**September 10, 1974**



**NASA Contract**
**NAS8-28055**

MASSACHUSETTS INSTITUTE OF TECHNOLOGY
DEPARTMENT OF MECHANICAL ENGINEERING
CAMBRIDGE, MASSACHUSETTS 02139

# MODAL ANALYSIS AND CONTROL
# OF FLEXIBLE MANIPULATOR ARMS

by

Octavio Maizza Neto

Eng. Mec., Escola Politécnica da U. S. P., São Paulo, Brazil
(1968)

M.S.M.E., Massachusetts Institute of Technology
(1973)

Mech. E., Massachusetts Institute of Technology
(1973)

SUBMITTED IN PARTIAL FULFILLMENT OF THE

REQUIREMENTS FOR THE DEGREE OF

DOCTOR OF PHILOSOPHY

at the

MASSACHUSETTS INSTITUTE OF TECHNOLOGY

September, 1974

Signature of Author.....
Department of Mechanical Engineering
September 10, 1974

Certified by.....
Thesis Supervisor

Accepted by.....
Chairman, Departmental Committee
on Graduate Students

# MODAL ANALYSIS AND CONTROL OF FLEXIBLE MANIPULATOR ARMS

Octavio Maizza Neto

Submitted to the Department of Mechanical Engineering
on September 10, 1974 in partial fulfillment of the
requirements for the Degree of Doctor of Philosophy

## ABSTRACT

This study examines the possibility of modeling and control of flexible manipulator arms. A modal approach is used throughout the work for obtaining the mathematical model and control techniques applied. The arm model is represented mathematically by a state space description defined in terms of joint angles and mode amplitudes obtained from truncation on the distributed systems, and includes the motion of a two link two joint arm.

The problem of controlling the system is examined via the linearized model and using a regulator type of control. Three basic techniques are used for this purpose: pole allocation with gains obtained from the rigid system with interjoint feedbacks, Simon-Mitter algorithm for pole allocation and sensitivity analysis with respect to parameter variations. An improvement in arm bandwidth is obtained that could replace more conservative designs currently in use.

Optimization of some geometric parameters is undertaken in order to maximize bandwidth for various payload sizes and programmed tasks.

The controlled system is examined under constant gains and using the nonlinear model for simulations following a time varying state trajectory. The procedure presented in this work is general and can be implemented to be used in more specific designs.

THESIS SUPERVISOR: Professor Daniel E. Whitney

TITLE: Associate Professor of Mechanical Engineering

ACKNOWLEDGEMENTS

The author wishes to express his appreciation to those who have been of great help in the preparation of this thesis. Professor Daniel E. Whitney has been a very helpful committee chairman. He has spent much time in consultation, and has provided valuable suggestions. The author is also grateful to Professor Leonard A. Gould, Professor Richard S. Sidell and Professor James H. Williams, Jr, for their valuable help both in committee meetings and in private consultation. For their valuable discussions on the thesis topic the author is indebted to Dr. Wayne J. Book, Mr. Sergio Simunovic and Mr. Jaime Szajner, as well as other members of the graduate student body.

Particular acknowledgement goes to my wife, Norma, for her valuable non-technical support at home, through four years leading to the completion of this degree. Sincere thanks also to my parents for providing moral support in earlier education.

The efficient staff of Joint Computer Facility, Civil-Mechanical Engineering has been on great help in programming and debugging. Special thanks go to Mr. Larry Hare and Mr. Stanley Knutson for their time and energy devoted to this good cause.

Appreciation is expressed to Alice J. Sanderson who typed this thesis with its several equations.

This research was supported in party by Fundação de Amparo a Pesquisa do Estado de São Paulo, Brazil, Escola Politécnica da Universidade de São Paulo, Brazil, and George C. Marshall Space Flight Center, contract number NAS8-28055.

# TABLE OF CONTENTS

# LIST OF TABLES

LIST OF FIGURES

## NOMENCLATURE

| | |
|---|---|
| $\underline{A},\underline{B},\ldots$ | matrices |
| $\underline{a},\underline{b},\ldots$ | vectors |
| $\vec{A},\vec{B},\ldots\ \vec{a},\vec{b},\ldots$ | geommetric vectors |
| $\overline{A},\overline{B},\ldots\ \overline{a},\overline{b},\ldots$ | nondimensionalized parameters |
| $c(\cdot)$ | cossine of $\cdot$ |
| E | Young's modulus |
| EI | stiffness |
| GRG | General control with gains obtained from rigid model with interjoint feedbacks |
| I | bending moment of inertia |
| $\underline{I}$ | Identity matrix |
| $k_{r1},k_{r2}$ | ratio of radii |
| m | mass |
| $m_p$ | payload mass |
| $m_j$ | joint mass |
| g | gravity acceleration |
| $J_{(\cdot)}$ | moment of inertia with respect to axis $\cdot$ |
| $J_{xxp}$ | moment of inertia of payload with respect to center of gravity |
| l | lenght |
| $q_{ij}$ | time dependent mode component |
| $Q_r$ | generalized force or torque |
| $s(\cdot)$ | sine of $\cdot$ |
| SMA | Simon-Mitter algorithm |

| | |
|---|---|
| $t$ | time |
| $T$ | kinetic energy |
| $\bar{T}_s$ | nondimensionalized settling time |
| $\bar{T}$ | nondimensionalized time |
| $u_{.E}$ | flexible displacement of beam $(\cdot)$ at end |
| $\underline{u}$ | control law |
| $V$ | potential energy |
| $w,\omega$ | angular frequency |
| $\dot{A},\dot{a}...$ | time derivative of A,a... |
| $.^T$ | transpose of a matrix or a vector |
| $.^{-1}$ | inverse of a matrix |
| $\theta_1,\theta_2,\theta_r$ | angles |
| $\phi_{ij}$ | spatial mode component |
| $\tau_1,\tau_2$ | torques |
| $\zeta$ | damping ratio |
| $\delta(\cdot)$ | finite variation of $\cdot$ |
| $\mu$ | density per unit lenght |
| $\rho$ | density per unity volume |
| $j$ | complex unity |

# CHAPTER I

# INTRODUCTION

## 1.1 Scope of the Work

Many recent studies deal with the design and control of mechanical manipulators that perform tasks similar to those of human arms. The possibility of using small computers located in the vicinity of the manipulator originated the so-called supervisory controlled devices, es--ecially important when the distance between the arm and the operator introduces a time lag in the information process [M2], [T1]. However, the arm dimensions or the velocity of performing a task can increase the effects of nonlinear factors that will complicate even more the control process. Such control procedures would require nonlinear techniques that may not be at hand. In the case of flexible mechanical arms, the vibrations originated by the elasticity of the links would affect the effectiveness of the system and even cause instability. In the interest of reducing these vibrations, this study deals with the control of the nonlinear system with results obtained from the linear control theory. A suitable mathematical model is developed to represent the plane motion of two flexible beams by considering the rigid and flexible motions. The hypothesis of controlling the dynamic motion of the nonlinear model is examined by means of modal control applied to the linearized model.

## 1.2 The System Mathematical Description

The approach assumed in this work is to derive the equations of motion of a system of two flexible beams pinned at one end and at the

joint. Lagrange's equation applied to a distributed system are used for this purpose. Basically the model is obtained by superposing the flexible motion over a hypothetical rigid body motion. For the purpose of this study, the elastic motion of the beams is truncated in the second mode and a six degree of freedom, nonlinear model is obtained. A good approximation for the dynamic shapes of the beams during the motion is achieved by using the appropriate boundary conditions. Some experimental results have shown good approximations for the values of natural frequencies of the uncontrolled system when compared with those obtained from the linearized mathematical model. Details of these procedures can be found in Chapter II.

## 1.3 Control from the Perspective of Manipulator Design

The basic idea for controlling the system is to find the forces of torques that must be exerted on the manipulator joints in order to move the system from its present configuration to the desired position. If fast motions have to be performed, the dynamic forces will become significant and a reasonable control must be achieved for the nonlinear system. On the other hand, slow motion with large payload might give rise to undesired large deflections of the links.

A broad analysis of manipulator design would depend upon geometric and elastic parameters, according to the tasks to be performed. In this work one considers the implications of applying modal control techniques to either short and rigid manipulators such as automation devices or long and flexible ones like the space shuttle boom. In both cases,

the control performance would depend upon physically available measurements. However, only a limited number of these quantities might be obtained for a given arm configuration. This suggests the comparison of control performance for cases where all of the variables could supposedly be measured and those when only some of them are vailable. Three different techniques are used in the present work resulting in a linear regulator type of control. The first technique works with the gains obtained in the allocation of poles in the rigid equivalent system and uses those gains in the control of the flexible model. The convenience of this method is accentuated by the fact that simple measurements are sufficient for controlling the system. The second procedure is the use of Simon-Mitter algorithm [S1], [S2] for independent positioning of poles. This procedure requires the measurement and/or estimation of some state variables that might require very sophisticated instruments. Finally, the third method makes use of the poles sensitivites with respect to parameters variations in order to find the elements of the feedback law. These procedures are described in Chapter III and a comparison of results is presented in Chapter IV. Estimates of maximum arm bandwidth are presented for the case of controlling the flexible system with a control law obtained from the rigid model.

Some simulations of the nonlinear system using the rigid control law and Simon-Mitter algorithm are presented in Chapter V for analyzing the system performance in tracking a time varying state trajectory.

## 1.4 Remarks

The study of controlling flexible manipulators was first undertaken by Mirro [M2] in which a single beam is analyzed from the point of view of optimal regulator theory. Before that, Townsend [T1], Kahn [K1] and many others were concerned with controlling essentially rigid manipulator arms. The most recent work on flexible systems is presented by Book [B2] and Whitney, Book, Lynch [W2] where the pertinent literature can be found.

# CHAPTER II

# SYSTEM DESCRIPTION

## 2.1 The Physical Model

The schematic of the general physical system is shown in Figure 2.1. The system is composed of two flexible bodies connected by a frictionless pinned joint. One end of the system is attached to the origin of a reference frame. The system is assumed to have planar motion and the relative motion of the two bodies results from torques applied at each joint of the system. In order to facilitate the description, the joints are numbered by 1 and 2 and the bodies will be represented by two flexible beams. At the end of beam 1, a concentrated mass representing the servo-motor at joint 2 and the joint itself; at the end of beam 2, a discrete mass can also appear, representing a payload to be moved between two points in the plane.

In order to describe the motions, three reference frames can be defined:

[0,X,Y] - an inertial reference frame with origin at joint 1

$[0,x_1y_1]$ - a reference frame with origin at 0 and the axis $x_1$ tangent to beam 1 at point 0

$[0_2,x_2,y_2]$ - a reference frame with origin at joint 2 and with axis $x_2$ tangent to beam 2 at point $0_2$

Also two angles can be defined:

$\theta_1(t)$ is the angle between the axes $x_1$ and X

$\theta_2(t)$ is the angle between the axes $x_1$ and $x_2$

If now a new system is defined as being formed by two segments $OO_1$ and $O_1O_3$, having the angle $\theta_2$ at $O_1$, the overall motion can be understood as a motion of a hypothetical rigid system $OO_1O_3$ and a flexible motion of the beams 1 and 2 with respect to this moving system. In order to simplify the notations a matrix representation form of the reference frames can be introduced.

Let

$\{\vec{U}\} = \begin{Bmatrix} \vec{u}_x \\ \vec{u}_y \end{Bmatrix}$ be the unit vector of reference frame OXY

$\{\vec{U}_1\} = \begin{Bmatrix} \vec{u}_{x1} \\ \vec{u}_{y1} \end{Bmatrix}$ the unit vector of reference frame $Ox_1y_1$,

$\{\vec{U}_2\} = \begin{Bmatrix} \vec{u}_{x2} \\ \vec{u}_{y2} \end{Bmatrix}$ the unit vector of reference frame $O_2x_2y_2$

then

$$\{\vec{U}_1\} = [C_1]\ \{\vec{U}\} \qquad (2.1.1)$$

$$\{\vec{U}_2\} = [C_2]\ \{\vec{U}\} \qquad (2.1.2)$$

$[C_1]$ and $[C_2]$ are the rotational-transformation matrices. (Reference [C2]).

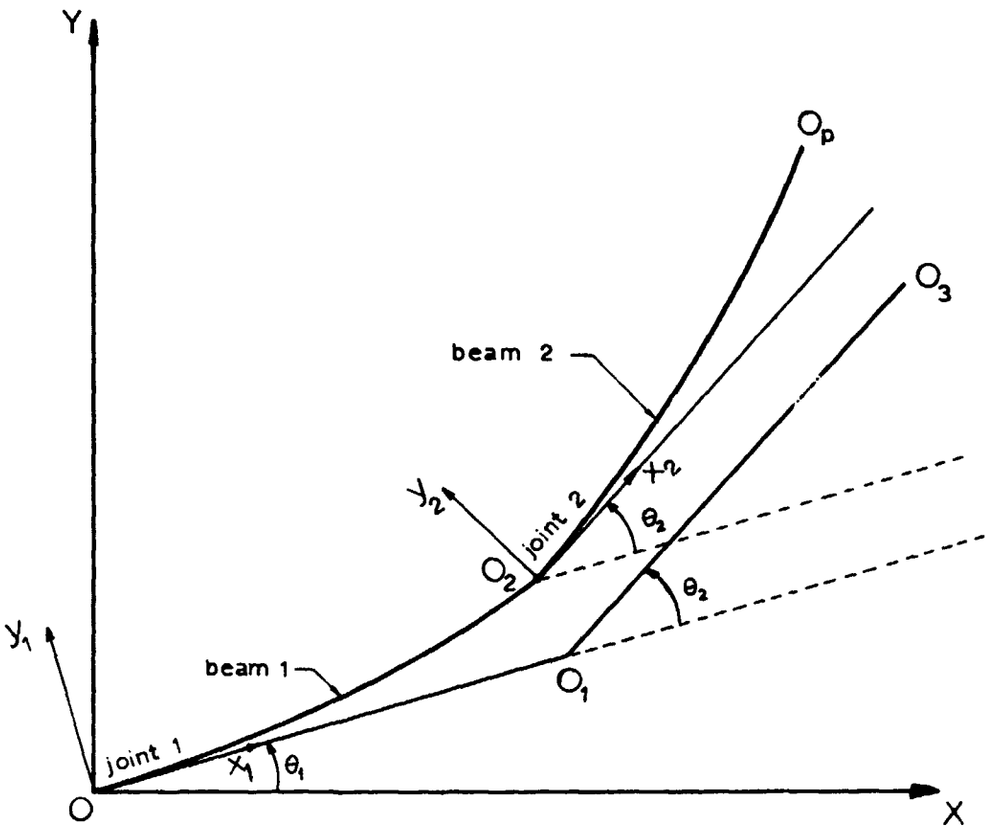


Figure 2.1

Schematic of the General Physical System

Then

$$\{\vec{U}_1\} = \begin{bmatrix} c\theta_1 & s\theta_1 \\ -s\theta_1 & c\theta_1 \end{bmatrix} \{\vec{U}\} \tag{2.1.3}$$

$$\{\vec{U}_2\} = \begin{bmatrix} c(\theta_1+\theta_2) & s(\theta_1+\theta_2) \\ -s(\theta_1+\theta_2) & c(\theta_1+\theta_2) \end{bmatrix} \{\vec{U}\} \tag{2.1.4}$$

$$[C_1] = \begin{bmatrix} c\theta_1 & s\theta_1 \\ -s\theta_1 & c\theta_1 \end{bmatrix} \tag{2.1.5}$$

$$[C_2] = \begin{bmatrix} c(\theta_1+\theta_2) & s(\theta_1+\theta_2) \\ -s(\theta_1+\theta_2) & c(\theta_1+\theta_2) \end{bmatrix} \tag{2.1.6}$$

where

$$c\theta_1 = \cos\theta_1 \tag{2.1.7}$$

$$s\theta_1 = \sin\theta_1 \tag{2.1.8}$$

$$c(\theta_1+\theta_2) = \cos(\theta_1+\theta_2) \tag{2.1.9}$$

$$s(\theta_1+\theta_2) = \sin(\theta_1+\theta_2) \tag{2.1.10}$$

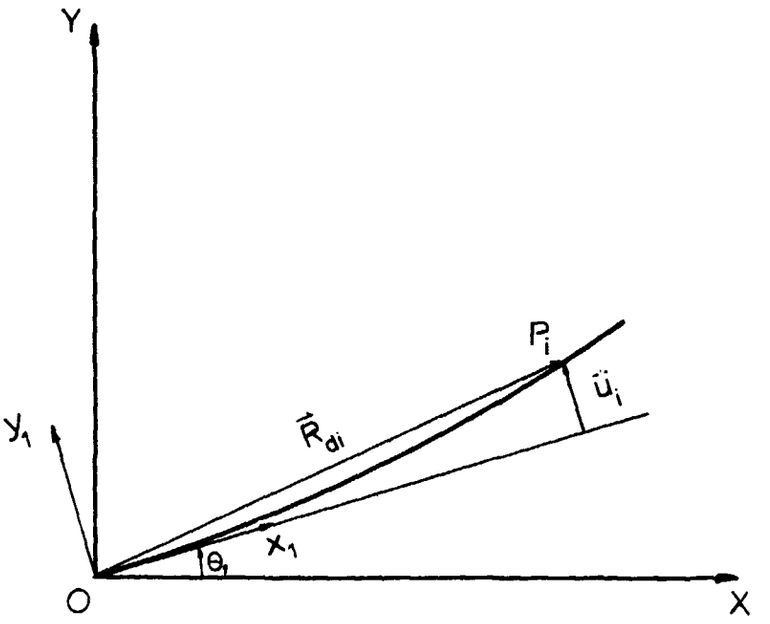


Vector Position of One Element in Beam 1

Figure 2.2

## 2.2 Kinematic Description

The position of any point in the system can be described by a convenient definition of a set of coordinates. As indicated in Figure 2.2, any point $P_i$ can be specified if a new variable $u_i(x_i,t)$ is defined as being the coordinate of the flexible motion with respect to the reference frame $[O_i x_i y_i]$. The vector position of point $P_i$ would be

$$\vec{R}_{di} = \{\vec{U}_i\}^t \begin{Bmatrix} x_i \\ y_i \end{Bmatrix} = x_i \vec{u}_{xi} + y_i \vec{u}_{yi} \tag{2.2}$$

### 2.2.1 Beam 1

The vector position of any point in beam 1 is

$$\vec{R}_{d1} = \{\vec{U}_1\}^t \begin{Bmatrix} x_1 \\ u_1 \end{Bmatrix} = \{\vec{U}\}^t [C_1]^t \begin{Bmatrix} x_1 \\ u_1 \end{Bmatrix} = (x_1 c\theta_1 - u_1 s\theta_1)\vec{u}_x$$

$$+ (x_1 s\theta_1 + u_1 c\theta_1)\vec{u}_y \tag{2.3}$$

### 2.2.2 Beam 2

In order to define the vector position of any point on beam 2, it will be necessary to assume that the displacements of the flexible bodies with respect to reference frames $[Ox_1y_1]$ and $[O_2x_2y_2]$ be small enough to consider the paths of points $O_2$ and $O_p$ as straight lines normal to the respective reference frames. Then, as shown in Figure 2.3,

the vector position of any point $P_2$ on beam 2 will be

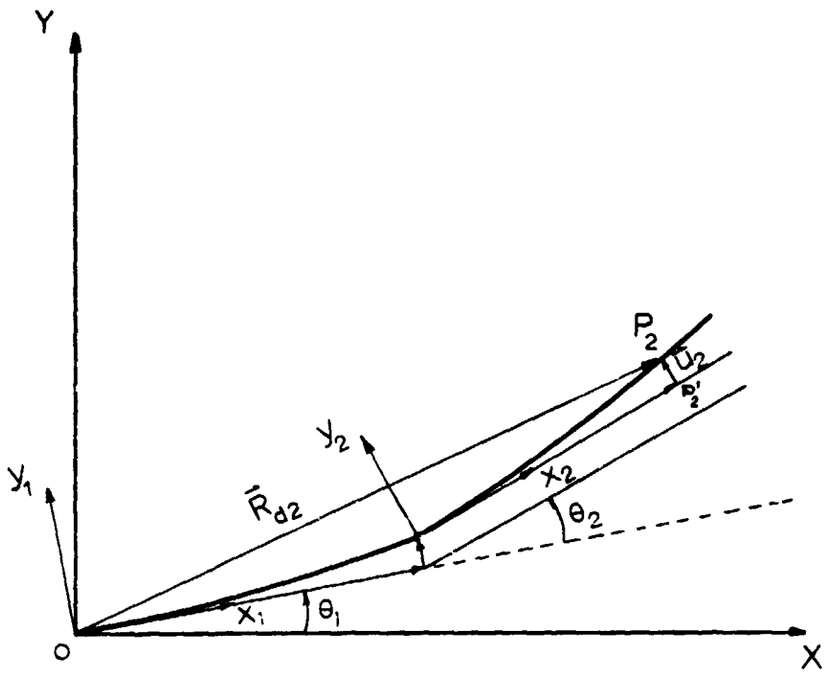


Vector Position of one Element in Beam 2

Figure 2.3

$$\vec{R}_{d2} = \vec{OO}_1 + \vec{O_1O_2} + \vec{O_2P_2'} + \vec{P_2'P_2} \tag{2.4}$$

If now

$u_{1E}$ = flexible linear displacement at end of beam 1

$l_1$ = length of beam 1

$l_2$ = length of beam 2

then

$$\vec{OO}_1 = \{\vec{U}\}^t \begin{Bmatrix} l_1 c\theta_1 \\ l_1 s\theta_1 \end{Bmatrix} = l_1 c\theta_1 \vec{u}_x + l_1 s\theta_1 \vec{u}_y \tag{2.5.1}$$

$$\vec{O_1O_2} = \{\vec{U}\}^t \begin{Bmatrix} -u_{1E} s\theta_1 \\ u_{1E} c\theta_1 \end{Bmatrix} = -u_{1E} s\theta_1 \vec{u}_x + u_{1E} c\theta_1 \vec{u}_y \tag{2.5.2}$$

$$\vec{O_2P_2'} = \{\vec{U}_1\}^t \begin{Bmatrix} x_2 \\ 0 \end{Bmatrix} = \{\vec{U}\}^t [C_1]^t \begin{Bmatrix} x_2 \\ 0 \end{Bmatrix} = x_2 c(\theta_1 + \theta_2)\vec{u}_x + x_2 s(\theta_1 + \theta_2)\vec{u}_y \tag{2.5.3}$$

$$\vec{P_2'P_2} = \{\vec{U}_2\}^t \begin{Bmatrix} 0 \\ u_2 \end{Bmatrix} = \{\vec{U}\}^t [C_2]^t \begin{Bmatrix} 0 \\ u_2 \end{Bmatrix} = -u_2 s(\theta_1 + \theta_2)\vec{u}_x + u_2 c(\theta_1 + \theta_2)\vec{u}_y \tag{2.5.4}$$

and

$$\vec{R}_{d2} = \{\vec{U}\}^t \left[ \begin{Bmatrix} l_1 c\theta_1 \\ l_1 s\theta_1 \end{Bmatrix} + \begin{Bmatrix} -u_{1E} s\theta_1 \\ u_{1E} c\theta_1 \end{Bmatrix} + [C_1]^t \begin{Bmatrix} x_2 \\ 0 \end{Bmatrix} + [C_2]^t \begin{Bmatrix} 0 \\ u_2 \end{Bmatrix} \right] \tag{2.6.1}$$

$$\vec{R}_{d2} = [l_1 c\theta_1 - u_{1E} s\theta_1 + x_2 c(\theta_1 + \theta_2) - u_2 s(\theta_1 + \theta_2)]\vec{u}_x$$

$$+ [l_1 s\theta_1 + u_{1E} c\theta_1 + x_2 s(\theta_1 + \theta_2) + u_2 c(\theta_1 + \theta_2)]\vec{u}_y \tag{2.6.2}$$

The respective velocities are

$$\dot{\vec{R}}_{d1} = [-\dot{\theta}_1 x_1 s\theta_1 - \dot{u}_1 s\theta_2 - \dot{\theta}_1 u_1 c\theta_1]\vec{u}_x + [\dot{\theta}_1 x_1 c\theta_1 + \dot{u}_1 c\theta_1 - u_1 \dot{\theta}_1 s\theta_1]\vec{u}_y \tag{2.7}$$

$$\dot{\vec{R}}_{d2} = [-l_1 \dot{\theta}_1 s\theta_1 - \dot{u}_{1E} s\theta_1 - u_{1E} \dot{\theta}_1 c\theta_1 - x_2(\dot{\theta}_1 + \dot{\theta}_2)s(\theta_1 + \theta_2)$$

$$-\dot{u}_2 s(\theta_1 + \theta_2) - u_2(\dot{\theta}_1 + \dot{\theta}_2)c(\theta_1 + \theta_2)]\vec{u}_x \; [l_1 \dot{\theta}_1 c\theta_1 + \dot{u}_{1E} c\theta_1 -$$

$$u_{1E} \dot{\theta}_1 s\theta_1 + x_2(\theta_1 + \dot{\theta}_2)c(\theta_1 + \theta_2) + \dot{u}_2 c(\theta_1 + \theta_2) - u_2(\dot{\theta}_1 + \dot{\theta}_2)$$

$$s(\theta_1 + \theta_2)]\vec{u}_y \tag{2.8}$$

where the dot means the derivative with respect to time.

For any mass $m_j$ concentrated at joint 2 the velocity will be the same as for the end of beam 1 and for any payload, the velocity will be the one at the end of beam 2.

## 2.3 Kinetic Energy

The kinetic energy of beams 1 and 2 can be expressed as

$$T_b = T_1 + T_2 = 1/2 \int_{m_1} \dot{\bar{R}}_{d1} \cdot \dot{\bar{R}}_{d1} dm + 1/2 \int_{m_2} \dot{\bar{R}}_{d2} \cdot \dot{\bar{R}}_{d2} dm \qquad (2.9)$$

where dm is the element of mass at point $P_i (i = 1,2)$ and $m_1$ and $m_2$ are the masses of beams 1 and 2 respectively.

If now (2.7) and (2.8) are substituted into (2.9) the result is:

$$T_b = 1/2\dot{\theta}_1^2 \int_{m_1} x_1^2 dm + 1/2 \int_{m_1} \dot{u}_1^2 dm + \dot{\theta}_1 \int_{m_1} \dot{u}_1 x_1 dm +$$

$$1/2\dot{\theta}_1^2 \int_{m_1} u_1^2 dm + 1/2 m_2 l_1^2 \dot{\theta}_1^2 + 1/2 m_2 \dot{u}_{1E}^2 + 1/2 m_2 u_{1E}^2 \dot{\theta}_1^2 + m_2 l_1 \dot{\theta}_1 \dot{u}_{1E}$$

$$+1/2(\dot{\theta}_1 + \dot{\theta}_2)^2 \int_{m_2} x_2^2 + 1/2 \int_{m_2} \dot{u}_2^2 dm + 1/2(\dot{\theta}_1 + \dot{\theta}_2)^2 \int_{m_2} u_2^2 dm$$

$$+ (\dot{\theta}_1 + \dot{\theta}_2) \int_{m_2} x_2 \dot{u}_2 dm + l_1 \dot{\theta}_1 (\dot{\theta}_1 + \dot{\theta}_2) c\theta_2 \int_{m_2} x_2 dm +$$

$$l_1 \dot{\theta}_1 c\theta_2 \int_{m_2} \dot{u}_2 dm + \dot{u}_{1E} (\dot{\theta}_1 + \dot{\theta}_2) c\theta_2 \int_{m_2} x_2 dm + \dot{u}_{1E} c\theta_2 \int_{m_2} \dot{u}_2 dm$$

$$\dot{u}_{1E} (\dot{\theta}_1 + \dot{\theta}_2) s(-\theta_2) \int_{m_2} u_2 dm + u_{1E} \dot{\theta}_1 (\dot{\theta}_1 + \dot{\theta}_2) s\theta_2 \int_{m_2} x_2 dm +$$

$$l_1 \dot{\theta}_1 (\dot{\theta}_1 + \dot{\theta}_2) s(-\theta_2) \int_{m_2} u_2 dm + u_{1E} \dot{\theta}_1 (\dot{\theta}_1 + \dot{\theta}_2) c\theta_2 \int_{m_2} u_2 dm +$$

$$u_{1E} \dot{\theta}_1 s\theta_2 \int_{m_2} \dot{u}_2 dm \qquad (2.10)$$

The same procedure can be applied to a mass concentrated at joint 2 and to a payload with moment of inertia $J_{xp}$ with respect to an axis normal to the plane of motion and through the center of gravity. In fact, for the mass at joint 2 expression (2.7) can be modified to

$$\vec{R}_j = [-\dot{\theta}_1 l_1 s\theta_1 - \dot{u}_{1E} s\theta_1 - \dot{\theta}_1 u_{1E} c\theta_1] \vec{u}_x + [\dot{\theta}_1 l_1 c\theta_1 + \dot{u}_{1E} c\theta_1$$

$$- u_{1E} \dot{\theta}_1 s\theta_1] \vec{u}_y \qquad (2.11)$$

and from expression (2.8)

$$\dot{\vec{R}}_p = [-l_1\dot{\theta}_1 s\theta_1 - \dot{u}_{1E}s\theta_1 - u_{1E}\dot{\theta}_1 c\theta_1 - l_2(\dot{\theta}_1 + \dot{\theta}_2)s(\theta_1 + \theta_2) - \dot{u}_{2E}s(\theta_1 + \theta_2)$$

$$-u_{2E}(\dot{\theta}_1 + \dot{\theta}_2)c(\theta_1 + \theta_2)]\vec{u}_x[l_1\dot{\theta}_1 c\theta_1 + \dot{u}_{1E}c\theta_1 - u_{1E}\dot{\theta}_1 s\theta_1 + l_2(\dot{\theta}_1 + \dot{\theta}_2)$$

$$c(\theta_1 + \theta_2) + \dot{u}_{2E}c(\theta_1 + \theta_2) - \dot{u}_{2E}(\dot{\theta}_1 + \dot{\theta}_2)s(\theta_1 + \theta_2)]\vec{u}_y \qquad (2.12.1)$$

where

$u_{2E}$ and $\dot{u}_{2E}$ are flexible displacement and velocity of the end of beam 2. If the moment of inertia of the payload with respect to an axis through point $O_2$ is defined by $J_p$ and the angular displacement

$$\left[\frac{\partial u_2}{\partial x_2}\right]_{x_2 = l_2} = u_{2E}' \qquad (2.12.2)$$

is taken into account, the total kinetic energy of the system can be finally expressed as:

$$T = 1/2 \int_{m_1} \dot{\vec{R}}_{d1}\cdot\dot{\vec{R}}_{d1}dm + 1/2 \int_{m_2} \dot{\vec{R}}_{d2}\cdot\dot{\vec{R}}_{d2}dm + 1/2 m_j \vec{R}_j \vec{R}_j +$$

$$+ \frac{1}{2} m_p \vec{R}_p \cdot \vec{R}_p + \frac{1}{2} J_p \dot{u}_{2E}^2 \qquad (2.13)$$

## 2.4 Potential Energy

The potential energy of the system will be assumed as composed of the energy associated to the rigid motion plus the elastic potential energy of the links. Then, assuming Ox as the reference position, the first approximation of the total potential of the system is (assuming $u_1$ and $u_2$ sufficiently small)

$$V = m_1 g \frac{l_1}{2}(1-c\theta_1) + m_j g l_1 (1-c\theta_1) + m_2 g[l_1(1-c\theta_1) + \frac{l_2}{2}(1-c(\theta_1+\theta_2))] + m_p g[l_1(1-c\theta_1) + l_2(1-c(\theta_1+\theta_2))] - 1/2 \int_0^{l_1} EI_1 \left(\frac{\partial^2 u_1}{\partial x_1^2}\right)^2 dx - 1/2 \int_0^{l_2} EI_2 \left(\frac{\partial^2 u_2}{\partial x_2^2}\right) dx \qquad (2.14)$$

where

g is the component of gravity acceleration in the Ox direction, i.e.,

$$\vec{G} = [\vec{U}]^t \begin{Bmatrix} g \\ 0 \end{Bmatrix} \tag{2.15}$$

$EI_1$, $EI_2$ are stiffnesses of links 1 and 2 respectively, assumed constant for the purpose of this model.

## 2.5 Equations of Motion

In order to write the equations of motion of the proposed system, it is possible to make use of the so called assume-modes method [M1]. Based upon this method, a solution of the flexible motions could be assumed as being composed of a linear combination of admissible functions multiplied by time-dependent generalized coordinates. Here, by admissible functions is meant any arbitrary function satisfying all the geometric or essential boundary conditions [C1]. Then, in case of the flexible displacements of beams 1 and 2, it is possible to assume

$$u_1 = \sum_{i=1}^{n} \phi_{1i}(x_1) q_{1i}(t) \tag{2.16.1}$$

$$u_2 = \sum_{i=1}^{n} \phi_{2i}(x_2) q_{2i}(t) \tag{2.16.2}$$

where the admissible functions $\phi_{ji}(x)$ must satisfy the geometric boundary conditions with respect to the representation of the links in the reference frames $[O_1 x_1 y_1]$ and $[O_2 x_2 y_2]$.

It is clear that the system is now represented by a $(2n + 2)$ de-

grees of freedom system where $[\theta_1(t),\theta_2(t)]$ and $[q_{1i}(t), q_{2i}(t), i=1, \ldots,n]$ are the generalized coordinates. Moreover, assuming that the amplitude of the higher modes of the flexible links is very small compared with the first one, the system can be truncated with n equal 2, resulting in a 6-degree of freedom problem.

The (2.16) assumes the form

$$u_1 = \phi_{11}(x_1)q_{11}(t) + \phi_{12}(x_1)q_{12}(t) \qquad (2.17.1)$$

$$u_2 = \phi_{21}(x_2)q_{12}(t) + \phi_{22}(x_2)q_{22}(t) \qquad (2.17.2)$$

if now, $\phi_{ij}(i,j = 1,2)$ are assumed to be the eigenfunctions of a clamped-free beam, the geometric boundary conditions will be satisfied and because the orthogonality of these functions

$$\int_0^{l_1} \phi_r(x)\phi_s(x)dx = \int_0^{l_1} \phi_r{}^{11}(x)\phi_s{}^{11}(s)dx = \begin{cases} 0 & (\neq s) \\ 1 & (r= s) \end{cases} \qquad (2.18)$$

where

$$\phi_r(x) = (\cosh\lambda_r x - \cos\lambda_r x) - \sigma_r(\sinh\lambda_r x - \sin\lambda_r x) \qquad (2.19)$$

as in reference [B1], where r is the mode of vibrations and $\lambda_r,\sigma_r$ are given by Table 2.1.

| r | $\lambda_r l$ | $\sigma_r$ |
|---|---|---|
| 1 | 1.875 | 0.7340 |
| 2 | 4.694 | 1.0184 |

Table 2.1 Characteristic Values for Clamped-free Beam

Now the integrals in equations (2.10) and (2.14) can be evaluated.

$$\int_{m_1} x_1^2 dm = J_0 \tag{2.18.1}$$

$$\int_{m_1} \dot{u}_1^2 dm = \int_{m_1} \phi_{11}^2 \dot{q}_{11}^2 dm + \int_{m_1} \phi_{12}^2 \dot{q}_{12}^2 dm = \dot{q}_{11}^2 \int_{m_1} \phi_{11}^2 dm +$$

$$\dot{q}_{12}^2 \int \phi_{12}^2 dm = m_1(\dot{q}_{11}^2 + \dot{q}_{12}^2) \tag{2.18.2}$$

$$\int_{m_1} \dot{u}_1 x_1 dm = \int_{m_1} (\phi_{11}\dot{q}_{11} + \phi_{12}\dot{q}_{12}) x_1 dm = \dot{q}_{11} \int_{m_1} \phi_{11} x_1 dm +$$

$$\dot{q}_{12} \int_{m_1} \phi_{12} x_1 dm = nw11\ \dot{q}_{11} + nw12\ \dot{q}_{12} \tag{2.18.3}$$

where

$$nw11 = \int_{m_1} \phi_{11} x_1 dm = \int_0^{l_1} \mu_1 x \phi_{11}(x) dx \qquad (2.18.4)$$

$$nw12 = \int_{m_1} \phi_{12} x_1 dm = \int_0^{l_1} \mu_1 x \phi_{12}(x) dx \qquad (2.18.5)$$

$\int_{m_1} u_1^2 dm$ - neglected in the model

$$\int_{m_2} x_2^2 dm = J_{01} \qquad (2.18.6)$$

$$\int_{m_2} \dot{u}_2^2 dm = m_2(\dot{q}_{21}^2 + \dot{q}_{22}^2) \qquad (2.18.7)$$

$\int_{m_2} u_2^2 dm$ = neglected in the model

$$\int_{m_2} x_2 \dot{u}_2 dm = nw21\dot{q}_{21} + nw22\dot{q}_{22} \qquad (2.18.8)$$

where

$$nw21 = \int_{m_2} \phi_{21} x_2 dm = \int_0^{l_2} \mu_2 x \phi_{21}(x) dx \qquad (2.18.9)$$

$$nw22 = \int_{m_2} \phi_{22} x_2 dm = \int_0^{l_2} \mu_2 x \phi_{22}(x) dx \qquad (2.18.10)$$

$$\int_{m_2} x_2 dm = m_2 \frac{l_2}{2} \qquad (2.18.11)$$

$$\int_{m_2} \dot{u}_2 dm = \int_{m_2} (\phi_{21}\dot{q}_{21} + \phi_{22}\dot{q}_{22})dm = \dot{q}_{21} \int_{m_2} \phi_{21} dm + \dot{q}_{22} \int \phi_{22} dm =$$

$$nq21\ \dot{q}_{21} + nq22\ \dot{q}_{22} \tag{2.18.12}$$

where

$$nq21 = \int_{m_2} \phi_{21} dm = \int_0^{l_2} \mu_2 \phi_{21}(x) dx \tag{2.18.13}$$

$$nq22 = \int_{m_2} \phi_{22} dm = \int_0^{l_2} \mu_2 \phi_{22}(x) dx \tag{2.18.14}$$

$$\int_{m_2} u_2 dm = \int_{m_2} (\phi_{21}q_{21} + \phi_{22}q_{22})dm = nq21\ q_{21} + nq22\ q_{22} \tag{2.18.15}$$

For the potential energy, assuming EI constant for each beam and neglecting the effect of shear forces one can write

$$\int_0^{l_1} EI_1 \left( \frac{\partial^2 u_1}{\partial x_1^2} \right)^2 dx = EI_1 \int_0^{l_1} (\phi''_{11}\ q_{11} + \phi''_{12}\ q_{12})^2 dx =$$

$$kw111 q_{11}^2 + kw122\ q_{12}^2 \tag{2.19}$$

where the generalized springs are

$$kw111 = EI_1 \int_0^{l_1} (\phi_{11}"\phi_{11}")dx \tag{2.20.1}$$

$$kw122 = EI_1 \int_0^{l_1} (\phi_{12}"\phi_{12}")dx \tag{2.20.2}$$

$$\int_0^{l_2} E\, I_2 \frac{\partial^2 u_2}{\partial x_2^2}\, dx = kw211\, q_{21}^2 + kw222\, q_{22}^2 \tag{2.21}$$

where

$$kw211 = E\, I_2 \int_0^{l_2} (\phi_{21}"\phi_{21}")dx \tag{2.22.1}$$

$$kw222 = E\, I_2 \int_0^{l_2} (\phi_{22}"\phi_{22}")dx \tag{2.22.2}$$

The total kinetic energy can then be written as

$$T = 1/2(J_0 + m_j l_1^2)\dot{\theta}_2^2 + 1/2m_1(\dot{q}_{11}^2 + \dot{q}_{12}^2) + 1/2m_j(\theta_{11E}\dot{q}_{11}^2 +$$

$$\theta_{12E}\dot{q}_{12}^2 + \phi_{11E}\phi_{12E}\,\dot{q}_{11}\dot{q}_{12}) + \dot{\theta}_2[nw11 + m_j l_1\phi_{11E})\dot{q}_{11} + (nw12 +$$

$$m_j l_1\phi_{12E})\dot{q}_{12}] + 1/2(m_2 + m_p)l_1^2\dot{\theta}_2^2 + 1/2(m_2 + m_p)(\phi_{11E}\dot{q}_{11} + \phi_{12E}\dot{q}_{12})^2$$

$$+ 1/2(m_2 + m_p)\dot{\theta}_2^2\,(\phi_{11E}q_{11} + \phi_{12E}q_{12})^2 + (m_2 + m_p)l_1\dot{\theta}_2\,(\phi_{11E}\dot{q}_{11} +$$

$$\phi_{12E}\dot{q}_{12}) + 1/2(J_{01} + J_p)(\dot{\theta}_2 + \dot{\theta}_3)^2 + 1/2m_2(\dot{q}_{21}^2 + \dot{q}_{22}^2) +$$

$$1/2m_p(\phi_{21E}\dot{q}_{21} + \phi_{22E}\dot{q}_{22})^2 + (\dot{\theta}_2 + \dot{\theta}_3)\,[(nw21 + m_p l_2\phi_{21E})\dot{q}_{21} +$$

$$(nw22 + m_p l_{2\ 22E})\dot{q}_{22}] + (m_2 + 2m_p)\frac{l_1 l_2}{2}\,\dot{\theta}_2(\dot{\theta}_2 + \dot{\theta}_3)c\theta_3 +$$

$$l_1\dot{\theta}_2 c\theta_3[(m_p\phi_{21E} + nq21)\dot{q}_{21} + (m_p\phi_{22E} + nq22)\dot{q}_{22}] + (\phi_{11E}\dot{q}_{11} +$$

$$\phi_{12E}\dot{q}_{12})(\dot{\theta}_2 + \dot{\theta}_3)(m_2 + 2m_p)\frac{l_2}{2}\,c\theta_3 + (\phi_{11E}\dot{q}_{11} + \phi_{12E}\dot{q}_{12})[(m_p\phi_{21E}$$

$$+ nq21)\dot{q}_{21} + (m_p\phi_{22E} + nq22)\dot{q}_{22}]c\theta_3 - (\phi_{11E}\dot{q}_{11} + \phi_{12E}\dot{q}_{12})$$

$$(\dot{\theta}_2 + \dot{\theta}_3)[(m_p\phi_{21E} + nq21)q_{21} + (m_p\phi_{22E} + nq22)q_{22}]s\theta_3 +$$

$$(m_2 + 2m_p)(\phi_{11E}q_{11} + \phi_{12E}q_{12})\dot{\theta}_2(\dot{\theta}_2 + \dot{\theta}_3)s\theta_3\frac{l_2}{2} + (\phi_{11E}q_{11} +$$

$$\phi_{12E}q_{12})\dot{\theta}_2[m_p\phi_{21E} + nq21)\dot{q}_{21} + (m_p\phi_{22E} + nq22)\dot{q}_{22}]s\theta_3 -$$

$$l_1\dot{\theta}_2(\dot{\theta}_2 + \dot{\theta}_3)[(m_p\phi_{21E}{}^{+}nq21)q_{21}{+}(m_p\phi_{22E} + nq22)q_{22}]s\theta_3 +$$

$$(\phi_{11E}q_{11} + \phi_{12E}q_{12})\dot{\theta}_2(\dot{\theta}_2 + \dot{\theta}_3)[(m_p\phi_{21E} + nq21)q_{21} + (m_p\phi_{22E} +$$

$$nq22)q_{22}]c\theta_3 + 1/2J_p(\phi_{21E}{}'\dot{q}_{21} + \phi'_{22E}\dot{q}_{22})^2 \qquad (2.23)$$

For the potential energy

$$V = \{(m_1 + 2m_j + 2m_p + 2m_2)\frac{l_1}{2}\,(1 - c\theta_1) + (m_2 + 2m_p)\frac{l_2}{2}$$

$$[1 - c(\theta_1 + \theta_2)]\}g + kw111\, q_{11}^2 + kw122\, q_{12}^2 + kw211\, q_{21}^2 +$$

$$kw222\, q_{22}^2 + k \qquad (2.24)$$

where:

k is the reference potential energy for the flexible components

$\phi_{11E}$, $\phi_{12E}$ are end deflections of beam 1

$\phi_{21E}$, $\phi_{22E}$ are end deflections of beam 2

$\phi_{21E}'$, $\phi_{22E}'$ are the angles at end of beam 2

g is the acceleration of gravity in X direction

If now $\theta_1$, $\theta_2$, $q_{11}$, $q_{12}$, $q_{21}$, $q_{22}$ are assumed to be a set of generalized coordinates and $\tau_1$ and $\tau_2$ are nonconservative torques acting at the joints of the system, it is possible to write the equations of motion using Lagrange's equations for a nonconservative system. These equations have the form

$$\frac{d}{dt}\left(\frac{\partial T}{\partial q_r}\right) - \frac{\partial T}{\partial q_r} + \frac{\partial V}{\partial q_r} = Q_r \qquad r = 1,2...6 \qquad (2.25)$$

where $Q_r$ are time-dependent nonconservative generalized forces (or torques). In this particular case, the torques $\tau_1$ and $\tau_2$ are going to realize work only for variations of $\theta_1$ and $\theta_2$. Then, if a variation $\delta\theta_1$ occurs at joint 1, with all other variables kept constant, the virtual work done is:

$$\delta W = \tau_1 \delta_1 \tag{2.26}$$

and

$$Q_1 = \frac{\delta W}{\delta \theta_1} = \tau_1 \tag{2.27}$$

Similarly

$$Q_2 = \tau_2 \tag{2.28}$$

Also, from the definition of the angle $\theta_2$ given at the beginning of this chapter it is possible to show that the remaining generalized forces are equal to zero.

Then, the equations of motion become

$$M_{11}\ddot{\theta}_1 + M_{12}\ddot{\theta}_2 + M_{13}\ddot{q}_{11} + M_{14}\ddot{q}_{12} + M_{15}\ddot{q}_{21} + M_{16}\ddot{q}_{22} =$$

$$- MB11 - F1 + \tau_1 \tag{2.29.1}$$

$$M_{21}\ddot{\theta}_1 + M_{22}\ddot{\theta}_2 + M_{23}\ddot{q}_{11} + M_{24}\ddot{q}_{12} + M_{25}\ddot{q}_{21} + M_{26}\ddot{q}_{22} =$$
$$- MB12 - F2 + \tau_2 \tag{2.29.2}$$

$$M_{31}\ddot{\theta}_1 + M_{32}\ddot{\theta}_2 + M_{33}\ddot{q}_{11} + M_{34}\ddot{q}_{12} + M_{35}\ddot{q}_{21} + M_{36}\ddot{q}_{22} =$$
$$- KW111\, q_{11} - F3 \tag{2.29.3}$$

$$M_{41}\ddot{\theta}_1 + M_{42}\ddot{\theta}_2 + M_{43}\ddot{q}_{11} + M_{44}\ddot{q}_{12} + M_{45}\ddot{q}_{21} + M_{46}\ddot{q}_{22} =$$
$$-KW122\, q_{12} - F4 \qquad (2.29.4)$$

$$M_{51}\ddot{\theta}_1 + M_{52}\ddot{\theta}_2 + M_{53}\ddot{q}_{11} + M_{54}\ddot{q}_{12} + M_{55}\ddot{q}_{21} + M_{56}\ddot{q}_{22} =$$
$$-KW211\, q_{21} - F5 \qquad (2.29.5)$$

$$M_{61}\ddot{\theta}_1 + M_{62}\ddot{\theta}_2 + M_{63}\ddot{q}_{11} + M_{64}\ddot{q}_{12} + M_{65}\ddot{q}_{21} + M_{66}\ddot{q}_{22} =$$
$$-KW222\, q_{22} - F6 \qquad (2.29.6)$$

where the coefficients are given by

$$M_{11} = (J_0 + m_j l_1^2) + (m_2 + m_p) l_1^2 + (m_2 + m_p)(\phi_{11E} q_{11} + \phi_{12E} q_{12})$$
$$+ (J_{01} + J_p) + (m_2 + 2m_p) l_1 l_2 c\theta_2 + 2(m_2 + 2m_p)(\phi_{11E} q_{11} + \phi_{12E} q_{12})$$
$$\frac{l_2}{2} s\theta_2 - 2(mp21\, q_{21} + mp22\, q_{22}) l_1 s\theta_2 + 2(\phi_{11E} q_{11} + \phi_{12E} q_{12})$$
$$(mp21\, q_{21} + mp22\, q_{22}) c\theta_2 \qquad (2.30.1)$$

$$M_{12} + (J_{01} + J_p) + (m_2 + 2m_p)\frac{l_1 l_2}{2} c\theta_2 + (m_2 + 2m_p)(\phi_{11E} q_{11} +$$
$$\phi_{12E} q_{12}) s\theta_2 - (mp21 q_{21} + mp22\, q_{22}) l_1 s\theta_2 + (mp21\, q_{21} + mp22\, q_{22})$$
$$(\phi_{11E} q_{11} + \phi_{12E} q_{12}) c\theta_2 \qquad (2.30.2)$$

$$M_{13} = (nw11 + m_j l_1 \phi_{11E}) + (m_2 + m_p) l_1 \phi_{11E} + (m_2 + 2m_p)\, \phi_{11E} \frac{l_2}{2} c\theta_2$$
$$- (mp21\, q_{21} + mp22\, q_{22}) \phi_{11E} s\theta_2 \qquad (2.30.3)$$

$$M_{14} = (mw12 + m_j l_1 \phi_{12E}) + (m_2 + m_p) l_1 \phi_{12E} + (m_2 + 2m_p)\frac{l_2}{2} \phi_{12E} \; c\theta_2 - (mp21\, q_{21} + mp22\, q_{22}) \phi_{12E} s\theta_2 \quad (2.30.4)$$

$$M_{15} = (mw21 + m_p l_2 \phi_{21E}) + l_1 c\theta_2 mp_{21} + mp21\, s\theta_2 (\phi_{11E} q_{11} + \phi_{12E} q_{12}) \quad (2.30.5)$$

$$M_{16} = (mw22 + mpl_2 \phi_{22E}) + mp22 l_1 c\theta_2 + mp22\, s\theta_2 (\phi_{11E} q_{11} + \phi_{12E} q_{12}) \quad (2.30.6)$$

$$K_{21} = M_{12} \quad (2.30.7)$$

$$M_{22} = J_{01} + Jp \quad (2.30.8)$$

$$M_{23} = \phi_{11E}(m_2 + 2m_p)\frac{l_2}{2} c\theta_2 - \phi_{11E}(mp21\, q_{21} + mp22 q_{22})\, s\theta_2 \quad (2.30.9)$$

$$M_{24} = \phi_{12E}(m_2 + 2m_p)\frac{l_2}{2} c\theta_2 - \phi_{12E}(mp21 q_{21} + mp22 q_{22})\, s\theta_2 \quad (2.30.10)$$

$$M_{25} = (mw21 + m_p l_2\, \phi_{21E}) \quad (2.30.11)$$

$$M_{26} = (mw22 + m_p l_2 \phi_{22E}) \quad (2.30.12)$$

$$M_{31} = M_{13} \quad (2.30.13)$$

$$M_{32} = M_{23} \quad (2.30.14)$$

$$M_{33} = m_1 + (m_2 + m_j + m_p)\phi_{11E}^2 \qquad (2.30.15)$$

$$M_{34} = (m_2 + m_p + m_j)\phi_{11E}\phi_{12E} \qquad (2.30.16)$$

$$M_{35} = \phi_{11E} m_{p21}\, c\theta_2 \qquad (2.30.17)$$

$$M_{36} = \phi_{11E}\, m_{p22}\, c\theta_2 \qquad (2.30.18)$$

$$M_{41} = M_{14} \qquad (2.30.19)$$

$$M_{42} = M_{24} \qquad (2.30.20)$$

$$M_{43} = M_{34} \qquad (2.30.21)$$

$$M_{44} = m_1 + (m_2 + m_j + m_p)\phi_{12E}^2 \qquad (2.30.22)$$

$$M_{45} = \phi_{12E} m_{p21}\, c\theta_2 \qquad (2.30.23)$$

$$M_{46} = \phi_{12E} m_{p22}\, c\theta_2 \qquad (2.30.24)$$

$$M_{51} = M_{15} \qquad (2.30.25)$$

$$M_{52} = M_{25} \qquad (2.30.26)$$

$$M_{53} = M_{35} \tag{2.30.27}$$

$$M_{54} = M_{45} \tag{2.30.28}$$

$$M_{55} = m_2 + m_p \phi_{21E}^2 + J_p \phi'^2_{21E} \tag{2.30.29}$$

$$M_{56} = m_p \phi_{21E}\phi_{22E} + J_p \phi'_{21E}\phi'_{22E} \tag{2.30.30}$$

$$M_{61} = M_{16} \tag{2.30.31}$$

$$M_{62} = M_{26} \tag{2.30.32}$$

$$M_{63} = M_{36} \tag{2.30.33}$$

$$M_{64} = M_{46} \tag{2.30.34}$$

$$M_{65} = M_{56} \tag{2.30.35}$$

$$M_{66} = m_2 + m_p \phi_{22E}^2 + J_p \phi'^2_{22E} \tag{2.30.36}$$

$$M_{11} = [(m_1 + 2m_j)\frac{l_1}{2} s\theta_2 + (m_2 + 2m_p)\frac{l_2}{2} s(\theta_1 + \theta_2) + (m_2 + m_p) l_1 s\theta_1]g \tag{2.30.37}$$

$$MB12 = (m_2 + 2m_p)\frac{l_2}{2} gs(\theta_1 + \theta_2) \qquad (2.30.38)$$

**and the nonlinear functions are**

$$F1 = 2(m_2 + m_p)(\phi_{11E}q_{11} + \phi_{12E}q_{12})(\phi_{11E}\dot{q}_{11} + \phi_{12E}\dot{q}_{12})\dot{\theta}_1 -$$

$$(m_2 + 2m_p)l_1 l_2\dot{\theta}_1\dot{\theta}_2 s\theta_2 - (m_2 + 2m_p)\frac{l_1 l_2}{2}\dot{\theta}_2^2 \; s\theta_2 - l_1\dot{\theta}_2 s\theta_2$$

$$(mp21\,\dot{q}_{21} + mp22\,.\,\dot{q}_{22}) - (m_2 + 2m_p)(\phi_{11E}\dot{q}_{11} + \phi_{12E}\dot{q}_{12})\frac{l_2}{2}\dot{\theta}_2 s\theta_2$$

$$- (\phi_{11E}\,\dot{q}_{11} + \phi_{12E}\,\dot{q}_{12})[mp21\,\dot{q}_{21} + mp22\,\dot{q}_{22})s\theta_2 + (mp21\,q_{21} +$$

$$mp22\,q_{22})\dot{\theta}_2 c\theta_2] + 2(m_2 + 2m_p)\frac{l_2}{2}\;[(\phi_{11E}\,\dot{q}_{11} + \phi_{12E}\,\dot{q}_{12})\dot{\theta}_1 s\theta_2$$

$$+ (\phi_{11E}\,q_{11} + \phi_{12E}\,q_{12})\dot{\theta}_1\dot{\theta}_2 c\theta_2] + (m_2 + 2m_p)[(\phi_{11E}\,\dot{q}_{11} +$$

$$\phi_{12E}\,\dot{q}_{12})\dot{\theta}_2 s\theta_2 + (\phi_{11E}\,q_{11} + \phi_{12E}\,q_{12})\dot{\theta}_2^2 c\theta_2]\;\frac{l_2}{2} +$$

$$(\phi_{11E}\,\dot{q}_{11} + \phi_{12E}\,\dot{q}_{12})(mp21\,\dot{q}_{21} + mp22\,\dot{q}_{22})s\theta_2 + (\phi_{11E}\,q_{11} +$$

$$\phi_{12E}\,q_{12})(mp21\,\dot{q}_{21} + mp22\,\dot{q}_{22})\dot{\theta}_2 c\theta_2 - (mp21\,\dot{q}_{21} + mp22\,\dot{q}_{22})$$

$$s\theta_2 l_1(2\dot{\theta}_1 + \dot{\theta}_2) - (mp21\,q_{21} + mp22\,q_{22})\dot{\theta}_2 l_1 c\theta_2(2\dot{\theta}_1 + \dot{\theta}_2) + (\phi_{11E}\dot{q}_{11} +$$

$$\phi_{12E}\dot{q}_{12})(mp21q_{21} + mp22q_{22})(2\dot{\theta}_1 + \dot{\theta}_2) + (\phi_{11E}q_{11} + \phi_{12E}q_{12})$$

$$[(mp21\dot{q}_{21} + mp22\dot{q}_{22})(2\dot{\theta}_1 + \dot{\theta}_2)c\theta_2 - (mp21q_{21} + mp22q_{22})\dot{\theta}_2$$

$$(2\dot{\theta}_1 + \dot{\theta}_2)s\theta_2] \qquad (2.31.1)$$

$$F2 = -(\phi_{11E}\dot{q}_{11} + \phi_{12E}\dot{q}_{12})(m_2 + 2mp)\frac{l_2}{2}\dot{\theta}_2 s\theta_2 + (m_2 + 2mp)(\phi_{11E}\dot{q}_{11}$$

$$+ \phi_{12E}\dot{q}_{12})\dot{\theta}_1 s\theta_2\frac{l_2}{2} - (mp21\dot{q}_{21} + mp22\dot{q}_{22})l_1\dot{\theta}_1 s\theta_2 + (\phi_{11E}\dot{q}_{11}+\phi_{12E}\dot{q}_{12})$$

$$\dot{\theta}_1(mp21q_{21} + mp22q_{22})c\theta_2 + (m_2 + 2mp)\frac{l_1 l_2}{2}\dot{\theta}_1^2 s\theta_2 + l_1\dot{\theta}_1 s\theta_2$$

$$(mp21\dot{q}_{21} + mp22\dot{q}_{22}) + (\phi_{11E}\dot{q}_{11} + \phi_{12E}\dot{q}_{12})\ (\dot{\theta}_1+\dot{\theta}_2)(m_2+2mp)\frac{l_2}{2}\ s\theta_2 +$$

$$(\phi_{11E}\dot{q}_{11} + \phi_{12E}\dot{q}_{12})\dot{\theta}_1(mp21q_{21} + mp22q_{22})c\theta_2 - (m_2 + 2mp)\frac{l_2}{2}(\phi_{11E}q_{11} +$$

$$\phi_{12E}q_{12})\dot{\theta}_1^2 c\theta_2 + (\phi_{11E}q_{11} + \phi_{12E}q_{12})\dot{\theta}_1^2(mp21q_{21} + mp22q_{22})s\theta_2 +$$

$$l_1\dot{\theta}_1^2\ (mp21q_{21} + mp22q_{22})c\theta_2 \qquad (2.31.2)$$

$$F3 = \phi_{11E}\frac{l_2}{2}(\dot{\theta}_1 + \dot{\theta}_2)(m_2 + 2mp)\dot{\theta}_2 s\theta_2 - \phi_{11E}(mp21\dot{q}_{21} + mp22\dot{q}_{22})$$

$$\dot{\theta}_2 s\theta_2 - \phi_{11E}(\dot{\theta}_1 + \dot{\theta}_2)[(mp21\dot{q}_{21} + mp22\dot{q}_{22})s\theta_1 + (mp21q_{21} + mp22q_{22})$$

$$\dot{\theta}_2 c\theta_2] - (m_2 + mp)\dot{\theta}_1^2\ (\phi_{11E}q_{11} + \phi_{12E}q_{12})\phi_{11E} - (m_2 + 2mp)\phi_{11E}\ddot{\theta}_1$$

$$(\dot{\theta}_1 + \dot{\theta}_2)s\theta_2 \frac{l_2}{2} - \phi_{11E}\dot{\theta}_1(mp21\dot{q}_{21} + mp22\dot{q}_{22})s\theta_2 - \phi_{11E}\dot{\theta}_1(\dot{\theta}_1 + \dot{\theta}_2)$$

$$(mp21q_{21} + mp22q_{22})c\theta_2 \qquad (2.31.3)$$

$$F4 = -\phi_{12E}\,\dot{\theta}_2(\dot{\theta}_1 + \dot{\theta}_2)(m_2 + 2mp)\,\frac{l_2}{2}\,s\theta_2 \cdot \phi_{12E}(mp21\dot{q}_{21} + mp22\dot{q}_{22})$$

$$\dot{\theta}_2\, s\theta_2 - \phi_{12E}(\dot{\theta}_1 + \dot{\theta}_2)[(mp21\dot{q}_{21} + mp22\dot{q}_{22})s\theta_2 + (mp21q_{21} + mp22q_{22})$$

$$\dot{\theta}_2\, c\theta_2] - (m_2 + m_p)\dot{\theta}_1^2\phi_{12E}(\phi_{11E}q_{11} + \phi_{12E}q_{12}) - (m_2 + 2m_p)\phi_{12E}\dot{\theta}_1$$

$$(\dot{\theta}_1 + \dot{\theta}_2)\, s\theta_2\, \frac{l_2}{2} - \phi_{12E}\dot{\theta}_1(mp21\dot{q}_{21} + mp22\dot{q}_{22})\, s\theta_2 - \phi_{12E}\dot{\theta}_1$$

$$(\dot{\theta}_1 + \dot{\theta}_2)(mp21q_{21} + mp22q_{22})\, c\theta_2 \qquad (2.31.4)$$

$$F5 = -mp21\, l_1\dot{\theta}_1\dot{\theta}_2 s\theta_2 + 2(\phi_{11E}\dot{q}_{11} + \phi_{12E}\dot{q}_{12})mp21\dot{\theta}_1 s\theta_2 + l_1\dot{\theta}_1$$

$$(\dot{\theta}_1 + \dot{\theta}_2)mp21 s\theta_2 - (\phi_{11E}q_{11} + \phi_{12E}q_{12})\dot{\theta}_1^2 mp21\, c\theta_2 \qquad (2.31.5)$$

$$F6 = -mp22\, l_1\dot{\theta}_1\dot{\theta}_2\, s\theta_2 + 2(\phi_{11E}\dot{q}_{11} + \phi_{12E}\dot{q}_{12})mp22\, \dot{\theta}_1 s\theta_2 + l_1\dot{\theta}_1$$

$$(\dot{\theta}_1 + \dot{\theta}_2)mp22\, s\theta_2 - (\phi_{11E}q_{11} + \phi_{12E}q_{12})\dot{\theta}_1^2\, mp22\, c\theta_2 \qquad (2.31.6)$$

where

$$mp21 = m_p\,\phi_{21E} + nq21 \qquad (2.32.1)$$

$$mp22 = m_p \phi_{22E} + nq22 \tag{2.32.2}$$

Equations (2.29) can be written in matrix form

$$\underline{M}_1 (t)\, \ddot{\underline{\xi}} = \underline{K}_1\, \underline{\xi} + \underline{F}_1 + \underline{C}\, \underline{u} \tag{2.33}$$

where

$$\underline{M}_1(t) = [M_{ij}] \qquad i,j = 1,\ldots, 6 \tag{2.34.1}$$

$$\underline{K}_1 = \begin{bmatrix} 0 & 0 & 0 & 0 & 0 & 0 \\ 0 & 0 & 0 & 0 & 0 & 0 \\ 0 & 0 & -kw111 & 0 & 0 & 0 \\ 0 & 0 & 0 & -kw122 & 0 & 0 \\ 0 & 0 & 0 & 0 & -kw211 & 0 \\ 0 & 0 & 0 & 0 & 0 & -kw222 \end{bmatrix} \tag{2.34.2}$$

$$\underline{F}_1 = \begin{bmatrix} +F1 - MB11 \\ +F2 - MB12 \\ -F3 \\ -F4 \\ -F5 \\ -F6 \end{bmatrix} \tag{2.34.3}$$

$$\underline{C} = \begin{bmatrix} 1 & 0 \\ 0 & 1 \\ 0 & 0 \\ 0 & 0 \\ 0 & 0 \\ 0 & 0 \end{bmatrix} \tag{2.34.4}$$

$$\underline{u} = \begin{bmatrix} \tau_1 \\ \tau_2 \end{bmatrix} \tag{2.34.5}$$

$$\ddot{\underline{\xi}} = \begin{bmatrix} \ddot{\theta}_1 \\ \ddot{\theta}_2 \\ \ddot{q}_{11} \\ \ddot{q}_{12} \\ \ddot{q}_{21} \\ \ddot{q}_{22} \end{bmatrix} \tag{2.34.6}$$

$$\underline{\xi} = \begin{bmatrix} \theta_1 \\ \theta_2 \\ q_{11} \\ q_{12} \\ q_{21} \\ q_{22} \end{bmatrix} \tag{2.34.7}$$

A new set of variables can now be defined in order to write the equations of motion (2.33) in state space form.

In fact, if

$\zeta_1 = \theta_1$ (2.35.1) $\qquad \zeta_4 = q_{12}$ (2.35.4)

$\zeta_2 = \theta_2$ (2.35.2) $\qquad \zeta_5 = q_{21}$ (2.35.5)

$\zeta_3 = q_{11}$ (2.35.3) $\qquad \zeta_6 = q_{22}$ (2.35.6)

equation (2.33) will be

$$\dot{\underline{\zeta}} = \underline{A}' \underline{\zeta} + \underline{F}' + \underline{C}'\underline{u} \tag{2.36}$$

where

$$\dot{\underline{\zeta}} = [\dot{\zeta}_i] \tag{2.37.1}$$

$$\underline{\zeta} = [\zeta_i]$$

$$i = 1, \ldots, 6 \tag{2.37.2}$$

$$\underline{A}' = \left[\begin{array}{c:c} \underline{0} & \underline{I} \\ \hdashline \underline{M_1}^{-1}\underline{K_1}' & \underline{0} \end{array}\right] \tag{2.37.3}$$

$$\underline{F}' = \left[\begin{array}{c} \underline{0} \\ \hdashline \underline{M_1}^{-1}\underline{F} \end{array}\right] \tag{2.37.4}$$

$$\underline{C}' = \left[\begin{array}{c} \underline{0} \\ \hdashline \underline{M_1}^{-1}\underline{B} \end{array}\right] \tag{2.37.5}$$

where $\dot{\underline{x}}$, $\underline{x}$ and $\underline{F}'$ are (12x1) vectors, $\underline{A}'$ is (12x12) and $\underline{C}'$ is (12x2) matrix.

## 2.6 Linearized Equations

Equation (2.36) is used to study the motions of the proposed system under some designed control component $\underline{u}$. For the purpose of design a linearized form of (2.36) is obtained. In doing so, all sines and cosines are first replaced by their series representation and then all terms of second- or higher degree in $x_i$, $i = 1,\ldots,6$ are dropped from the equations. The resulting linearized system of equations can then be written as

$$\dot{\underline{x}} = \underline{A}\,\underline{x} + \underline{B}\,\underline{u} \tag{2.38}$$

where

$$\underline{A} = \begin{bmatrix} \underline{0} & \underline{I} \\ \underline{M}^{-1}\underline{K} & \underline{0} \end{bmatrix} \tag{2.39.1}$$

$$\underline{B} = \begin{bmatrix} \underline{0} \\ \underline{M}^{-1}\underline{B} \end{bmatrix} \tag{2.39.2}$$

and

$$\underline{M} = [M_{ij}] \qquad i, j = 1, \ldots, 6 \tag{2.39.3}$$

$$\underline{K} = \begin{bmatrix} -MB111 & -MB112 & 0 & 0 & 0 & 0 \\ -MB121 & -MB122 & 0 & 0 & 0 & 0 \\ 0 & 0 & -kw111 & 0 & 0 & 0 \\ 0 & 0 & 0 & -kw122 & 0 & 0 \\ 0 & 0 & 0 & 0 & -kw211 & 0 \\ 0 & 0 & 0 & 0 & 0 & -kw222 \end{bmatrix} \quad (2.39.4)$$

where now

$$M_{11} = (J_0 + m_j l_1^2) + (m_2 + m_p) l_1^2 + (J_{01} + J_p) + (m_2 + 2m_p) l_1 l_2 c\bar{\theta}_2 \quad (2.40.1)$$

$$M_{12} = (J_{01} + J_p) + (m_2 + 2m_p)\frac{l_1 l_2}{2} c\bar{\theta}_2 \quad (2.40.2)$$

$$M_{13} = (nw11 + m_j l_1 \phi_{11E}) + (m_2 + m_p) l_1 \phi_{11E} + (m_2 + 2m_p)\phi_{11E} \frac{l_2}{2} c\bar{\theta}_2 \quad (2.40.3)$$

$$M_{14} = (nw12 + m_j l_1 \phi_{11E}) + (m_2 + m_p) l_1 \phi_{12E} + (m_2 + 2m_p)\frac{l_2}{2} \phi_{12E} c\bar{\theta}_2 \quad (2.40.4)$$

$$M_{15} = (nw21 + m_p l_2 \phi_{21E}) + mp21\ l_1 c\bar{\theta}_2 \quad (2.40.5)$$

$$M_{16} = (nw22 + m_p l_2 \phi_{22E}) + mp22\ l_1 c\bar{\theta}_2 \quad (2.40.6)$$

$$M_{21} = M_{12} \quad (2.40.7)$$

$$M_{22} = J_{01} + Jp \tag{2.40.8}$$

$$M_{23} = \phi_{11E}(m_2 + 2m_p)\frac{l_2}{2}\,c\bar{\theta}_2 \tag{2.40.9}$$

$$M_{24} = \phi_{12E}(m_2 + 2m_p)\frac{l_2}{2}\,c\bar{\theta}_2 \tag{2.40.10}$$

$$M_{25} = mw21 + m_p l_2 \phi_{21E} \tag{2.40.11}$$

$$M_{26} = mw22 + m_p l_2 \phi_{22E} \tag{2.40.12}$$

$$M_{31} = M_{13} \tag{2.40.13}$$

$$M_{32} = M_{23} \tag{2.40.14}$$

$$M_{33} = m_1 + m_2 + m_j + m_p)\phi^2_{11E} \tag{2.40.15}$$

$$M_{34} = (m_2 + m_p + m_j)\phi_{11E}\,\phi_{12E} \tag{2.40.16}$$

$$M_{35} = \phi_{11E} mp21\; c\bar{\theta}_2 \tag{2.40.17}$$

$$M_{36} = \phi_{11E} mp22\; c\bar{\theta}_2 \tag{2.40.18}$$

$$M_{41} = M_{14} \tag{2.40.19}$$

$$M_{42} = M_{24} \tag{2.40.20}$$

$$M_{43} = M_{34} \tag{2.40.21}$$

$$M_{44} = m_1 + (m_2 + m_j + m_p)\phi_{12E}^2 \tag{2.40 22}$$

$$M_{45} = \phi_{12E} mp21\ c\bar{\theta}_2 \tag{2.40.23}$$

$$M_{46} = \phi_{12E} mp22\ c\bar{\theta}_2 \tag{2.40.24}$$

$$M_{51} = M_{15} \tag{2.40.25}$$

$$M_{52} = M_{25} \tag{2.40.26}$$

$$M_{53} = M_{35} \tag{2.40.27}$$

$$M_{54} = M_{45} \tag{2.40.28}$$

$$M_{55} = m_2 + mp\phi_{21E}^2 + Jp\phi_{21E}^2 \tag{2.40.29}$$

$$M_{56} = m_p \phi_{21E} \phi_{22E} + J_p \phi'_{21E}\ \phi'_{22E} \tag{2.40.30}$$

$$M_{61} = M_{16} \tag{2.40.31}$$

$$M_{62} = M_{26} \tag{2.40.32}$$

$$M_{63} = M_{36} \tag{2.40.33}$$

$$M_{64} = M_{46} \tag{2.40.34}$$

$$M_{65} = M_{56} \tag{2.40.35}$$

$$M_{66} = m_2 + mp\phi_{22E}^2 + Jp\phi_{22E}^{'2} \tag{2.40.36}$$

$$MB111 = [(m_1 + 2m_j + 2m_2 + 2m_p)\frac{l_1}{2} c\bar{\theta}_1 + (m_2 + 2m_p)\frac{l_2}{2}$$

$$c(\bar{\theta}_1 + \bar{\theta}_2)]g \tag{2.40.37}$$

$$MB112 = [(m_2 + 2m_p)\frac{l_2}{2} g\, c(\bar{\theta}_1 + \bar{\theta}_2)] \tag{2.40.38}$$

$$MB121 = [(m_2 + 2m_p)\frac{l_2}{2} g\, c(\bar{\theta}_1 + \bar{\theta}_2)] \tag{2.40.39}$$

$$MB122 = [(m_2 + 2m_p)\frac{l_2}{2} g\, c(\bar{\theta}_1 + \bar{\theta}_2)] \tag{2.40.40}$$

and

$$x_1 = \theta_1 - \bar{\theta}_1 \tag{2.41.1}$$

$$x_2 = \theta_2 - \bar{\theta}_2 \tag{2.41.2}$$

$$x_3 = q_{11} \tag{2.41.3}$$

$$x_4 = q_{12} \tag{2.41.4}$$

$$x_5 = q_{21} \tag{2.41.5}$$

$$x_6 = q_{22} \tag{2.41.6}$$

with $\bar{\theta}_1$ and $\bar{\theta}_2$ being constant angles at some instant t.

## 2.7 Experimental Verification

To know how well the model represents a real system an experiment was designed and built. It consisted of two carbon steel beams pinned together by a joint that allows motion only in the plane of the beams. One of the ends was connected to a torque motor for excitation and at the other extreme a payload was clamped as indicated in Figure 2.4. The joint was represented in the model by a lumped mass at the end of the first beam. The experiment was performed in the vertical plane in order to have the effects of the gravitational field. The frequency spectrum shown in Figure 2.5 was obtained by automatic frequency sweeping and measurement of the acceleration of the end point via an accelerometer mounted on the payload. As the model only takes into account two nodes for each beam, the overall system presents two rigid and four flexible natural frequencies. Table 2.2 summarizes the flexible resonant frequencies and the error relative to the experiment. As one can verify, the results are quite good if one takes into account all the possible measurement errors that might have been introduced by the automatic sweeping without allowing the system to reach the steady state. Another source of errors could well be introduced by the value of moment of inertia of the torque

Units: slug-ft-sec (kg-m-sec)

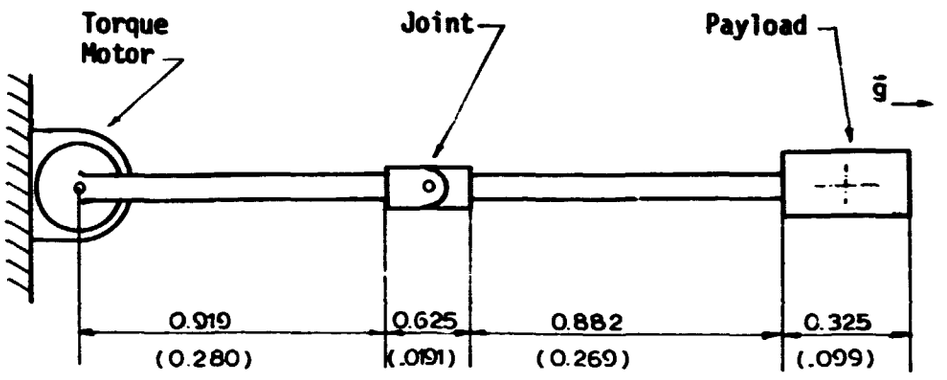


Torque Motor Rotor Inertia = $3.98 \times 10^{-4}$ ft-lbf-sec$^2$
($5.75 \times 10^{-4}$ nt-m-sec$^2$)

Beams: diameter = 0.25 in (0.00635 m)

material: carbon-steel

Joint material: Aluminum

mass = $1.23 \times 10^{-3}$ slugs (0.0179 kg)

Payload mass = $4.875 \times 10^{-3}$ slugs ( 0.0711 kg)

$J_{cg} = 0.395 \times 10^{-4}$ slug-ft$^2$ ( $0.669 \times 10^{-4}$ kg-m$^2$)

Figure 2.4 - Experimental Verification - System Parameters

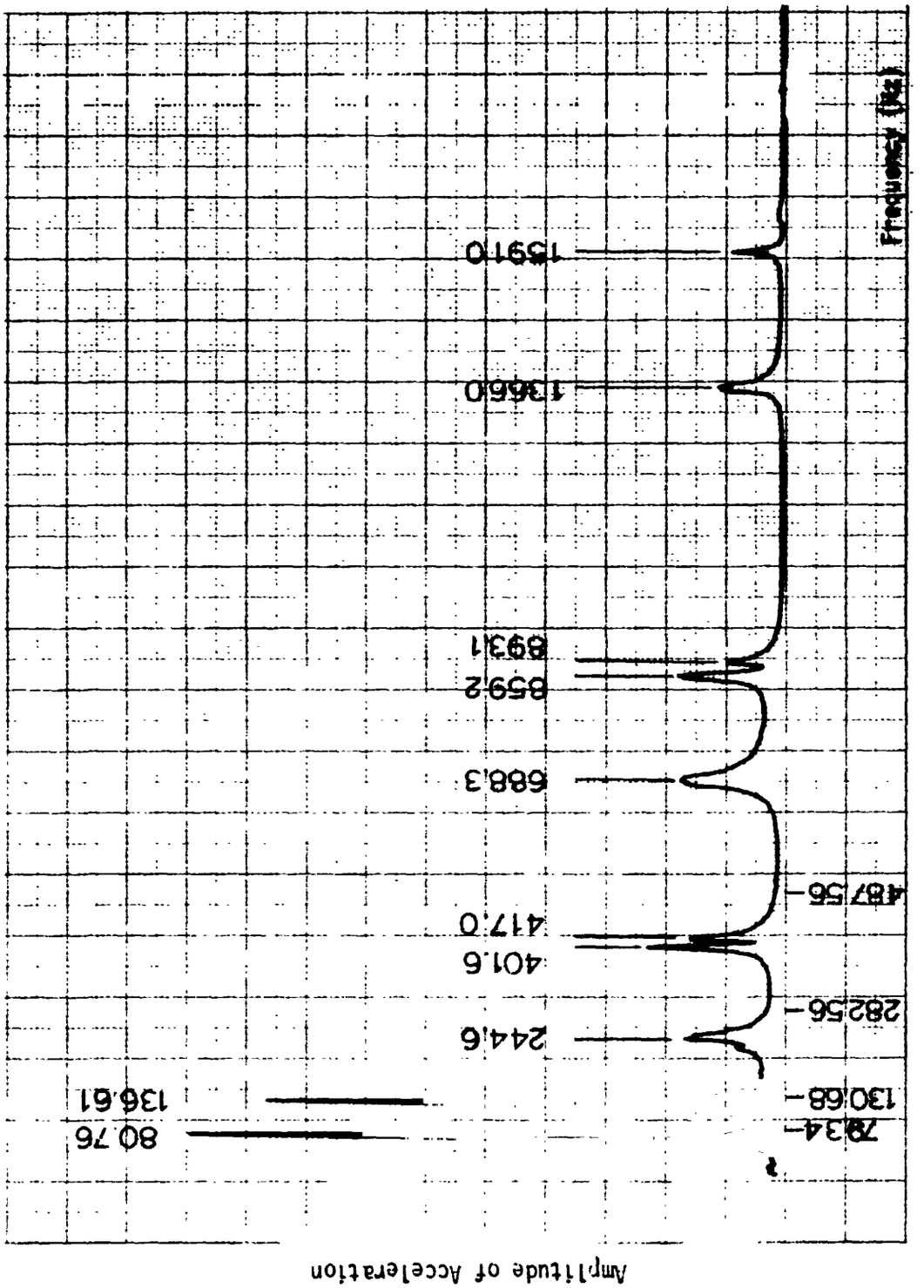


Figure 2.5 - Frequency Spectrum - Experimental Results

motor, which was obtained from a motor catalogue. As has been observed by W.J. Book [B2], a reduction of 30% in this value would lower the first three natural frequencies about 3.7%.

Another comparison of results was performed between the proposed model and the transfer-matrix procedure used in [B2]. For this purpose the chosen system was the correspondent model of a 53.4 ft. long manipulator. The dimensions are summarized in Figure 2.6 and the results in Table 2.3. In this case no gravity was taken into account and Table 2.3 presents the first four flexible natural frequencies.

From the results presented in these two comparisons, one might assume that the model gives a good representation of the proposed physical system with probably loss of significance only in the highest frequency due to truncation error. This kind of error was also observed when the proposed modeling procedure was applied to a single pinned-free beam. Table 2.4 presentes some results comparing the proposed model applied to a single pinned-free beam in two situations: forced by the same torque motor and analytical values with dimensions shown in Figure 2.7, both cases assuming truncation at the second flexible mode.

## 2.8 Numerical Evaluations

As the number of modes introduced in the model increases, the system becomes more and more numerically stiff [L1]. This fact is reflected in the numerical calculations of the eigenvalues of the mathematical model. The previous results in this work were obtained by using a minicomputer Interdata Model 70, with 40K 16 bit words of core storage ail-

Units: slug-ft-sec ( kg-m-sec)

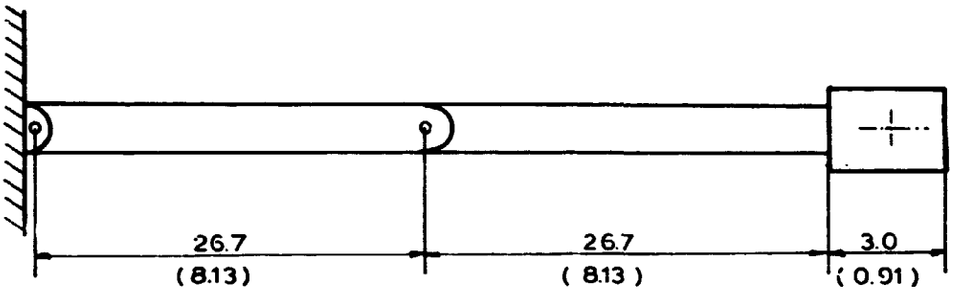


Beams: External diameter = 0.75 ft (0.228 m)

Internal diameter = 0.734 ft (0.223 m)

mass = 5.278 slugs (77.021 kg)

Joint lumped mass = 1 slug (14.592 kg)

Payload

mass = 15.54 slugs (226.76 kg)

$J_{c.g.}$ = 12.62 slug-ft$^2$ ( 21.37 kg-m$^2$)

diameter = 1.0 ft (0.304 m)

Figure 2.6 - Characteristics of system used for comparison with transfer-matrix method

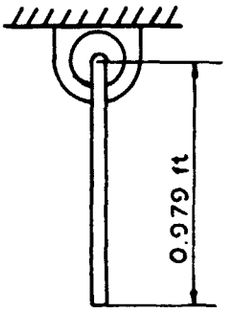


Torque motor rotor inertia: $3.98 \times 10^{-4}$ (lbf-ft-sec$^2$)
($5.75 \times 10^{-4}$ mt-m-sec$^2$)

diameter = 0.25 in (0.0635 m)

material: carbon steel

a) laboratory experiment

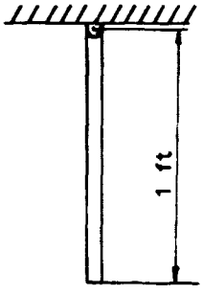


material: carbon steel

diameter = 0.01 ft (0.00304m)

b) analytical example

Figure 2.7 - Characteristics of a single pinned-free beam for model verification

| Experiment | Model | Error (%) |
|---|---|---|
| 80.76 | 79.34 | 1.7 |
| 136.6 | 130.68 | 4.3 |
| 244.6 | 282.56 | 15.5 |
| 401.6<br>417.0 | 487.56 | 21.4<br>16.9 |

Table 2.2 Flexible Resonant Frequencies and Relative Error

| Model | Transfer-Matrix |
|---|---|
| 39.7 | 38.1 |
| 57.9 | 53.2 |
| 144.5 | 143.6 |
| 189.1 | 279.5 |

unit: rd/sec

Table 2.3 Comparison between the proposed model and transfer-matrix procedure

Analytical

| Model | Exact | Error |
|---|---|---|
| 313.2 | 308.3 | 1.5% |
| 1016.16 | 1191.58 | 17.2% |

Experimental

| Model | Lab. Exper. | Error |
|---|---|---|
| 615.7 | 606.46 | 1.5% |
| 2513.3 | 2112.16 | 15.9% |

units: rd/sec

Table 2.4 Analytical and Experimental Results from a Single Pinned-Free Beam

able at M.I.T. Joint Civil-Mechanical Engineering Computer Facility. The general programs are listed in Appendix A. As the storage capacity of the computer used was small compared with the size of the program, the operations were performed utilizing disk storage.

# CHAPTER III

# CONTROL TECHNIQUES

## 3.1 Introduction

This chapter gives a general description of the techniques that were applied to the analysis of controlling flexible manipulators. These techniques, with one exception, were applied to the models presented in Chapter IV and the results are discussed in the next chapter. In order to introduce these control procedures one can start with equation (2.36) which represents the nonlinear model of the physical system

$$\dot{\tau} = \underline{A}' \, \underline{\tau} + \underline{F}' + \underline{C}' \, \underline{u} \qquad (2.36)$$

The objective is to find a control law $\underline{u}(\underline{\tau},\dot{\underline{\tau}},t)$ such that the system response follows the desired specifications. This task is complicated by the presence of the nonlinear terms in the system representation.

Even in the case for which the control law can be exactly specified, it would in principle be useful only in very specific cases. To avoid this type of design of the control one can always design the compensation for the linearized model and verify how good the approach is when applied to the nonlinear system.

From the linearized equations of motion

$$\dot{\underline{x}} = \underline{A} \, \underline{x} + \underline{B} \, \underline{u} \qquad (2.38)$$

the structure of a linear regulator can be represented as in the block diagram of Figure 3.1

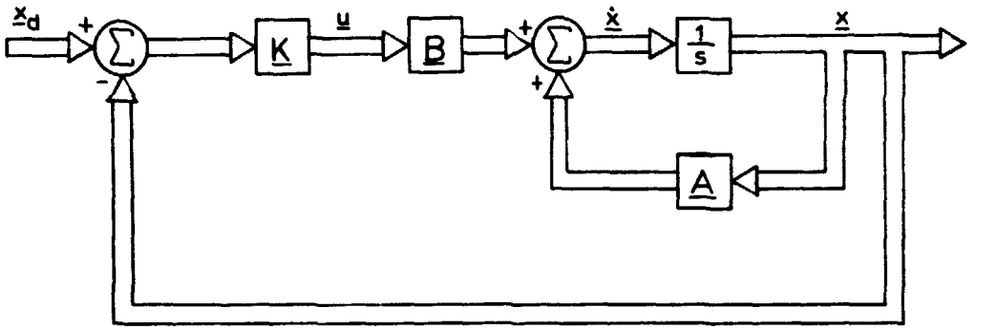


Figure 3.1 Block Diagram of the Compensated System.

where the control has been replaced by the linear equation

$$\underline{u} = \underline{K}\,\underline{x} \tag{3.1}$$

and $\underline{x}_D$ is the desired trajectory.

The purpose of this chapter is to present several techniques that were used to compute the set of gains $\underline{K}$ for different feedback alternatives.

## 3.2 Modal Analysis

It is well known that in the case of linear time invariant systems described by state equations of the form

$$\dot{\underline{x}} = \underline{A}\,\underline{x} + \underline{B}\,\underline{u} \tag{3.2}$$

where $\underline{A}$ and $\underline{B}$ are (n x n) and (n x r) matrices respectively, a model representation can be obtained by using a nonsingular transformation of state [C3], [S1].

$$\underline{x} = \underline{U}\,\underline{z} \tag{3.3}$$

In the case of distinct eigenvalues of matrix $\underline{A}$, matrix $\underline{U}$ is the modal matrix of $\underline{A}$ and its columns are the eigenvectors of $\underline{A}$ [G1] [C3].

Then equation (3.1) becomes

$$\dot{\underline{Z}} = \underline{\Delta}\,\underline{Z} + \underline{P}^T\,\underline{u} \tag{3.4.1}$$

where $\underline{\Delta}$ is the diagonal matrix of the eigenvalues of $\underline{A}$

$$\underline{\Delta} = \begin{bmatrix} \lambda_1 & & & \\ & \lambda_2 & & \mathbf{0} \\ & & \ddots & \\ \mathbf{0} & & & \lambda_n \end{bmatrix} \tag{3.4.2}$$

and

$$\underline{P}^T = \underline{U}^{-1}\underline{B} = \underline{V}^T\,\underline{B} \tag{3.4.3}$$

is the mode controllability matrix with

$$\underline{U}\,\underline{V}^T = \underline{I} \tag{3.4.4}$$

where $\underline{I}$ is the identity matrix.

It is clear from equations (3.4) that the transformation (3.3) uncouples the n-th order system into n uncoupled subsystems. Also it is evident from equations (3.4) that the ith mode of the uncoupled system is controllable by the jth control input if and only if

$$P_{ij} = \underline{v}_i^T \underline{b}_j \neq 0 \qquad (3.5)$$

The controllability of the system is immediately verified by examining the components of the mode controllability matrix $\underline{P}^T$.

Equations (3.3) represent an uncoupled system giving rise to one important question: is it possible to find a control law $\underline{u}$ such that the eigenvalues can be specified a priori? The answer to this question was initially given by Rosenbrock [R1] and his presentation of modal control. Several extensions and improvements have been made since then [E1], [P1], [P2] and a very useful algorithm was presented in the work of Simon and Mitter [S1], [S2] for the case of distinct eigenvalues. A more recent work by Gould, Murphy and Berkman [G3] extends this algorithm for repeated eigenvalues. The constraints in the number of inputs in the present work make the Simon-Mitter algorithm the most suitable for applications. For this reason a brief presentation of this method will follow in a simplified way as it was applied. A rigorous and general formulation can be found in reference [S2].

## 3.3 Simon-Mitter Algorithm (SMA)

This algorithm is capable of shifting all the eigenvalues to desired

location with only one application. However, this procedure may cause numerical difficulties in the solution of a large number of ill-conditioned equations. On the other hand, the shifting technique is recursive, that is, a small number of poles can be shifted in each application of the algorithm and this procedure may be applied as many times as is necessary. If a number p of poles is to be shifted the solution involves an inversion of a (p x p) matrix. For this reason a recursive design shifting two poles each time was used, which means that the procedure would involve a small amount of computer core for each change of poles. When two poles are moved, the gains to form the control law $\underline{u}$ are such that two poles go to a new specified position while all the others remain fixed. If a new pair of poles is modified, the gains are all added to the old ones in order to maintain the former shifting of poles. This procedure has a disadvantage with respect to numerical errors accumulation but it is useful when few poles have to be shifted. Again, the only restriction is that the system has no repeated poles.

In order to illustrate the two pole shift procedure one can recall the canonical form (3.4.1)

$$\dot{\underline{Z}} = \underline{\Delta}\,\underline{Z} + \underline{P}^T\,\underline{u} \qquad (3.4.1)$$

The question is to find a linear state variable feedback law

$$\underline{u} = \underline{G}\,\underline{z} = \underline{K}\,x \qquad (\underline{K} = \underline{G}\,\underline{V}^T) \qquad (3.6)$$

which moves the two selected poles to specified location while the other poles remain constant. If one chooses to change the poles $\lambda_1$ and $\lambda_2$ to $\gamma_1$ and $\gamma_2$ and assume that the system has r inputs the feedback law becomes

$$\underline{u} = \underline{g}_1 \underline{Z}_1 + \underline{g}_2 Z_2 = \begin{bmatrix} g_{11} \\ g_{21} \\ \vdots \\ g_{r1} \end{bmatrix} \underline{v}_1^T \underline{x} + \begin{bmatrix} g_{12} \\ g_{22} \\ \vdots \\ g_{r2} \end{bmatrix} \underline{v}_2^T \underline{x} \qquad (3.7)$$

Substitution of (3.6) into (3.4.1) yields the new system

$$\dot{\underline{z}} = \bar{\underline{\Delta}} \underline{z} \qquad (3.8.1)$$

where

$$\bar{\underline{\Delta}} = \underline{\Delta} + \underline{P}^T \underline{G} \qquad (3.8.2)$$

$$\bar{\underline{\Delta}} = \begin{bmatrix} \lambda_1 + \delta'_{11} & \delta'_{12} & & & \\ \delta'_{21} & \lambda_2 + \delta'_{22} & & \underline{0} & \\ \hline \delta'_{31} & \delta'_{32} & \lambda_3 & & \underline{0} \\ \vdots & \vdots & & \lambda_4 & \\ \delta'_{i1} & \delta'_{n2} & \underline{0} & & \lambda_n \end{bmatrix} \qquad (3.9.1)$$

where

$$\delta'_{ik} = \underline{p}_i^T \underline{g}_k \qquad \text{for } i = 1,\ldots,n \quad k = 1,\ldots,r \qquad (3.9.2)$$

To determine the new eigenvalues it is sufficient [S1] to examine the eigenvalues of

$$\bar{\underline{\Delta}}_{11} = \begin{bmatrix} \lambda_1 + \delta'_{11} & \delta'_{12} \\ \delta'_{21} & \lambda_2 + \delta'_{22} \end{bmatrix} \qquad (3.10.1)$$

In fact, from the mode decomposition property (Appendix B)

$$\det(s\underline{I} - \bar{\underline{\Delta}}) = \prod_{j=3}^{n} (s - \lambda_j) \cdot \det(s\underline{I} - \bar{\underline{\Delta}}_{11}) \qquad (3.10.2)$$

If now the new pair of eigenvalues is $\gamma_1$ and $\gamma_2$ it is sufficient to equate the coefficients of like powers of the identity

$$(s - \gamma_1)(s - \gamma_2) = \det[s\underline{I} - \bar{\underline{\Delta}}_{11}] \qquad (3.11)$$

and consequently find the conditions that must be satisfied by $\underline{g}_1$ and $\underline{g}_2$. However, $\underline{g}_1$and $\underline{g}_2$ are vectors whose dimension depends upon the number of inputs to the system. If the system has a single input it is clear that (3.10) will give a unique solution for the control law $\underline{u}$. On the other hand, if $r \neq 1$ there exist an infinite number of components for $\underline{g}_1$ and $\underline{g}_2$ that satisfy (3.10). Several alternatives exist to produce a unique sol-

ution for the control. Among these techniques are those based on power requirements of the system, sensitivities, proportionality between control elements, etc. For the purpose of this application the criterion used is the fixed ratio of feedback gains, that is, the vectors $g_1$ and $g_2$ were replaced by $\eta_1 g_0$ and $\eta_2 g_0$ respectively. The vector $g_0$ is usually chosen on the sense of satisfying some desired condition. In particular, the selection of the elements of $g_0$ by the rule [S1]

$$g_{i0} = \text{sign}\,(p_{i1}) \qquad i = 1,\ldots,r \tag{3.12}$$

maximizes the measure of controllability and hence requires the least absolute value of feedback gains. This rule was used throughout the applications. Since $g_0$ is specified the algorithm gives a unique solution for a shift of a pair of poles. This solution can be presented for two cases: pair of real poles and a complex conjugate pair. In particular, the numerical implementation becomes easier when these two cases are taken into account.

### 3.3.1 Real Pair of Poles $\lambda_1$ and $\lambda_2$ ($\lambda_1 \neq \lambda_2$)

In this case, (3.11) yields

$$\begin{bmatrix} \eta_1 \\ \eta_2 \end{bmatrix} = \begin{bmatrix} \alpha_{10} & \alpha_{20} \\ \lambda_2\alpha_{10} & \lambda_1\alpha_{20} \end{bmatrix}^{-1} \cdot \begin{bmatrix} \varepsilon_1 \\ \varepsilon_2 \end{bmatrix} \tag{3.13.1}$$

where

$$\epsilon_1 = \gamma_1 + \gamma_2 - \lambda_1 - \lambda_2 \tag{3.13.2}$$

$$\epsilon_2 = \gamma_1 \gamma_2 - \lambda_1\lambda_2 \tag{3.13.3}$$

$$\alpha_{ko} = \underline{p}_k^T \underline{g}_o \qquad k = 1,\ldots,n \tag{3.13.4}$$

and the control law

$$\underline{u} = \underline{g}_o [\eta_1 \underline{v}_1 + \eta_2 \underline{v}_2]^T \underline{x} \tag{3.13.5}$$

3.3.2 Complex Conjugated Poles

For this case, in order to assure that $\underline{u}$ is real let

$$\lambda_1 = \lambda_1' + j\lambda_1'' \tag{3.14.1}$$

$$\lambda_2 = \lambda_1^* = \lambda_1' - j\lambda_1'' \tag{3.14.2}$$

and from the mode controllability matrix let

$$\underline{p}_1 = \underline{p}_1' + j\underline{p}_1'' \tag{3.14.3}$$

$$\underline{p}_2 = \underline{p}_1^* = \underline{p}_1' - j\,\underline{p}_1'' \tag{3.14.4}$$

$$\underline{v}_1 = \underline{v}_1' + j\,\underline{v}_1'' \tag{3.14.5}$$

$$\underline{v}_2 = \underline{v}_1^* = \underline{v}_1' - j\underline{v}_1'' \tag{3.14.6}$$

Then, the solution of

$$\begin{bmatrix} \eta' \\ \eta'' \end{bmatrix} = \begin{bmatrix} \underline{P}_1^T \cdot \underline{g}_0 & -\underline{P}_1^T \cdot \underline{g}_0 \\ \underline{P}_1^T \cdot \underline{g}_0 & \underline{P}_1^T \cdot \underline{g}_0 \end{bmatrix}^{-1} \cdot \begin{bmatrix} \epsilon_{1/2} \\ (\epsilon_2 - \lambda_1' \epsilon_1)/2\lambda_1'' \end{bmatrix} \tag{3.14.7}$$

leads to the control law

$$\underline{u} = 2\underline{g}_0[\eta' \underline{v}_1' - \eta'' v_1'']^T \underline{x} \tag{3.15}$$

The transformation of a real pair of poles into a complex pair and vice versa can be easily obtained by successive numerical applications. Appendix A presents the computer program used for the applications of modal control using this algorithm in a recursive way.

## 3.4 General Rigid Gains - Cross Joint Feedback (GRG)

The preceding algorithm when applied to system (2.38) can move any pole to the desired position. However, the control law $\underline{u}$ used for this pole shifting will involve the measurements and/or estimation of all state variables associated with the physical system. Although the possibility of using measurements of all of the variables is not impossible, another technique was used in order to compare the results Essentially,

this other procedure is to compute the gains ror the control of a two link rigid manipulator and apply them to the flexible model. The control for the rigid system would use only position and velocity feedback gains involving the joint state variables. Several methods exist to compute this kind of gains butone particular procedure suggested by Professor D.E. Whitney [W1] seems appealing because of its similarity to a modal approach. A brief description of this method is presented below.

Cons der a pure rigid two link system with no damping and no joint compliance represented by the equations

$$\underline{J}\,\ddot{\underline{\Omega}} = \underline{\tau} \tag{3.16}$$

where $\underline{J}$ is the (2x2) inertia matrix of the system, $\underline{\tau}$ is the (2x1) vector of control torques and $\underline{\Omega}$ is a vector with components $\Omega_1$ and $\Omega_2$, shoulder and elbow angles in the rigid system respectively. In terms of state variables (3.16) can be written

$$\begin{bmatrix} \dot{\underline{\Omega}} \\ \ddot{\underline{\Omega}} \end{bmatrix} = \begin{bmatrix} \underline{0} & \underline{I} \\ \underline{0} & \underline{0} \end{bmatrix} \begin{bmatrix} \underline{\Omega} \\ \dot{\underline{\Omega}} \end{bmatrix} + \begin{bmatrix} \underline{0} \\ \underline{J}^{-1} \end{bmatrix} \underline{\tau} \tag{3.17}$$

where $\underline{I}$ is the identity matrix.

The torques are obtained via a control law

$$\underline{\tau} = \underline{B}\,\underline{u} \tag{3.18}$$

with $\underline{B}$ a (2x2) matrix and

$$\underline{u} = \underline{k_T}\underline{\Omega} + \underline{k_{TD}}\dot{\underline{\Omega}} \tag{3.19}$$

where $\underline{k}_T$ is a (2x2) angular position feedback matrix and $\underline{K}_{TD}$ is a (2x2) angular velocity feedback matrix. The elements of $\underline{K}_T$ and $\underline{K}_{TD}$ can be obtained for some desired specifications with respect to the position of the poles in the complex plane. The system (3.16) with (3.17) and (3.18) becomes

$$\begin{bmatrix} \dot{\underline{\Omega}} \\ \ddot{\underline{\Omega}} \end{bmatrix} = \begin{bmatrix} \underline{0} & \underline{I} \\ \underline{J}^{-1}\underline{B}\underline{k}_r & \underline{J}^{-1}\underline{B}\underline{k}_{TD} \end{bmatrix} \begin{bmatrix} \underline{\Omega} \\ \dot{\underline{\Omega}} \end{bmatrix} \qquad (3.20)$$

If now $\underline{k}_T$ and $\underline{k}_{TD}$ are chosen so that (*)

$$\underline{J}^{-1}\underline{B}\underline{K}_T = \begin{bmatrix} -w_1^2 & 0 \\ 0 & -w_2^2 \end{bmatrix} \qquad (3.21.1)$$

$$\underline{J}^{-1}\underline{B}\underline{K}_{TD} = \begin{bmatrix} -2\zeta_1 w_1 & 0 \\ 0 & -2\zeta_2 w_2 \end{bmatrix} \qquad (3.21.2)$$

it is clear that the system (3.16) will become a set of two uncoupled differential equations with natural frequencies $w_1$ and $w_2$ and damping ratios $\zeta_1$ and $\zeta_2$ respectively. This choice of $\underline{K}_T$ and $\underline{K}_{TD}$ is not unique but it is convenient because it allows one to place the poles by inspection. Then, this procedure enables one to specify the desired characteristic of the system and as a consequence find the corresponding angular position and velocity feedbacks.

Since for a real system the inertia matrix is always non-singular,

(*) w and $\omega$ are used interchangebly to represent angular frequency

the only restriction to the technique is that the control matrix $\underline{B}$ is non-singular. This fact makes impossible the application of this procedure to the flexible model itself but some variations of the control derived from a corresponding rigid model can be applied to the flexible system. Also it is important to notice that the matrices $\underline{K}_T$ and $\underline{K}_{TD}$ are not necessarily diagonal which means that the control can take into account feedback between the joints. Finally this procedure can be applied to a rigid arm with any number of joints. A trivial generalization allows the procedure to be applied to any controllable and observable lumped passive dynamic system although an observer may be needed.

## 3.5 Rigid Gains - No Cross Joint Feedback

This case is a particular way to find the $\underline{K}_T$ and $\underline{K}_{TD}$ matrices in the preceding method. As was mentioned before, the effect of cross joint feedback disappears when $\underline{K}_T$ and $\underline{K}_{TD}$ are chosen diagonal matrices. Using this procedure W.J. Book [B2] achieved interesting results for the design of control for flexible manipulators. This method was not applied in the present work except as a means of comparison of different control techniques.

## 3.6 Sensitivity Analysis

Another procedure used to find the components of the control law $\underline{u}$ deals with the sensitivities of the poles with respect to variations in the gains. If one assumes only angular position and velocity feedbacks, the number of control elements would be considerably reduced and by inspection the gains could be changed based on their corresponding sensi-

tivities.

Consider the system represented by

$$\dot{\underline{x}} = \underline{A}\,\underline{x} + \underline{B}\,\underline{u} \tag{2.37}$$

and assume that

$$\underline{u} = \underline{K}\,\underline{x} \tag{3.22}$$

where $\underline{A}$ is (nxn) matrix, $\underline{B}$ is (nxr) control matrix and $\underline{K}$ is (rxn) gain matrix. For example, equation (2.38) could represent the linearized model of a flexible manipulator. The eigenvector $\underline{u}_j$ associated with the jth eigenvalue $\lambda_j$ is defined by the equation

$$\underline{A}\,\underline{u}_j = \lambda_j \underline{u}_j \tag{3.23}$$

If $\underline{v}_j$ is the corresponding element in the reciprocal basis, from the orthogonality of the modes

$$\underline{v}_i^T \underline{u}_j = \delta_{ij} \begin{cases} \delta_{ij} = 0 \text{ for } i \neq j \\ \delta_{ij} = 1 \text{ for } i = j \end{cases} \tag{3.24}$$

From (3.23) and (3.24)

$$\underline{v}_j^T \underline{A}\,\underline{u}_j = \lambda_j \tag{3.25.1}$$

It is easy to verify that the only left hand side term involving the element $a_{ik}$

$$\ldots + v_{ji} a_{ik} u_{kj} + \ldots = \lambda_j \tag{3.25.2}$$

Then, from (3.24) and (3.25) the sensitivity of the eigenvalue $\lambda_j$ with respect to variations in the element $a_{ik}$ of the $\underline{A}$ matrix is given by [V1]

$$\frac{\delta \lambda_j}{\delta a_{ik}} = v_{ji} u_{kj} \tag{3.26}$$

If now the control law (3.22) is taken into account, equation (2.38) re-decues to

$$\dot{\underline{x}} = \bar{\underline{A}}\, \underline{x} \tag{3.27.1}$$

where

$$\bar{\underline{A}} = \underline{A} + \underline{B}\, \underline{K} \tag{3.27.2}$$

with components

$$\bar{a}_{ij} = a_{ij} + \sum_{k=1}^{r} b_{ik} g_{kj} \tag{3.27.3}$$

Now, the sensitivity of a pole $\lambda_\alpha$ with respect to gain $g_{kj}$ is

$$\frac{\partial \lambda_\alpha}{\partial g_{kj}} = \sum_{i=1}^{n} \sum_{k=1}^{r} \frac{\partial \lambda_\alpha}{\partial \bar{a}_{ij}} \cdot \frac{\partial \bar{a}_{ij}}{\partial g_{kj}} = \sum_{i=1}^{n} \frac{\partial \lambda_\alpha}{\partial \bar{a}_{ij}} \left( \sum_{k=1}^{r} \frac{\partial \bar{a}_{ij}}{\partial g_{kj}} \right) \quad (3.28)$$

But

$$\frac{\partial \bar{a}_{ij}}{\partial g_{kj}} = b_{ik} \quad (3.29)$$

Then it follows from (3.28) and (3.29) that

$$\frac{\partial \lambda_\alpha}{\partial g_{kj}} = \sum_{i=1}^{n} \frac{\partial \lambda_\alpha}{\partial \bar{a}_{ij}} b_{ik} \quad (3.30)$$

From (3.30) and (3.26) one can see that if the eigenvectors corresponding to a certain configuration are known, it is possible to analyze the effects of local pole variations for each component of the gain matrix. This procedure will be explained numerically in the next chapter.

## 3.7 Summary

This chapter presented a brief description of the control techniques used in this work. The next chapter presents the application of these techniques to some nondimensionalized examples and general results obtained.

# CHAPTER IV

# APPLICATIONS AND RESULTS

## 4.1 Introduction

The purpose of this chapter is to introduce the example systems used in the applications of the mathematical techniques and the general results obtained from the several control methods. Two examples have been chosen, both with circular ring cross sections. The first one (example 1) is a very long and flexible beam of two equal segments carrying a payload that might vary in size and weight. The overall dimensions are shown in Figure 4.1 and were obtained from reference [N1].

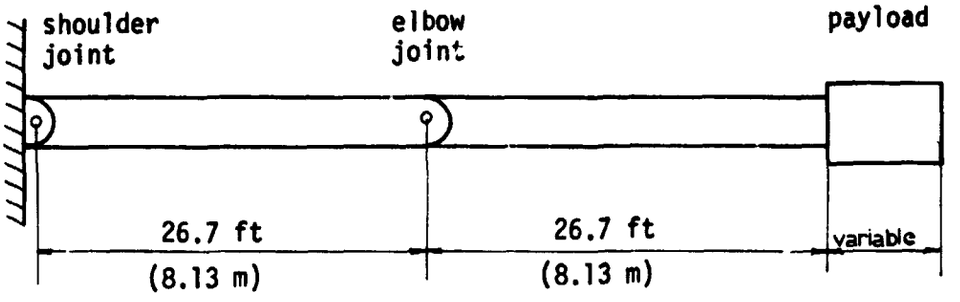


Beams: external diameter = 0.75 ft (0.228 m)
internal diameter = 0.734 ft (0.223 m)
material: Aluminum
$E = 10^7$ psi ($7.0 \times 10^{10}$ Pa)

Figure 4.1 Example 1 Characteristics

The second example (example 2) is a more rigid system with fixed payload. The most important difference is that the beams have different radii and were chosen such that the stiffness EI for the first beam is approximately equal to six times the value for the second beam. The main geometric characteristics are presented in Figure 4.2 and were obtained from reference [R2].

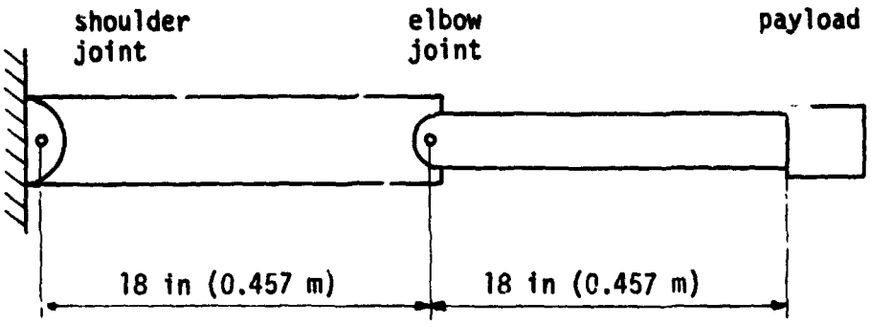


Beam 1: external diameter = 3.74 in (0.095 m)
internal diameter = 3.15 in (0.080 m)

Beam 2: external diameter = 2.36 in (0.060 m)
internal diameter = 2.00 in (0.051 m)

Material: Aluminum E = $10^7$ psi ($7.0 \times 10^{10}$ Pa)

Joint lumped mass = 0.932 slugs (13.6 kg)

Assumed payload:

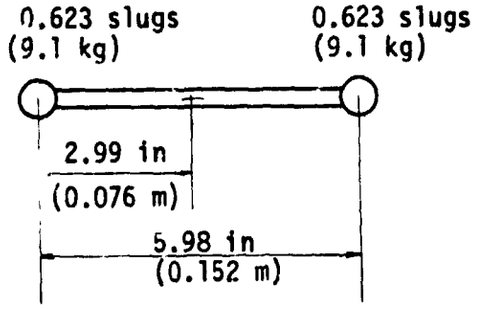


Figure 4.2 Example 2 Characteristics

With respect to all the applications of the described models, the motions were assumed to be in the plane of the beams, no structural damping was considered and gravity was neglected. However, the computer programs presented in Appendix A can accommodate damping and gravity.

## 4.2 Nondimensionalization

In order to have a better idea about the effect of the system parameters and also to obtain more general results, a system nondimensionalization was performed using the quantities given in Table 4.1.

| Physical Quantity | Symbol | Dimension |
|---|---|---|
| Stiffness constant of beam 1 | $EI_1$ | $FL^2$ |
| Total length | $l$ | $L$ |
| Average Mass/unit length | $\mu$ | $FL^{-2}T^2$ |

Table 4.1 Parameters for Nondimensionalization

where

$$l = l_1 + l_2 \tag{4.1.1}$$

$$\mu = \frac{\mu_1 l_1 + \mu_2 l_2}{l} \tag{4.1.2}$$

Two important quantities can be derived from Table 4.1

- time $$T_d = \sqrt{\frac{\mu l^3}{EI_1}} \tag{4.2.1}$$

-frequency $$w_d = \sqrt{\frac{EI_1}{\mu l^3}} \qquad (4.2.2)$$

It is important to observe that frequency $w_d$ has no associated physical system but can be easily related to any system natural frequency. For example, if one considers a beam with stiffness $EI_1$, length $l$ and density per unit length $\mu$, the clamped-free natural frequency is given by

$$w_c = 3.52 \sqrt{\frac{EI_1}{\mu l^3}} \qquad (4.3)$$

Then it follows that the relationship between frequencies $w_d$ and $w_c$ is simply given by

$$w_c = 3.52\, w_d \qquad (4.4)$$

Any results with respect to $w_d$ can then be extended to compare with $w_c$. If now one introduces:

- ratio of the radii of beam 1

$$k_{r1} = \frac{r_{i1}}{r_{e1}} \qquad (4.5)$$

- ratio of the radii of beam 2

$$k_{r2} = \frac{r_{i2}}{r_{e2}} \qquad (4.6)$$

it is possible to establish a constraint among the stiffness constant, the radius and the density of the beams. In fact, if one assumes the ratio of the radii for each beam and also the nondimensionalized stiffness constant of beam 2, the following relationships are useful for the

nondimensionalization of the remaining parameters.

In fact, if

$$\bar{EI}_2 = \frac{EI_2}{EI_1} = \left(\frac{r_{e2}}{r_{e1}}\right)^4 \frac{(1-k_{r2}^4)}{(1-k_{r1}^4)} \tag{4.7.1}$$

then

$$\left(\frac{r_{e2}}{r_{e1}}\right)^2 = \sqrt{\bar{EI}_2 \frac{(1-k_{r1}^4)}{(1-k_{r2}^4)}} \tag{4.7.2}$$

Also, from (4.1.1)

$$\mu = \frac{\mu_1 l_1 + \mu_2 l_2}{l} = \mu_1 \bar{l}_1 + \mu_2 \bar{l}_2 \tag{4.8.1}$$

or

$$\bar{\mu}_1 \bar{l}_1 + \bar{\mu}_2 \bar{l}_2 = 1 \tag{4.8.2}$$

On the other hand, for cylindrical be..

$$\mu = \rho\pi[\bar{l}_1 r_{e1}^2(1-k_{r1}^2) + \bar{l}_2 r_{e2}^2(1-k_{r2}^2)] \tag{4.9}$$

and

$$\bar{\mu}_1 = \frac{\mu_1}{\mu_2} = \frac{\rho\pi r_{e1}^2(1-k_{r1}^2)}{\rho\pi[\bar{l}_1 r_{e1}^2(1-k_{r1}^2) + \bar{l}_2 r_{e2}^2(1-k_{r2}^2)]} \tag{4.10}$$

or, using (4.7) into (4.10)

$$\bar{\mu}_1 = \frac{1}{\bar{l}_1 + \bar{l}_2 \sqrt{\overline{EI}_2 \dfrac{(1 + k_{r1}^2)(1 - k_{r2}^2)}{(1 + k_{r2}^2)(1 - k_{r1}^2)}}} \tag{4.11}$$

and from (4.6)

$$\bar{\mu}_2 = \frac{1 - \bar{\mu}_1 \bar{l}_1}{\bar{l}_2} \tag{4.12}$$

Then, assuming the value of $\overline{EI}_2$, the ratio $k_{r1}$ and $k_{r2}$, the lengths $\bar{l}_1$ and $\bar{l}_2$ and one of the external radii, expressions (4.7), (4.11) and (4.12) define the other characteristics of the system.

Using $EI_1$, $\mu$ and $l$ the nondimensionalized groups are shown in Table 4.2.

| Nondimensionalized Quantity | Equations |
|---|---|
| stiffness constant of beam 1 | $\bar{EI}_1 = EI_1/EI_1$ |
| stiffness constant of beam 2 | $\bar{EI}_2 = EI_2/EI_1$ |
| length of beam 1 | $\bar{l}_1 = l_1/l$ |
| length of beam 2 | $\bar{l}_2 = l_2/l$ |
| length of payload | $\bar{l}_p = l_p/l$ |
| internal diameter of beam 1 | $\bar{d}_{i1} = d_{i1}/l$ |
| internal diameter of beam 2 | $\bar{d}_{i2} = d_{i2}/l$ |
| external diameter of beam 1 | $\bar{d}_{e1} = d_{e1}/l$ |
| external diameter of beam 2 | $\bar{d}_{e2} = d_{e2}/l$ |
| density per unity length: beam 1 | $\bar{\mu}_1 = \mu_1/\mu$ |
| density per unity length: beam 2 | $\bar{\mu}_2 = \mu_2/\mu$ |
| payload mass | $\bar{m}_p = m_p/\mu l$ |
| elbow joint lumped mass | $\bar{m}_j = m_j/\mu l$ |
| mass moment of inertia | $\bar{J} = J/\mu l^3$ |
| time | $\bar{T} = t/T_d$ |
| frequency | $\bar{w} = w/w_d$ |
| angular position feedback gain | $\bar{k}_{ap} = k_{ap}/(EI_1/l)$ |
| linear position feedback gain | $\bar{k}_{1p} = k_{1p}/EI_1/l^2)$ |
| angular velocity feedback gain | $\bar{k}_{av} = k_{av}/(EI_1/w_d l)$ |
| linear velocity feedback gain | $\bar{k}_{1v} = k_{1v}(EI_1/w_d l^2)$ |

Table 4.2 Nondimensionalized groups

## 4.3 The Control Application and Arm Bandwidth Definitions

In order to apply the control techniques described in Chapter III it is helpful to know some details of the gain matrix $\underline{K}$ that appears in equation (3.1). The model described in Chapter II was assumed to have two inputs, namely the torques $\tau_1$ and $\tau_2$ applied at shoulder and elbow joints, respectively. As the model is described by 12 state variables, $\underline{K}$ is a (2x12) matrix. The general form of this matrix is

$$\underline{K} = \begin{bmatrix} k_{11} & k_{12} & k_{13} & k_{14} & k_{15} & k_{16} & k_{17} & k_{18} & k_{19} & k_{110} & k_{111} & k_{112} \\ k_{21} & k_{22} & k_{23} & k_{24} & k_{25} & k_{26} & k_{27} & k_{28} & k_{29} & k_{210} & k_{211} & k_{212} \end{bmatrix} \tag{4.13}$$

where

$k_{11}$, $k_{12}$, $k_{21}$, $k_{22}$ are angular position feedback gains; $k_{13}$, $k_{14}$, $k_{15}$, $k_{16}$, $k_{17}$, $k_{23}$, $k_{24}$, $k_{25}$, $k_{26}$, $k_{27}$ are linear position feedback gains; $k_{17}$, $k_{18}$, $k_{27}$, $k_{28}$ are angular velocity feedback gains; $k_{19}$, $k_{110}$, $k_{111}$, $k_{112}$, $k_{29}$, $k_{210}$, $k_{211}$, $k_{212}$ are linear velocity feedback gains.

It is obvious that the linear feedbacks will necessarily require measurements and/or estimation of flexible displacements and velocities while the angular feedbacks are based essentially on the measurements of angles. This is an important fact in comparing the results from the application of general rigid gains design method and Simon-Mitter algorithm. Modal control will involve the set of 24 gains while in the

other case 8 at most are necessary. In the special case where no cross joint feedback is taken into account, only four gains are used [B2]. Due to the large number of gains, the analysis via a root locus for gains variations is impractical.

The remaining parts of this work will frequently mention arm bandwidth when comparisons or simulations are presented. There is a certain arbitrariness in defining the bandwidth of a manipulator arm. For this reason this work defines arm bandwidth as the maximum undamped frequency for which the two first dominant poles are as close as possible to 0.707 damping ratio. The following results are concerned with the arm bandwidth obtained by using the control techniques presented in the previous chapter.

## 4.4 General Rigid Gains Method Applications

For the implementation of this method one nondimensionalized example was chosen with the following parameters:

| | |
|---|---|
| $k_{r1} = k_{r2} = 0.9$ | $\bar{J}_p = 0.0$ |
| $\bar{EI}_1 = 1.$ | $\bar{l}_p = 0.0$ |
| $\bar{EI}_2 = 1.0$ | $\bar{l}_1 = 0.5$ |
| $\bar{\mu}_1 = 1.0$ | $\bar{l}_2 = 0.5$ |
| $\bar{\mu}_2 = 1.0$ | $\bar{r}_{e1} = 0.05$ |
| $\bar{m}_p = 0.0$ | $\bar{r}_{e2} = 0.05$ |
| $\bar{m}_j = 0.0$ | $\theta_1 = 0°$ |
| | $\theta_2 = 0°$ |

Tabe 4.3 Nondimensionalized Parameters of Example 3

Similar tables for examples 1 and 2 can be found in Appendix C.

In order to obtain some results using this method one has to use an equivalent rigid model that in the case of present work is represented by a double pendulum with inputs at both pinned joints. It is evident that only angular position and velocity feedback gains will be present in such a model. If equations (3.2.1) are recalled, one will notice that to find the matrices $\underline{K}_T$ and $\underline{K}_{TD}$, it is necessary to specify four parameters of the desired system, namely, $w_1$, $w_2$, $\zeta_1$, $\zeta_2$. Once these values are specified, one can obtain $\underline{K}_T$ and $\underline{K}_{TD}$ such that the poles of the closed loop system will be exactly at the desired location. These gains can now replace the angular position and velocity feedbacks on the gain matrix (4.13), corresponding to the flexible case. In this way it is possible to analyze how effective the method is for several variations in the parameters. The following steps represent the application procedure:

a) choose the desired values of the first two dominant modes, that is, $w_1$, $w_2$, $\zeta_1$, $\zeta_2$;

b) using (3.21) applied to the rigid equivalent model obtain the gain matrices $\underline{K}_T$, $\underline{K}_{TD}$;

c) construct the gain matrix $\underline{K}$ expression (4.13) using $\underline{K}_T$ and $\underline{K}_{TD}$;

d) examine the closed-loop poles of the flexible system.

The limiting range of this method will be determined by the deviation of the dominant poles of the flexible model from the desired specifications.

This sequence was applied to the example of Table 4.3 with the frequencies nondimensionalized by (4.2) and the assumption

$$\bar{w}_1 = \bar{w}_2 = \bar{w} \tag{4.14a}$$

$$\zeta_1 = \zeta_2 = \zeta \tag{4.14b}$$

where

$$\bar{w} = w/w_d$$

It is important to mention that assumption (4.14) was used because it yields symmetric matrices $\underline{K}_T$ and $\underline{K}_{TD}$. This fact will make the control of the flexible model analogous to spring and dashpots actuating among the joints and consequently assuring stability for the system. Some results were obtained for $w_1 \neq w_2$ as can be seen in Figure 4.3 However to assure stability (4.14) assumption was used throughout the work with damping ratio $\zeta = 0.7$ as a constant parameter.

For this damping ratio $\zeta$ the frequency $\bar{w}$ was specified and gains $\underline{\bar{K}}_T$ and $\underline{\bar{K}}_{TD}$ were obtained via the rigid model; these gains when applied to the flexible model returned a pair of dominant poles which were plotted as a root-locus of the first two dominant flexible poles. The locus is shown in Figure 4.4 for damping ratios of 0.5, 0.7 and 0.8. A reasonable understanding of the results can be obtained by plotting both poles on the same graph. One can see that for $\bar{w} = 1.0$ the resulting behavior of the flexible system is essentially the same as the rigid one; the dominant poles are close together with damping ratio 0.7. As the value of $\bar{w}$ is increased, the poles of the flexible system start separating and for $\bar{w}$ over 3.0 there is a shift with respect to the distance to origin

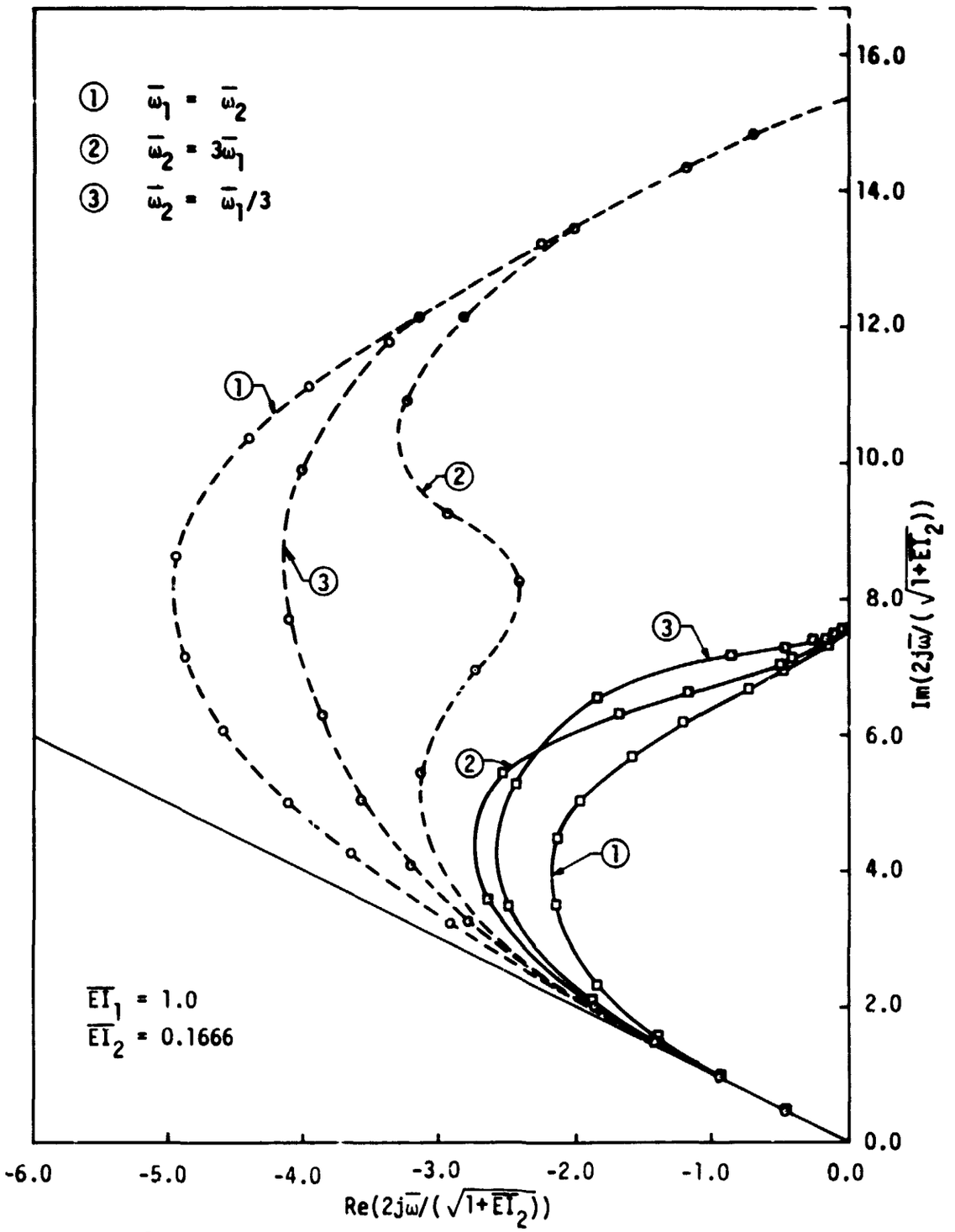


Figure 4.3 - Root loci of dominant poles - GRG Control for constant damping ratio $\zeta = 0.7$ and $\bar{\omega}_1 \neq \bar{\omega}_2$

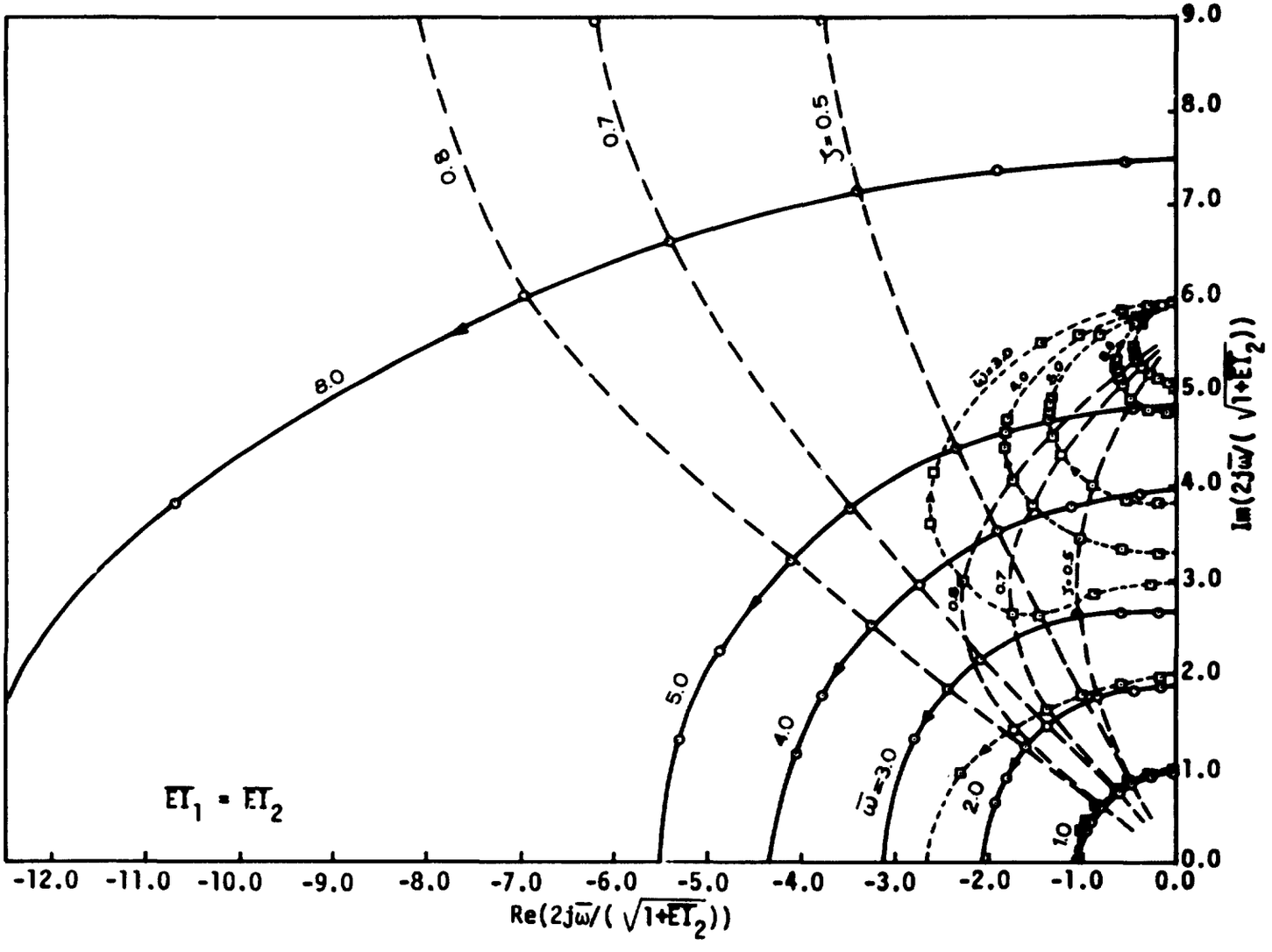


Figure 4.4 - Summary of complex root loci for two dominant poles - GRG Control

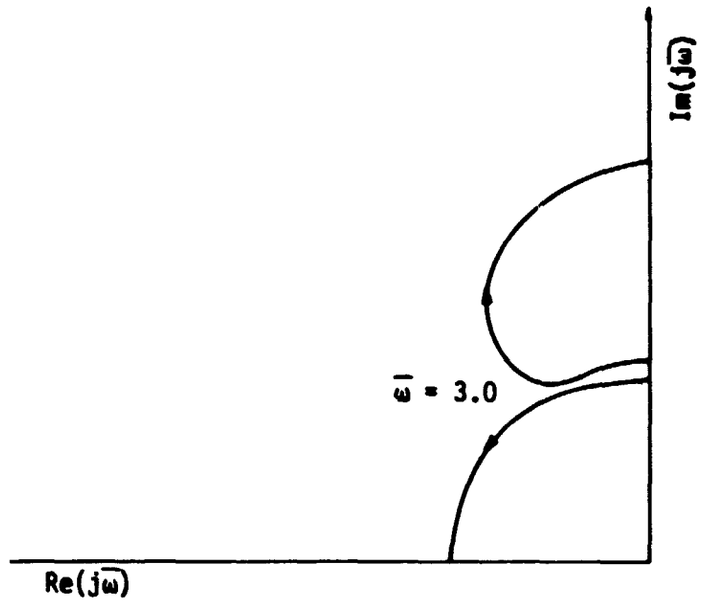


Figure 4.4a - Detail root loci of dominant poles
GRG Control varying $\zeta$

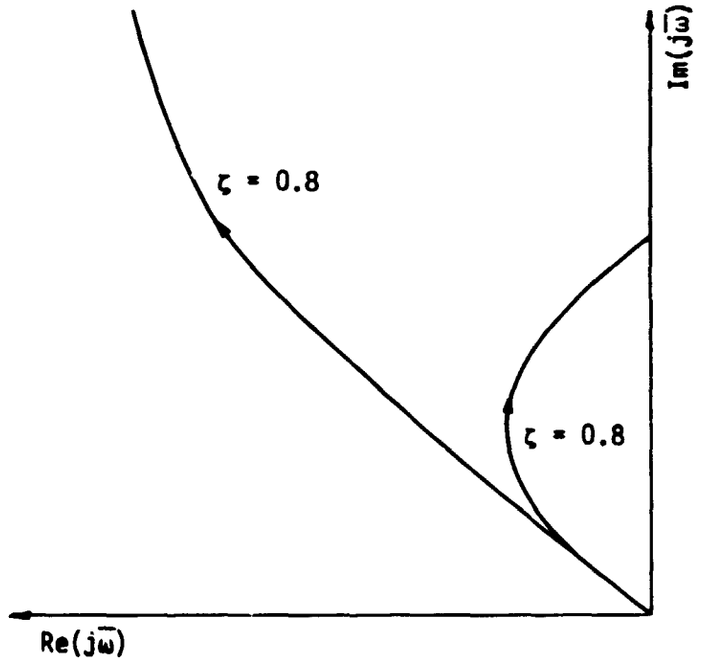


Figure 4.4b - Detail root loci of dominant poles
GRG Control varying $\bar{\omega}$

and the dominant pole becomes the one that has a smaller damping ratio. On the other hand, if one recalls expression (4.4) it is easy to see that this relationship holds for the present example. Consequently

$$\bar{w} = \frac{w}{w_d} = \frac{1}{3.52} \cdot \frac{w}{w_c} \qquad (4.15)$$

is useful to compare the preceding explanation with respect to the natural frequency of a clamped-free beam associated with the system. Using (4.15) one might say that the method of general rigid gains yields very reasonable results for manipulator bandwidth up to the natural frequency of the clamped-free equivalent system. Faster response can be obtained only with a considerable reduction in the damping ratio of the dominant mode. For constant specified damping ratio of $\zeta = 0.7$ Figure 4.5 shows the dominant flexible poles for variations in $\bar{w}$. This plot presents a better view of the limitations obtained from the general rigid gains method.

## 4.5 Effect of Payload

In order to analyze the effect of the payload in the design of the control, a comparison was made between three different payloads for the example presented in Table 4.3. The payloads were assumed to be lumped masses at the end of the second beam with values indicated in Table 4.4

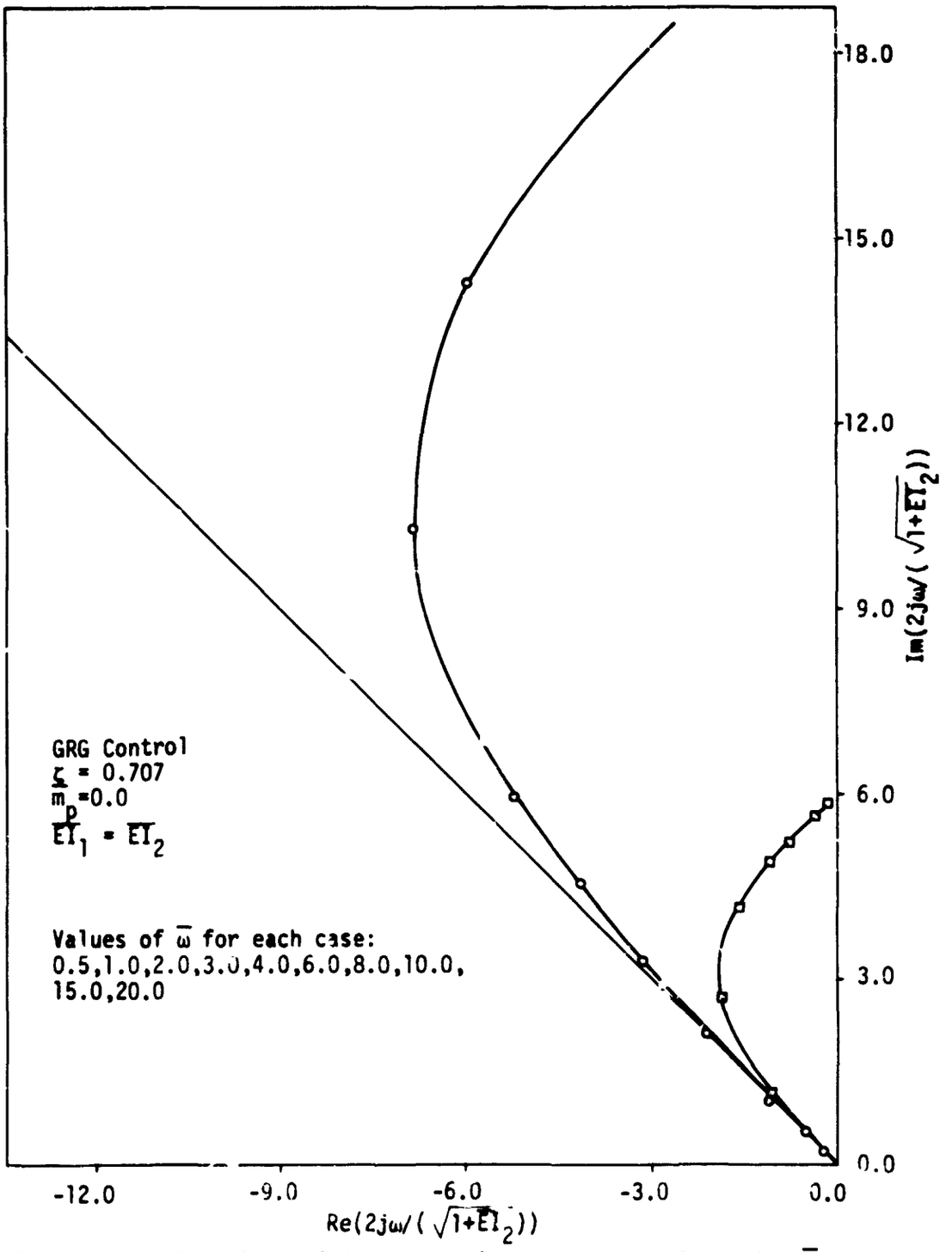


Figure 4.5 - Root loci of dominant poles - GRG Control varying $\bar{\omega}$

| case | $m_p$ | $\alpha$ |
|---|---|---|
| 1 | 0.8 | 1.63 |
| 2 | 1.0 | 1.44 |
| 3 | 5.0 | 0.75 |

Table 4.4 Lumped Payloads Assumed for Example 3

The natural frequency of the clamped-free equivalent system is $w_c = \alpha\sqrt{EI/\mu l^4}$ with $\alpha$ obtained using the method presented in reference [B1]. The results can be seen in Figure 4.6 As the payload is increased, the arm bandwidth is reduced as a consequency of the lower system natural frequencies. If one assumes the best design situation to be as close as possible to a damping ratio of 0.7 one sees that the general rigid gains method can still be applied with good results up to close to the clamped-free equivalent natural frequency. The situation would be considerably different if rotary inertia of the payload were considered.

## 4.6 Variations in System Geometry

In the preceding discussion only the case of equal cross section was verified from the point of view of control application. However, it would be useful to know how the system geometry has to be taken into account in order to improve the arm bandwidth. In order to implement this idea it is necessary to mention some important aspects. First, the system is going to be assumed, as in the previous cases, with two beams of equal length. Then, in order to keep a good reference for comparisons, the sum of the masses of the beams is assumed to be constant and the only variations must occur in the radii of the beams. In doing

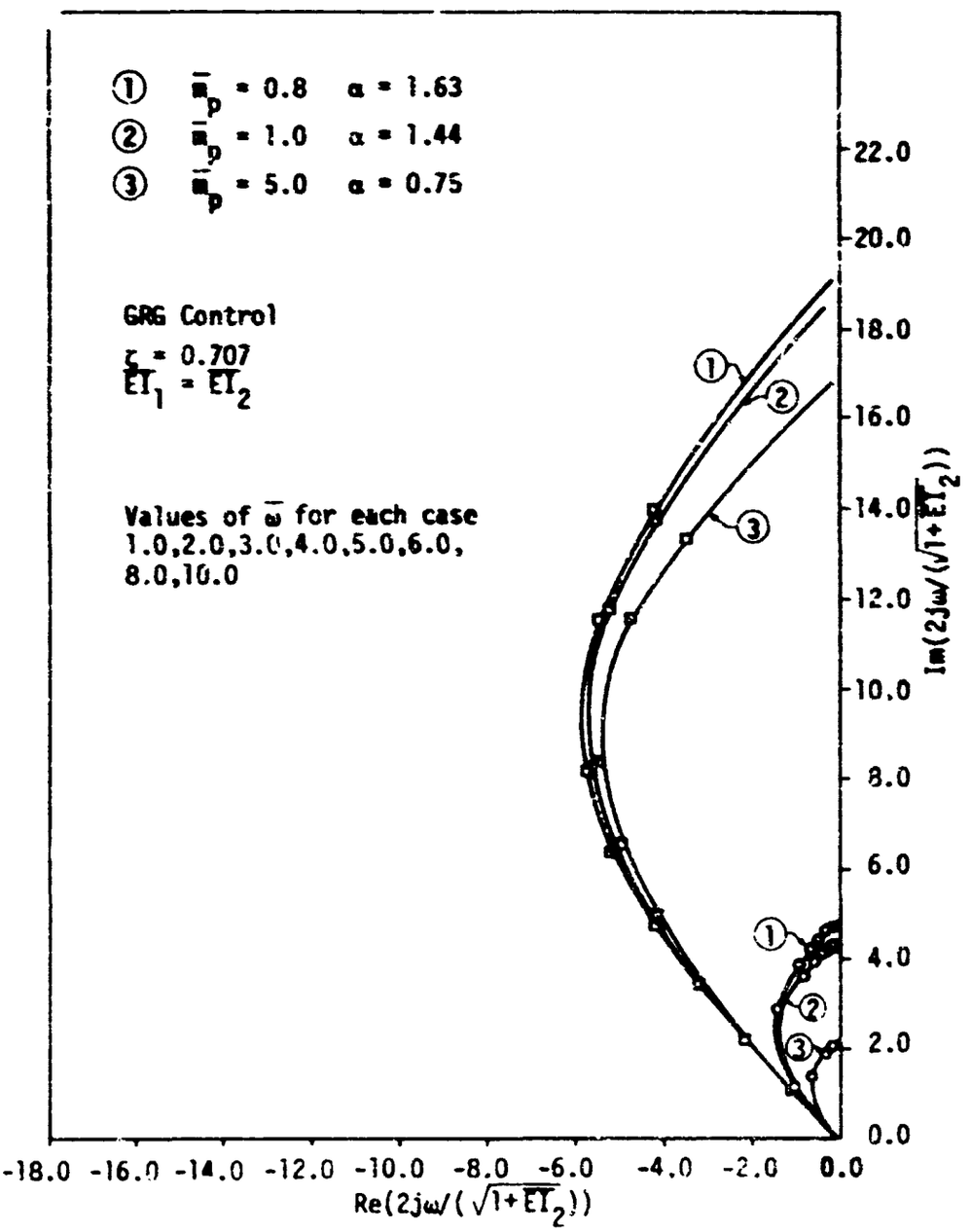


Figure 4.6 - Root loci of dominant poles - GRG Control

so let one assume

$$m_1 + m_2 = m = \text{constant} \tag{4.16}$$

$$l_1 + l_2 = l = \text{constant} \tag{4.17}$$

If $\rho$ is the density of the material, equation (4.16) can be written

$$\rho\, l_1 \frac{\pi}{4} d_{e1}^2(1-k_{r1}^2) = \rho\, l_2 \frac{\pi}{4} d_{e2}^2(1-k_{r2}^2) = m \tag{4.18}$$

or, using the nondimensionalization from Table 4.1, (4.18) can be reduced to

$$\bar{l}_1(1-k_{r1}^2) + \left(\frac{r_{e2}}{r_{e1}}\right)^2 \bar{l}_2(1-k_{r2}^2) = \frac{m}{\rho\, d_{e1}^2 \frac{\pi}{4} l^3} \tag{4.19}$$

If now one uses equation (4.7) there results

$$\bar{d}_{e1}^2 = \left(\frac{m}{\rho \frac{\pi}{4} l^3}\right) \left(\frac{1}{\bar{l}_1(1-k_{r1}^2) + \bar{l}_2(1-k_{r2}^2 \sqrt{\frac{\bar{l}_2}{\bar{l}_1}\frac{(1-k_{r1}^2)}{(1-k_{r2}^2)}}}\right) \tag{4.20}$$

However, by definition

$$\rho = \frac{m}{V} \tag{4.21}$$

where V is the total volume of the system.

Then, with (4.21) one can define a system coefficient

$$c.s. = \frac{d_{e1}^2(1-k_{r1}^2)l_1 + d_{e2}^2(1-k_{r2}^2)l_2}{l^3} \tag{4.22}$$

This coefficient can be calculated for any initial system configuration and remains constant as long as the mass is kept invariant. Then, for a given physical system it is possible to find the nondimensionalized diameters by using

$$\bar{d}_{e1}^2 = \frac{c.s.}{\bar{l}_1(1-k_{r1}^2) + \bar{l}_2(1-k_{r2}^2)\sqrt{\bar{EI}_2 \frac{(1-k_{r1}^2)}{(1-k_{r2}^2)}}} \tag{4.23}$$

together with relationship (4.7)

Another useful parameter to analyze the effect of variations of the system geometry is the natural frequency of the corresponding clamped-free system. For the purpose of comparison, W.J. Book (personal communication) based on the nondimensionalization described before and using a transfer matrix model, determined those natural frequencies for different ratios of the stiffness EI and several payloads. The results are shown in Figure 4.7 where

$$\bar{w} = \frac{w_{clamped}}{w_d} \tag{4.24}$$

and the factor $(2/(1 + \sqrt{EI_2/EI_1}))$ corresponds to a correction factor which takes into account the definition of $w_d$ based upon $EI_1$. With these elements it is possible to analyze the benavior of a stepped beam under the general rigid gains type of control.

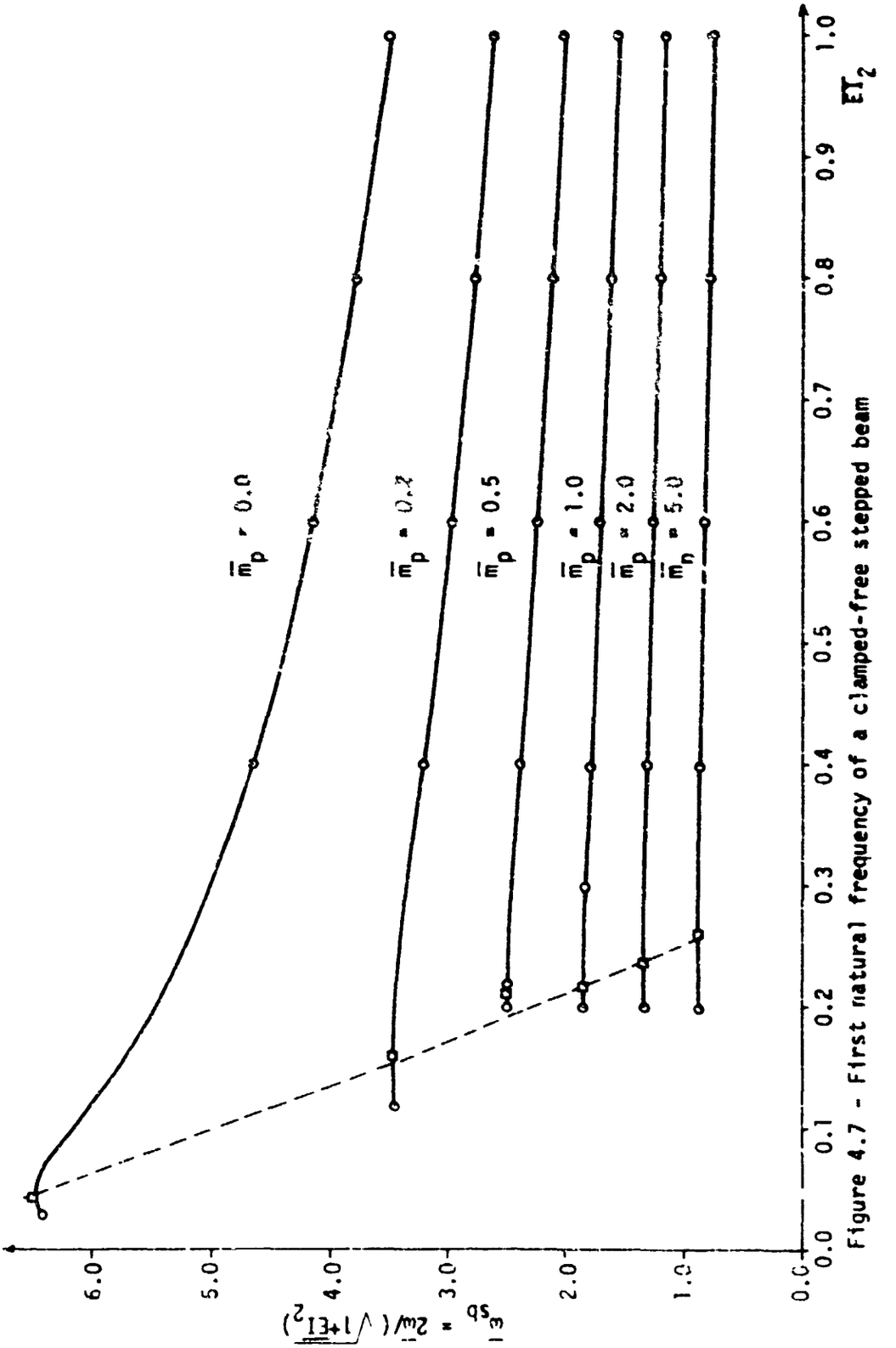


Figure 4.7 - First natural frequency of a clamped-free stepped beam

In order to get some insight into the effect of cross section variations, the control method was applied to the system described in Table 4.3 assuming constant length and constant total mass. Two cases were chosen: no payload at all and lumped payload mass of the same order of magnitude as the mass of the total arm.

## 4.7 No Payload - $\overline{EI}_2$ Variations

In this case the procedure was applied as before for each chosen $\overline{EI}_2$ ratio. The results can be seen in Figure 4.8 for $\overline{EI}_2$ varying from 0.2 to 0.8. As one can notice, if no payload is present, the arm bandwidth becomes better as one decreases the $\overline{EI}_2$ ratio. However, if one uses the results presented in Figure 4.7 it is expected that the best bandwidth for the system would be obtained for $\overline{EI}_2$ ratio equal to 0.045, which corresponds to the maximum clamped-free frequency of the equivalent system. This has not been verified and is included in the suggestions for further work.

## 4.8 With Payload-$\overline{EI}_2$ Variations

The effect of payload seems to be very important in the search for the best geometry of the system. While an accentuated stepped-beam appears to be the best design for no payload situation, a uniform system looks the best indicated for carrying payloads. This can be seen in Figure 4.9 where the method of general rigid gains was applied in the same way as without payload, for the case of $\overline{m}_p = 1.0$. A close look reveals that the system seems to converge for the best bandwidth when

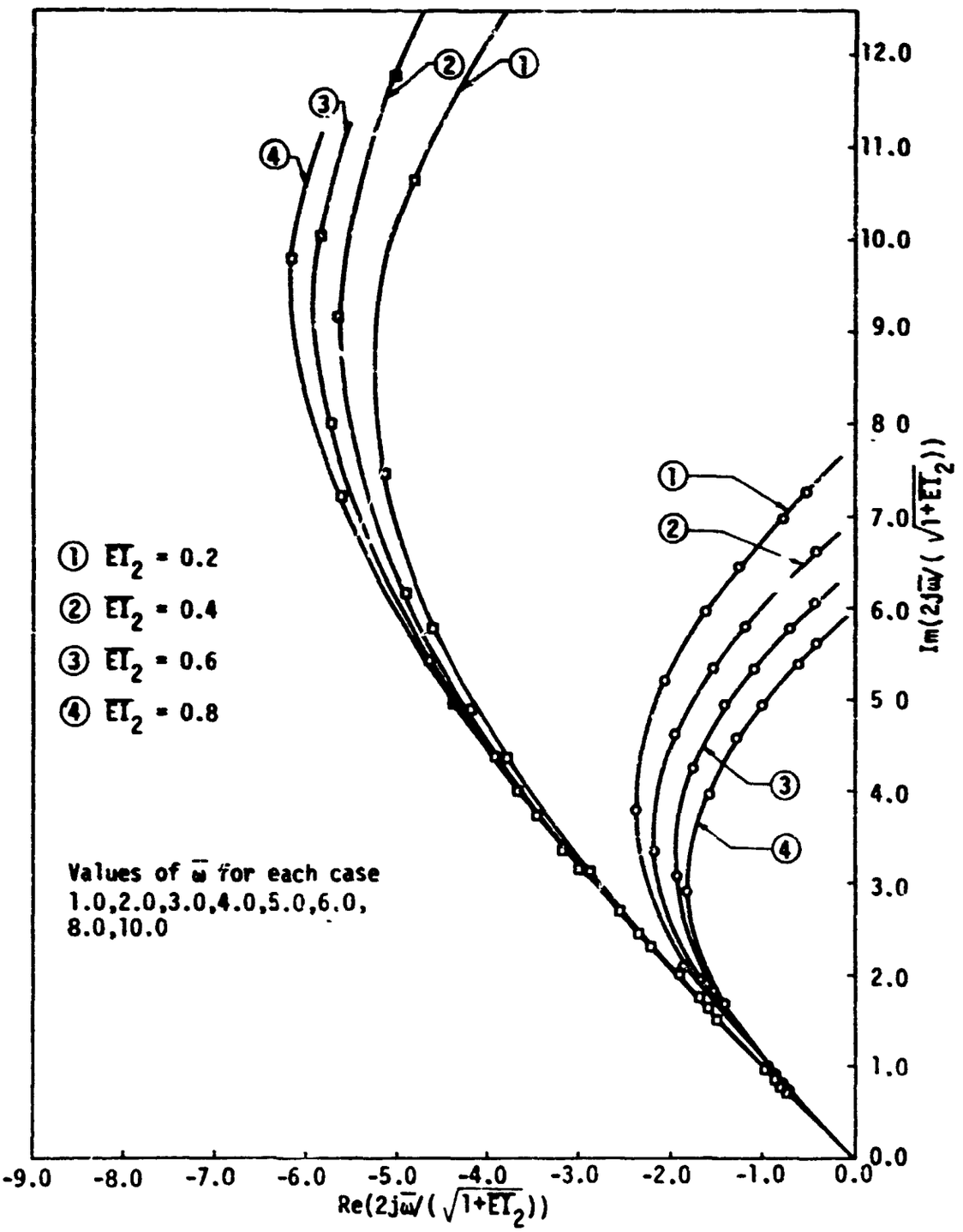


Figure 4.8 - Root loci of dominant poles - GRG Control
stiffness variations payload

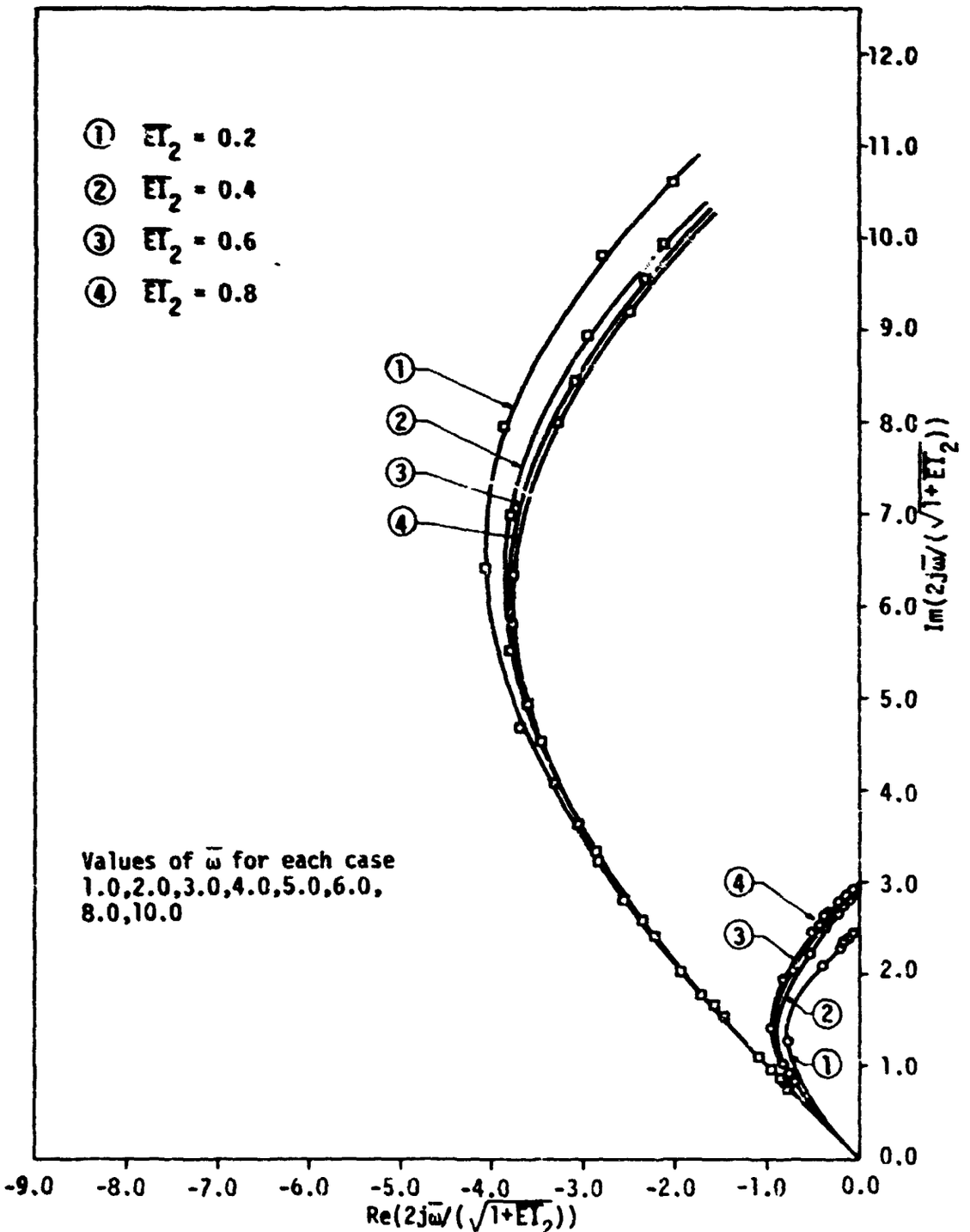


Figure 4.9 - Root loci of dominant poles - GRG Control stiffness variations - $\bar{m}_p$ = 1.0

$\overline{EI}_2$ approaches 1.0, that is, when the two beams have the same dimensions.

Comparing the maximum reasonable bandwidth with the results from Figure 4.7 it appears that the best results are those for $\overline{EI}_2 = 1.0$, where the system bandwidth is about the natural frequency of the equivalent clamped free system. Also, as was expected for lumped payload, the bandwidth is considerably lower than in the case of no payload. These two sets of results show that the designer should be very careful in specifying the system geometry with respect to the kind of work the arm has to perform. Also it is very important the analysis of the system based upon the payload geometry because of natural frequency reduction caused by the increasing rotary inertia. This fact was not considered in the present work.

## 4.9 Simon-Mitter Algorithm Applications

At the beginning of the present work, the idea was to apply modal control in order to place the poles of the system at any desired position. However, after a number of applications it was verified that the particular algorithm (SMA) used for the modal control design would not solve the problem due to the fact that poles were moved to positions that did not correspond to minimum sensitivity. As a consequency any small variation that appeared in the process would shift the poles to other locations and even to undesired unstable situations. Once reasonable results were obtained using the general rigid gain method, the idea of applying modal control changed to simply trying to improve the system bandwidth obtained

from rigid gains. Even in this case, if some improvement was obtained it should really be significant in order to compensate for the required measurements and/or estimation of the remaining state variables of the system.

Finally, assuming that a good bandwidth was achieved with the (SMA), the final decision should be made by comparing the required torque with the ones obtained from the application of the other design procedures.

In order to present some results from (SMA) applications the example of Table 4.3 was used with equal beams. Initially the system was assumed with no feedback at all. In terms of pole locations, all poles lay on the imaginary axis with four poles at the origin. As the modal control algorithm was not implemented in this work for applications to cases with repeated eigenvalues, very small gains were assumed in order to disturb numerically the poles at origin. The initial configuration is indicated in Table 4.5 where $\varepsilon_1 \neq \varepsilon_2 \neq 0$.

It was shown before that when the general rigid gain method was applied to this system, the best control situation was achieved for the two dominant poles close to the natural frequencies of the clamped-free equivalent system. As this frequency has the value $\bar{w} = 3.52$, the first movement using the Simon-Mitter algorithm was to shift the two first dominant poles of Table 4.5 to the point$(-3 \pm 3_j)$, that is, trying an improvement of about 20% with respect to the rigid method. For comparison, the rigid gain procedure was used in an attempt to obtain similar dominant pole locations. All the eigenvalues are shown in Table 4.6.

| Eigenvalue | Real Part | Imaginary Part |
|---|---|---|
| 1 | 0.0 | $+\varepsilon_1$ |
| 2 | 0.0 | $-\varepsilon_1$ |
| 3 | 0.0 | $+\varepsilon_2$ |
| 4 | 0.0 | $-\varepsilon_2$ |
| 5 | 0.0 | 44.3 |
| 6 | 0.0 | -44.3 |
| 7 | 0.0 | 68.6 |
| 8 | 0.0 | -68.6 |
| 9 | 0.0 | 151.0 |
| 10 | 0.0 | -151.0 |
| 11 | 0.0 | 161.0 |
| 12 | 0.0 | -161.0 |

Table 4.5 Initial Configuration for Application of Modal Control Algorithm

| Eigenvalue | Real Part | Imaginary Part |
|---|---|---|
| 1 | -2.8 | 2.9 |
| 2 | -2.8 | -2.9 |
| 3 | -1.5 | 3.7 |
| 4 | -1.5 | -3.7 |
| 5 | -6.1 | 0.0 |
| 6 | -8.4 | 53.9 |
| 7 | -8.4 | -53.9 |
| 8 | -16.4 | 103.8 |
| 9 | -16.4 | -103.8 |
| 10 | -44.9 | 129.0 |
| 11 | -44.9 | -129.0 |
| 12 | -1361.5 | 0.0 |

Table 4.6 Configuration From General Rigid Gains For Comparison With (SMA)

One important distinction between the two control procedures is that in the case of rigid gains the high frequency poles are free to move during gains variations (Table 4.6) and in case of (SMA) all poles were specified to remain at the same position (Table 4.5) except the ones chosen for relocation. The control is not only acting to move a pair of poles but also to keep the other poles at a fixed position. This fact is displayed very well in Table 4.7 where the gains using both methods for obtaining the same dominant eigenvalues (of Table 4.6) appear in the same order as in expression (4.13). One notices that for the first input to the system the gains corresponding to angular position and velocity feedbacks are smaller in case of (SMA) while for the second input (SMA) appears with bigger gains probably because of the specification of the second dominant pole to a better position than rigid gains gave. On the other hand, due to the fact that the high frequency poles remain constant, (SMA) presents reasonably large linear feedback gains. Again this fact requires high accuracy in the measurements or estimation that must be made to apply the Simon-Mitter technique because of observed high sensitivity of the poles with respect to gain variations.

A second shift using the Simon-Mitter algorithm was performed moving the first dominant poles to $(-5 \pm 5j)$. In this case the modal control gains increased up to 10 times more than those presented in Table 4.7. The rigid gain method cannot yield both dominant poles near this position, so no direct comparison is possible.

Another important effect of the modal control feedbacks, especially

the positive ones, is with respect to system stability. For small motions around the equilibrium position used for control design (shoulder and elbow joints with zero degrees) the linearized model presented stable eigenvalues. However, due to high sensitivity of the poles to parameter variations, the achieved arm bandwidth is rapidly lost as the joint angles change. For gross motion of the elbow joint from 0° to 90° using constant gains obtained by the application of (SMA) at 0°, some high frequency poles change rapidly to the right half complex plane, making the system unstable. This fact was one of the bad characteristics of (SMA) application because for different equilibrium position designs, the gross motion always presented unstable high frequency poles. This fact was not observed using constant gains obtained at the same position using general rigid gains method. As a result, the Simon-Mitter algorithm could not be applied using constant gains for a given gross motion but would only give some improvement for small motions around equilibrium position. This implies that the use of (SMA) for this kind of system would bring some reasonable results only if one has a kind of adaptive modal control. Finally, depending upon the tasks to be performed there is a possibility of controlling the gross motion with the rigid gain method and the fine motion using modal control techniques, using different sets of constant gains.

## 4.10 System Analysis Using Sensitivities

Another procedure to achieve desired pole allocations for the pre-

| Nomenclature | Gain | Rigid Method | Modal Control | Gain | Rigid Method | Modal Control |
|---|---|---|---|---|---|---|
| Angular Position Feedbacks | $k_{11}$ | -5.3 | -3.9 | $k_{21}$ | -1.6 | -4.2 |
| | $k_{12}$ | -1.6 | -1.2 | $k_{22}$ | -0.7 | -1.5 |
| Linear Position Feedbacks | $k_{13}$ | 0.0 | -10.6 | $k_{23}$ | 0.0 | -10.6 |
| | $k_{14}$ | 0.0 | +3.2 | $k_{24}$ | 0.0 | +4.4 |
| | $k_{15}$ | 0.0 | -3.9 | $k_{25}$ | 0.0 | -4.8 |
| | $k_{16}$ | 0.0 | -1.6 | $k_{26}$ | 0.0 | -1.3 |
| Angular Velocity Feedbacks | $k_{17}$ | -1.8 | -1.4 | $k_{27}$ | -0.6 | -1.5 |
| | $k_{18}$ | -0.5 | -0.4 | $k_{28}$ | -0.2 | -0.5 |
| Linear Velocity Feedbacks | $k_{19}$ | 0.0 | -3.7 | $k_{29}$ | 0.0 | -3.7 |
| | $k_{110}$ | 0.0 | +2.9 | $k_{210}$ | 0.0 | +3.4 |
| | $k_{111}$ | 0.0 | -1.3 | $k_{211}$ | 0.0 | -1.7 |
| | $k_{112}$ | 0.0 | -0.5 | $k_{212}$ | 0.0 | -0.5 |

Table 4.7 Comparison of Gains from General Rigid Method and Modal Control

sented system was the use of eigenvalues sensitivites using the analytical expressions described in Chapter III. To understand the procedure let one consider the same example presented in Tables 4.3 and 4.6 with the two pairs of dominant poles described with greater precision in Table 4.8

| Eigenvalue | Real Part | Imaginary Part | Magnitude | Damping Ratio |
|---|---|---|---|---|
| 1 | -2.792 | +2.957 | 4.066 | 0.686 |
| 2 | -1.540 | +3.775 | 4.077 | 0.377 |

Table 4.8 Initial Configuration for Sensitivities Application

Let one assume that only angular feedbacks are available for controlling the system. Then, only sensitivities corresponding to eight gains are necessary for analyzing the system despite the fact that all poles must be checked for stability. In order to illustrate the procedure let one cosider only the sensitivities of the two poles indicated in Table 4.8. The values of the sensitivities are presented in Table 4.9 and they represent the real and imaginary part of the right hand side of expression (3.30).

Let one assume that a small improvement should be obtained in both poles in the sense of shifting them as close as possible to a damping ratio of $\zeta = 0.707$ while keeping about the same magnitude. From Table 4.9 it is possible to see that pole 1 is much more sensitive to gain variations than pole 2. However, as it would be more desirable to move pole 2 rather than pole 1, it is obvious that one should base the cal-

| | Gain | Sensitivity | |
|---|---|---|---|
| | | Real Part | Imaginary Part |
| POLE 1 | $k_{11}$ | -0.12378 | -1.6737 |
| | $k_{12}$ | -0.28930 | +3.9537 |
| | $k_{17}$ | +5.5841 | +8.2614 |
| | $k_{18}$ | -12.2098 | -6.2314 |
| | $k_{21}$ | -11.7945 | -0.60046 |
| | $k_{22}$ | -13.1803 | -19.5332 |
| | $k_{27}$ | -30.9911 | -34.0298 |
| | $k_{28}$ | +28.8638 | +14.7419 |
| POLE 2 | $k_{11}$ | -0.39584 | -0.17209 |
| | $k_{12}$ | -0.20609 | -0.03951 |
| | $k_{17}$ | 1.0579 | -1.3176 |
| | $k_{18}$ | 0.44946 | -0.72977 |
| | $k_{21}$ | 0.53836 | -0.54829 |
| | $k_{22}$ | 0.54781 | -0.60792 |
| | $k_{27}$ | -0.05030 | -0.09906 |
| | $k_{28}$ | 0.23709 | -0.38123 |

Table 4.9 Sensitivities of Poles from Table 4.8

culations upon sensitivities of pole 2. From expression (3.39) and for small variations of the gains, one can write

$$\frac{\Delta\lambda\sigma}{\Delta g_{kj}} = s_{kj}^{(\sigma)} \qquad (4.25)$$

where $s_{kj}^{(\sigma)}$ is the sensitivity of the real (imaginary) part of pole$\sigma$ with respect to variations in the gain $k_{kj}$. Also, if the sensitivity is positive (negative) and the eigenvalue is negative (positive) an improvement in the poles would be obtained by decreasing the corresponding gain and vice versa. If now one turns to Table 4.9 it is verified that the maximum shift of pole two would be obtained for small variations in the gain $k_{17}$. However, for this same gain variations, pole 1 has five times more sensitivity which means it would undergo a bigger shift. It must be kept in mind that this analysis is true only for small variations of the gains since expression (4.25) holds only for linear deviations from the dynamic equilibrium point. Let one assume for example that it was decided to vary gain $k_{17}$ from its original value of -1.873 to a new value -1.9 while the other gains were maintained constant. As one sees, the variation on the gain was about 1.44%. The new pole location is shown in Tables 4.10a and 4.10b.

| Eigenvalue | Real Part | Imaginary Part | Magnitude | Damping Ratio |
|---|---|---|---|---|
| 1 | -2.942 | 2.733 | 4.016 | 0.732 |
| 2 | -1.560 | 3.310 | 4.120 | 0.380 |

Table 4.10a New Poles Using Expression (4.25) for Sensitivities

| Eigenvalue | Real Part | Imaginary Part | Magnitude | Damping Ratio |
|---|---|---|---|---|
| 1 | -2.948 | 2.840 | 4.093 | 0.729 |
| 2 | -1.571 | 3.806 | 4.117 | 0.381 |

Table 4.10b New Poles Using Computer Programs from Appendix A.

As one sees, the predicted values from Table 4.10a are very close to the numbers obtained from the gain variation using the model in a digital computer. The discrepancy observed in the imaginary part of pole 1 might be explained by the fact that the corresponding sensitivity is not constant for the assumed gain variation. The new location is better than the one in Table 4.8 but still is not enough since pole 2 still has a small damping ratio. Further modifications can be obtained by repeating the procedure with the sensitivities calculated for the positions represented in Table 4.10. In applying the sensitivities procedure for some of the poles, it is also necessary to know what happens with the high frequency eigenvalues since they might go unstable for a desired gain variation to shift a specified pole.

This procedure was applied to several cases in order to improve a few of the poles, especially the dominant ones. However, fair results were obtained only for a large number of trials since the gains variations must be relatively small. For this reason no general results from sensitivities are presented for comparison and the procedure is left only for fine adjustments in a final phase of the design. A more systematic procedure might be designed for computer implementation.

Finally, it should be noticed that sensitivity played a very important role in the present work in the sense of analyzing the numerical results

obtained. Each time a given set of gains was obtained the sensitivities helped to judge how accurate the gains had to be in order to have only small deviation in the poles corresponding to truncation error. Also in applying the modal control algorithm, sensitivity of the high frequency poles was always analyzed for the purpose of stability because the pole sensitivity may increase considerably when the gains are specified to keep the pole at constant position.

## 4.11 Comparison of Results with Rigid Gains - No Cross Joint Feedback

In order to show the effect of the cross joing feedback some results obtained in the present work were compared with those obtained by W.J. Book using independent joint feedback and a transfer matrix model of the physical system, as described in [B2]. The values of the gains were obtained from a rigid design technique which yielded a desirable relative position of the four most dominant poles. These gains were presented for the case of equal beams in [B2] and slightly modified to allow for the changes in inertia where the beams are not equal. All results are presented for the non-dimensionalized case of Table 4.3 with changes in the parameters payload and cross section of the component beams. In the case of equal beams ($\overline{EI}_2 = 1.0$) and no payload Figure 4.10 shows the results obtained from no cross joint feedback. Although only one dominant pole is shown, one can see that the maximum arm bandwidth is about 50% of the clamped-free equivalent natural frequency. Variation of the mass distribution of the system from equal beams to a stepped configuration with no payload shows a slight increase in the ratio of arm bandwidth to clamped natural frequency as can be seen from Figure 4.11 ($\overline{EI}_2 = .05$)

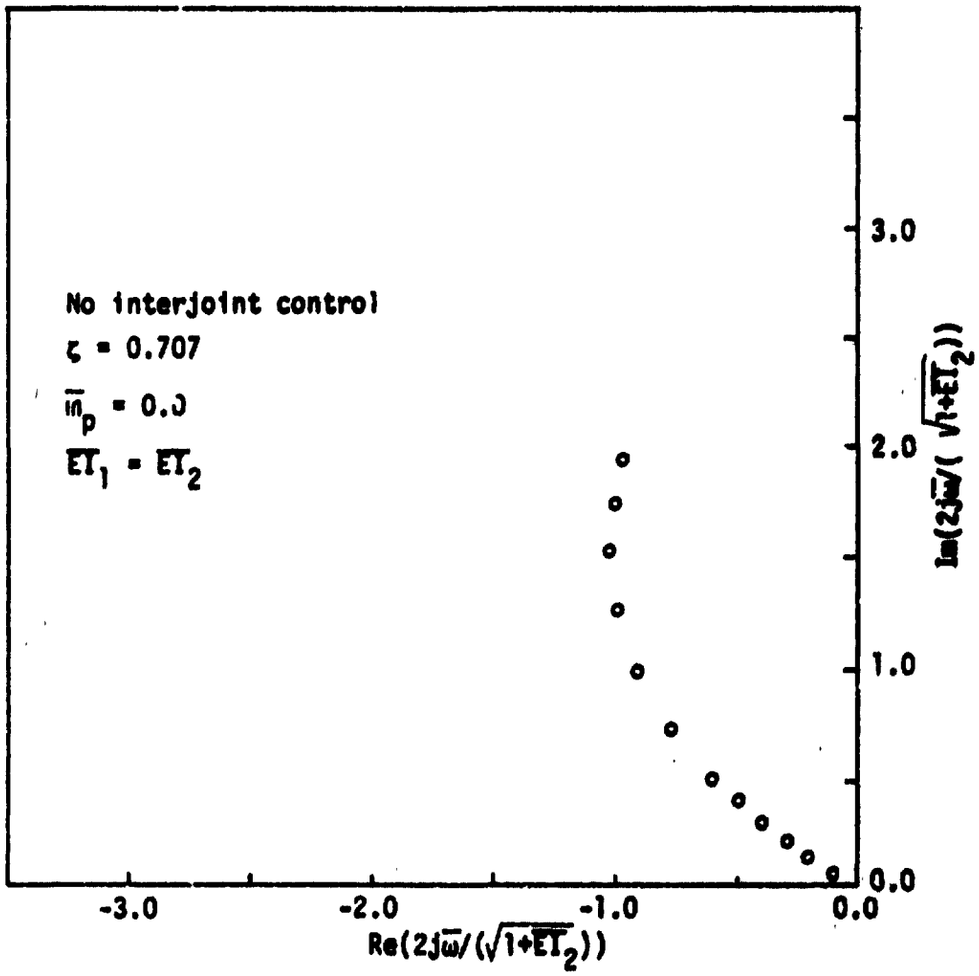


Figure 4.10 - Root loci of first dominant pole no interjoint feedback, varying $\bar{\omega}$

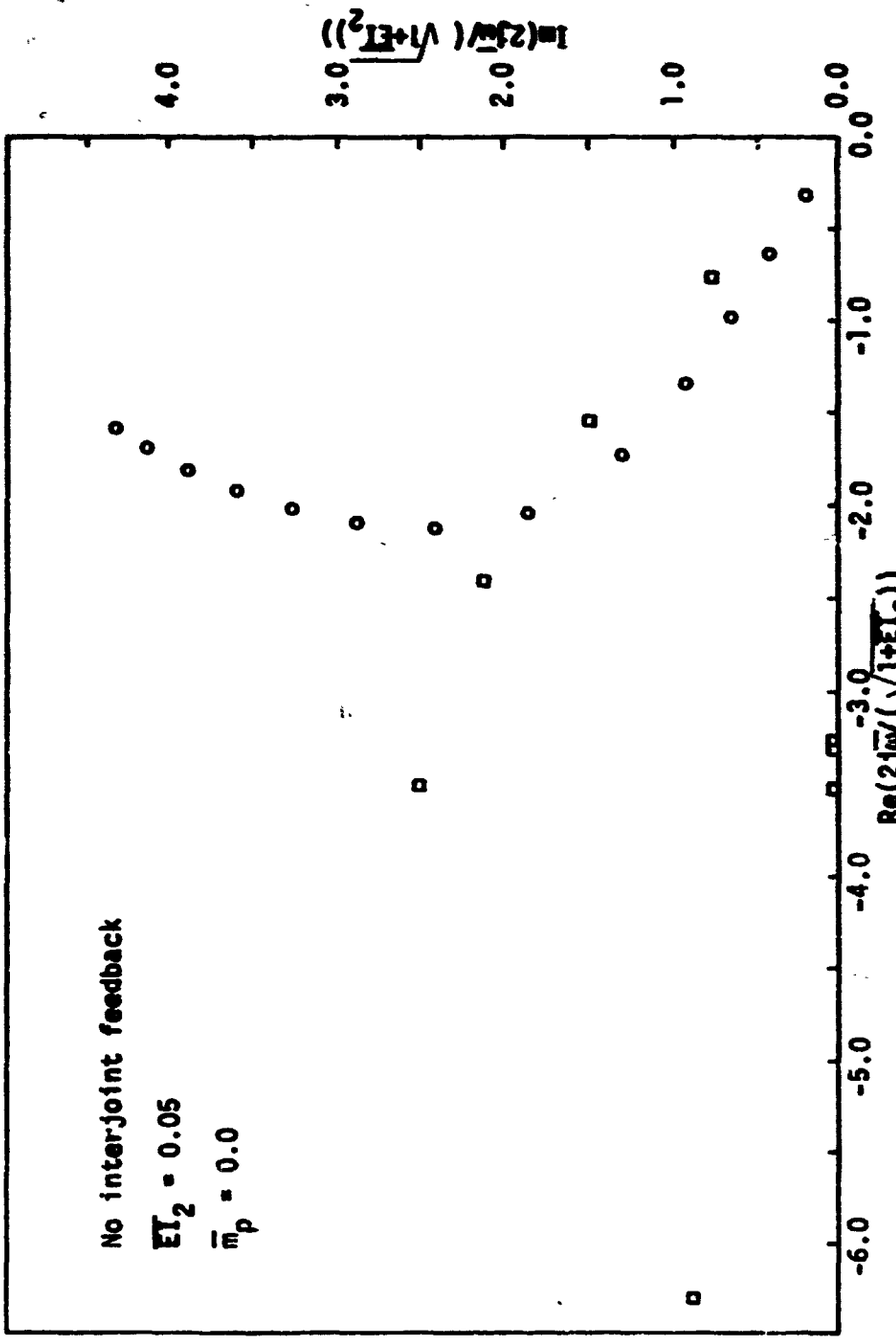


Figure 4.11 - Root locI of dominant poles - no interjoint feedbacks varying $\overline{\omega}$, stiffness $\overline{EI}_2$ = 0.05

and the corresponding plot in Figure 4.7. The effect of payload results in a reduction in this ratio as can be seen in Figure 4.12. These results indicate the importance of the information between the joints. However, as the control has more dynamics the feedback between the joints may cause system instability in case of failure. (The examples of rigid gains are stable even when the cross joint feedback gains are set to zero individually or together).

## 4.12 The Measurement of Feedback Angles

One observes from the definition of coordinates in the proposed model for the physical system that the angle corresponding to shoulder position ($\theta_1$) can be measured by a simple potentiometer or other type readout. However, for the elbow angle the definition of coordinates requires that not only the rigid angle must be measured but also the slope at the end of the first beam. Here, by rigid angle ($\theta_r$) is meant the angle between the tangent at the end of the first beam and the tangent at the beginning of the second beam that also can be measured by a potentiometer. Measurement of the slope at the end of the first beam is more difficult. In order to present some results comparing the feedbacks measuring the flexible or rigid angle, a brief transformation of coordinates has to be presented. The rigid angle can be defined as

$$\theta_r = \theta_2 - u_{1E}' \tag{4.26}$$

with

$$u_{1E}' = \phi_{11E}' q_{11} + \phi_{12E}' q_{12} \tag{4.27}$$

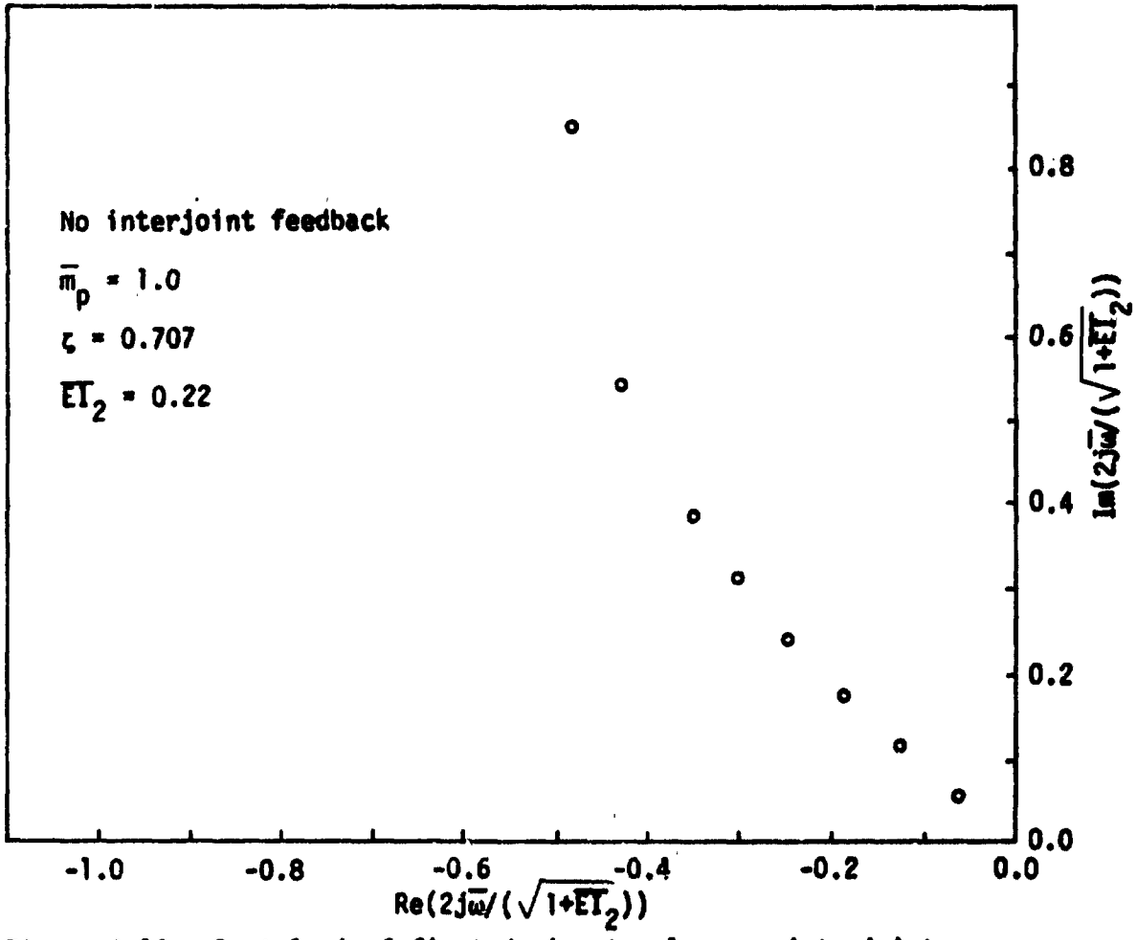


Figure 4.12 - Root loci of first dominant pole - no interjoint feedback-varying $\bar{\omega}$ and fixed payload

where the signs of the components $\phi'_{11E}$ and $\phi'_{12E}$ have been described with respect to the reference frames in Chapter II. Then, in order to use the rigid angle in the feedback law from the general rigid method one must have

$$\begin{bmatrix} \tau_1 \\ \tau_2 \end{bmatrix} = \begin{bmatrix} K_{T1} & K_{T3} \\ K_{T2} & K_{T4} \end{bmatrix} \begin{bmatrix} \theta_1 \\ \theta_r \end{bmatrix} + \begin{bmatrix} K_{TD1} & K_{TD3} \\ K_{TD2} & K_{TD4} \end{bmatrix} \begin{bmatrix} \theta_1 \\ \theta_r \end{bmatrix} \tag{4.28}$$

with the relation of coordinates given by

$$\begin{bmatrix} \theta_1 \\ \theta_r \end{bmatrix} = \begin{bmatrix} 1 & 0 & 0 & 0 & 0 & 0 \\ 0 & 1 & -\phi'_{11E} & -\phi'_{12E} & 0 & 0 \end{bmatrix} \begin{bmatrix} \theta_1 \\ \theta_2 \\ q_{11} \\ q_{12} \\ q_{21} \\ q_{22} \end{bmatrix} \tag{4.29.1}$$

$$\begin{bmatrix} \dot{\theta}_1 \\ \dot{\theta}_r \end{bmatrix} = \begin{bmatrix} 1 & 0 & 0 & 0 & 0 & 0 \\ 0 & 1 & -\phi'_{11E} & -\phi'_{12E} & 0 & 0 \end{bmatrix} \begin{bmatrix} \dot{\theta}_1 \\ \dot{\theta}_2 \\ \dot{q}_{11} \\ \dot{q}_{12} \\ \dot{q}_{21} \\ \dot{q}_{22} \end{bmatrix} \tag{4.29.2}$$

Using relations (4.29.1) and (4.29.2) in the proposed model, some results were obtained in order to analyze the effect of the measured angle in the design of the control. In Figure 4.13 one can see the effect of using

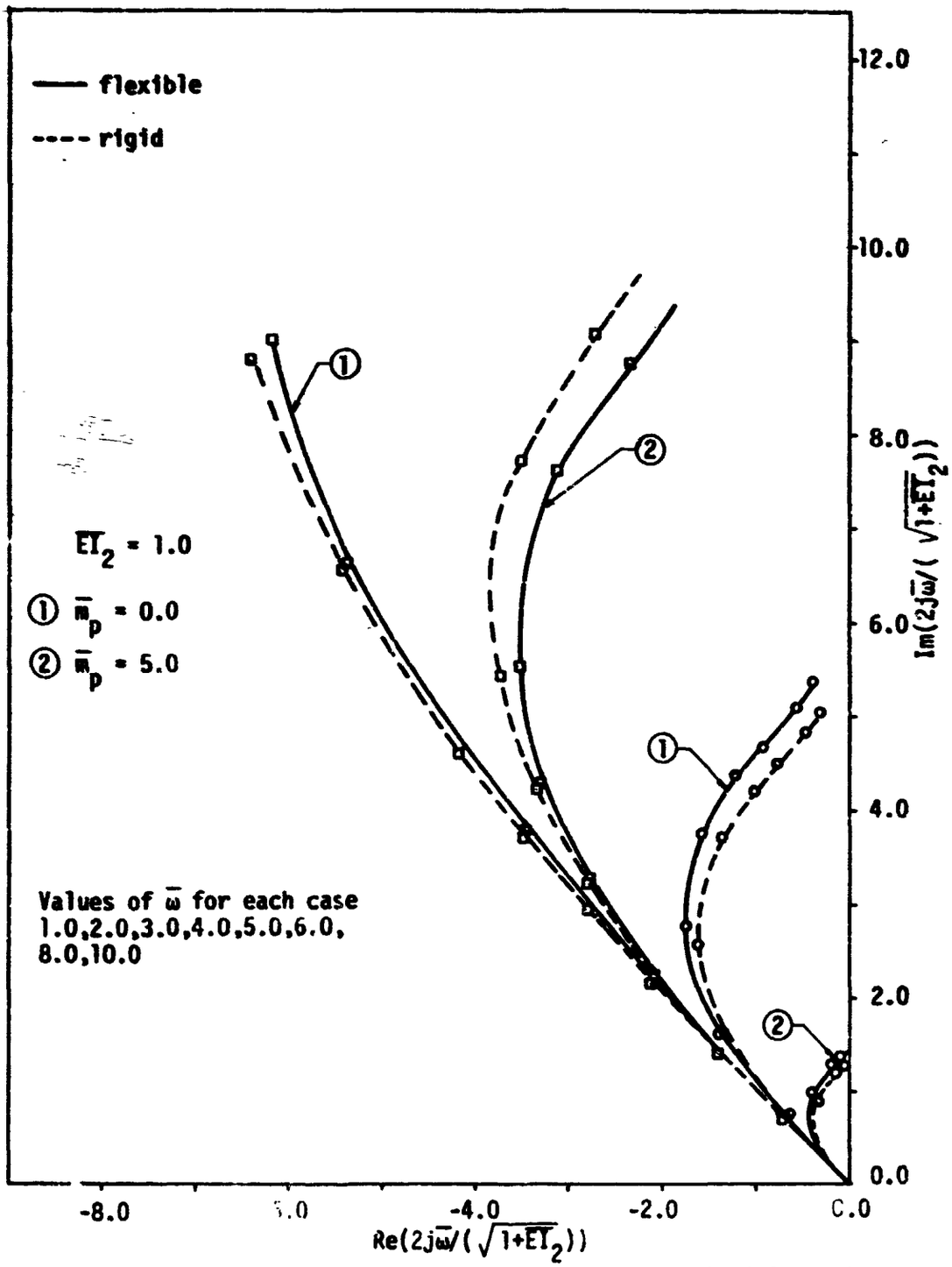


Figure 4.13 - Root loci of dominant poles - Rigid and flexible angle definition - variations in payload

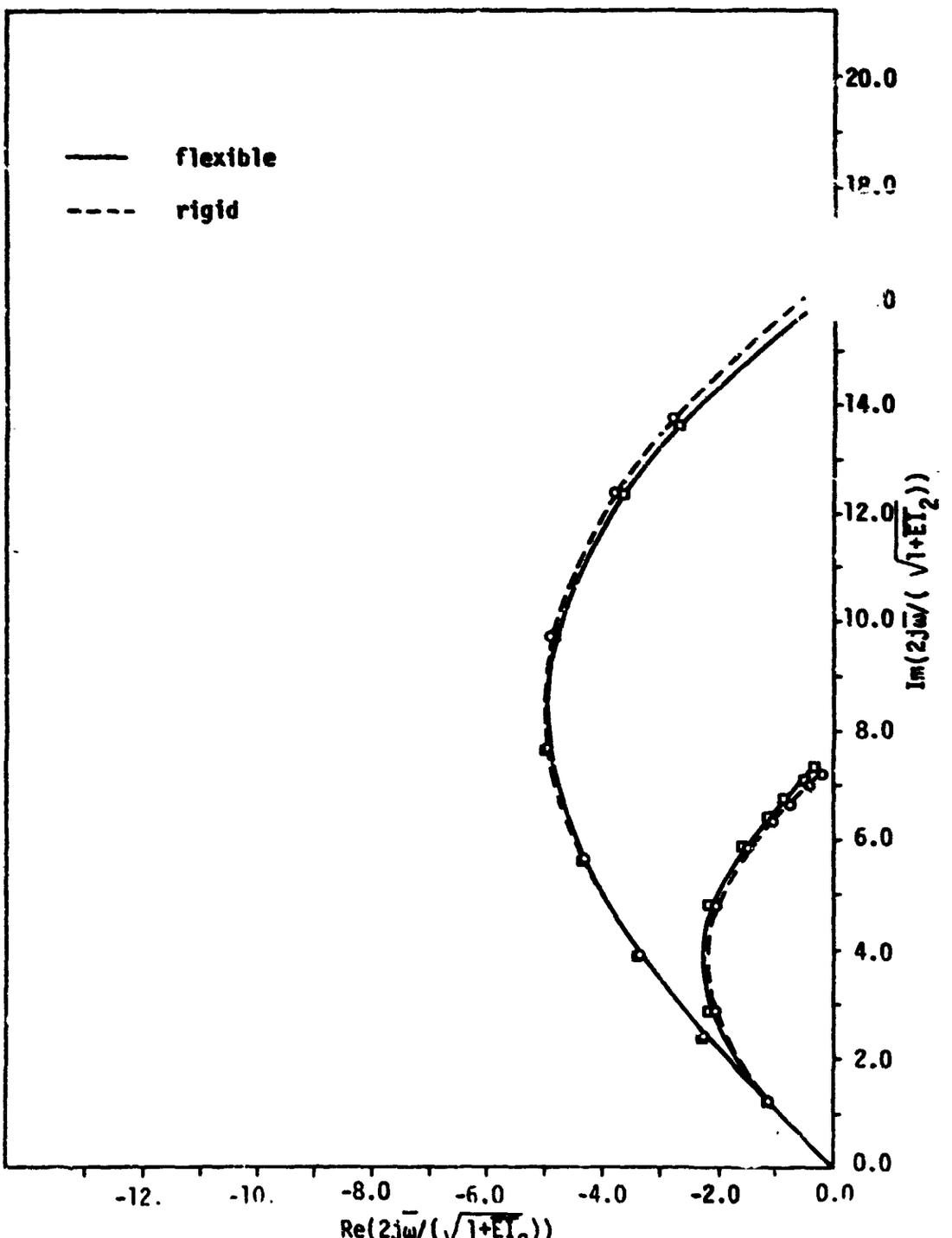


Figure 4.14 - Root loci of dominant poles - rigid and flexible angle definition - no payload - $\overline{EI}_2 = 0.045$

the rigid angle in comparison with flexible feedback for the system of Table 4.3 with $\overline{EI}$ ratio equal to unity. The graph shows the results for no payload and for $\overline{m}_p = 5.0$. It is clear that feeding back information about the flexible motion allows the design of a better control. However, the improvement in the arm bandwidth may not justify the considerable complications of measuring the deflection at the end of the first beam. For the case of stepped like system with $\overline{EI}_2 = 0.045$ Figure 4.14 shows essentially the same behavior.

## 4.13 Summary

This chapter presented the general results obtained from the applications of the control techniques presented in Chapter III. A general comparison of the results was presented. Some digital computer simulations applying these results are presented in Chapter V.

# CHAPTER V

# SIMULATION OF SPECIAL CASES

## 5.1 General Results

This chapter presents some results from digital simulation of the examples presented in the previous chapter. The results are non-dimensionalized as indicated in Table 4.2 and the main physical characteristics were presented in Figures 4.1 and 4.2. The values of the parameters for nondimensionalization are presented in Table 5.1 for the case of no payload and no joint mass.

| Physical Quantity | Symbol | Example 1 | Example 2 |
|---|---|---|---|
| System Coefficient | c.s. | $1.6303 \times 10^{-5}$ | $1.936 \times 10^{-3}$ |
| Stiffness Constant | $EI_i$ | $1.848 \times 10^{6}$ lbf - $ft^2$ | $1.39 \times 10^{5}$ Nt-$m^2$ |
| Total Length | $l$ | 53.4 ft | 9.914m |
| Average Mass per Unit Length | $\mu$ | 0.19769 lbm/ft | 3.955 $kg/m$ |
| Dimensionalization Frequency | $w_d$ | 1.072 rd/sec | 224.5 rd/sec |
| Dimensionalization Time | $T_d$ | 5.86 sec | 0.028 sec |

Table 5.1 Parameters for Non-Dimensionalization of the Simulated Examples

The simulations are divided into torque impulse responses and parabola tracking performance. The flexible amplitudes are the amplitudes of each mode component, that is, $\bar{q}_{11}$, $\bar{q}_{12}$, $\bar{q}_{21}$, $\bar{q}_{22}$. The joint dis-

placement means the linear deviation of the end of second beam with respect to the rigid system ($\overline{O_p O_3}$ in Figure 2.1).

In order to analyze the behavior of the system under the (SMA) modal control algorithm, Example 2 was chosen for the physical case of zero reference state variables. Following the procedure and results presented in the previous chapters, a control was designed using the general rigid gains method, specifying the dominant poles at 60% of the corresponding clamped-free natural frequency ($\bar{w} = 0.6\,\bar{w}_c$ where $\bar{w}_c$ is obtained from Figure 4.7). Once the control law was obtained the eigenvalues corresponding to the closed-loop situation were calculated. Then one returned to the original uncontrolled system and applied (SMA) to obtain the closed-loop system with exactly the same eigenvalues as those obtained using the general rigid method. The purpose of this procedure was to compare the response under modal control (SMA) to the response under [illegible] and to study the effect of pole sensitivity under both. The results presented in Figures 5.1 and 5.2 correspond to the elbow torque impulse response of the same magnitude. As one can see from Figures 5.1a and 5.2a modal control allows a smaller total angle variation for the elbow but varies the shoulder more. Both systems settle down at about the same time. The oscillatory behavior of modal control at the beginning might be caused by the large number of feedbacks necessary for controlling the system, especially those from the flexible components. From the torque point of view the (SMA) presents a more oscillatory behavior as can be seen from Figures 5.2a and 5.2b.

The maximum torque is bigger in case of modal control, especially

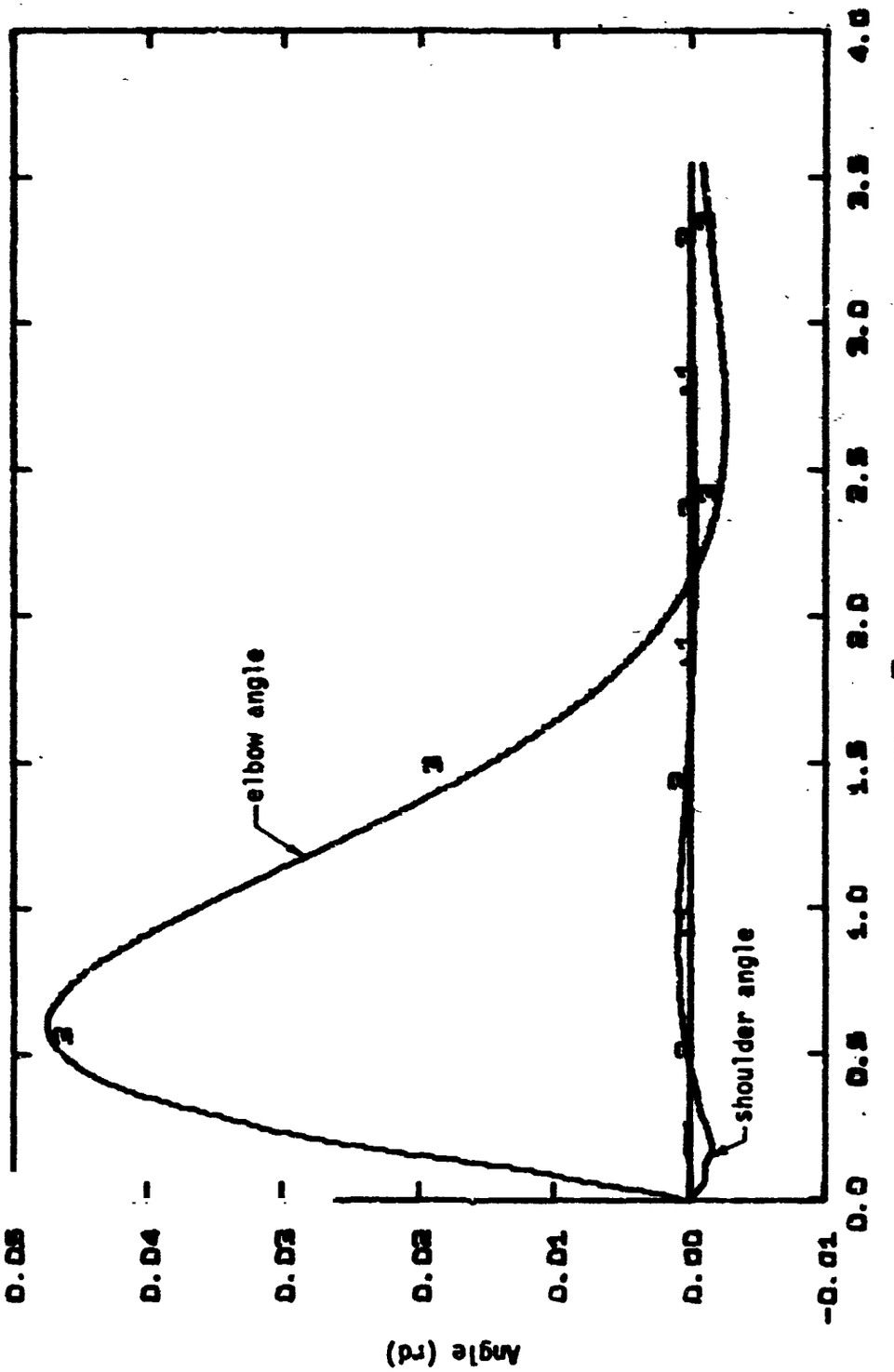


Figure 5.1a - Angle Response of Example 2 for Impulse at Elbow
GRG Control for $\bar{\omega}=0.6\bar{\omega}_c$

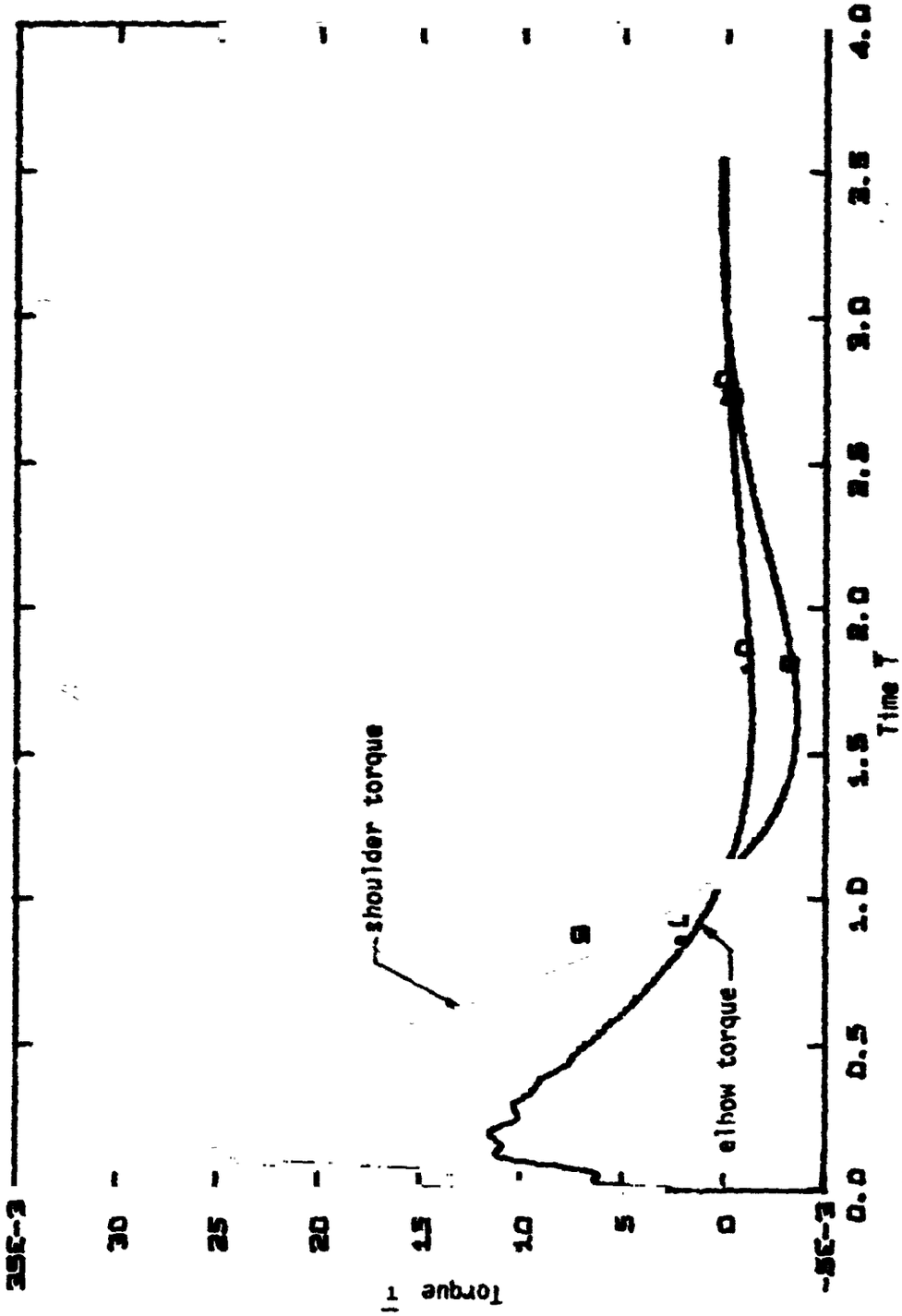


Figure 5.1b - Torque Response of Example 2 for Impulse at Elbow
GRG Control for $\bar{\omega} = 0.6\ \bar{\omega}_c$

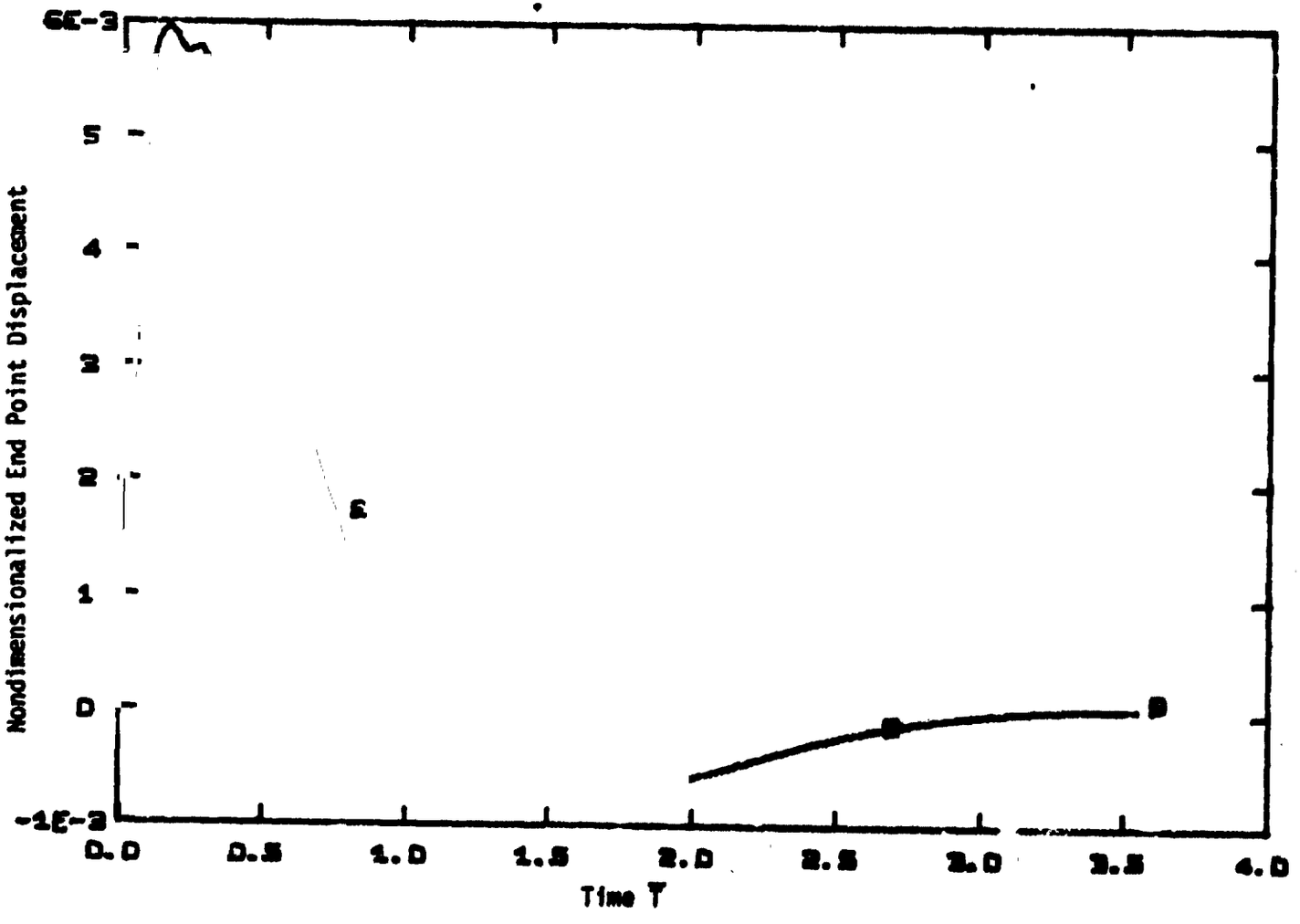


Figure 5.1c - End Point Displacement of Example 2 for Impulse at Elbow
GRG Control for $\bar{\omega} = 0.6\ \bar{\omega}_c$

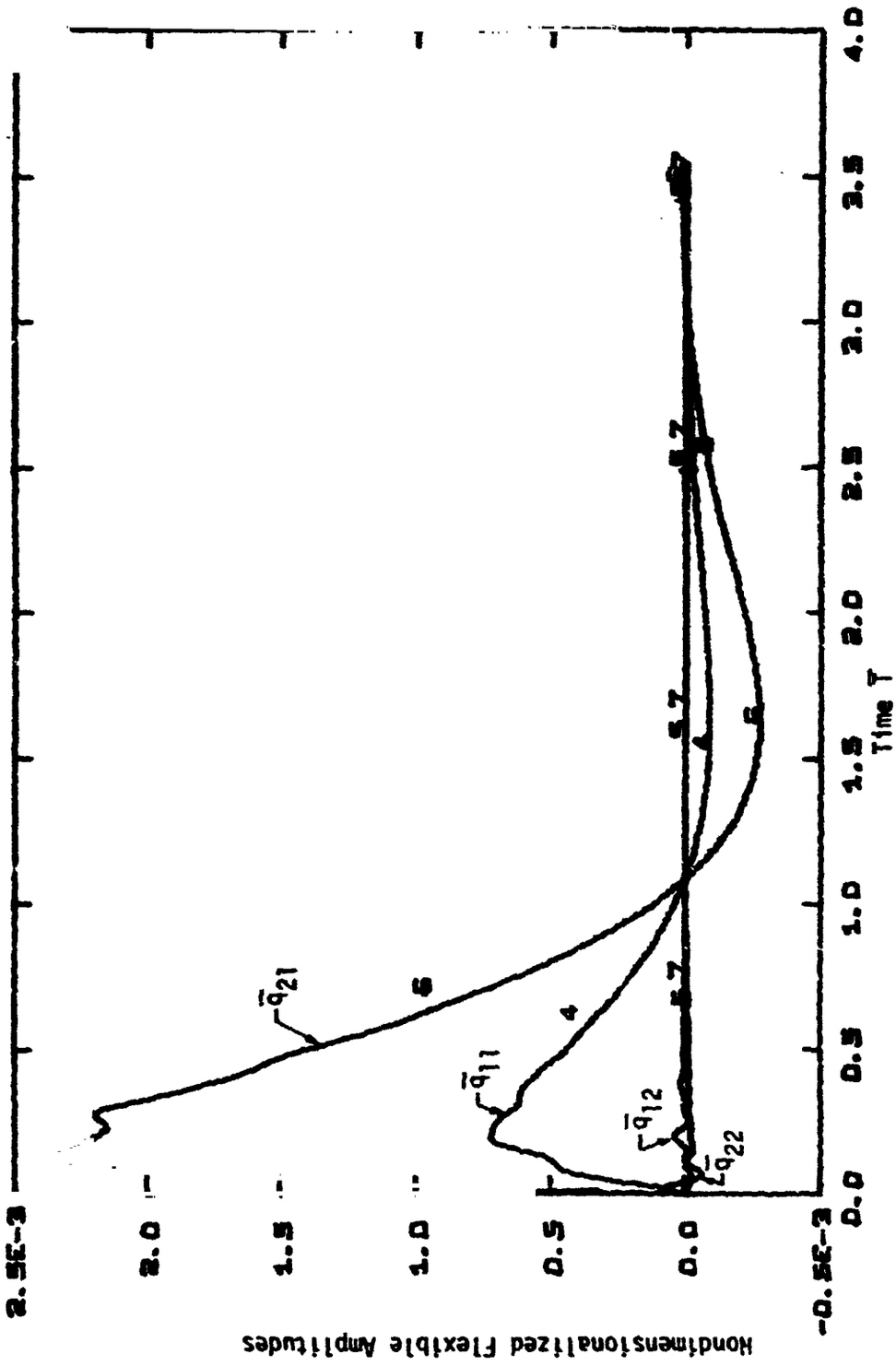


Figure 5.1d - Flexible Amplitudes Response of Example 2 for Impulse at Elbow GRG Control for $\bar{\omega} = 0.6\,\bar{\omega}_c$

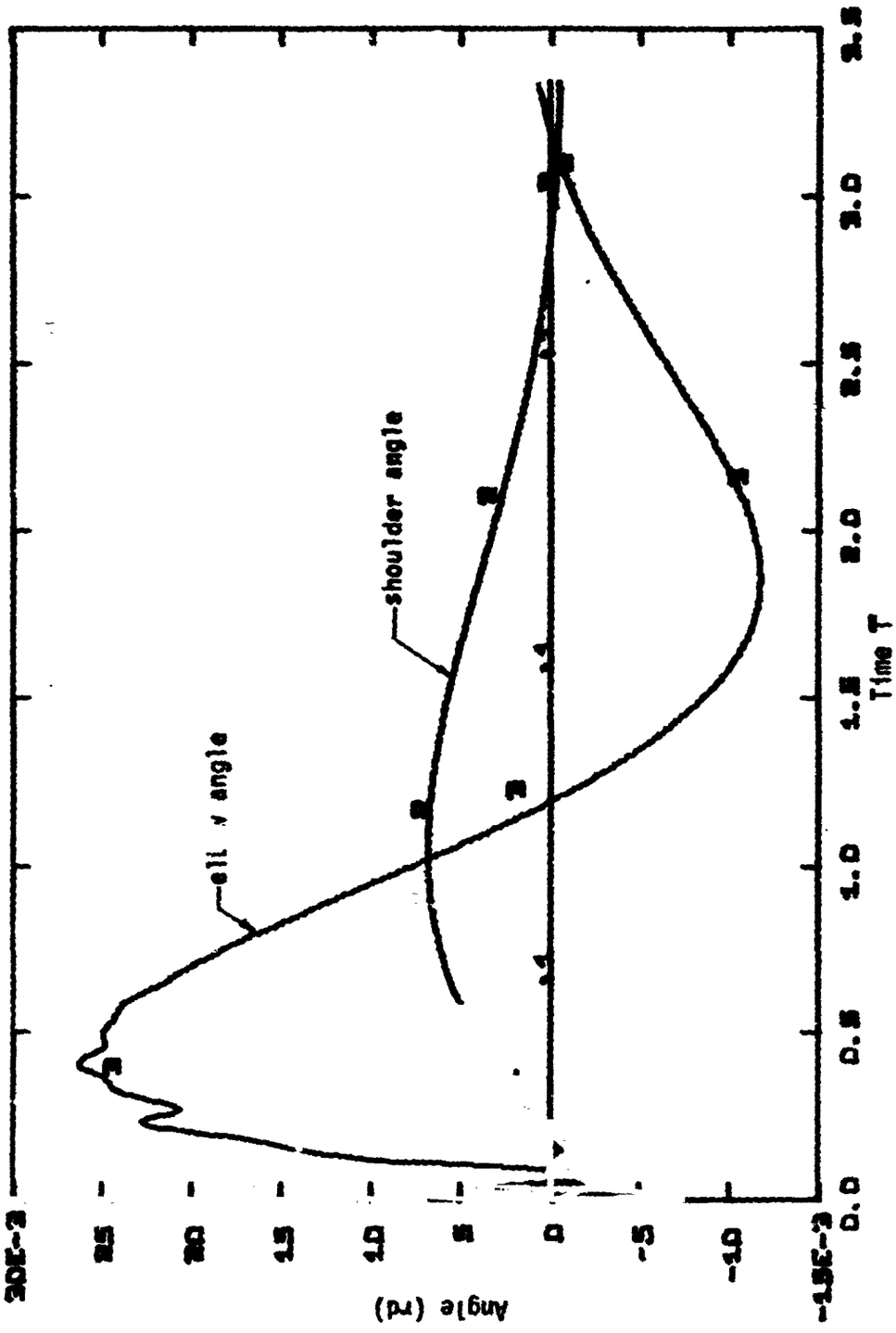


Figure 5.2a - Angle Response of Example 2 for Impulse at Elbow
SMA Control for same poles of GRG with $\tilde{\omega} = 0.6\tilde{\omega}_c$

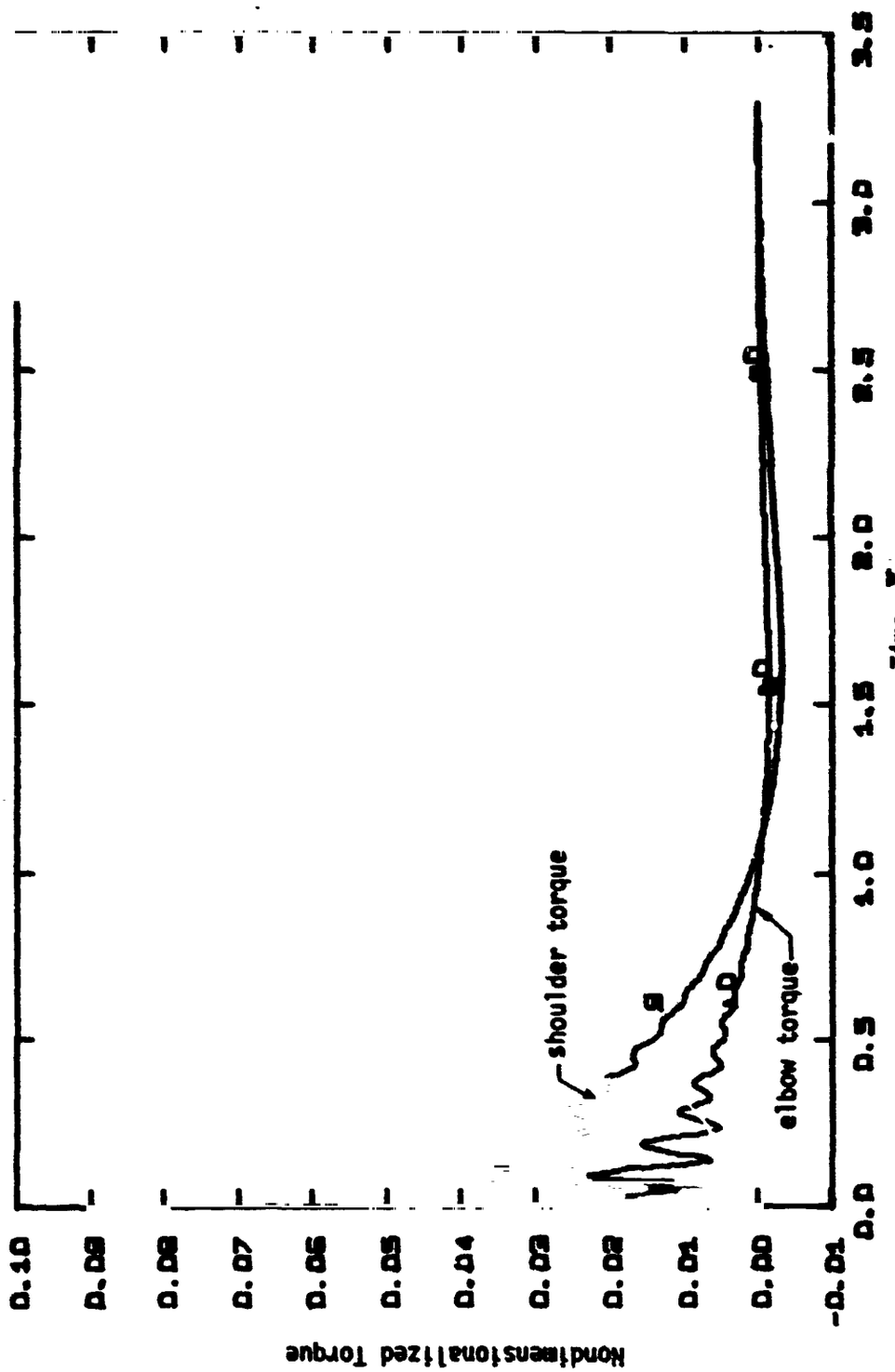


Figure 5.2b - Torque Response of Example 2 for Impulse at Elbow SMA Control for same poles of GRG with $\bar{\omega} = 0.6\ \bar{\omega}_c$

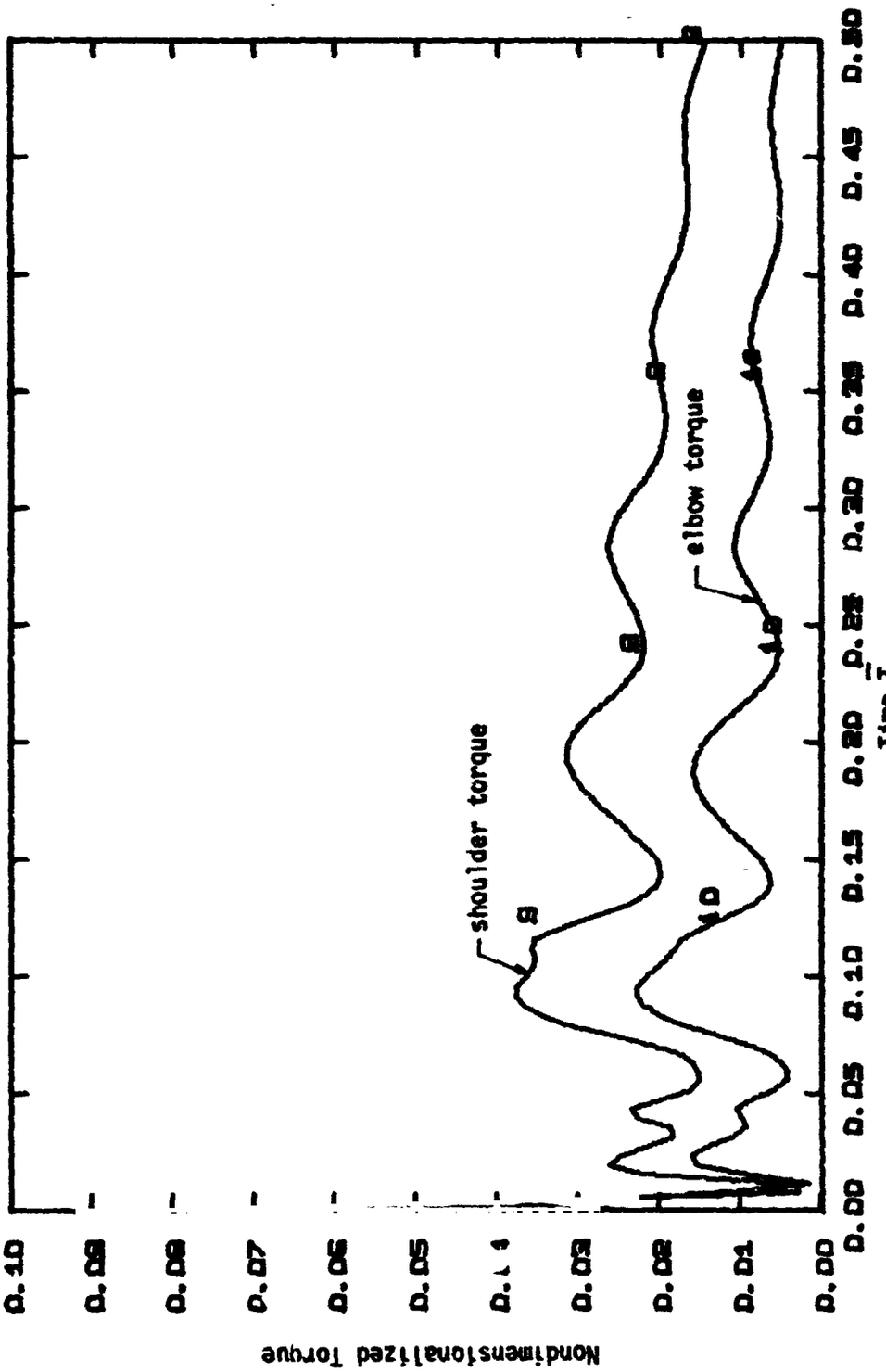


Figure 5.2c - Torque at Starting Simulation of Figure 5.2b

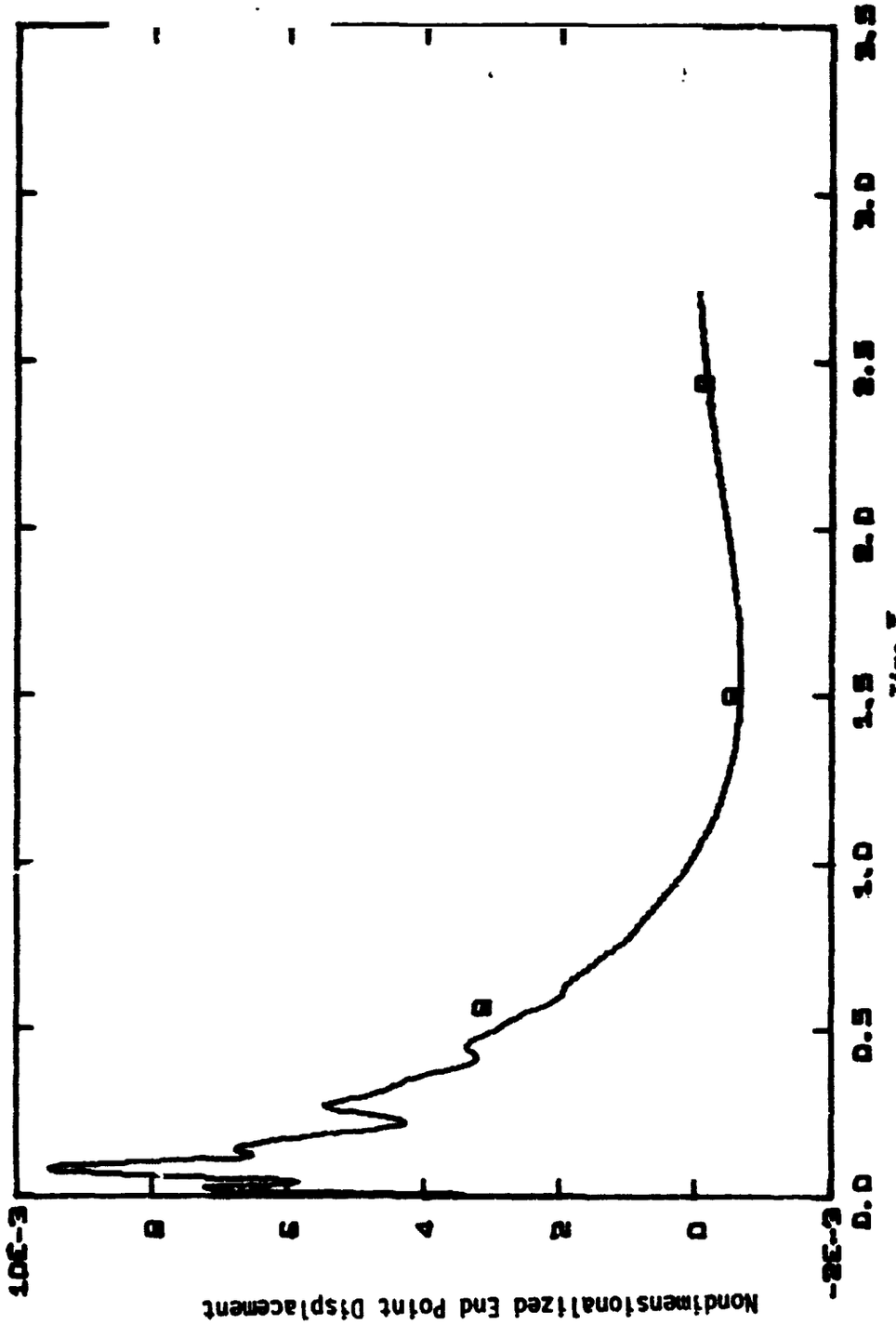


Figure 5.2d - End Point Displacement of Example 2 for Impulse at Elbow
SMA Control for same poles of GRG with $\bar{\omega} = 0.6\bar{\omega}_c$

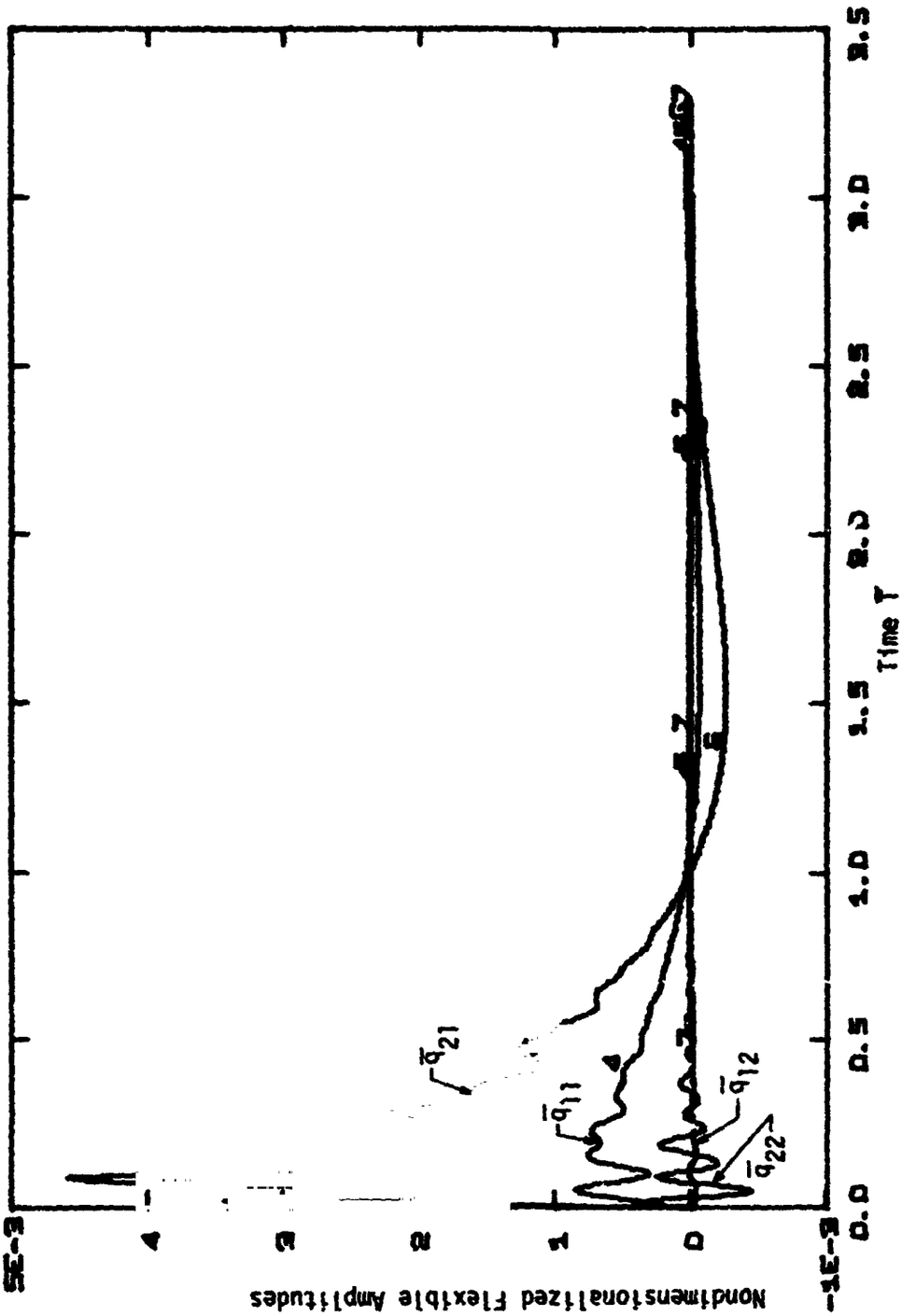


Figure 5.2e - Flexible Amplitude Response of Example 2 for Impulse at Elbow SMA Control for same poles of GRG with $\bar{\omega} = 0.6\,\bar{\omega}_c$

at the starting point. Finally, the end point displacement and flexible amplitudes are about twice as large when modal control is applied, as can be seen in Figures 5.1c, 5.1d, 5.2c, 5.2d. Here it is important to notice that the different behavior presented by the system when using modal control algorithm with poles equivalent to the general rigid gains application can be justified by the fact that the eigenvectors are not the same. That is, with the modal control algorithm it is possible to bring the poles to some desired location but it is not necessarily true that the eigenvectors will be the same.

Following the previous results an attempt was made to improve the system response by applying modal control (SIA) to the general rigid gain (Figure 5.2) case and move the two dominant poles to a value of $\bar{W}$ about 2.5 times larger than the case of Figure 5.2 ($\bar{W}$ equals 1.5 of $\bar{W}_c$ the dimensionless clamped-free natural frequency). The remaining poles in this application were not moved. The results for the same impulse response can be seen in Figure 5.3. The angles variations are smaller than the previous case (Figure 5.2) with relatively higher oscillation. Despite the fact that the poles were moved to a position of $\zeta = 0.707$ damping, the sensitivities are so high that as soon as the system starts moving the new pole locations indicate a considerable loss in system damping. The torque history presents about the same maximum as the previous case but acting for a longer period of time. The end point displacement and flexible amplitudes represent a considerable increase from the previous case as can be seen in Figures 5.3c and 5.3d.

Another control was then designed for example 2 using the general

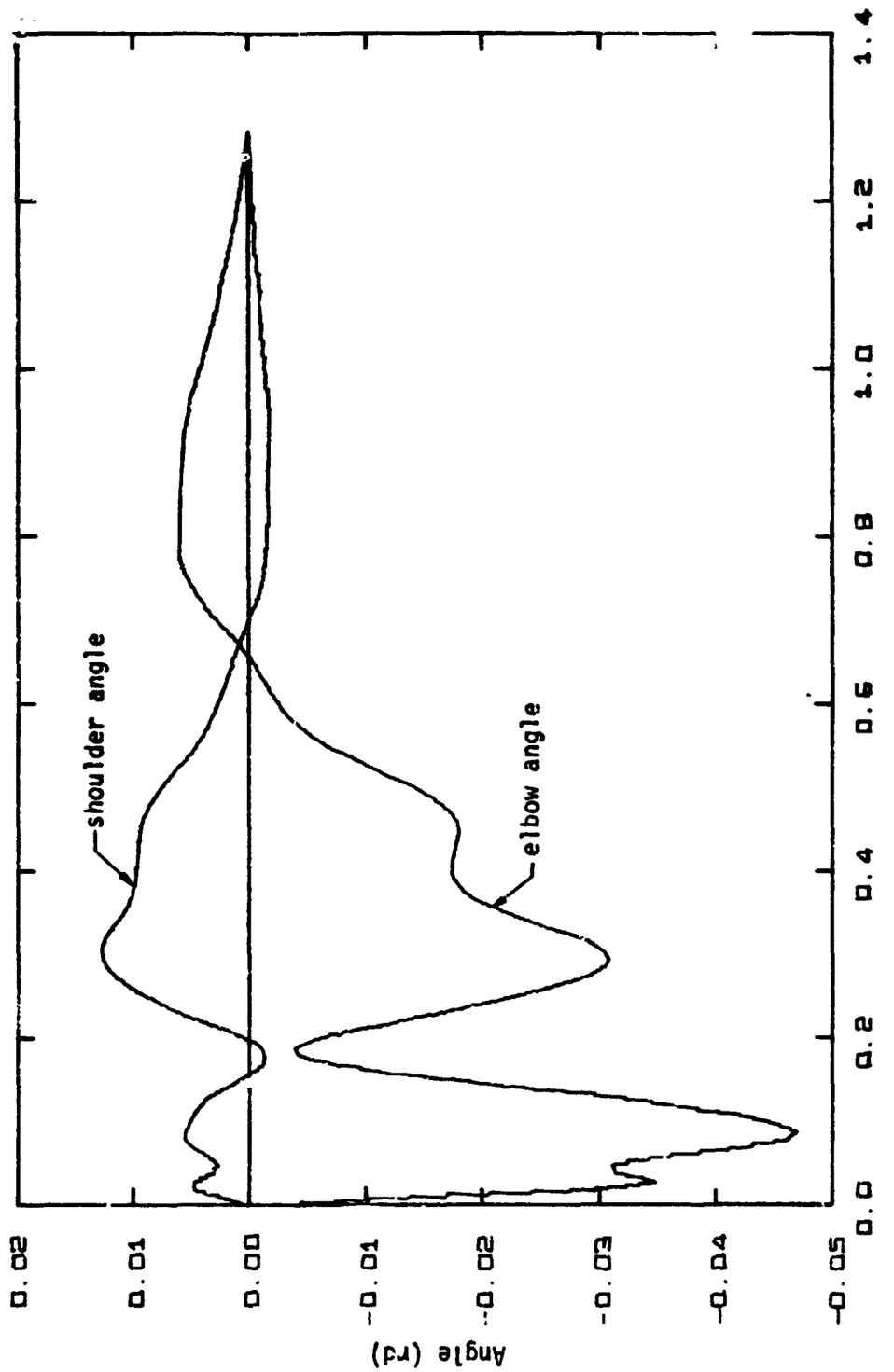


Figure 5.3a - Angle Response of Example 2 for Impulse at Elbow
SMA Control with dominant poles at $\bar{\omega} = 1.5\bar{\omega}_c$

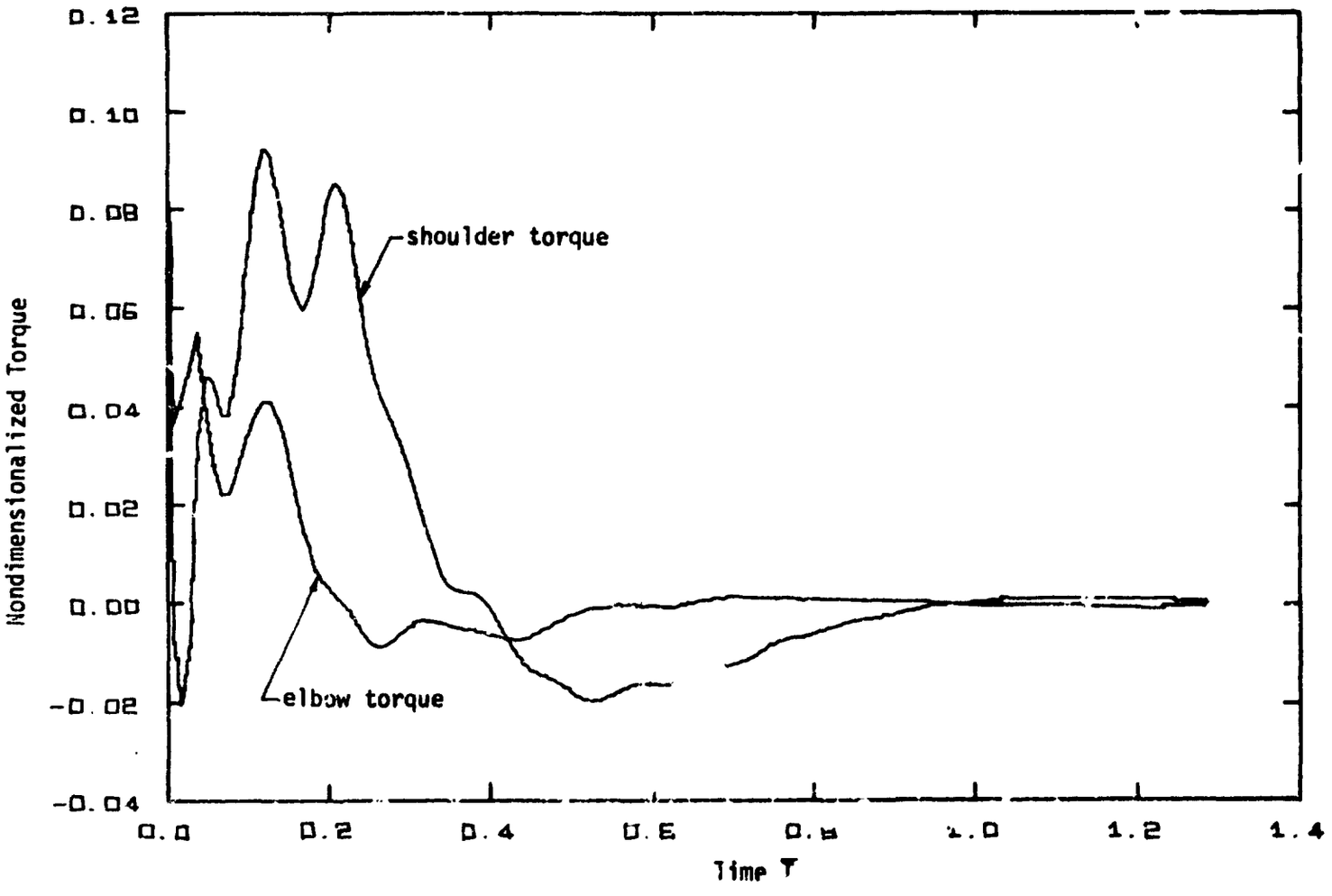


Figure 5.3b - Torque Response of Example 2 for Impulse at Elbow
SMA Control with dominant poles at $\bar{\omega} = 1.5\ \bar{\omega}_c$

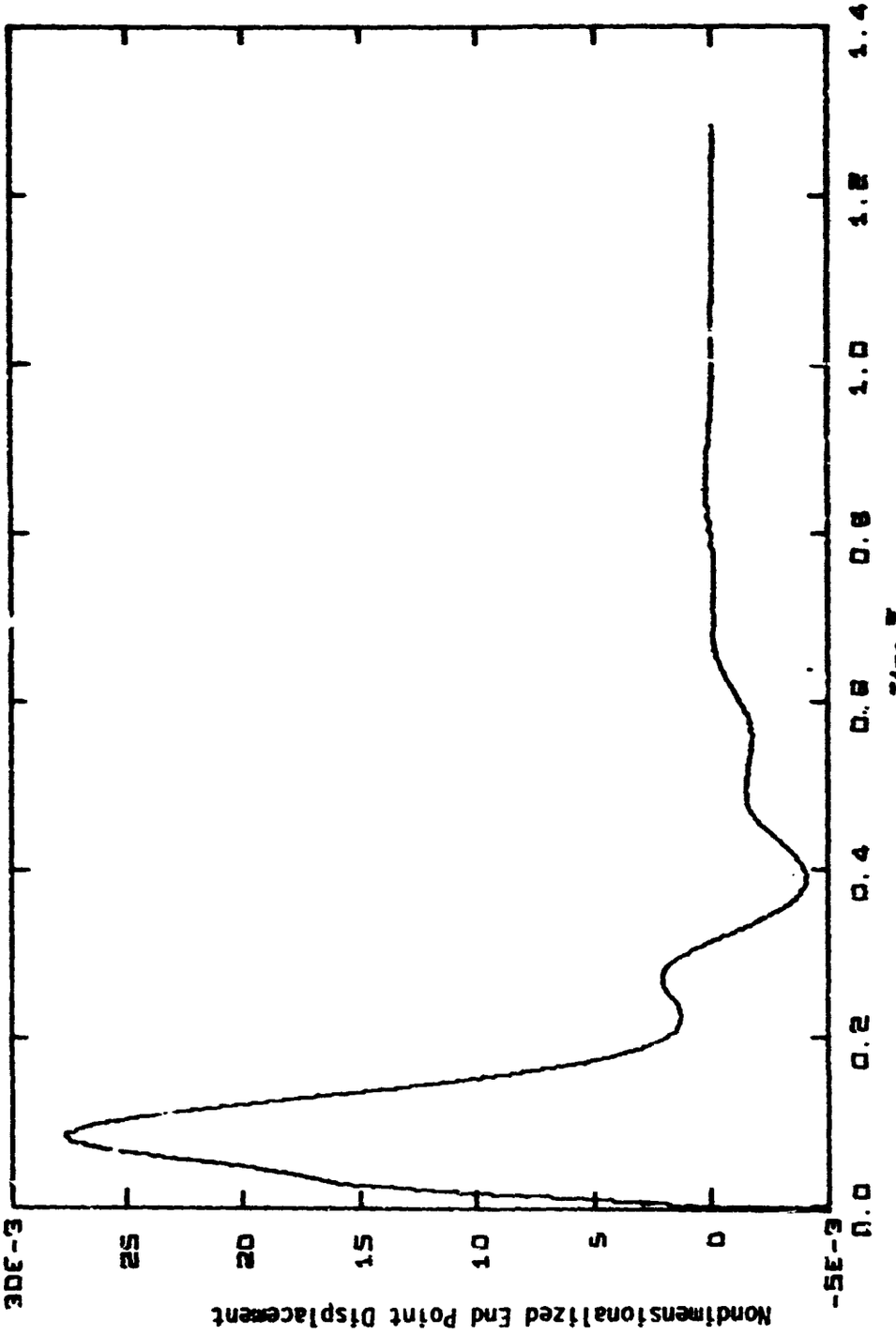


Figure 5.3c - End Point Displacement of Example 2 for Impulse at Elbow
SMA Control with dominant poles at $\bar{\omega} = 1.5\bar{\omega}_c$

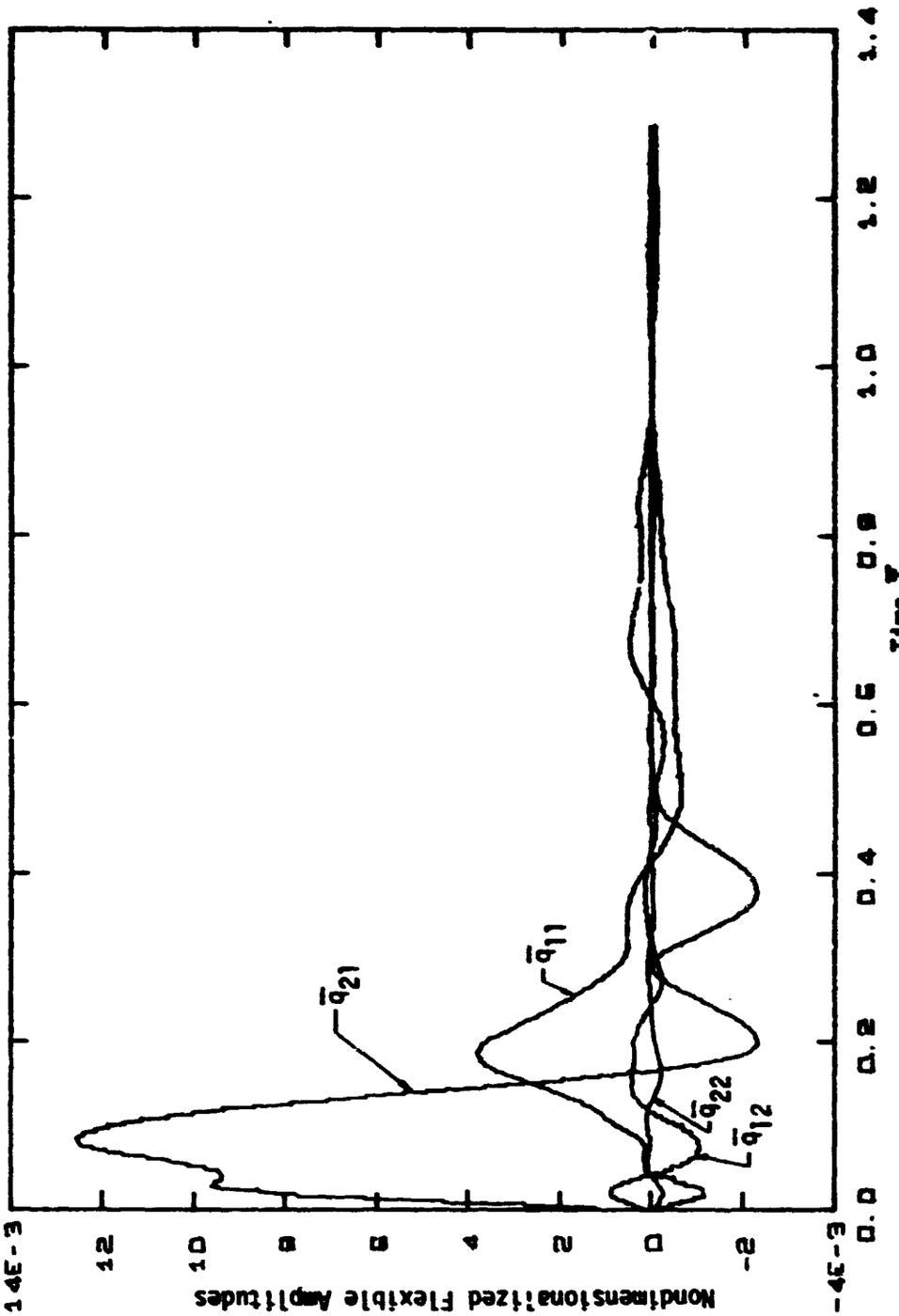


Figure 5.3d - Flexible Amplitude Response of Example 2 for Impulse at Elbow SMA Control with dominant poles at $\bar{w} = 1.5\ \bar{w}_c$

rigid gain method. For this situation the gains were obtained by specifying the dominant poles of the rigid system at 0.9 ($\bar{w} = 0.9\bar{w}_c$) of the dimensionless natural frequency of the clamped-free associated system. The results are shown in Figure 5.4a which correspond to a response to torque impulse at the shoulder. The response presents a smooth behavior that is similar to the simulation of a rigid system.

Again for example 2 some gross motion simulations were performed. In all cases the system was supposed to move the elbow angle from -15° to +15° according to a double parabola specified as reference input. In Figure 5.4 it is shown the pole variations when the control remains constant and the elbow angle is changed from 0° to ± 90°. Since the control was designed for 0° elbow angle (the same as in Figure 5.1 with GRG) the arm bandwidth is decreased for working at elbow angle of 90°.

If one recalls Figures 5.1 it is seen that the nondimensionalized settling time is of the order of $\bar{T}_s = 3.5$. The system was simulated tracking double parabolas of joint angle $\theta_2$ of durations $0.5\bar{T}_s$, $1.0\bar{T}_s$ and $2.0\ \bar{T}_s$ respectively. This set of results can be seen in Figures 5.5, 5.6 and 5.7 and one could say that the recommended time to perform the motion should be set equal to the settling time of the system at zero angle position. With this in mind all the conclusions were applied to the example 2 with $\bar{w} = 0.9$, that is, maximum bandwidth for the general rigid method and settling time from the parabola tracking. The results can be seen in Figure 5.8. It is important to notice that Figure 5.8d represents the flexible components appearing in the system as described in equation (2.36), representing an additional torque generated by the

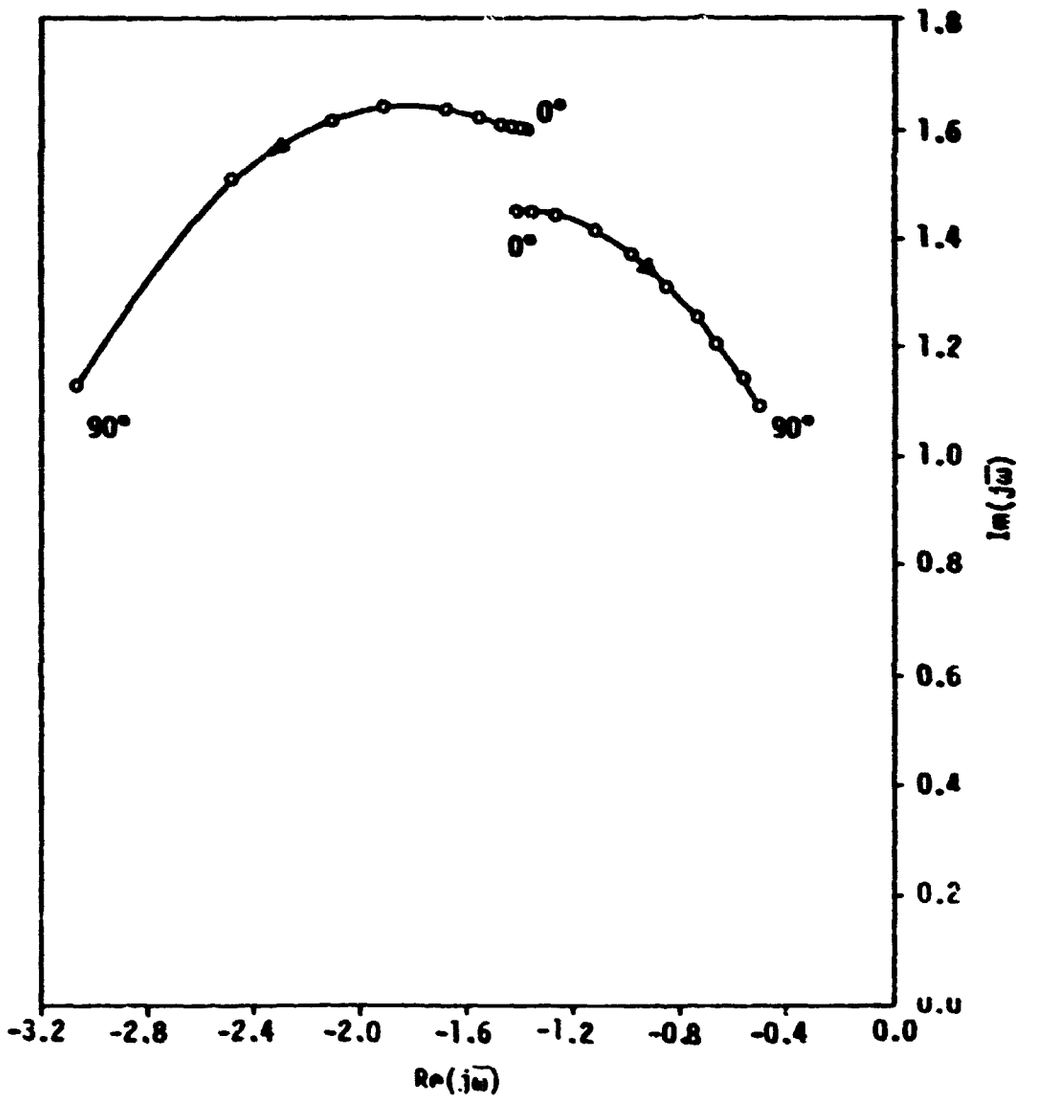


Figure 5.4 - Root locus of dominant poles for variations of elbow angle - Example 2 - GRG Control for $\bar{\omega} = 0.6\bar{\omega}_c$

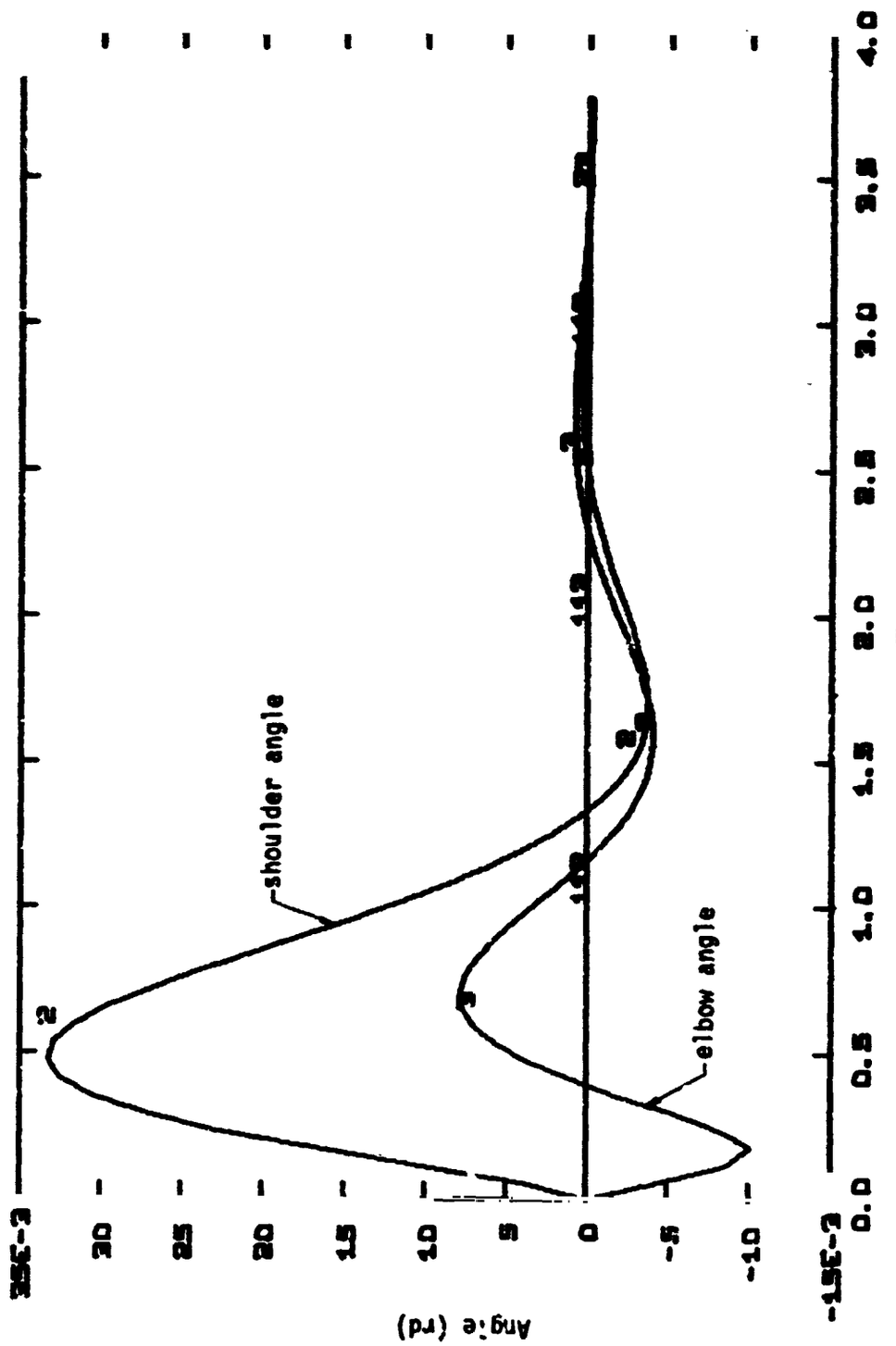


Figure 5.4a - Angle Response of Example 2 for Impulse at Shoulder
GRG Control for $\bar{\omega} = 0.9\bar{\omega}_c$

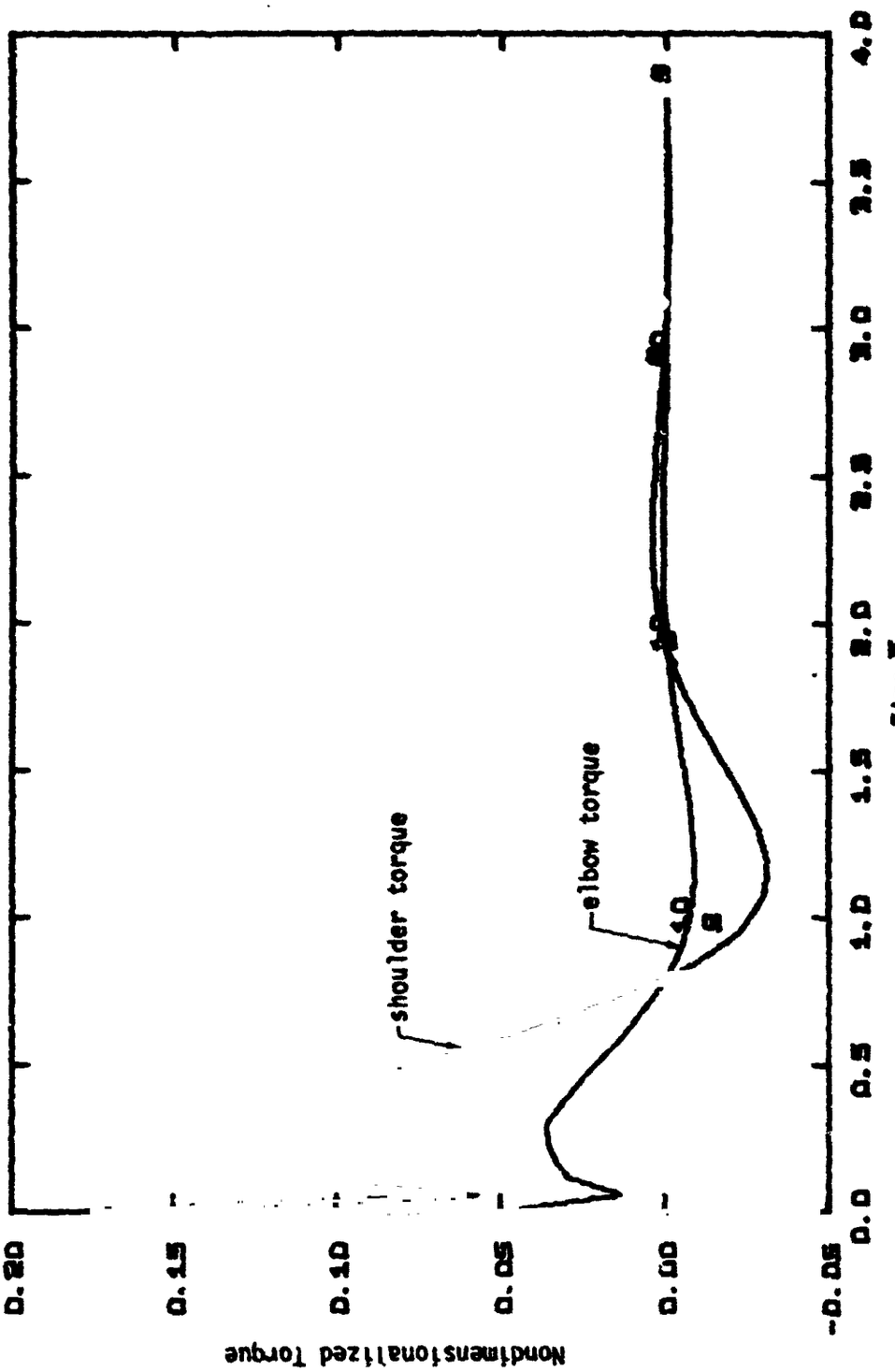


Figure 5.4b - Torque Response of Example 2 for Impulse at Shoulder
GRG Control for $\bar{\omega} = 0.9\bar{\omega}_c$

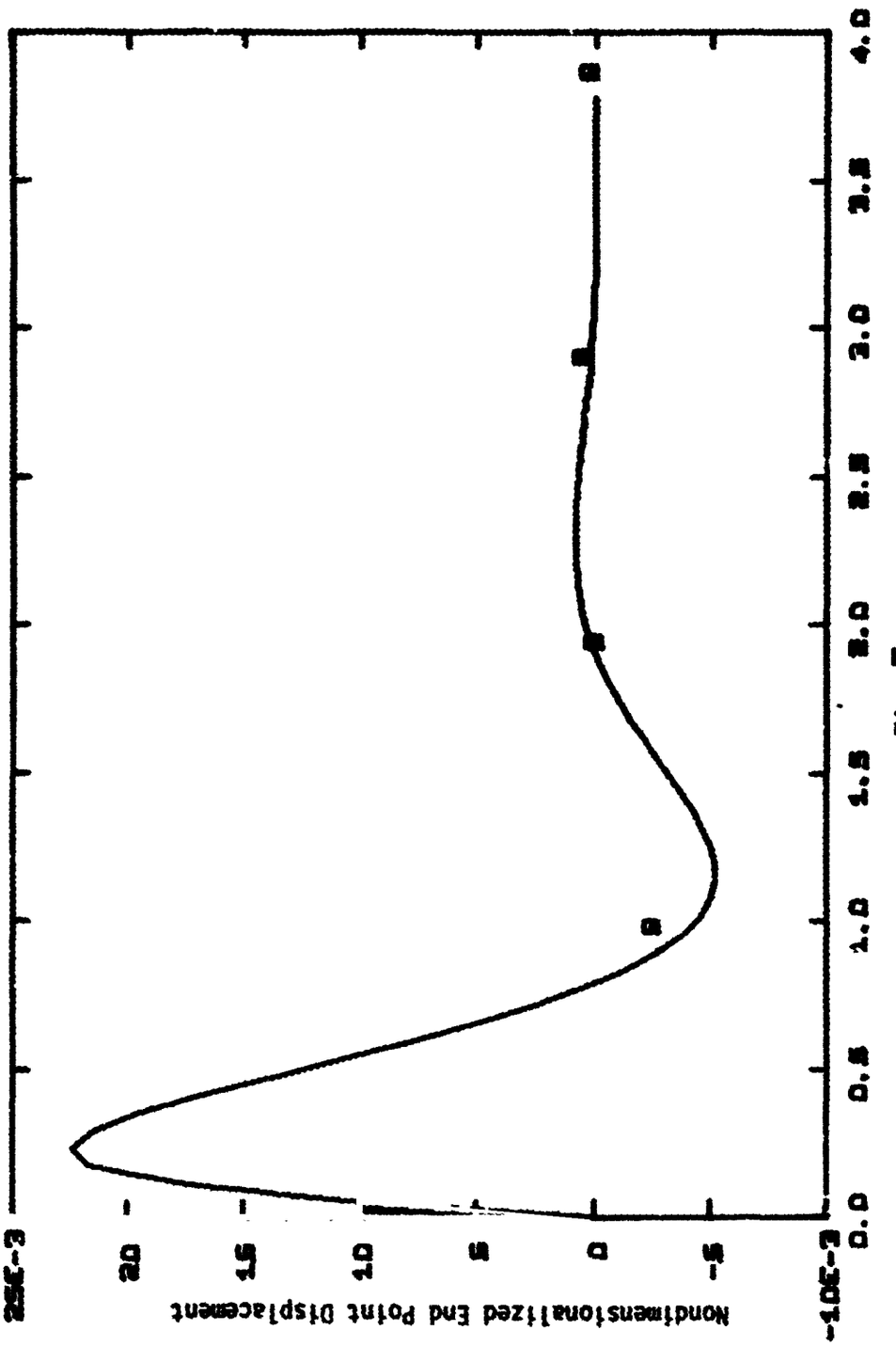


Figure 5.4c - End Point Displacement of Example 2 for Impulse at Shoulder
GRG Control for $\bar{\omega} = 0.9\,\bar{\omega}_c$

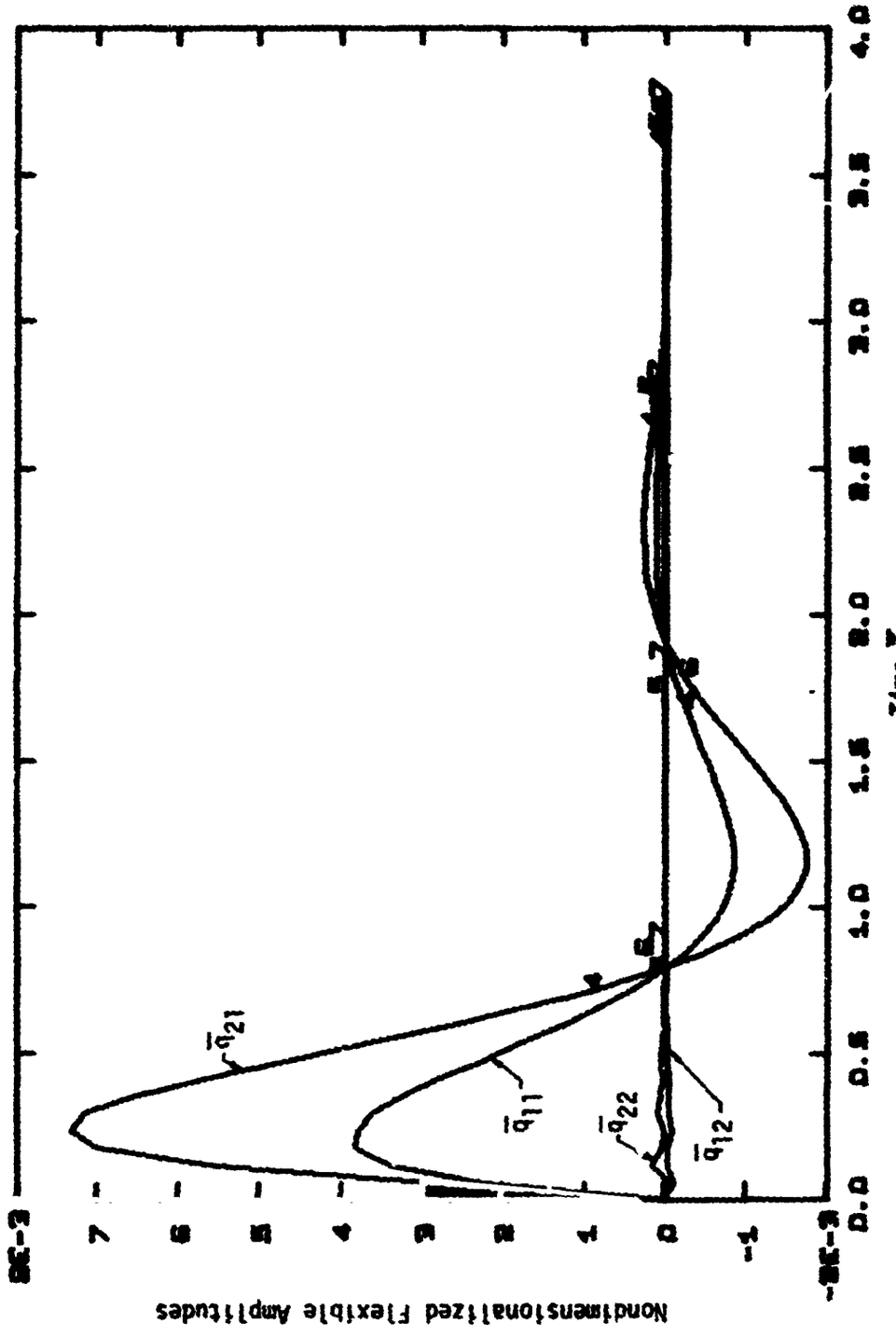


Figure 5.4d - Flexible Amplitude Response of Example 2 for Impulse at Shoulder
GRG Control for $\bar{\omega} = 0.9\,\bar{\omega}_c$

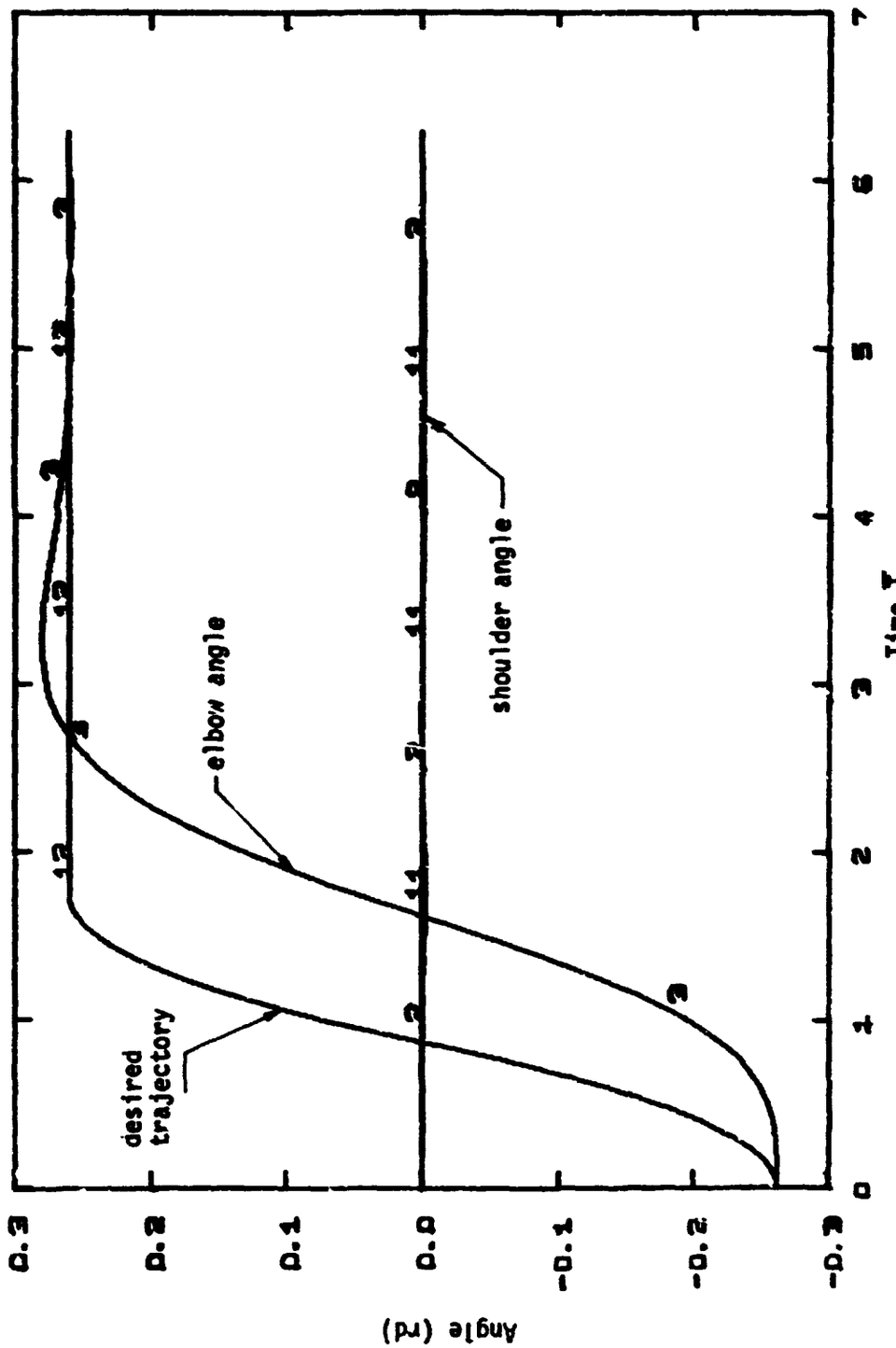


Figure 5.5a - Angle Response of Example 2 Tracking a double-parabola GRG Control for $\bar{\omega} = 0.6\ \bar{\omega}_c$ - Tracking Time Interval 1/2 of Settling Time of Figure 5.1

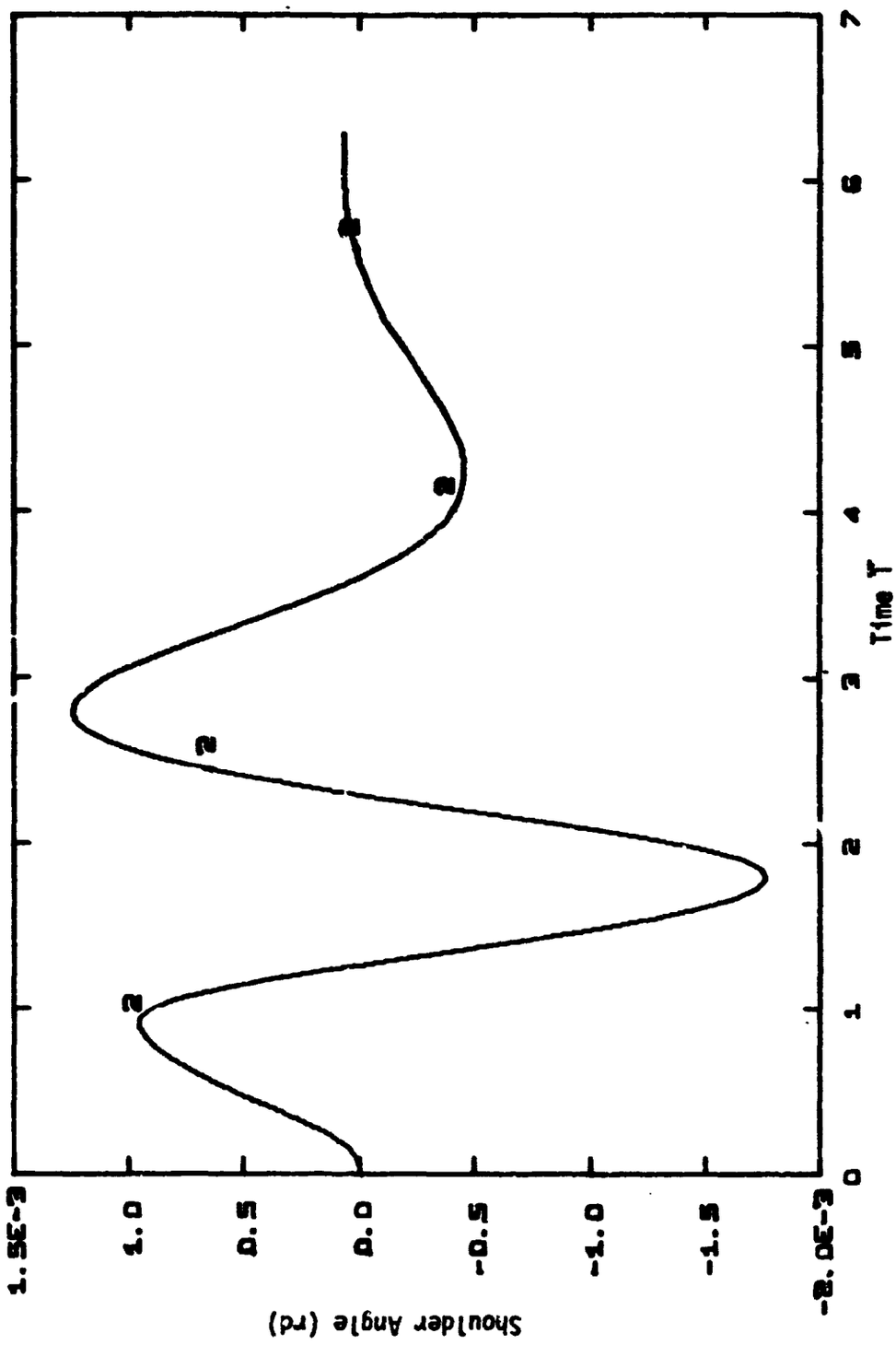


Figure 5.5b - Shoulder Angle Response of Example 2
Same Conditions of Figure 5.5a

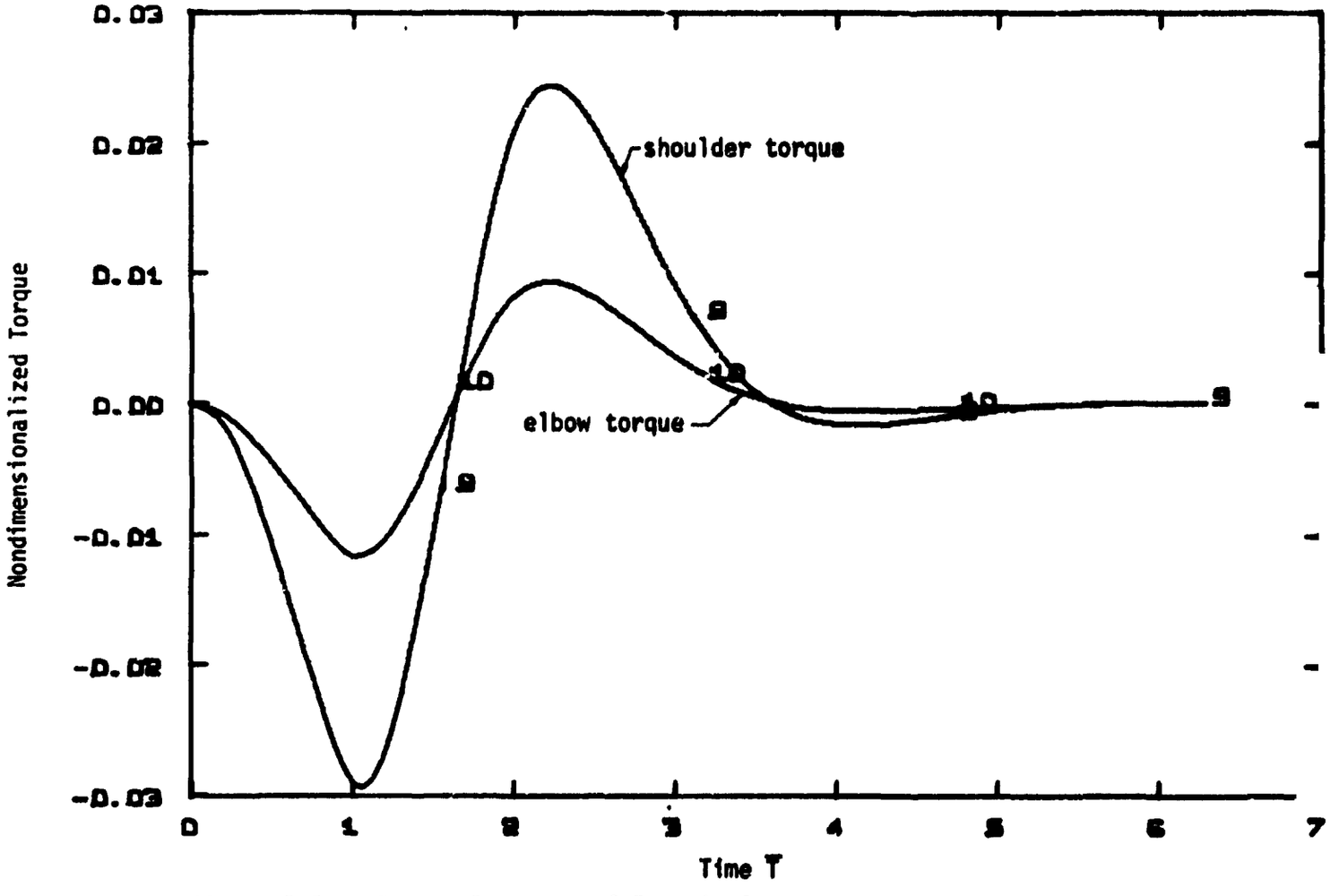


Figure 5.5c - Torque Response of Example 2
Same Conditions of Figure 5.5a

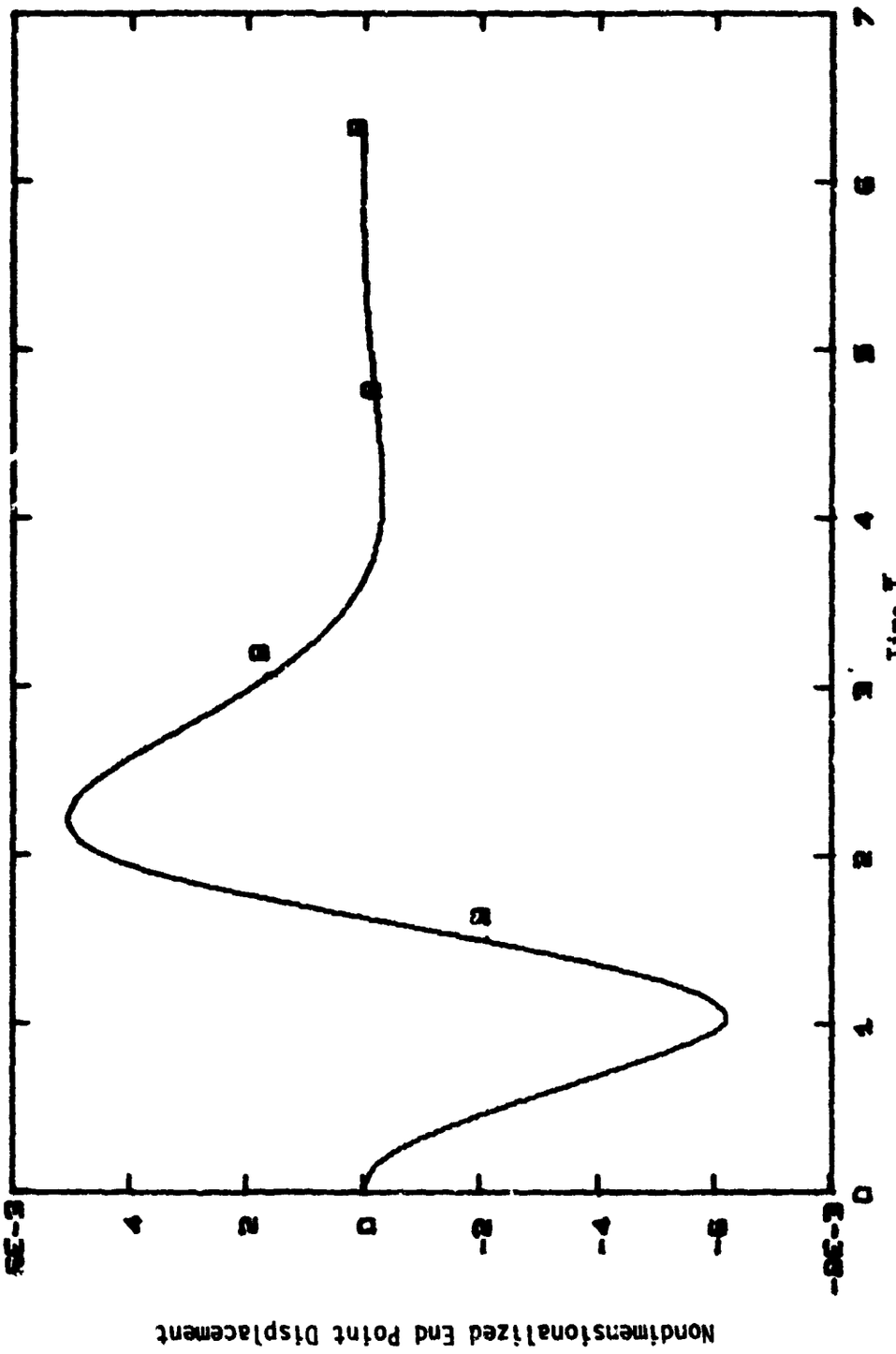


Figure 5.5d - End Point Displacement of Example 2
Same Conditions of Figure 5.5a

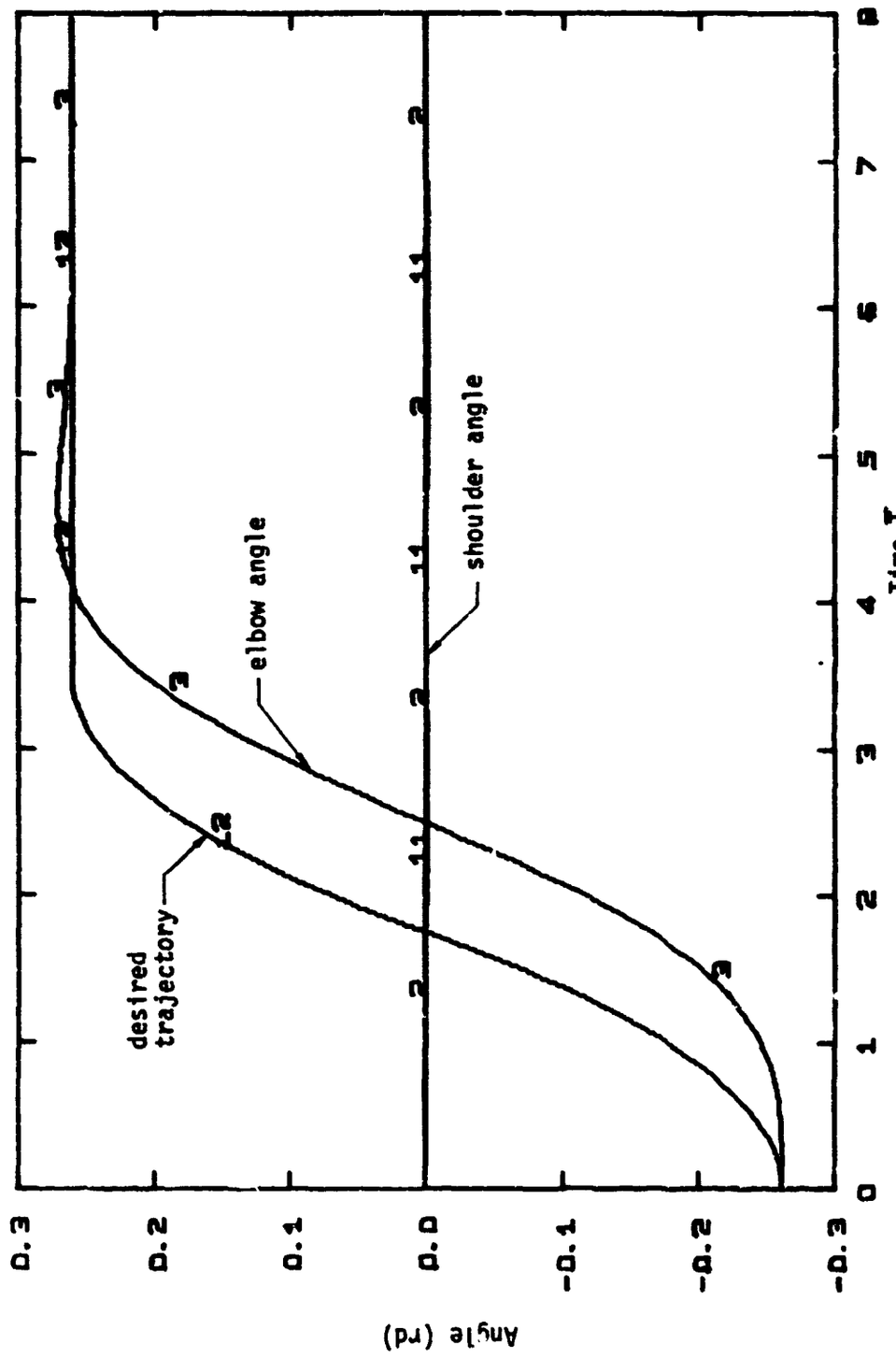


Figure 5.6a - Angle Response of Example 2 tracking a double-parabola GRG Control for $\bar{\omega} = 0.6\ \bar{\omega}_c$ - Tracking Time Interval Equal Settling Time of Figure 5.1

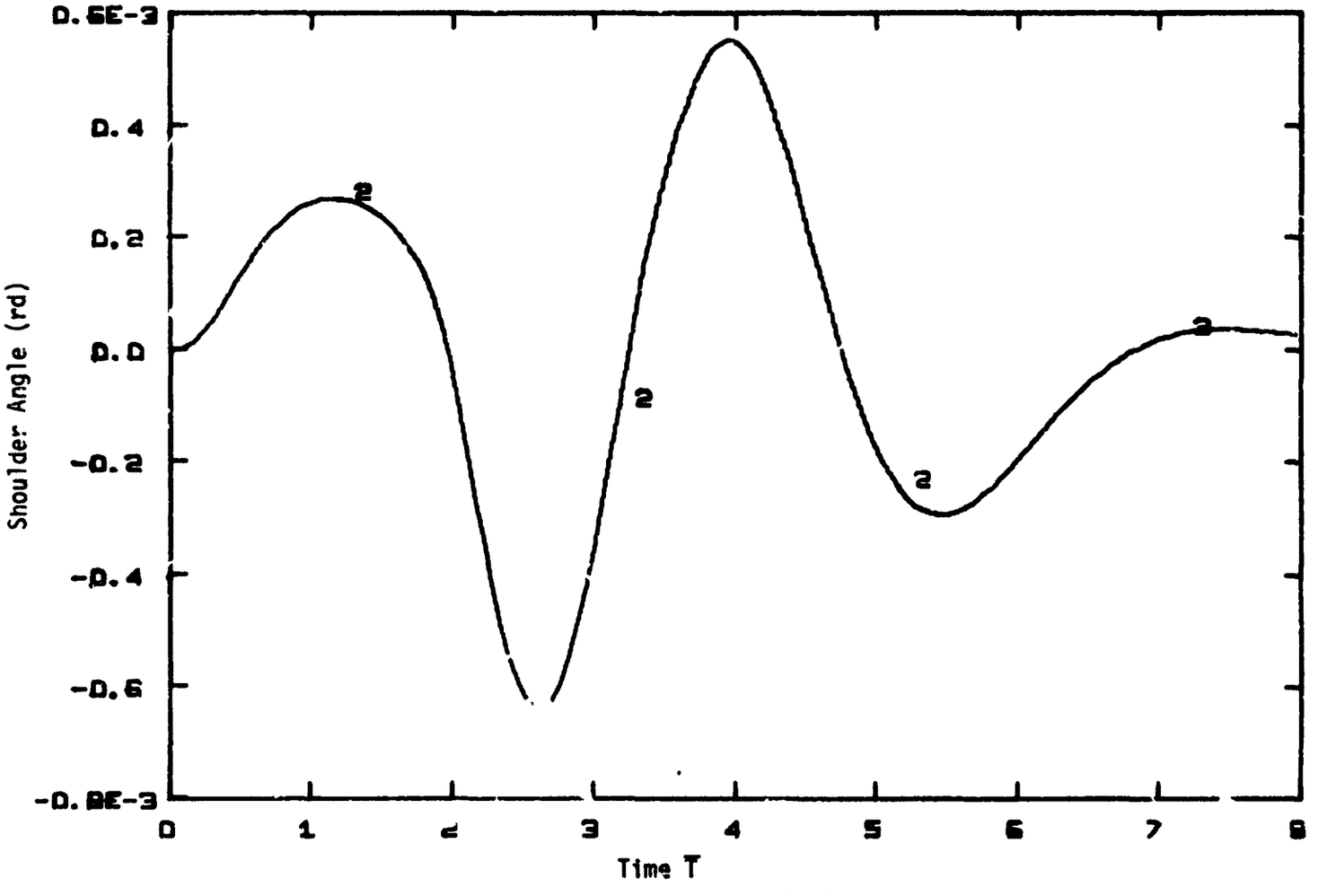


Figure 5.6b - Shoulder Angle Response of Example 2
Same Conditions of Figure 5.6a

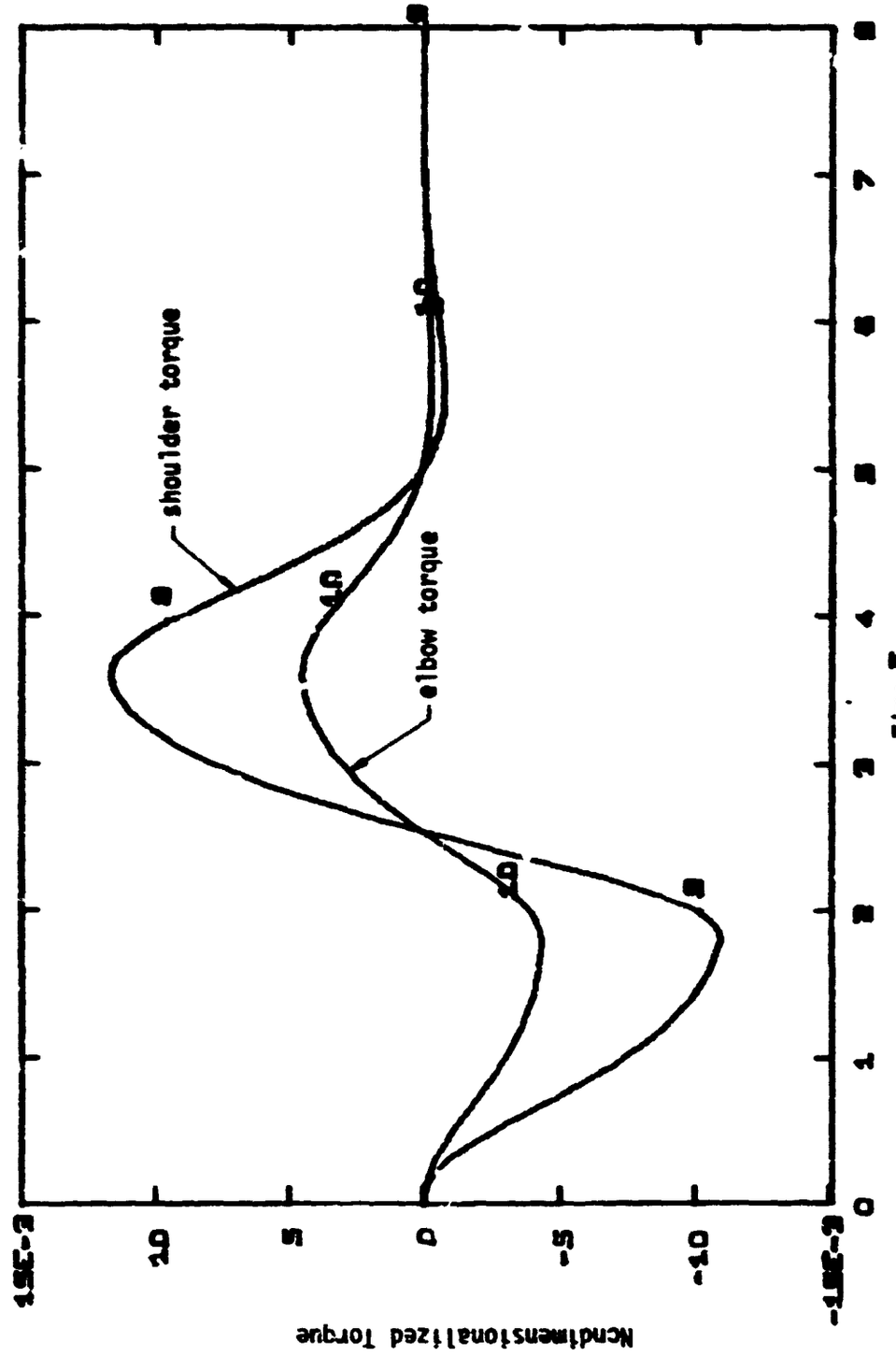


Figure 5.6c - Torque Response of Example 2
Same Conditions of Figure 5.6a

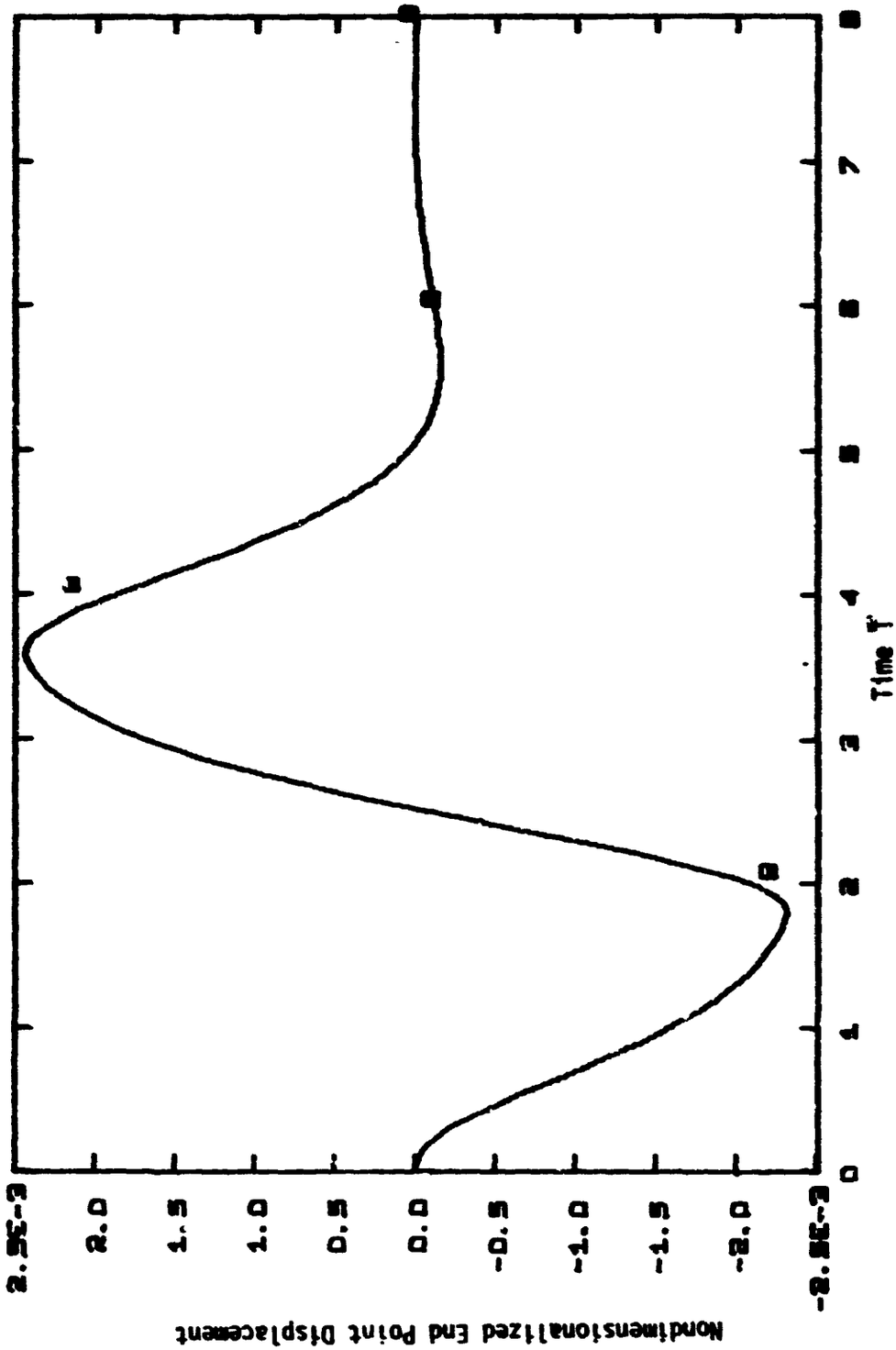


Figure 5.6d - End Point Displacement of Example 2
Same Conditions of Figure 5.6a

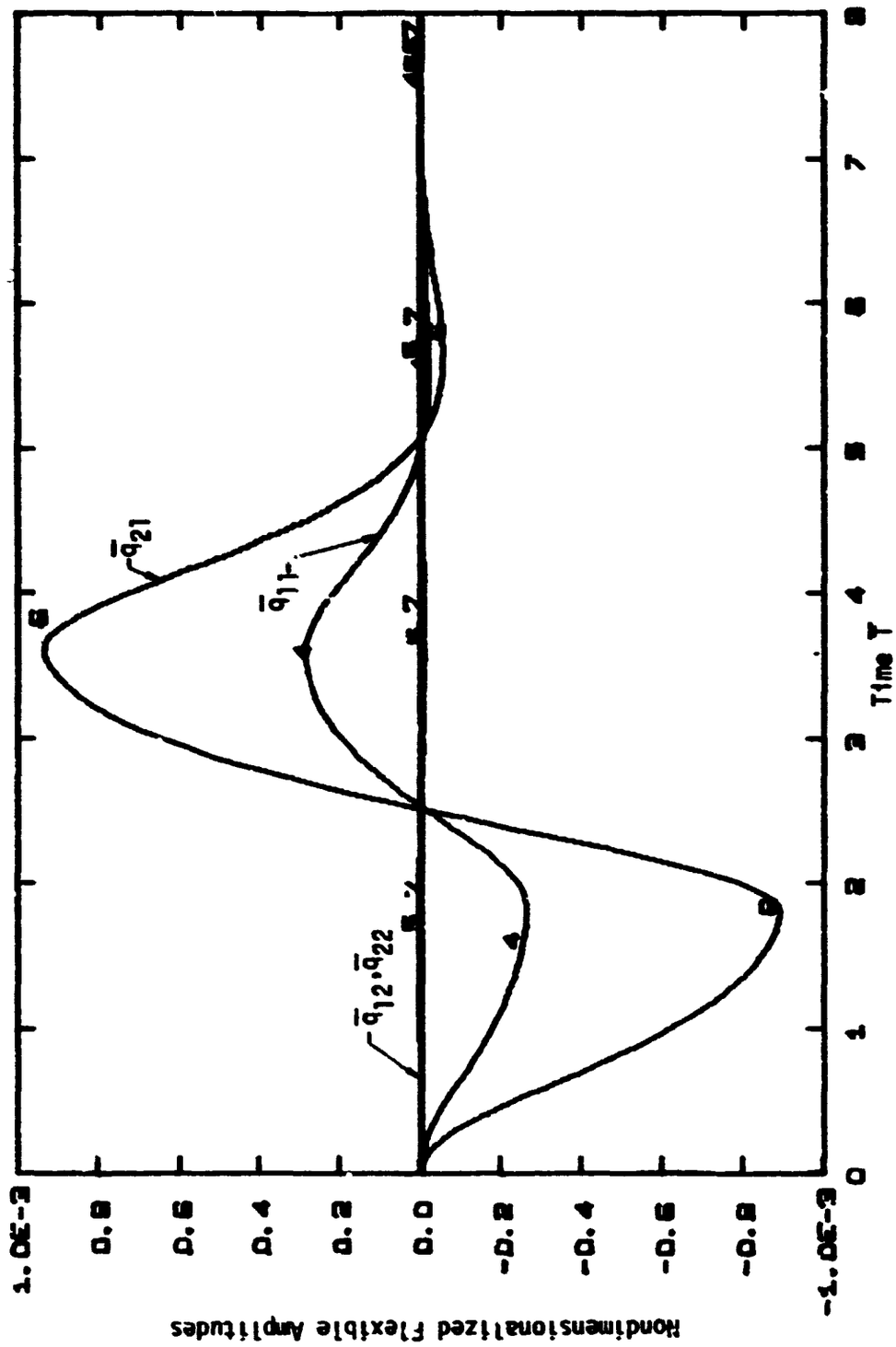


Figure 5.6e - Flexible Amplitudes of Example 2
Same Conditions of Figure 5.6a

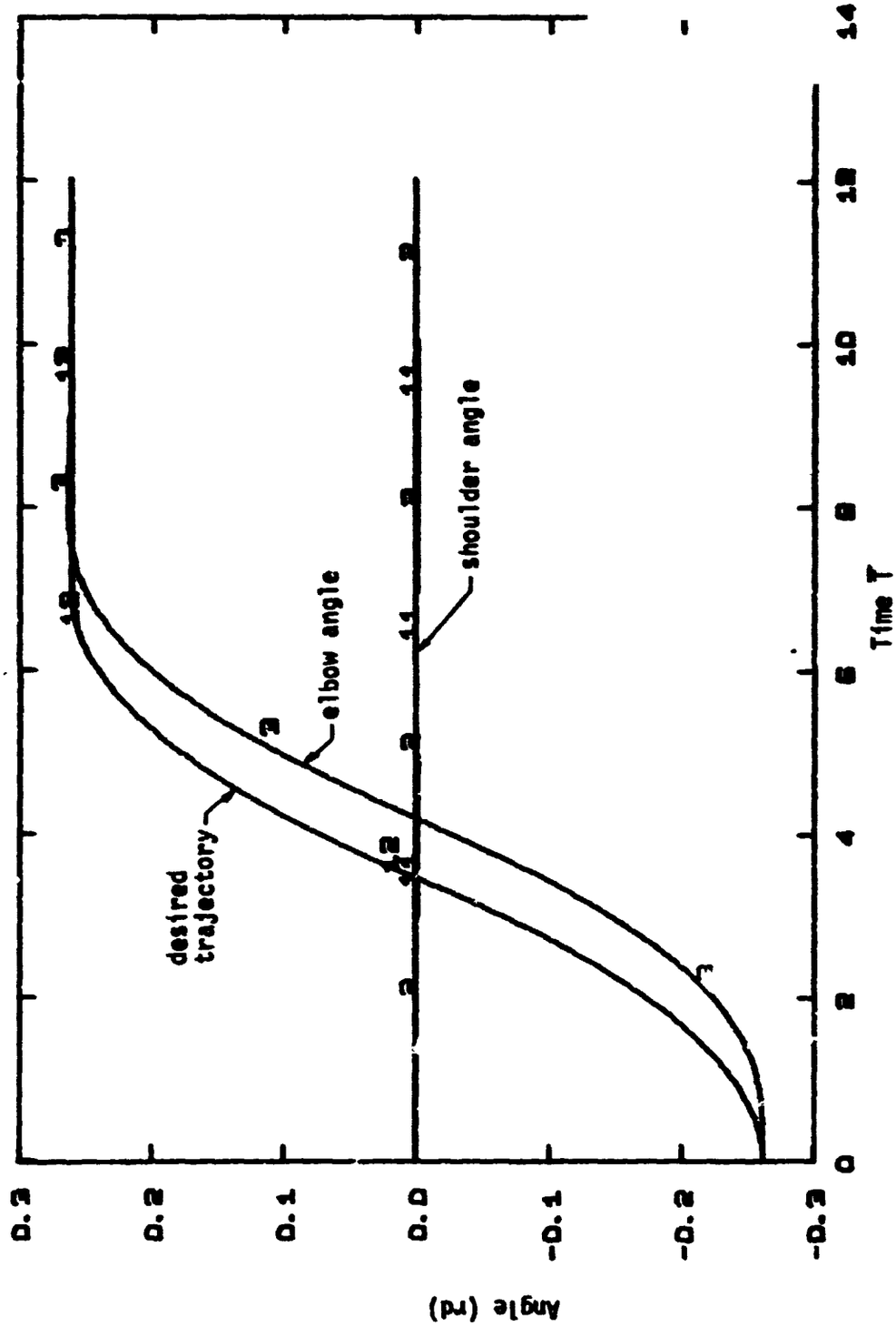


Figure 5.7a - Angle Response of Example 2 tracking a double-parabola
GRG Control for $\bar{\omega} = 0.6\ \bar{\omega}_c$ - Tracking Time Interval
Twice Settling Time of Figure 5.1

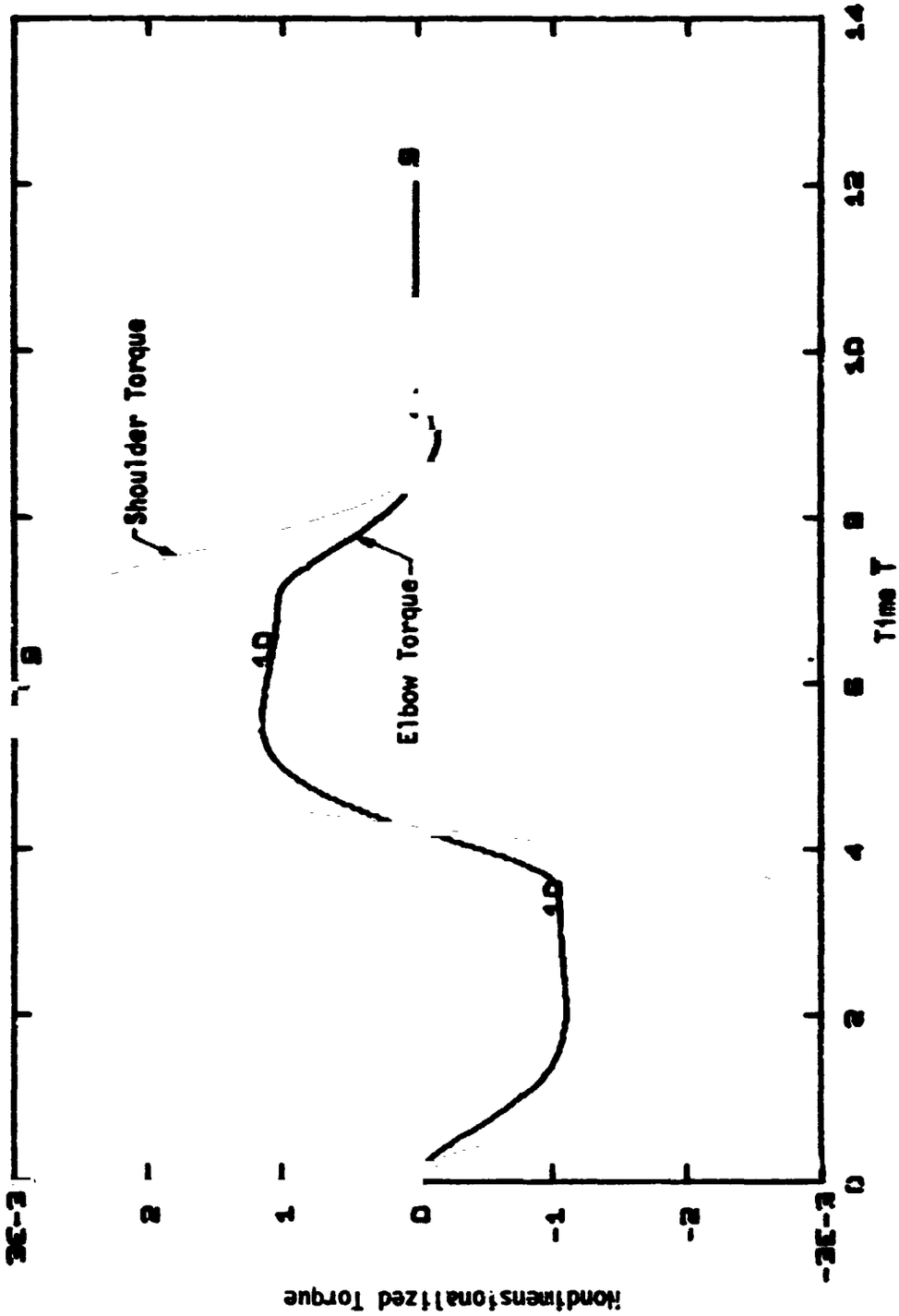


Figure 5.7b - Torque Response of Example 2
Same Conditions of Figure 5.7a

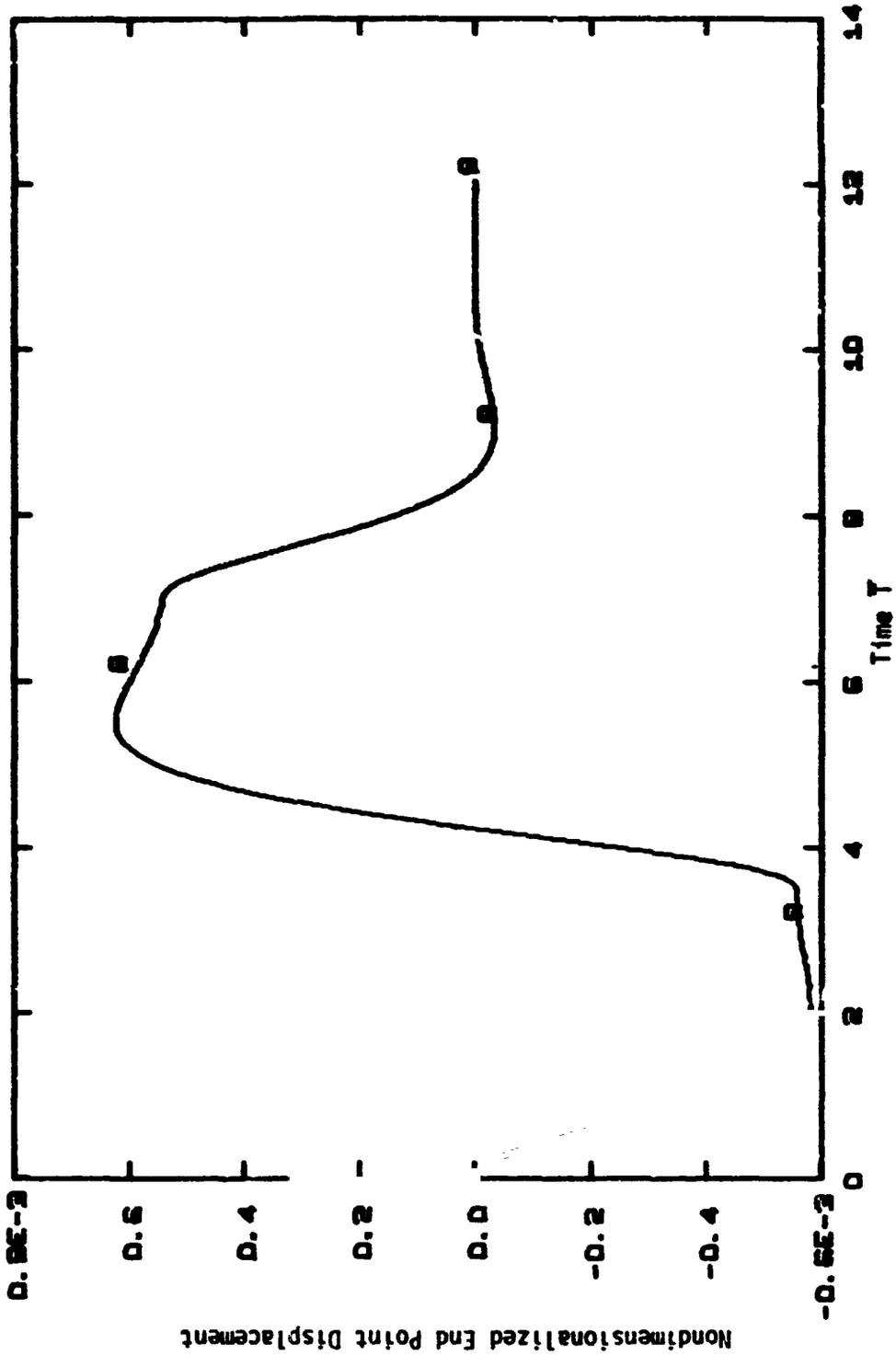


Figure 5.7c - End Point Displacement of Example 2
Same Conditions of Figure 5.7a

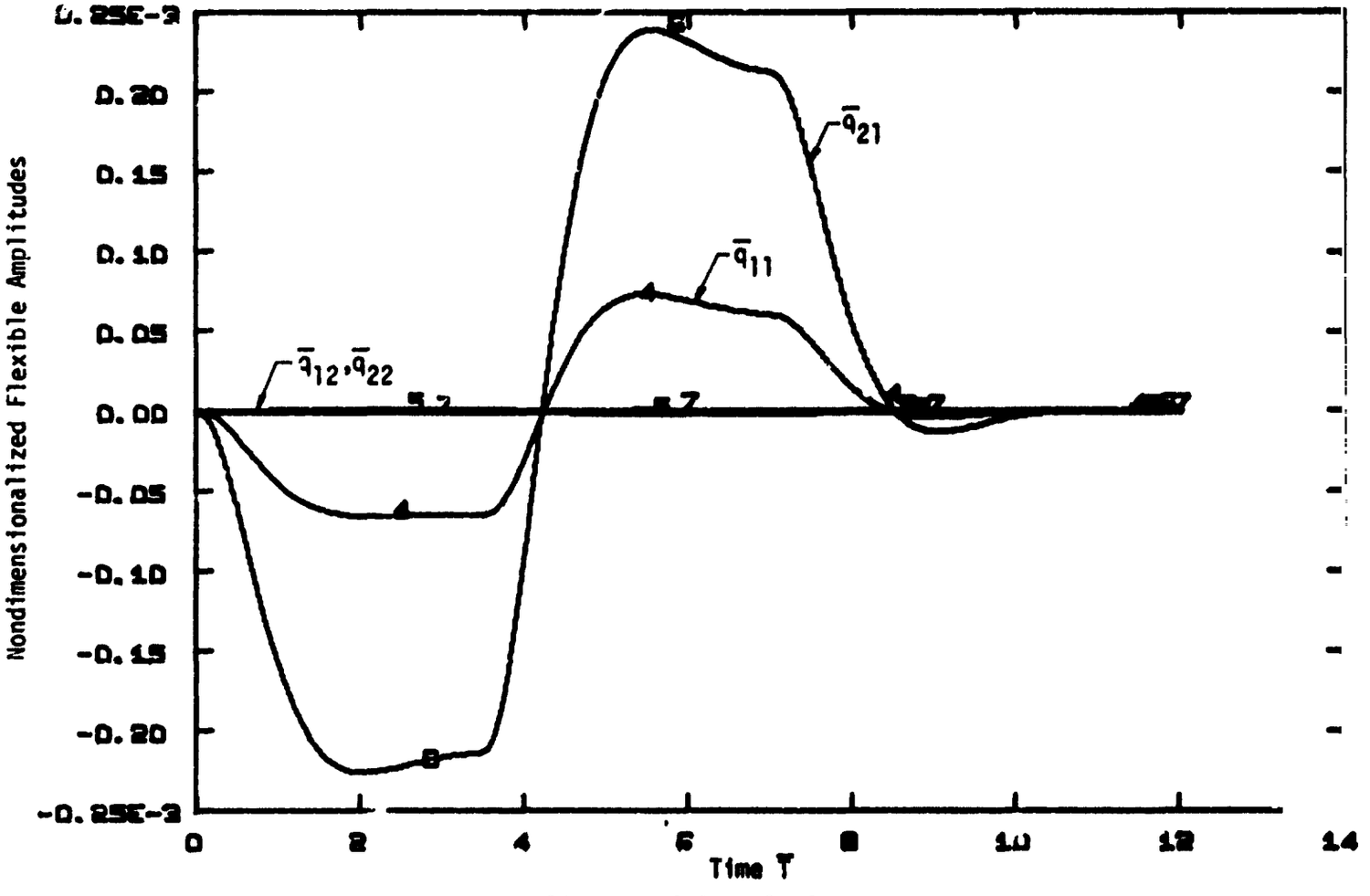


Figure 5.7d - Flexible Amplitudes of Example 2
Same Conditions of Figure 5.7a

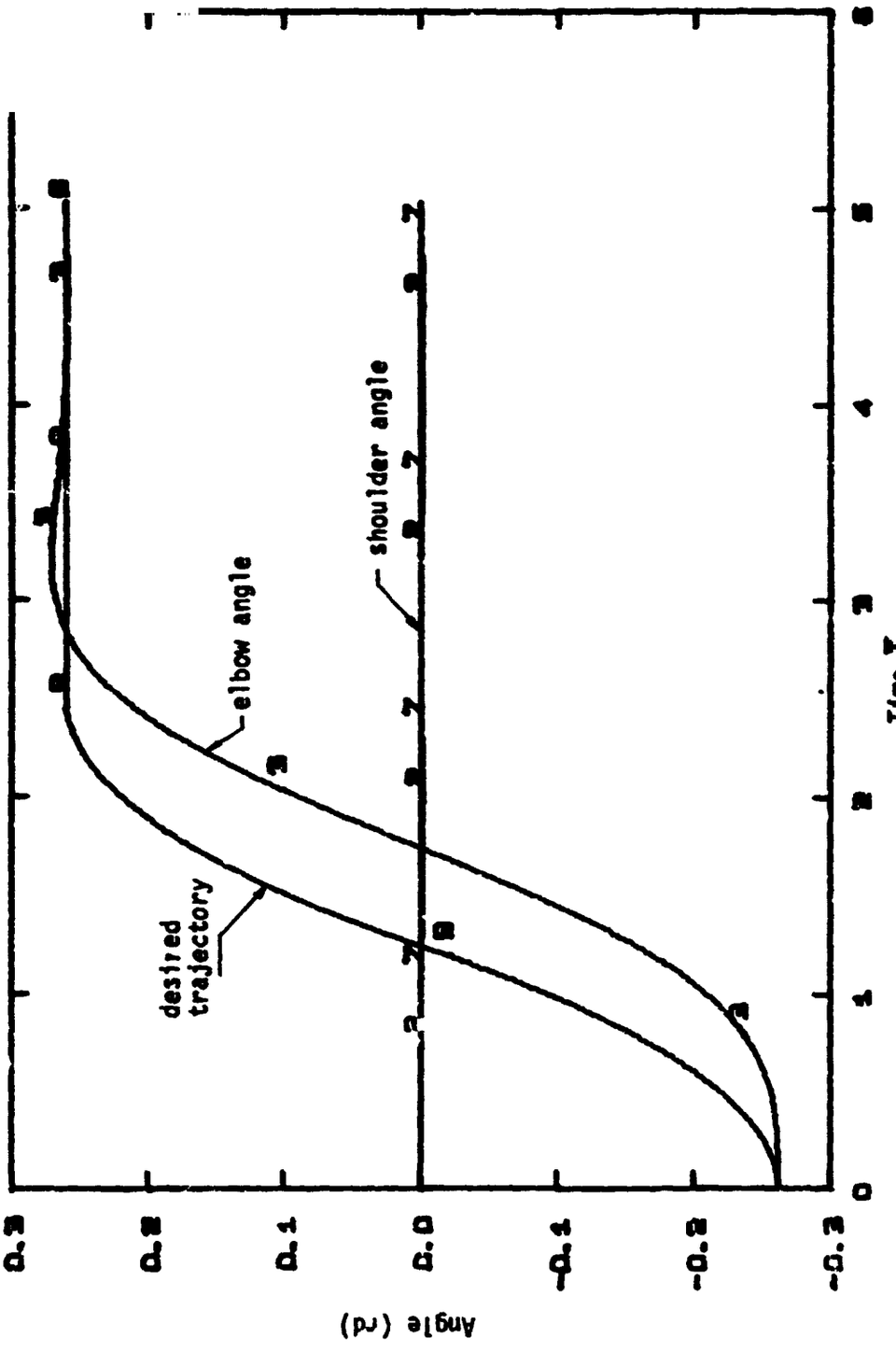


Figure 5.8a - Angle Response of Example 2 Tracking a double-parabola GRG Control for $\bar{\omega} = 0.9\,\bar{\omega}_c$ - Tracking Time Interval Equal Settling Time of Figure 5.4a

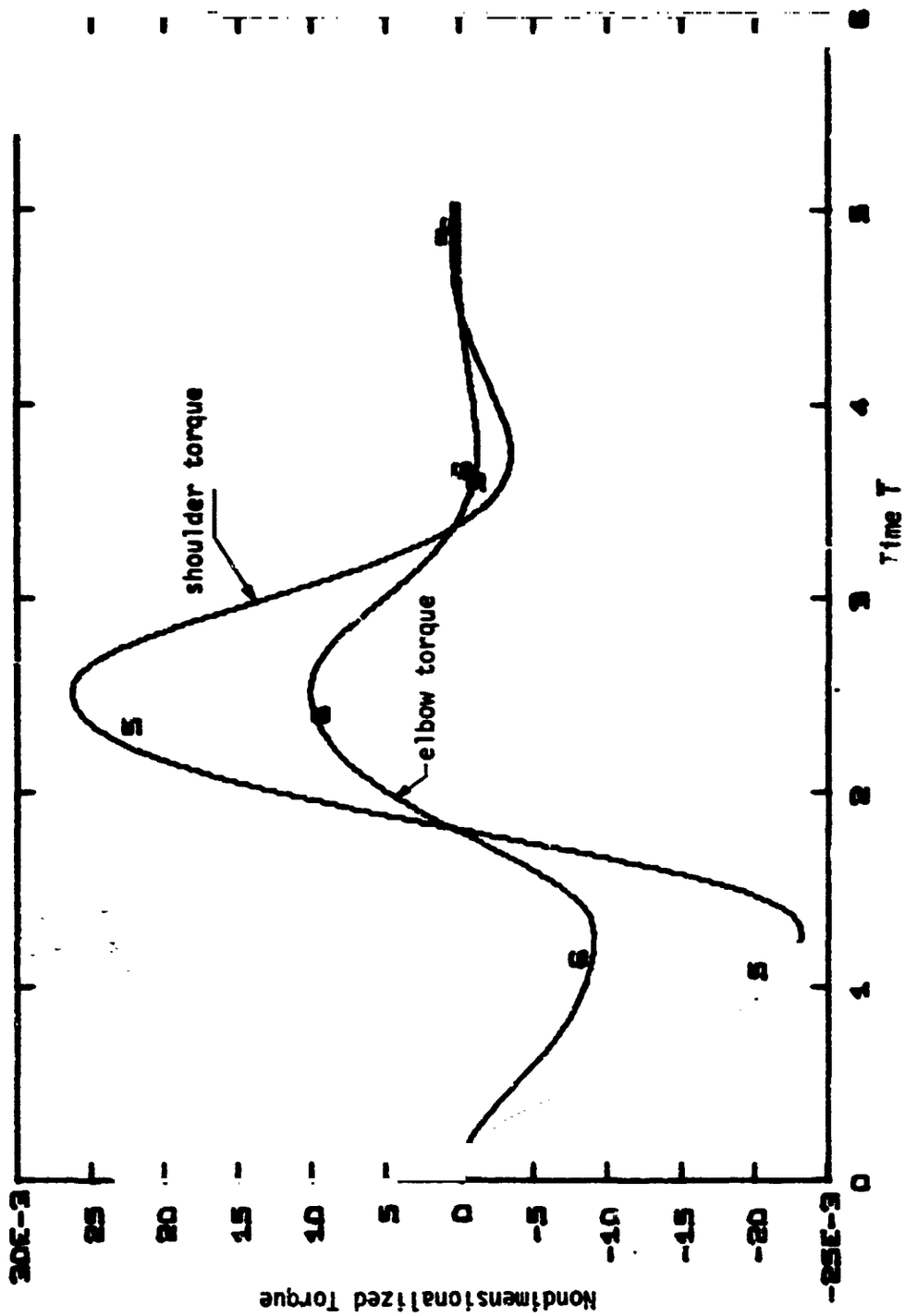


Figure 5.8b - Torque Response of Example 2
Same Conditions of Figure 5.8a

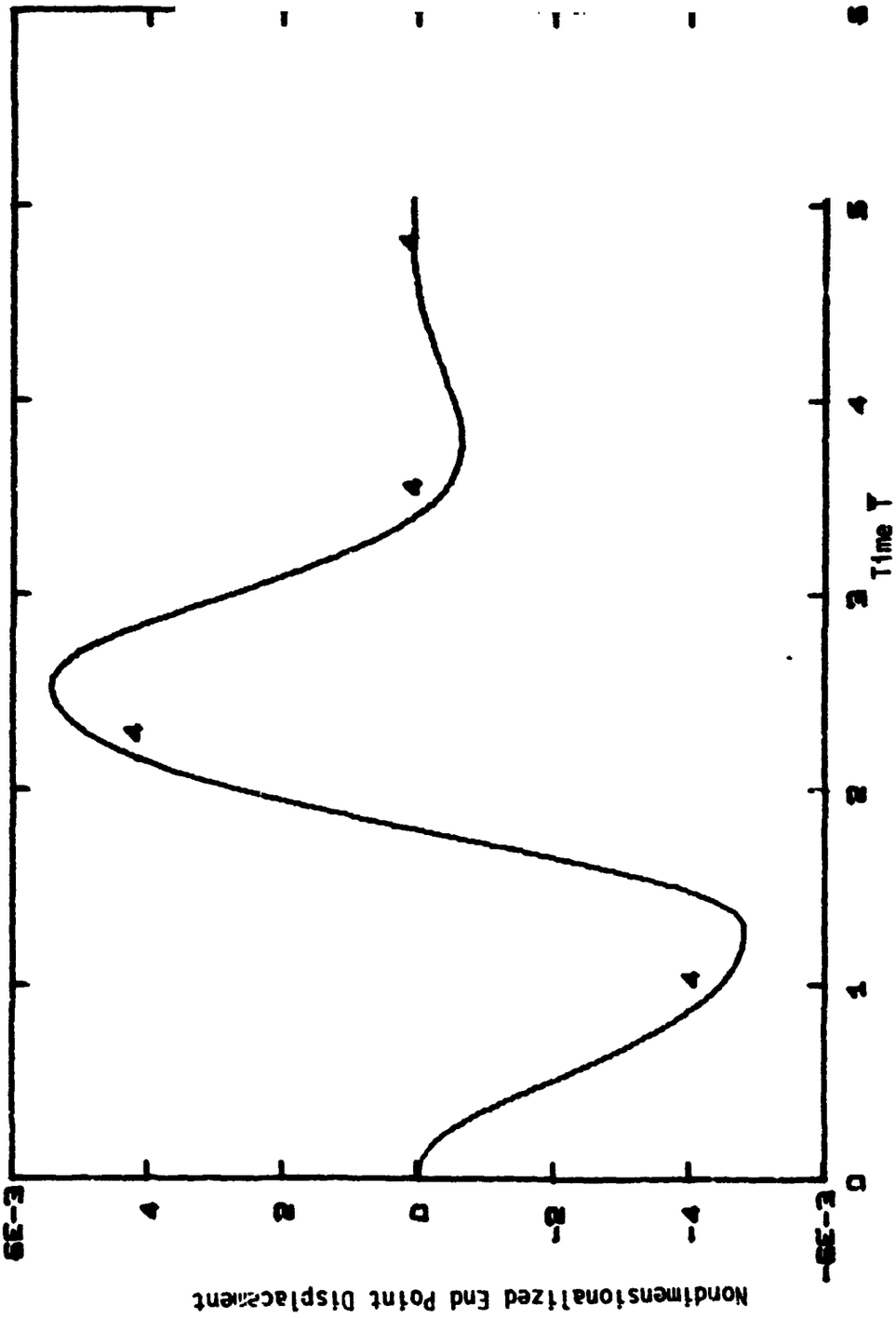


Figure 5.8c - End Point Displacement of Example 2
Same Conditions of Figure 5.8a

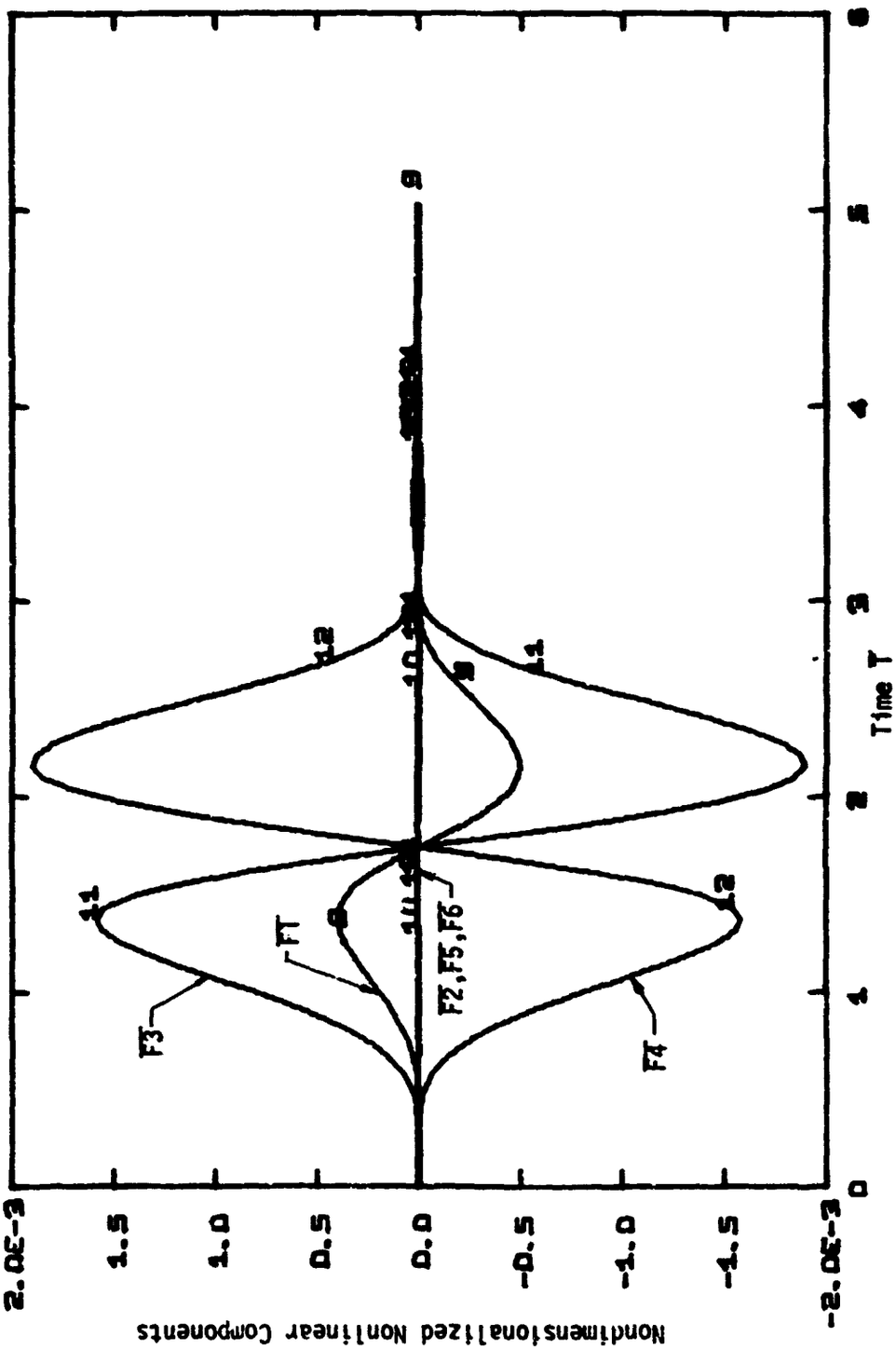


Figure 5.8d - Nonlinear Components
Same Conditions of Figure 5.8a

nonlinearities which in this simulation amounts to only about 10% of the total torque acting in the system.

Finally, Figures 5.9 presents the elbow impulse response of example 1 for $\bar{w} = 0.3\ \bar{w}_c$. This case is a more flexible system and this can be noticed by the oscillatory behavior of the response in Figure 5.9b that indicates the system torques have to act in a vibrating way in order to keep decreasing the effect of a higher flexibility.

## 5.2 Summary

This chapter presented some special simulations using results obtained from the previous chapter. The systems were simulated for the condition of no payload because of large computer time necessary to simulate other configurations. The computer programs are presented in Appendix A and are capable of simulations for any configurations.

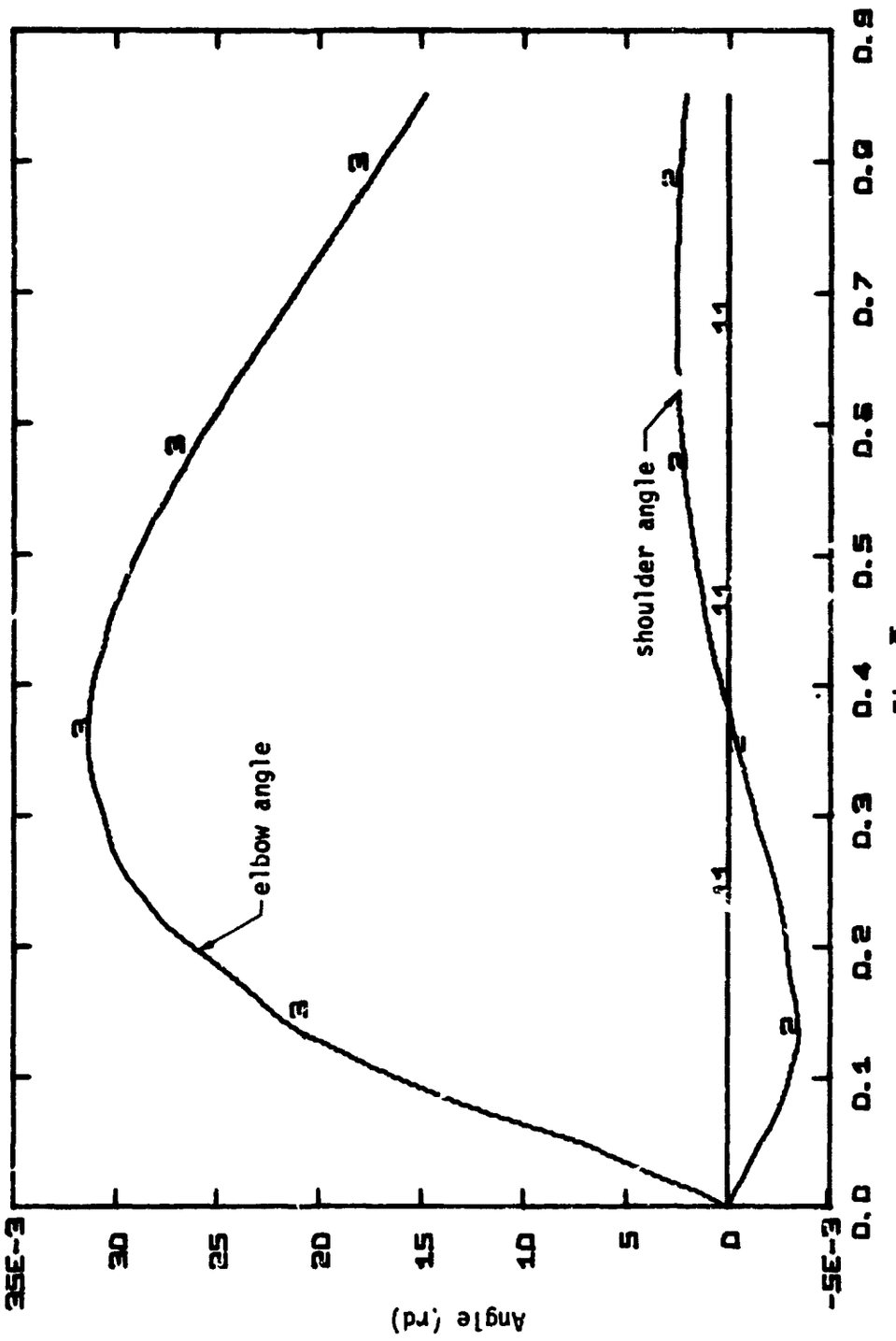


Figure 5.9a - Angle Response of Example 1 for Impulse at Elbow
GRG Control for $\bar{\omega} = 0.9\ \bar{\omega}_c$

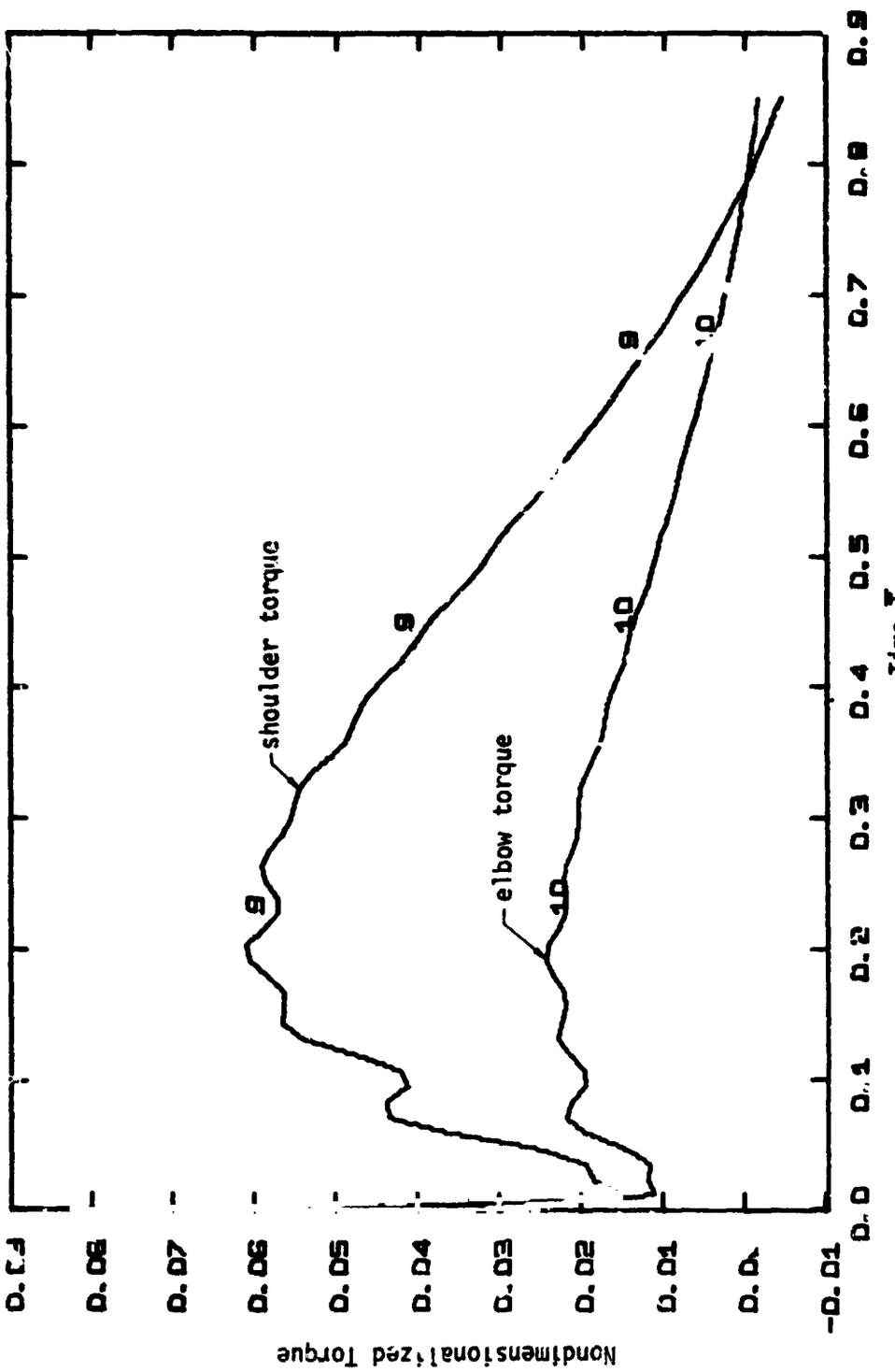


Figure 5.9b : Torque Response of Example 1 for Impulse at Elbow
GRG Control for $\bar{\omega} = 0.9\,\bar{\omega}_c$

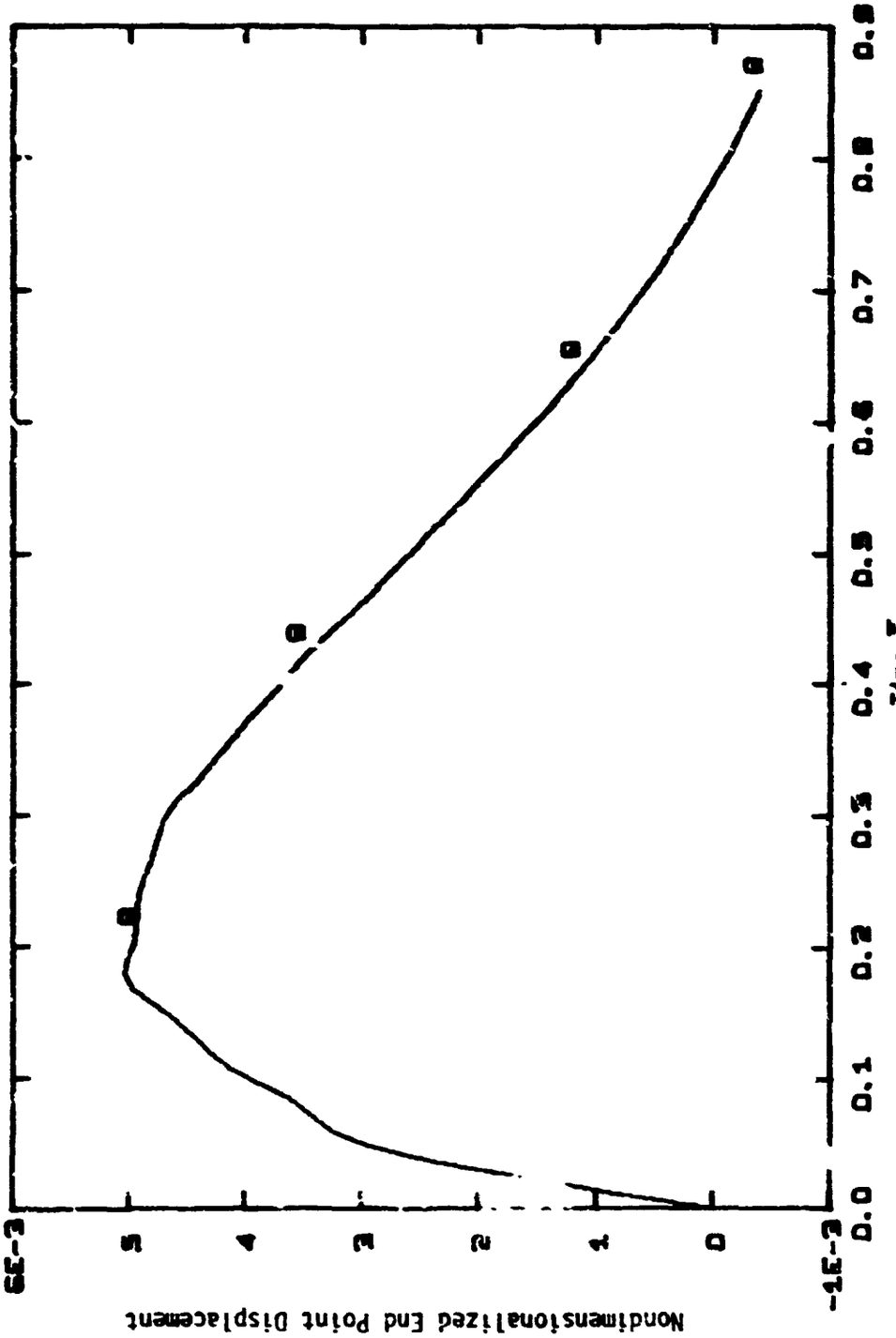


Figure 5.9c - End Point Displacement of Example 1 for Impulse at Elbow GRG Control for $\bar{\omega} = 0.9\,\bar{\omega}_c$

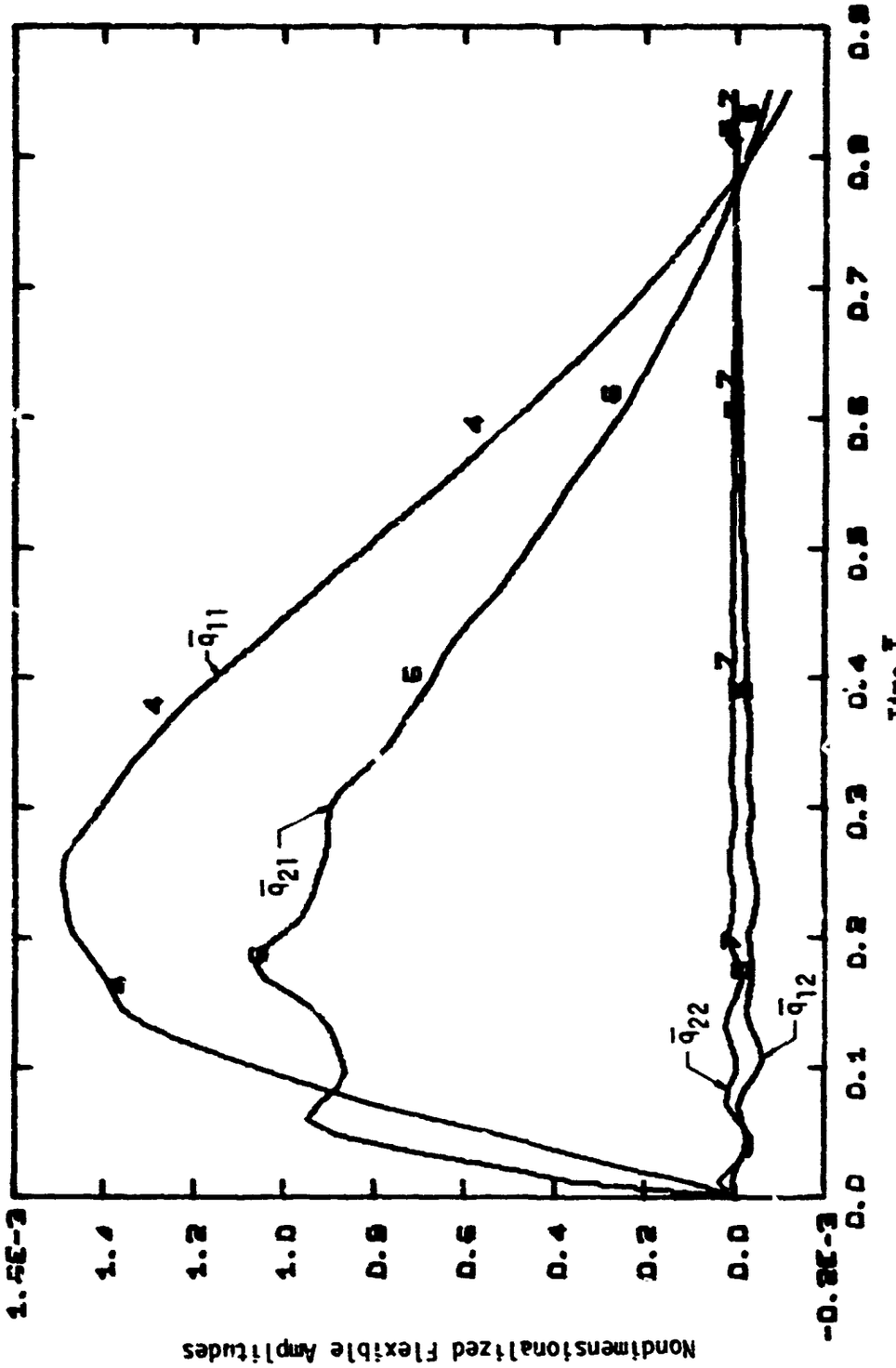


Figure 5.9J - Flexible Amplitudes of Example 1 for Impulse at Elbow GRG Control for $\bar{\omega} = 0.9\ \bar{\omega}_c$

# CHAPTER VI

# CONCLUSIONS AND SUGGESTIONS FOR FURTHER WORK

## 6.1 Introduction

In this chapter, the principal results of the analysis in this dissertation are summarized. Some conclusions about the proposed model for manipulator arms are presented and the overall results concerning control applications and discussed. Suggestions for future work are given in the final section of this chapter.

## 6.2 Summary of the Conclusions on the Model

This study has presented a new model of a two-link flexible manipulator arm. The fact that the model introduces the flexible behavior with respect to a hypothetical rigid motion is important in studying overall task performance. The experimental results from an uncontrolled situation have shown that the truncation at the second mode of each flexible component is a good approximation. The generalized coordinates used in this model, regardless of the number of modes chosen, are suitable for obtaining the system configuration at any time t, which would be very helpful from a design point of view.

The fact that the model is presented in a pseudo-standard form $\dot{\underline{x}} = \underline{A}\,\underline{x} + \underline{F}(\underline{x}, \dot{\underline{x}}, t) + \underline{B}\,\underline{u}$ simplifies the linearization procedure that can be used for application of linear control theory as well as allowing simulations of the controlled nonlinear system. However, if the control law requires more than the simple measuring of joing angles, the use

of such a model may need more sophisticated techniques for measuring the flexible components.

A more detailed study of the planar motion is also possible by introducing compliance and damping associated with the actuators, for example.

## 6.3 Control via (S"A)

From the point of view of controlling a flexible manipulator the basic idea of the present work was to design a control technique that could allow high speed without extreme deviations from rigid behavior. This means that the desired flexible position and velocity during the motion should be considered as being zero. With this in mind, this work was started considering the possibility of using one particular modal control algorithm as a means to assign desired closed-loop eigenvalues configuration. However, despite the efforts to obtain desirable results from this technique, the attempts did not produce a good control design because specifying the eigenvalues does not necessarily mean that the controlled system has reached a desired situation with respect to the eigenvectors. This fact, related to the non-uniqueness of control law for a multiple-input system, makes the system very sensitive to gains variations which essentially eliminates the possibility of using constant gains for controlling gross motions of manipulators. Even in case of obtaining desirable results from the application of (S"A) in manipulator control there exists the problem of measurement and/or estimation of some state variables present in the system modeling.

## 6.4 Control Using General Rigid Gains Method

With respect to the rigid like control technique, the addition of cross joint feedback seems to work very well in controlling the flexible system. The application of this method in the present work improved the speed of response by about a factor of two when compared with the control without feedback between the joints. In other words, the arm bandwidth is increased up to the value of the corresponding clamped-free natural frequency. This procedure also eliminates the necessity of flexible measurements and the use of an estimator. Finally, the most important feature of this method is the possibility of working under constant gains since the poles are less sensitive than using (SMA).

This method was applied to controlling the system under different geometric configurations. When a lumped payload mass is present, the results have shown that the arm bandwidth with control decreases compared to the no-payload case. As the payload becomes bigger, the effect of its rotary inertia becomes more and more important. With the increasing of the rotary inertia the associated clamped-free system will have its first natural frequency decreased, consequently reducing the arm bandwidth under control design via rigid gains method.

However, as a wide range of payloads must eventually be considered this work did not deal with all possible alternatives with respect to payload geometry.

It has also been shown in this work that decreasing the relative ratio of stiffness $\overline{EI}_2$ in case of no-payload increases the arm bandwidth. The existence of an optimum stiffness ratio with respect to the clamped-free natural frequency may indicate a limit for improvement in

the closed-loop system performance when this ratio is varied and the system carries no payload or if the payload range is small. On the other hand, it has been shown that for handling large payloads the best indicated ratio is of the order of unity.

## 6.5 The Use of Pole Sensitivities to Gains Variations

The use of pole sensitivity analyses has shown that in most cases it is a matter of finding a set of convenient numbers in order to move the poles to some desirable location. The fact that this process involves a large amount of trials makes it not very useful for the overall design but only for fine adjustments.

## 6.6 General Remarks

In measuring the state of the system it has been shown that the variables included in the proposed model take into account the flexible displacement of the end of the first beam. The improvement in the control when this measurement is used may not justify the complications and accuracy of measuring devices. This means that potentiometer and tachometer measurements may be enough to achieve the desired results using the general rigid gains method.

With respect to system stability, the rigid gains method with cross joint feedbacks and symmetric matrices $\underline{K}_T$ and $\underline{K}_{TD}$ presented very good results since the system is always stable. However, if some of the interjoint feedbacks fail, the results have shown that the system remains stable at least for arm bandwidth of order of the clamped-free natural

frequency of the equivalent system. However, despite the loss of desirable response a good safety policy would be to cut all cross feedbacks in case of failure in one of them.

In this work a linearized control technique was applied to a system that in some cases may present severe nonlinear effects. This fact is strongly dependent upon the system itself and this work did not analyze all possible cases of gross motion. In the cases where linear control was applied the results obtained were satisfactory if one considered that the control was designed to keep the system as close as possible to rigid motions. The nonlinear components, as appearing in the equations of the proposed model, act like additional torques and forces to the system during task motions. In the simulations of several cases it was observed that the nonlinear torques amounts to about ten percent of the total torque. However, in cases where the nonlinear effects are significant this effect has to be carefully analyzed.

Finally Table 6.1 summarizes the major results obtained in this work when compared with rigid method cross joint feedback.

## 6.7 Suggestions for Further Work

The work presented in this dissertation suggests several problems for future investigators:

1. Compare the results obtained with the proposed model with those from a model with only one component mode for each beam;

2. Extend the proposed model to represent spatial motions considering also torsional compliances;

| Method | Arm Band. | Stability of high frequency poles (during motion) for constant gain | Stability after failure of one feedback | Relative torques | Bandwidth under high payload |
|---|---|---|---|---|---|
| Rigid without cross joint feedback | up to $w_c/2$ | Good-always stable for any angle variations | Good-nonexistence of cross joint feedback | A little higher than general rigid gains | Poor-caused by reduction in the clamped-free natural frequency |
| General Rigid | up to $w_c$ | Good-always stable for any angle variation using symmetric matrices $\underline{K}_T$ and $\underline{K}_{TD}$ | Good-for cases analyzed with arm bandwidth up to $w_c$ | Lower than rigid method | Fair-poor increases in the arm bandwidth |
| Modal using (S**) | any | Poor-stable only for small motions around design position | Unstable-very sensitive to gains variation | The highest torques obtained | Not considered at all due to high sensitivity to gains variations |

Table 6.1 Summary of Major Results

# APPENDIX A

# COMPUTER PROGRAMS

```
      SUBROUTINE EQSIM
C**** MAINLINE FOR EQUATIONS OF MOTION
C**** FREE-ELBOW MODEL - TWO MODES FOR EACH BEAM
C        THIS SUBROUTINE IS USED TO CONSTRUCT
C        THE STATE SPACE EQUATIONS FOR
C        INTEGRATION VIA RUNGE-KUTTA FOUR
C        METHOD USING A STANDARD PROGRAM
C        DYSYS AVAILABLE AT JOINT COMPUTER
C        FACILITY CIVIL-MECHANICAL ENGINEERING
C        M.I.T..  IT IS ALSO USED AS A STARTING
C        POINT TO CONSTRUCT THE INITIAL MATRIX A
C        TO BE USED IN APPLICATIONS OF SIMON-
C        MITTER ALGORITHM AND SENSITIVITY ANALISES
      IMPLICIT INTEGER*2 (I-N)
      REAL*8 T1,BCR1,GSTO
      REAL*8 TEMP,DBLE
      REAL SENX(4),COSFX(4),FP(4),FI(4),LR(4)
      REAL LE(4),MU(4),NW(4),KW(4)
      REAL L1,L2,M1,M2,LP,MP,MJ,JXX1,JXX2,JXXP,JXXJ,JO,JP
      REAL JMT,JOMEG,JPOM,LR1,LR2,LR3,LR4,NW11,NW12,NW21,NW22
      REAL M11,M12,M13,M14,M15,M16,M21,M22,M23,M24,M25,M26
      REAL M31,M32,M33,M34,M35,M36,M41,M42,M43,M44,M45,M46
      REAL M51,M52,M53,M54,M55,M56,M61,M62,M63,M64,M65,M66
      REAL MR11,MR12,KW111,KW122,KW211,KW222
      REAL MU1,MU2,INER,MP21,MP22
      REAL INER1,INER2
      REAL FI(4)
      REAL LPM
      INTEGER L(6),M(6),NN
      COMMON /WORK/R(144)
      COMMON/SIMUL/T,DT,Y(30),DY(30),STIME,FTIME,NEWDT,IFWRT,NSYS,IPLOT
      COMMON/TOLD/A(12,12)
      COMMON/HOLD/BC(12,4),GSTO(4,12),NEX,NM,NN,KIN,KOUT,IGO
```

```
      DIMENSION BB(12),BI(12),F(6),FR(6),FC(12)
      DIMENSION AS(36)
      DIMENSION X(4),C(36),R(36)
      DIMENSION HS(4),HC(4),SI(4)
      DIMENSION SET(12),GFIN(12,12)
      EQUIVALENCE(SI(1),SIGM1),(SI(2),SIGM2),(SI(3),SIGM3),(SI(4),SIGM4)
      EQUIVALENCE (SENX(1),SEN1),(SENX(2),SEN2)
      EQUIVALENCE (SENX(3),SEN3),(SENX(4),SEN4)
      EQUIVALENCE (COSEX(1),COS1),(COSEX(2),COS2)
      EQUIVALENCE(COSEX(3),COS3),(COSFX(4),COS4)
      EQUIVALENCE (LR(1),LR1),(LR(2),LR2),(LR(3),LR3),(LR(4),LR4)
      EQUIVALENCE(FP(1),FP11E),(FP(2),FP12F),(FP(3),FP21E),(FP(4),FP22E)
      EQUIVALENCE(FI(1),FI11E),(FI(2),FI12E),(FI(3),FI21E),(FI(4),FI22E)
      EQUIVALENCE (A(1),M11),(A(2),M21),  (A(3),M31),(A(4),M41)
      EQUIVALENCE (B(5),M51),(B(6),M61),(B(7),M12),(B(8),M22)
      EQUIVALENCE (B(9),M32),(B(10),M42),(B(11),M52),(B(12),M62)
      EQUIVALENCE (B(13),M13),(B(14),M23),(B(15),M33),(B(16),M43)
      EQUIVALENCE (B(17),M53),(B(18),M63),(B(19),M14),(B(20),M24)
      EQUIVALENCE (B(21),M34),(B(22),M44),(B(23),M54),(B(24),M64)
      EQUIVALENCE (B(25),M15),(B(26),M25),(B(27),M35),(B(28),M45)
      EQUIVALENCE (B(29),M55),(B(30),M65),(B(31),M16),(B(32),M26)
      EQUIVALENCE (B(33),M36),(B(34),M46),(B(35),M56),(B(36),M66)
      EQUIVALENCE (HS(1),HSN1),(HS(2),HSN2),(HS(3),HSN3),(HS(4),HSN4)
      EQUIVALENCE (HC(1),HCS1),(HC(2),HCS2),(HC(3),HCS3),(HC(4),HCS4)
      EQUIVALENCE (LE(1),L1),(LE(3),L2)
      EQUIVALENCE (MU(1),MU1),(MU(3),MU2)
      EQUIVALENCE (NW(1),NW11),(NW(2),NW12),(NW(3),NW21),(NW(4),NW22)
      EQUIVALENCE(KW(1),KW111),(KW(2),KW122),(KW(3),KW211),(KW(4),KW222)
      EQUIVALENCE (EI(1),EI1),(EI(3),EI2)
      EQUIVALENCE (TET2,Y(1)),(TET3,Y(2))
      EQUIVALENCE (Y(18),F1),(Y(19),F2),(Y(20),F3),(Y(21),F4)
      EQUIVALENCE (Y(22),F5),(Y(23),F6)
      EQUIVALENCE (Y(14),TEMP1),(Y(15),TEMP2)
```

```
      LOGICAL LDATS
      DATA X/1.875,4.694,1.875,4.694/
      DATA IM,IB,ID/'ME','EN','NO'/
      DATA IPARA/0/
  609 FORMAT(1H1)
   72 FORMAT(1H1)
  320 FORMAT(12X,6(G14.4,3X)/)
   10 FORMAT(8F10.0)
   15 FORMAT(4F20.0)
  344 FORMAT(1H )
  345 FORMAT(1X,9G14.4)
 8002 FORMAT(A2)
      SEND=SIN(Y(2))
      COSE=COS(Y(2))
      IF(NEWDT)1,2,3
    1 CONTINUE
C**** BB IS THE CONTROL VECTOR IN THE
C     ORIGINAL FORM
C**** READ SYSTEM CHARACTERISTICS
C**** IU CAN BE 'METRIC','ENGLISH' OR
C**** 'NONDIMENSIONALIZED'
C**** NN,MM,LL ARE EQUAL TO N/2 WHERE
C**** N IS THE ORDER OF THE SYSTEM
C**** OF EQUATIONS  =  N=12
C**** NEX IS THE NUMBER OF INPUTS
C**** NEX CAN BE 1 OR 2
C**** IPLOT IS TO SAVE PRINTING
C**** IPLOT EQUAL N WILL LOOSE (N-1) POINTS
C**** IMODAL EQU     FOR SIMULATION
C**** IMODAL < 1       IMON-MITTER ALGORITHM
C**** IGO = 0 FOR    LATION
C**** IGO = 2 FOR     ACCUMULATION OF CONTROL
C**** GAINS IN THE APPLICATION OF (SMA)
```

```
C**** L1,L2  LENGHTS OF BEAMS
C**** MU1,MU2  DENSITIES OF BEAMS
C**** D1E,D2E  EXTERNAL DIAMETERS
C**** D1I,D2I  INTERNAL DIAMETERS
C**** MP  PAYLOAD MASS
C**** MJ  JOINT MASS
C**** E1,E2 STIFFNESS OF THE BEAMS IN
C**** THE CASE 'NONDIMENSIONALIZED' AND
C**** YOUNG'S MODULUS IN METRIC OR
C**** ENGLISH CASES
C**** G  GRAVITY
C**** LP  PAYLOAD LENGHT
C**** JMT  MOMENT OF INERTIA OF
C**** THE MOTOR AT SHOULDER
C**** JXXP  MOMENT OF INERTIA OF THE
C**** PAYLOAD AT C.G.
C**** GSTO  FEEDBACK GAINS
C**** SET  DESIRED POSITIONS AND
C**** VELOCITIES FOR SIMULATIONS
      READ(8,8021)IU
      READ(8,111)NM,LL,NFX,IPLOT,IGO,IMODAL
      READ(8,101)L1,L2,MU1,MU2,D1I,D1F,D2I,D2E
      READ(8,103)MP,MJ,E,G,LP,JMT
      READ(8,104)JXXP,E1,EP
      IF(IGO.EQ.1)  GO TO 8211
      READ(8,15)(GSTO(1,I),I=1,12)
      READ(8,15)(GSTO(2,I),I=1,12)
 8211 CONTINUE
      READ(8,20)(SET(I),I=1,12)
      KOUT=5
      TCTRL=1.00.
      SLP1=2.0
      SLP2=2.2
```

```
      MU(2)=MU1
      MU(4)=MU2
      LE(2)=L1
      LE(4)=L2
   11 FORMAT(40I2)
      M1=MU1*L1
      M2=MU2*L2
C ******* FOR HOLLOW CILYNDER
      PI=3.14159
      R1I=(D1I/2.)
      R1E=(D1E/2.)
      R2I=(D2I/2.)
      R2E=(D2E/2.)
      JOMEG=M2*(((R2I**2 )+(R2E**2 ))/4.+(L2**2 )/12.)+M2*((L2/2.)**2 )
      JO=JMT+M1*(((R1I**2 )+(R1E**2 ))/4.+(L1**2 )/12.)+M1*((L1/2.)**2 )
C ******* FOR THE PAYLOAD
      JPOM=MP*((L2+LP/2.)**2 )+JXXP
      JP=MP*((LP/2.)*(LP/2.))+JXXP
C ******* FOR THE STIFFNESS
      IF(IU.NE.IO)  GO TO 8010
      EI1=E1
      EI2=E2
      GO TO 8001
 8010 CONTINUE
      INER1=(PI/64.)*((D1E**4)-(D1I**4))
      INER2=(PI/64.)*((D2E**4)-(D2I**4))
      EI1=E1*INER1
      EI2=E2*INER2
      IF(IU.EQ.1)  GO TO 8001
      EI1=EI1*144.
      EI2=EI2*144.
 8001 CONTINUE
C
```

```
      EI(2)=EI1
      EI(4)=EI2
C ******* COMPUTE THE PARAMETERS OF FLEXIBLE PART
      DO 655 I=1,4
      LR(I)=X(I)/LE(I)
      HS(I)=(EXP(X(I))-EXP(-X(I)))/2.
      HC(I)=(EXP(X(I))+EXP(-X(I)))/2.
      SENX(I)=SIN(X(I))
      COSEX(I)=COS(X(I))
      SI(I)=(HS(I)-SENX(I))/(HC(I)+COSEX(I))
      TR(I)=LR(I)*(HS(I)+SENX(I)-SI(I)*(HC(I)-COSEX(I)))
      FI(I)=HC(I)-COSEX(I)-SI(I)*(HS(I)-SENX(I))
      T1=1./(LR(I)*LR(I))
      KW(I)=MU(I)*T1*(-HC(I)-COSEX(I)+X(I)*(HS(I)+SENX(I))+2.
     1+SI(I)*(-X(I)*(HC(I)+COSEX(I))+HS(I)+SENX(I)))
      KW(I)=EI(I)*LE(I)*(LR(I)**4)
  655 CONTINUE
      FI21=(MU2/LR3)*(HSN3-SEN3-SIGM3*(HCS3+COS3-2.))
      FI22=(MU2/LR4)*(HSN4-SEN4-SIGM4*(HCS4+COS4-2.))
      MP21=MP*FI21E+FI21
      MP22=MP*FI22E+FI22
      WRITE(5,609)
      WRITE(KOUT,159)
      IF(IU.NE.1D)  GO TO 8011
      WRITE(KOUT,1.3)
      GO TO 8004
 8011 CONTINUE
      IF(IU.EQ.1A)  GO TO 8003
      WRITE(KOUT,102)
      GO TO 8004
 8003 WRITE(KOUT,101)
C ****** PRINT HEADLINE
 8004 CONTINUE
```

```
      WRITE(KOUT,159)
  101 FORMAT(45X,'* SYSTEM PARAMETERS - ENGLISH UNITS *')
  102 FORMAT(45X,'* SYSTEM PARAMETERS - METRIC  UNITS *')
  103 FORMAT(45X,'* SYSTEM PARAMETERS - NON-DIMENSIONALIZED *')
  159 FORMAT(45X,'**********************************')
      WRITE(5,22)L1,L2,M1,M2,G
   22 FORMAT(10X,'L1=',G14.5,2X,'L2=',G14.5,2X,'M1=',G14.5,2X,'M2=',
     1G14.5,2X,'G= ',G14.5/)
      WRITE(5,23)D1I,D1E,D2I,D2E,TET3,TET2
   23 FORMAT(10X,'D1I=',G14.5,2X,'D1E=',G14.5,2X,'D2I=',G14.5,2X,
     1'D2E=',G14.5,2X,'TET3=',G14.5,2X,'TET2=',G14.4/)
      WRITE(5,24)MP,MJ,E,INER1,INER2,EI1
   24 FORMAT(10X,'MP=',G14.5,2X,'MJ=',G14.5,2X,'E=',G14.5,2X,
     1'I1=',G14.5,2X,'I2=',G14.5,2X,'EI1=',G14.5/)
      WRITE(5,25)JMT,JXXP,JD,JOMEG,EI2
   25 FORMAT(10X,'JMOTOR=',G14.5,2X,'JXXP=',G14.5,2X,'JC  =',G14.5,
     12X,'JOMEG=',G14.5,2X,'EI2=',G14.5/)
      WRITE(5,60)X(1),X(2),X(3),X(4)
   60 FORMAT(10X,'LAMB1=',G14.5,2X,'LAMB2=',G14.5,2X,'LAMB3=',
     1G14.5,2X,'LAMB4=',G14.5/)
      WRITE(5,153)SIGM1,SIGM2,SIGM3,SIGM4
  153 FORMAT(10X,'SIGM1=',G14.4,2X,'SIGM2=',G14.4,2X,'SIGM3=',G14.4,
     12X,'SIGM4=',G14.4/)
      WRITE(KOUT,156)
  156 FORMAT(10X,'FEEDBACK GAINS'/)
      NPR=2*NN
      DO 154 J=1,NPR
  154 WRITE(KOUT,346)J,GSTO(1,J),J,GSTO(2,J)
  346 FORMAT(10X,'GAIN( 1,',I2,')',G20.8,10X,'GAIN( 2,',I2,')',G20.8/)
      WRITE(KOUT,161)
  161 FORMAT(10X,'REFERENCES FOR TET1,TET2,Q11,Q12,Q21,Q22,DTET1,DTET2,D
     1Q11,DQ12,DQ21,DQ22'/)
      WRITE(KOUT,345)(SET(I),I=1,NPR)
```

```
      WRITE(5,609)
      KHZ=6
      WRITE(KHZ,872)
  872 FORMAT(3X,' *** SWITCH 3 DOWN TO FOLLOW A PARABOLA ***')
      WRITE(KHZ,222)
  222 FORMAT(3X,' ***  SWITCH 4 DOWN TO CHANGE TIME STEP *** ')
       RITE(KHZ,225)
  225  ORM.T(3X,' ***  SWITCH 7 DOWN TO STOP SIMULATION *** ')
    3 CONTINUE
      IF(NEWDT.LT.0)  GO TO 4
      IF(LOATS(5))  GO TO 2
    4 CONTINUE
C ****** COMPUTE COEFFICIENTS OF
C         INERTIA MATRIX (H)
      SUM1=M2+MP
      SUM2=M2+2.*MP
      FLE11=FI11E*Y(3)+FI12E*Y(4)
      FLE21=MP21*Y(5)+MP22*Y(6)
      FLE31=-W11+MJ*L1*FI11E
      FLE41=-W12+MJ*L1*FI12E
      FLE51=-W21+MP*L2*FI21E
      FLE61=-W22+MP*L2*FI22E
      FLE71=FI11(.Y(9)+FI12E*Y(10)
      FLE81=MP21*Y(11)+MP22*Y(12)
      M11=(JO+MJ*L1*L1)+SUM1*(L1*L1+FLE11)+JOMEG+JPOM+SUM2*L1*L2*COSE+
     12.*SUM2*FLE11*SENO*L2/2.-2.*FLE21*L1*SENO+2.*FLF11*FLE21*COSE
      M12=JOMEG+JPOM+SUM2*L1*L2*COSE/2.+SUM2*FLE11*SENO-
     1FLE21*L1*SENO+FLE21*FLE11*COSE
      M13=FLE31+SUM1*L1*FI11F+SUM2*FI11E*L2*COSE/2.-FLE21*FI11E*SENO
      M14=FLE41+SUM1*L1*FI12F+SUM2*L2*FI12F*COSE/2.-FLE21*FI12E*SENO
      M15=FLE51+MP21*L1*COSE+MP21*SENO*FLE11
      M16=FLE61+MP22*L1*COSE+FLE11*MP22*SENO
      M21=M12
```

```
      M22=JOMEG+JPOM
      M23=FI11E*SUM2*L2*COSE/2.+FI11E*FLE21*SENO
      M24=FI12E*SUM2*L2*COSE/2.+FI12E*FLE21*SENO
      M25=FLE51
      M26=FLE61
      M31=M13
      M32=M23
      M33=M1+(MP+MJ+MP)*FI11E*FI11E
      M34=(M2+MP+MJ)*FI11E*FI12E
      M35=FI11E*MP21*COSE
      M36=FI11E*MP22*COSE
      M41=M14
      M42=M24
      M43=M34
      M44=M1+(MP+MJ+MP)*FI12E*FI12E
      M45=FI12E*MP21*COSE
      M46=FI12E*MP22*COSE
      M51=M15
      M52=M25
      M53=M35
      M54=M45
      M55=M2+MP*FI21E*FI21E+JP*FP21E*FP21E
      M56=MP*FI21E*FI22E+JP*FP21E*FP22E
      M61=M16
      M62=M26
      M63=M36
      M64=M46
      M65=M56
      M66=M2+MP*FI22E*FI22E+JP*FP22E*FP22E
      IF(NEWDT.GE.0)  GO TO 7930
C ****** PRINT INERTIA MATRIX (M)
C        AND COMPUTE INVERSE(B)
      WRITE(KOUT,7903)
```

```
 7900 FORMAT('1 B MATRIX'/)
      DO 7901 J=1,6
 7901 WRITE(KOUT,349)(B(I),I=J,36,6)
 7930 CONTINUE
      CALL INVERT
      J1=?
      J2=6
      DO 1012 J=1,5
      J3=5
      DO 1011 I=J1,J2
      I1=I+J3
      TJ=(B(I)+B(I1))/2.
      B(I)=TJ
      B(I1)=TJ
 1011 J3=J3+5
      J2=J2+6
 1012 J1=J1+7
      IF(NEWDT.GE.0)  GO TO 7940
      WRITE(KOUT,7902)
 7902 FORMAT(1X,' INV(B)'/)
      DO 7903 J=1,6
 7903 WRITE(KOUT,349)(B(I),I=J,36,6)
      WRITE(KOUT,609)
  349 FORMAT(1X,6G19.8)
 7940 CONTINUE
      LC=NN*NN
C ****** NONLINEAR COMPONENTS F(X,DX,T)
      F11=2.*SUM1*FLE11*FLE71*Y(7)-SUM2*L1*L2*Y(8)*Y(7)*SENO
     1-SUM2*L1*L2*Y(8)*Y(8)*SENO/2.-L1*Y(8)*SENO*FLE81-
     2SUM2*FLE71*L2*Y(8)*SENO/2.-FLE71*(FLE81*SENO+FLE21*Y(8)*COSE)+
     32.*SUM2+(FLE71*Y(7)*SENO+FLE11*Y(7)*Y(8)*COSE)*L2/2.
      F12=SUM2*(FLE71*Y(8)*SENO+FLE11*Y(8)*Y(8)*COSE)*L2/2.
     1+FLE71*FLE81*SENO+FLE11*FLE81*Y(8)*COSE-
```

```
     2FLE71*L1*SENO*(2.*Y(7)+Y(8))-FLE21*Y(8)*L1*COSE*(2.*Y(7)+Y(8))+
     3FLE71*FLE21*(2.*Y(7)+Y(8))*COSE+
     4FLE11*(FLE81*(2.*Y(7)+Y(8))*COSE-FLE21*Y(8)*(2.*Y(7)+Y(8))*SENO)
      F1=F11+F12
      F21=-FLE71*SUM2*L2*Y(8)*SENO/2.+SUM2*FLE71*Y(7)*SENO*L2/2.
     1+FLE81*L1*Y(7)*SENO+FLE71*Y(7)*FLE21*COSE+
     3SUM2*L1*L2*Y(7)*Y(7)*SENO/2.+L1*Y(7)*SENO*FLE81
      F22=FLE71*(Y(7)+Y(8))*SUM2*L2*SENO/2.+FLE71*Y(7)*FLE21*COSE
     1+SUM2*FLE11*Y(8)*Y(8)*COSE*L2/2.+FLE11*Y(7)*Y(7)*FLE21*SENO+
     2L1*Y(7)*Y(7)*FLE21*COSE
      F2=F21+F22
      F31=-FI11E*L2*(Y(7)+Y(8))*SUM2*Y(8)*SENO/2.
     1-FI11E*FLE81*Y(8)*SENO-
     2FI11E*(Y(7)+Y(8))*(FLE81*SENO+FLE21*Y(8)*COSE)
      F32=-SUM1*Y(7)*Y(7)*FLE11*FI11E-SUM2*FI11E*Y(7)*(Y(7)+Y(8))*SENO*
     3L2/2.-FI11E*Y(7)*FLE81*SENO-FI11E*Y(7)*(Y(7)+Y(8))*FLE21*COSE
      F3=F31+F32
      F41=-FI12E*Y(8)*(Y(7)+Y(8))*SUM2*L2*SENO/2.-
     1FI12E*FLE81*Y(8)*SENO-
     2FI12E*(Y(7)+Y(8))*(FLE81*SENO+FLE21*Y(8)*COSE)
      F42=-SUM1*Y(7)*Y(7)*FI12E*FLE11-SUM2*FI12E*Y(7)*(Y(7)+Y(8))*SENO*
     1L2/2.-FI12E*Y(7)*FLE81*SENO-FI12E*Y(7)*(Y(7)+Y(8))*FLE21*COSE
      F4=F41+F42
      F5=-MP21*L1*Y(7)*Y(8)*SENO+2.*FLE71*MP21*Y(7)*SENO+
     1L1*Y(7)*(Y(7)+Y(8))*MP21*SENO-FLE11*Y(7)*Y(7)*MP21*COSE
      F6=-MP22*L1*Y(7)*Y(8)*SENO+2.*FLE71*MP22*Y(7)*SENO+
     1L1*Y(7)*(Y(7)+Y(8))*MP22*SENO-FLE11*Y(7)*Y(7)*MP22*COSE
      MB11=(M1+2.*MJ)*G*L1*SENO/2.+((M2+2.*MP)*SIN(Y(1)+Y(2)))*G*L2
     1/2.+(M2+MP)*G*L1*SENO
      MB12=(MP+2.*MP)*G*L2*SIN(Y(1)+Y(2))/2.
C ****** CONSTRUCT STATE SPACE FORM
      F(1)=F =MB11
      F(2)=-F2-MB12
```

```
      F(3)=F3
      F(4)=F4
      F(5)=F5
      F(6)=F6
      DO 61 I=1,LO
   61 C(I)=0.0
      C(15)=KW111
      C(22)=KW122
      C(29)=KW211
      C(36)=KW222
      NNA=NN*2
      DO 71 I=1,NNB
   71 BB(I)=0.0
      IF(NEX.EQ.2) GO TO 73
      BB(1)=1.2
      BB(2)=1.0
      GO TO 74
   73 CONTINUE
      BB(1)=1.0
      BB(8)=1.0
   74 CONTINUE
      CALL GMPRD(B,C,R,NN,MM,LL)
      CALL GMPRD(B,AB,BI,NN,MM,2)
      CALL GMPRD(B,F,FR,NN,MM,1)
      DO 901 I=1,NN
      J=I+NN
      FC(I)=0.0
  901 FC(J)=FR(I)
      NB=NNB
      DO 42 I=1,NNB
      DO 42 J=1,NNB
   42 A(I,J)=0.0
      NNN=NN
```

```
      NN1=NNN+1
      KP=1
      DO 82 J=1,NNN
      J1=J+6
      DO 82 I=NN1,NNB
      A(I,J)=R(KP)
   82 KP=KP+1
      DO 83 I=1,NNN
      J=I+NNN
   83 A(I,J)=1
      DO 84 I=1,NB
      DO 84 J=1,NEX
   84 BC(I,J)=0.0
      KI=1
      DO 85 J=1,NEX
      DO 85 I=NN1,NNB
      BC(I,J)=BI(KI)
   85 KI=KI+1
      DO 341 I=1,NP
      DO 341 J=1,NP
      T1=0.0
      DO 342 K=1,NEX
      BCR1=BC(I,K)
  342 T1=T1+BCR1*GSTO(K,J)
  341 GFIN(I,J)=T1
 9871 CONTINUE
      IF(LDATS(13))  IMODAL=1
      IF(IMODAL.EQ.0)  GO TO 9901
      DO 9902 I=1,NNB
      DO 9902 J=1,NNB
 9902 A(I,J)=A(I,J)+GFIN(I,J)
      CALL LINK('POLE1 ')
 9901 CONTINUE
```

```
    2 CONTINUE
      IF(NEWDT.EQ.6)  GO TO 221
C ****** ACCEPT NEW TIME STEP
      IF(.NOT.LDATS(4))  GO TO 223
      WRITE(KHZ,224)
  224 FORMAT(3X,' NEW TIME STEP DT ')
      READ(KHZ,10)DT
      WRITE(KOUT,226)DT
  226 FORMAT(1H ,10X,'NEW TIME STEP DT = ',G14.4/)
  223 CONTINUE
      IF(.NOT.LDATS(3))  GO TO 7000
C ****** ACCEPT PARAMETERS FOR TRACKING
      WRITE(KHZ,7001)
 7001 FORMAT(3X,'PARAMETERS FOR PARABOLA')
      WRITE(KHZ,7002)
 7002 FORMAT(3X,'TINTERVAL,TETAFINAL')
      READ(KHZ,7003)TINT,TETB
 7003 FORMAT(4F10.0)
      TFIN=T+TINT
      TETO=SET(2)
      TIN=T
      IPARA=1
      WRITE(KOUT,7251)
 7251 FORMAT(10X,'STARTING PARABOLA'/)
 7000 CONTINUE
      IF(IPARA.EQ.0)  GO TO 7005
      AUX1=4.*((TETB/2.)-TETO)
      AUX2=TFIN-TIN
      IF(T.LT.TFIN)  GO TO 16
      SET(2)=TEND
      SET(7)=TENDV
      GO TO 18
   16 CONTINUE
```

```
      TM=(TFIN+TIN)/2.
      IF(T.GT.TM)  GO TO 19
      SET(2)=TETO+(AUX1/(AUX2*AUX2))*(T-TIN)*(T-TIN)
      SET(7)=(AUX1/(AUX2*AUX2))*2.*(T-TIN)
      GO TO 12
   19 CONTINUE
      SET(2)=TETB/2.+(AUX1/AUX2)*(T-TM)-(AUX1/(AUX2*AUX2))*
     1(T-TM)*(T-TM)
      SET(7)=(AUX1/AUX2)-(AUX1/(AUX2*AUX2))*2.*(T-TM)
      TEND=SET(2)
      TENDV=SET(7)
   12 CONTINUE
   18 CONTINUE
 7005 CONTINUE
      IF(LDATS(15)) SET(1)=SET(2)
      Y(16)=SET(1)
      Y(17)=SET(2)
      IF(NPLOT-IPLOT)200,201,201
  200 CONTINUE
      IFWRT=1
      NPLOT=NPLOT+1
      GO TO 202
  201 IFWRT=0
      NPLOT=1
  202 CONTINUE
C ****** DATS 7 DOWN TO STOP SIMULATION
      IF(LDATS(7))  FTIME=T
  221 CONTINUE
      IF(NEWDT.EQ.2)  RETURN
C ****** CONSTRUCT FINAL EQUATIONS
      DO 850 I=1,NNB
      TEMP=0.0D0
      DO 851 J=1,NNB
```

```
  851 TEMP=TEMP+DBLE(A(I,J))*DBLE(Y(J))-DBLE(GFIN(I,J))*(DBLE(SET(J))-
     1DBLE(Y(J)))
  850 DY(I)=SNGL(TEMP+DBLE(FC(I)))
C ****** END POINT DISPLACEMENT WITH
C         RESPECT TO END POINT OF THE RIGID
C         MODEL
      Y(13)=((FI11E*Y(3)+FI12E*Y(4))*COSE+FI21E*Y(5)+FI22E*Y(6))
C ****** TORQUES
C         Y(15) IS THE TORQUE TO JOINT 1
C         Y(16) IS THE TORQUE TO JOINT 2
       EMP1=0.0
      TEMP2=0.0
      J=1
      DO 853 I=1,NNB
      T2=SET(I)-Y(I)
      TEMP1=TEMP1+GSTO(J,I)*T2
  853 TEMP2=TEMP2+GSTO(J+1,I)*T2
      RETURN
      END
```

```
C         POLE1 MAINLINE
C         MAINLINE FOR COMPUTING EIGENVALUES
C         EIGENVECTORS AND SENSITIVITIES
      IMPLICIT REAL*8(A-H,O-Z)
      IMPLICIT INTEGER*2 (I-N)
      REAL REAL,AIMAG,RC
      REAL C
      INTEGER L(12),M(12),N
      INTEGER IFORT,IBALAN,IVAL,IVEC,ISNGL
      COMPLEX VV(12,12),B(12,4),BR(12,4),CMPLX
      COMPLEX T1,T2
      COMMON/SOLD/BR,VV
      COMMON/FOLD/A(12,12),WR(12),WI(12)
      COMMON/TOLD/C(12,12)
      COMMON/HOLD/BC(12,4),GSTO(4,12),NEX,NM,N,KIN,KOUT,IGO
      DIMENSION Z(12,12),V(12,12)
      DIMENSION GRADR(50.,GRADI(50),LI(50),LJ(50)
      LOGICAL ZERO
      LOGICAL LDATS
      KOUT=5
      NM=12
      KIN=5
C         IGO MUST BE EQ 2 IN THE FIRST RUN
C         NENT IS THE NUMBER OF ENTRIES FOR SENSITIVITIES
C         (LI,LJ) SPECIFY THE ELEMENTS OF A MATRIX FOR SENSITIVITY
  700 FORMAT(40I2)
  110 FORMAT(16I5)
C         BC IS THE CONTROL VECTOR IN STATE
C         SPACE FORM
C         READ PARAMETERS FOR EISPAC
C         NENT DIFFERENT OF ZERO
C         TO COMPUTE SENSITIVITIES
C         IGO NOT EQUAL 5 WILL ACCEPT
```

```
C         THE A MATRIX FROM EQSIM
      READ(KIN,110)N,IFORT,IBALAN,IVAL,IVEC,ISNGL,NENT
      IGO1=5
      IF(IGO.EQ.10)  IGO1=IGO
      IF(IGO.EQ.5)  GO TO 851
      DO 849 I=1,N
      DO 849 J=1,N
  849 A(I,J)=C(I,J)
      IGO=5
      IGO=IGO1
  851 CONTINUE
      IF(LDATS(7))  IVEC=0
      IF(IVEC.GE.1.AND.LDATS(4))  IVEC=IVEC+100
  112 CONTINUE
C         COMPUTE EIGENVALUES, EIGENVECTROS
C         AND USE MORDER TO ORDER THEM
      CALL EISPAC (N,N,IBALAN,IFORT,A,WR,WI,V,IER,IVAL,IVEC,ISNGL)
      CALL MORDER(WR,WI,V,N)
      DO 117 I=1,N
      DO 117 J=1,N
  117 Z(I,J)=V(I,J)
      IF(IVEC.EQ.0)  GO TO 1705
      CALL GMINV(V,V,N,DET,L,M,N)
      IF(DET.NE.0.0)  GO TO 114
      WRITE(KOUT,113)
  113 FORMAT(1X,'DETERMINANT ZERO FOR GMINV ON SENS2'/)
      STOP
  114 CONTINUE
  606 FORMAT(20X,G20.8,20X,G20.8/)
 1707 FORMAT('1 SYSTEM MATRIX A'/)
 1709 FORM  ('0',I4,10G12.4/(5X,10G12.4))
      IF(IGO.EQ.2)  GO TO 1705
      IF(IGO.EQ.3)  GO TO 1705
```

```
      IF(.NOT.LDATS(7)) GO TO 1706
 1705 CONTINUE
      IF(IGO.EQ.10)  GO TO 1706
      WRITE(KOUT,1707)
      DO 1710 I=1,N
 1710 WRITE(KOUT,1709)I,(A(I,J),J=1,N)
 1706 CONTINUE
      KH7=4
      KOP=5
      ITRA=1
C ..... PRINT EIGENVALUES IN ORDER
      WRITE(KOUT,846)
      WRITE(KOUT,844)(I,WR(I),WI(I),I=1,N)
      WRITE(KOUT,893)
  893 FORMAT(5X,'NOTE: THE EIGENVALUES ARE IN ORDER WITH RESPECT TO DIST
     1ANCE TO ORIGIN'/)
  844 FORMAT(2X,I3,15X,G20.8,20X,G20.8/)
  846 FORMAT('1EIGENVALUES',16X,'REAL PART',29X,'IMAGINARY PART'/)
      IF(LDATS(7))  STOP
      IF(INT.NE.0)  GO TO 1200
C
C ..... MODIFY EIGENVECTORS TO COMPLEX FORM
      J1=1
      DO 730 J=1,N
      IF(J1.GT.N)  GO TO 800
      IF(ZERO(WI(J1)))  GO TO 710
      DO 705 K=1,N
      VJK=V(J1,K)/2.
      VJK1=-V(J1+1,K)/2.
      ZJK=Z(K,J1)
      ZJK1=Z(K,J1+1)
      VV(J1,K)=CMPLX(VJK,VJK1)
      VV(J1+1,K)=CMPLX(VJK,-VJK1)
```

```
 705 CONTINUE
     J1=J1+2
     GO TO 750
 710 DO 720 K=1,N
     VV(J1,K)=CMPLX(V(J1,K),0.0)
 720 CONTINUE
     J1=J1+1
 750 CONTINUE
 800 CONTINUE
     DO 10 I=1,N
     DO 10 J=1,NEX
  10 B(I,J)=CMPLX(BC(I,J),0.0)
     IF(.NOT.LDATS(5))  GO TO 915
     WRITE(KHZ,15)
     WRITE(KOUT,15)
  15 FORMAT(1H1,'COMPLEX CONTROL VECTOR'/)
     DO 12 I=1,N
     WRITE(KOUT,11)(B(I,J),J=1,NEX)
  12 WRITE(KHZ,11)(B(I,J),J=1,NEX)
 915 CONTINUE
11   FORMAT(1X,2(G14.4,1X,G14.4,2X),1X,2(G14.4,1X,G14.4,2X)/)
     DO 5 I=1,N
     DO 5 J=1,NEX
   5 BR(I,J)=(0.0,0.0)
     DO 100 I=1,N
     DO 100 J=1,NEX
     DO 100 K=1,N
 100 BR(I,J)=BR(I,J)+VV(I,K)*B(K,J)
     WRITE(KOUT,16)
  16 FORMAT(1H1,'MODE CONTROLLABILITY MATRIX'/)
     DO 13 I=1,N
  13 WRITE(KOUT,11)(BR(I,J),J=1,NEX)
 320 FORMAT(1X,4(G14.4,1X,G14.4,5X))
```

```
  321 FORMAT(1H )
      CALL LINK('POLE2 ')
 1200 CONTINUE
C         FOR SENSITIVITIES OF ALL POLES
C         WITH RESPECT TO VARIATIONS
C         ON GAINS GSTO(LI,LJ)
  623 FORMAT (20X,G20.8,20X,G20.8,/)
  609 FORMAT('1SENSITIVITIES',/)
  615 FORMAT(2I10,G20.8,20X,G20.8)
  616 FORMAT(' ')
  604 FORMAT(1H1)
      READ(KIN,700)(LI(I),I=1,NENT)
      READ(KIN,700)(LJ(I),I=1,NENT)
      WRITE(KOUT,604)
      WRITE(KOUT,609)
      DO 610 IC=1,N
      IF(WI(IC))610,611,611
  611 WRITE(KOUT,623)WR(IC),WI(IC)
      TEMP1=0.0
      TEMP2=0.0
      DO 612 J=1,NENT
      IB=LJ(J)
      INEX=LI(J)
      DO 1613 I=1,N
      IA=I
      IF(WI(IC))614,613,614
  613 GRADR(I)=Z(IB,IC)*V(IC,IA)*BC(IA,INEX)
      GRADI(I)=0.0D0
      GO TO 1614
  614 GRADR(I)=0.5D0*(Z(IB,IC)*V(IC,IA)+Z(IB,IC+1)*V(IC+1,IA))
     1*BC(IA,INEX)
      GRADI(I)=0.5D0*(Z(IB,IC+1)*V(IC,IA)-Z(IB,IC)*V(IC+1,IA))
     1*BC(IA,INEX)
```

```
1614 TEMP1=TEMP1+GRADR(I)
     TEMP2=TEMP2+GRADI(I)
1613 CONTINUE
     WRITE(KOUT,1615)LI(J),LJ(J),TEMP1,TEMP2
1615 FORMAT(1X,'GAIN(',I2,',',I2,')=',7X,D20.8,20X,D20.8)
 612 CONTINUE
     WRITE(KOUT,616)
 610 CONTINUE
     END
```

```
C         POLE2 MAINLINE
CC        MAINLINE FOR SIMON-MITTER ALGORITHM
C         USING CONSOLE FOR INTERACTION
C         CHANGES TWO REAL POLES OR A
C         COMPLEX CONJUGATE PAIR
      IMPLICIT REAL*8(A-H,O-Z)
      REAL REAL,AIMAG,BC
      REAL C
      IMPLICIT INTEGER*2 (I-N)
      INTEGER*2 IR,IC,IA
      INTEGER L,M,NN,NSMINV,N
      COMPLEX BR(12,4),VV(12,12)
      COMMON/SOLD/BR,VV
      COMMON/FOLD/A(12,12),WR(12),WI(12)
      COMMON/TOLD/C(12,12)
      COMMON/HOLD/BC(12,4),GSTO(4,12),NEX,NM,N,KIN,KOUT,IGO
      DIMENSION L(2),M(2),GAMR(12),GAMI(12),PP(2,2)
      DIMENSION GF(12,12),GI(12),GG(4,12)
      LOGICAL ZERO
      LOGICAL LDATS
      DATA IR,IC/'RE','CO'/
 1003 FORMAT(40I2)
      KHZ=6
C         IGO MUST BE EQ 2 IN FIRST STEP
 1201 FORMAT(40I2)
      IF(IGO.NE.2)  GO TO 1207
      DO 1200 I=1,N
      DO 1200 J=1,NEX
 1200 GSTO(J,I)=0.0
 1207 CONTINUE
      WRITE(KHZ,846)
      WRITE(KHZ,844)(I,WR(I),WI(I),I=1,N)
  844 FORMAT(2X,I3,5X,G20.8,20X,G20.8)
```

```
  846 FORMAT('1EIGENVALUES',6X,'REAL PART',29X,'IMAGINARY PART'/)
C
C         READ SPECIFICATION OF POLES TO BE SHIFTED
C         IA CAN BE 'REAL' OR 'COMPLEX'
C
      WRITE(KHZ,1352)
 1352 FORMAT(' **********   SET SWITCH 7 DOWN IF YOU WANT TO STOP'/)
      WRITE(KHZ,1505)
 1505 FORMAT(1X,'SWITCH 4 DOWN PRINT EIGENVECTORS'/)
      WRITE(KHZ,1210)
 1210 FORMAT(5X,'POLES TO BE SHIFTED'/)
      READ(KHZ,1201)IP1,IP2
      IPART=IABS(IP2-IP1)
      WRITE(KHZ,1211)
 1211 FORMAT(5X,'TYPE NATURE OF POLES - REAL/COMPLEX'/)
      READ(KHZ,1213)IA
 1213 FORMAT(A2)
      IF(IA.NE.IR)  GO TO 1217
      WRITE(KHZ,1215)
 1215 FORMAT(2X,'NEW PAIR OF REAL POLES'/)
      READ(KHZ,1004)(GAMR(I),I=IP1,IP2,IPART)
      DO 1410 I=IP1,IP2,IPART
 1410 GAMI(I)=0.0
      GO TO 1218
 1217 CONTINUE
      WRITE(KHZ,1216)
 1216 FORMAT(2X,'REAL AND IMAG. PART OF NEW COMPLEX POLE'/)
      READ(KHZ,1004)GAMR(IP1),GAMI(IP1)
      GAMR(IP2)=GAMR(IP1)
      GAMI(IP2)=-GAMI(IP1)
 1218 CONTINUE
 1004 FORMAT(12G16.9)
      WRITE(KOUT,1005)
```

```
 1005 FORMAT('1SUGGESTED POLE ALLOCATION'/////)
      DO 1006 I=IP1,IP2,IPART
      WRITE(KOUT,1007)WR(I),WI(I),GAMR(I),GAMI(I)
 1006 WRITE(KOUT,1011)
 1011 FORMAT(1H )
 1007 FORMAT(12X,G16.9,5X,G16.9,1X,'J   .... TO ....    ',G16.9,5X,
     1G16.9,'J'/)
      IF(IA.NE.IC)  GO TO 1100
C        SET UP GAINS FOR COMPLEX PAIR
      DO 1079 I=1,NEX
      TTT=AIMAG(BR(IP1,I))
      IF(.NOT.ZERO(WR(IP1)))   TTT=REAL(BR(IP1,I))
 1079 GI(I)=DSIGN(1.,TTT)
      IF(NEX.EQ.1)  GI(1)=1.0
      TEMP1=0.0
      TEMP2=0.0
      DO 1080 I=1,NEX
      PP1=(REAL(BR(IP1,I)))*GI(I)
      PP2=(-AIMAG(BR(IP1,I)))*GI(I)
      TEMP1=TEMP1+PP1
 1080 TEMP2=TEMP2+PP2
      PP(1,1)=TEMP1
      PP(1,2)=TEMP2
      PP(2,1)=-PP(1,2)
      PP(2,2)=PP(1,1)
      NCMINV=2
      NN=2
C        GMINV IS A DOUBLE PRECISION
C        VERSION OF IBM MINV SUBROUTINE
      CALL GMINV(PP,PP,NCMINV,DET,L,M,NN)
      IF(DET.NE.0.0)  GO TO 1052
      WRITE(KOUT,1051)
 1051 FORMAT(2X,'DET. ZERO IN DEIGS/COMPLEX - PROGRAM ABORTED'/)
```

```
      STOP
 1052 CONTINUE
      EPS1=GAMR(IP1)-WR(IP1)
      EPSP=GAMR(IP1)*GAMR(IP1)+GAMI(IP1)*GAMI(IP1)-WR(IP1)*WR(IP1)-
     1WI(IP1)*WI(IP1)
      EPS2=(EPSP-WR(IP1)*2.*EPS1)/(2.*WI(IP1))
      GAC1=PP(1,1)*EPS1+PP(1,2)*EPS2
      GAC2=PP(2,1)*EPS1+PP(2,2)*EPS2
C        SET UP FEEDBACK GAINS
      DO 1030 J=1,NEX
      DO 1030 I=1,N
      V11P=REAL(VV(IP1,I))
      V11PP=AIMAG(VV(IP1,I))
      TEMP=2.*(GAC1*V11P-GAC2*V11PP)
 1030 GG(J,I)=TEMP*GI(J)
      GO TO 1101
 1100 CONTINUE
C        SET UP GAINS FOR REAL PAIR OF POLES
      DO 1070 I=1,NEX
      TTT=REAL(BR(IP1,I))
 1070 GI(I)=DSIGN(1.,TTT)
      IF(NEX.EQ.1) GI(1)=1.0
      TEMP1=0.0
      TEMP2=0.0
      DO 1071 I=1,NEX
      PP1=(REAL(BR(IP1,I)))*GI(I)
      PP2=(REAL(BR(IP2,I)))*GI(I)
      TEMP1=TEMP1+PP1
 1071 TEMP2=TEMP2+PP2
      PP(1,1)=TEMP1
      PP(1,2)=TEMP2
      PP(2,1)=WR(IP2)*PP(1,1)
      PP(2,2)=WR(IP1)*PP(1,2)
```

```
      NCMINV=2
      NN=2
      CALL GMINV(PP,PP,NCMINV,DET,L,M,NN)
      IF(DET.NE.0.0)  GO TO 1062
      WRITE(KOUT,1061)
 1061 FORMAT(2X,'DET. ZERO IN DEIG5/REAL - PROGRAM ABORTED'/)
      STOP
 1062 CONTINUE
      EPS1=GAMR(IP1)+GAMR(IP2)-WR(IP1)-WR(IP2)
      EPS2=GAMR(IP1)*GAMR(IP2)-WR(IP1)*WR(IP2)
      GAC1=PP(1,1)*EPS1+PP(1,2)*EPS2
      GAC2=PP(2,1)*EPS1+PP(2,2)*EPS2
C        SET UP FEEDBACK GAINS
      DO 1039 J=1,NEX
      DO 1039 I=1,N
      V11P=REAL(VV(IP1,I))
      V11PP=REAL(VV(IP2,I))
      TEMP=GAC1*V11P+GAC2*V11PP
 1039 GG(J,I)=TEMP*GI(J)
 1101 CONTINUE
      DO 1400 J=1,NEX
      DO 1400 I=1,N
      TEMP2=GSTO(J,I)
 1400 GSTO(J,I)=GG(J,I)+TEMP2
      WRITE(KOUT,1020)
 1020 FORMAT(1H0,'GAINS FOR CANONICAL FORM'//)
      WRITE(KOUT,1009)GAC1,GAC2
 1009 FORMAT(5X,G16.8,2X,G16.8,1X,'J'//)
      WRITE(KOUT,1060)
 1060 FORMAT(1X,'CONTROLLER GAINS'//)
      DO 1072 J=1,NEX
      WRITE(KOUT,1034)(GG(J,I),I=1,N)
      WRITE(KOUT,1500)
```

```
 1072 CONTINUE
      WRITE(KOUT,1401)
 1401 FORMAT(1X,'ACCUMULATED GAINS'//)
      DO 1402 J=1,NEX
      WRITE(KOUT,1034)(GSTO(J,I),I=1,N)
      WRITE(KOUT,1500)
 1402 CONTINUE
 1500 FORMAT(1H0)
      DO 1031 I=1,N
      DO 1031 J=1,N
      TEMP1=0.0D0
      DO 1073 K=1,NEX
      BCR1=BC(I,K)
 1073 TEMP1=TEMP1+BCR1*GG(K,J)
 1031 GF(I,J)=TEMP1
      WRITE(KOUT,1032)
 1032 FORMAT('1FINAL GAINS IN THE ORIGINAL FORM'/)
      DO 1033 I=1,N
      WRITE(KOUT,1034)(GF(I,J),J=1,N)
 1033 WRITE(KOUT,1011)
 1034 FORMAT(1X,4(G20.8,5X))
C        FINAL MATRIX INCLUDING THE
C        PRODUCT OF CONTROL VECTOR TIMES
C        THE NEW GAIN MATRIX(CLOSED-LOOP
C        A MATRIX)
      DO 1050 I=1,N
      DO 1050 J=1,N
 1050 A(I,J)=A(I,J)+GF(I,J)
      IF(IGO.EQ.10)  IGO=5
C        RETURN TO POLE1  FOR EIGENVALUES
C        AND EIGENVECTORSS CALCULATIONS
      CALL LINK('POLE1 ')
      END
```

```
C         RIGID MAINLINE
C         CONSTRUCT STATE EQUATIONS FOR A
C         DOUBLE PENDULUM WITH TORQUE
C         INPUTS AT JOINTS AND FIND THE
C         GAINS USING GENERAL RIGID METHOD
C      FIND THE EIGENVALUES, EIGENVECTORS, NATURAL
C      FREQUENCIES AND SENSITIVITY OF LINEARIZED
C      FREE-ELBOW MODEL - RIGID MODEL
       IMPLICIT INTEGER*2 (I-N)
       REAL*8 T1,T2,GSTO,WR,WI
       REAL KT(4),KTD(4),KAUX(4)
       REAL L1,L2,M1,M2,LP,MP,MJ,JXX1,JXX2,JXXP,JXXJ,JO,JP
       REAL JMT,JOMEG,JPOM
       REAL M11,M12,M21,M22
       REAL MB11,MB12
       REAL MB111,MB121,MB112,MB122
       REAL MU1,MU2,LPM
       INTEGER L(6),M(6),NN
       COMMON/WORK/DUM1(144)
       COMMON/SIMUL/T,DT,Y(30),DY(30),STIME,FTIME,NEWDT,IFWRT,NSYS,IPLOT
       COMMON/TOLD/A(12,12)
       COMMON/HOLD/BC(12,4),GSTO(4,12),NEX,NM,NN,KIN,KOUT,IGO
       DIMENSION BB(12),BI(12)
       DIMENSION D(36),RD(36),BS(36)
       DIMENSION B(36),C(36),R(36)
       LOGICAL LDATS
  609  FORMAT(1H1)
  320  FORMAT(10X,6(G14.4,3X)/)
   10  FORMAT(8F10.0)
   15  FORMAT(4F20.0)
       DO 800 I=1,4
       DO 800 J=1,12
  800  GSTO(I,J)=0.0D0
```

```
      READ(8,11)NN,MM,LL,NEX,IGO
      READ(8,10)L1,L2,MU1,MU2,D1I,D1E,D2I,D2E
      READ(8,10)MP,MJ,E,TET2,TET3,G,LP,JMT
      READ(8,10)JXXP
      READ(8,15)(GSTO(1,I),I=1,4)
      READ(8,15)(GSTO(2,I),I=1,4)
      READ(8,10)Z1,Z2,Z3,Z4,Z5,Z6
      READ(8,10)W1,W2,W3,W4,W5,W6
      KOUT=5
C ........ GSTO ARE FEEDBACK GAINS
C         NEX EQ 1 SINGLE OUTPUT
C         NEX EQ 2 TWO OUTPUTS
   11 FORMAT(40I2)
      COSE=COS(TET3)
      M1=MU1*L1
      M2=MU2*L2
C ******* FOR HOLLOW CILYNDER
      PI=3.14159
      R1I=(D1I/2.)
      R1E=(D1E/2.)
      R2I=(D2I/2.)
      R2E=(D2E/2.)
      JOMEG=M2*(((R2I**2.)+(R2E**2.))/4.+(L2**2.)/12.)+M2*((L2/2.)**2.)
      JO=JMT+M1*(((R1I**2.)+(R1E**2.))/4.+(L1**2.)/12.)+M1*((L1/2.)**2.)
C ******* FOR THE PAYLOAD
      JPOM=MP*((L2+LP/2.)**2.)+JXXP
      JP=MP*((LP/2.)*(LP/2.))+JXXP
      LPM=L2+LP/2.
      WRITE(KOUT,101)
  101 FORMAT('1SYSTEM PARAMETERS  -  RIGID CASE  -  DIMENSIONS SLUG-FT-S
     1EC ')
      WRITE(5,22)L1,L2,M1,M2,G
   22 FORMAT(10X,'L1=',G14.5,2X,'LP=',G14.5,2X,'M1=',G14.5,2X,'M2=',
```

```
     1G14.5,2X,'G= ',G14.5/)
      WRITE(5,23)D1I,D1E,D2I,D2E,TET3,TET2
   23 FORMAT(10X,'D1I=',G14.5,2X,'D1E=',G14.5,2X,'D2I=',G14.5,2X,
     1'D2E=',G14.5,2X,'TET3=',G14.5,2X,'TET2=',G14.4/)
      WRITE(5,24)MP,MJ
   24 FORMAT(10X,'MP=',G14.5,2X,'MJ=',G14.5/)
      WRITE(5,25)JMT,JXXP,JO,JOMEG
   25 FORMAT(10X,'JMOTOR=',G14.5,2X,'JXXP=',G14.5,2X,'JO  =',G14.5,
     12X,'JOMEG=',G14.5/)
      WRITE(KOUT,156)
  156 FORMAT(10X,'FEEDBACK GAINS'/)
      NPR=2*NN
      DO 154 I=1,NEX
      WRITE(KOUT,345)(GSTO(I,J),J=1,NPR)
  154 WRITE(KOUT,344)
      B(1)=(JO+MJ*(L1**2.)+(M2+MP)*(L1**2.)
     1+JOMEG+JPOM+(M2+2.*MP)*L1*L2*COSE)
      B(3)=(JOMEG+JPOM+(M2+2.*MP)*L1*L2*0.5*COSE)
      B(2)=B(3)
      B(4)=JOMEG+JPOM
      MB111=((M1+2.*MJ)*0.5+(M2+MP))*L1*G+(M2+2.*MP)*L2*G*0.5
      MB112=(M2+2.*MP)*G*L2*0.5
      MB121=MB112
      MB122=(M2+2.*MP)*G*L2*0.5
      LO=NN*NN
      WRITE(KOUT,33)
   33 FORMAT(1H1,'INERTIA MATRIX '/)
      DO 32 I=1,NN
   32 WRITE(KOUT,345)(B(J),J=I,LO,NN)
      DO 61 I=1,LO
      KT(I)=0.0
      KTD(I)=0.0
   61 C(I)=0.0
```

```
      KTD(1)=-2.*Z1*W1
      KTD(4)=-2.*Z2*W2
      KT(1)=-W1*W1
      KT(4)=-W2*W2
      C(1)=-MB111
      C(2)=-MB121
      C(3)=-MB112
      C(4)=-MB122
      DO 70 I=1,LO
   70 C(I)=0.0
      IF(IGO.EQ.10)  GO TO 51
      D(1)=-2.*Z1*W1
      D(4)=-2.*Z2*W2
   51 CONTINUE
      NPR=NN
      NNB=NN*2
      DO 71 I=1,NNB
   71 BB(I)=0.0
      IF(NEX.EQ.2)  GO TO 73
      BB(1)=1.0
      BB(2)=1.0
      GO TO 74
   73 CONTINUE
      BB(1)=1.0
      BB(4)=1.0
   74 CONTINUE
      CALL GMPRD(B,KT,KAUX,NN,MM,LL)
      DO 31 I=1,LO
   31 KT(I)=KAUX(I)
      WRITE(KOUT,34)
   34 FORMAT(1X,'KT MATRIX '/)
      DO 35 I=1,NN
   35 WRITE(KOUT,345)(KT(J),J=I,LO,NN)
```

```
      CALL GMPRD(B,KTD,KAUX,NN,MM,LL)
      DO 36 I=1,LO
   36 KTD(I)=KAUX(I)
      WRITE(KOUT,37)
   37 FORMAT(1X,'KTD MATRIX '/)
      DO 38 I=1,NN
   38 WRITE(KOUT,345)(KTD(J),J=I,LO,NN)
      WRITE(5,1100)W1,W2,Z1,Z2
 1100 FORMAT(10X,'W1=',G14.4,2X,'W2=',G14.4,2X,'Z1=',G14.4,2X,'Z2=',G14.
     A4)
      IF(IGO.NE.10)  GO TO 39
      GSTO(1,1)=KT(1)
      GSTO(1,2)=KT(3)
      GSTO(2,1)=KT(2)
      GSTO(2,2)=KT(4)
      GSTO(1,7)=KTD(1)
      GSTO(1,8)=KTD(3)
      GSTO(2,7)=KTD(2)
      GSTO(2,8)=KTD(4)
      IF(.NOT.LDATS(10))  GO TO 40
C        TO USE ONLY RIGID ANGLES
      FP11E=1.46819
      FP12E=-2.03693
      GSTO(1,3)=-KT(3)*FP11E
      GSTO(1,4)=KT(3)*FP12E
      GSTO(2,3)=-KT(4)*FP11E
      GSTO(2,4)=KT(4)*FP12E
      GSTO(1,9)=-KTD(3)*FP11E
      GSTO(1,10)=KTD(3)*FP12E
      GSTO(2,9)=-KTD(4)*FP11E
      GSTO(2,10)=KTD(4)*FP12E
   40 CONTINUE
      IF(IGO.EQ.10)  CALL LINK('NONLI ')
```

```
 39 CONTINUE
    CALL MINV(B,NN,DET,L,M)
    CALL GMPRD(B,C,R,NN,MM,LL)
    CALL GMPRD(B,D,RD,NN,MM,LL)
    CALL GMPRD(B,BB,BI,NN,MM,NEX)
 41 NN=NN*2
    DO 42 I=1,NN
    DO 42 J=1,NN
 42 A(I,J)=0.0
    NNN=NN/2
    NN1=NNN+1
    KP=1
    DO 82 J=1,NNN
    J1=J+NNN
    DO 82 I=NN1,NN
    A(I,J)=R(KP)
    A(I,J1)=RD(KP)
 82 KP=KP+1
    DO 83 I=1,NNN
    J=I+NNN
 83 A(I,J)=1.0
    DO 84 I=1,NN
    DO 84 J=1,NEX
 84 BC(I,J)=0.0
    KI=1
    DO 85 J=1,NEX
    DO 85 I=NN1,NN
    BC(I,J)=BI(KI)
 85 KI=KI+1
    WRITE(5,609)
    WRITE(5,330)
330 FORMAT(10X,'..... CONTROL VECTOR .....'/)
    DO 331 I=1,NN
```

```
      WRITE(KOUT,320)(BC(I,J),J=1,NEX)
  331 WRITE(KOUT,344)
      N=NN
  343 FORMAT('1 INITIAL SYSTEM MATRIX A '/)
  345 FORMAT(1X,6G20.8)
  344 FORMAT(1H )
      WRITE(KOUT,343)
      DO 346 I=1,N
      WRITE(KOUT,345)(A(I,J),J=1,N)
C        FINAL MATRIX INCLUDING THE PRODUCT
C        OF CONTROL VECTOR TIMES THE GAIN
C        MATRIX(CLOSE-LOOP A MATRIX)
  346 WRITE(KOUT,344)
      DO 341 I=1,N
      DO 341 J=1,N
      T1=0.0
      DO 342 K=1,NEX
      BCR1=BC(I,K)
  342 T1=T1+BCR1*GSTO(K,J)
  341 A(I,J)=A(I,J)+T1
      CALL LINK('POLE1 ')
      END
```

# APPENDIX B

## B.1 Modal Decomposition Property [S2]

This property is better introduced through an example. Suppose the representation (3.4.1) with n=4 and assume poles 1 and 3 have to be changed. Then the control law u becomes:

$$\underline{u} = \underline{g}_1 \underline{z}_1 + \underline{g}_3 \underline{z}_3 \qquad (1.B)$$

where $\underline{g}_1$ and $\underline{g}_3$ are r-dimensional vectors. Then $\bar{\underline{\Delta}}$ is given by

$$\bar{\underline{\Delta}} = \begin{bmatrix} \lambda_1 + \delta'_{11} & 0 & \delta'_{13} & 0 \\ \delta'_{21} & \lambda_2 & \delta'_{23} & 0 \\ \delta'_{31} & 0 & \lambda_3 + \delta'_{33} & 0 \\ \delta'_{41} & 0 & \delta'_{43} & \lambda_4 \end{bmatrix} \qquad (2.B)$$

Using properties for interchanging rows and columns of determinants (2.B) yields to

$$\det(s\underline{I}-\bar{\underline{\Delta}}) = \det \begin{bmatrix} s-\lambda_1-\delta'_{11} & -\delta'_{13} & 0 & 0 \\ -\delta'_{31} & s-\lambda_3-\delta'_{33} & 0 & 0 \\ -\delta'_{21} & -\delta'_{23} & s-\lambda_2 & 0 \\ -\delta'_{41} & -\delta'_{43} & 0 & s-\lambda_4 \end{bmatrix} \qquad (3.B)$$

On the other hand, if $\underline{A}_{11}$ and $\underline{A}_{22}$ are square matrices

$$\det \begin{bmatrix} \underline{A}_{11} & \underline{A}_{12} \\ \underline{0} & \underline{A}_{22} \end{bmatrix} = \det (\underline{A}_{11}) \cdot \det (\underline{A}_{22}) \tag{4.B}$$

Using (4.B) into (3.B) one finally has

$$\det(s\underline{I}-\Delta) = (s-\lambda_2)(s-\lambda_4) \cdot \det \begin{bmatrix} s-\lambda_1-\delta'_{11} & -\delta'_{13} \\ -\delta'_{31} & s-\lambda_3-\delta'_{33} \end{bmatrix} \tag{5.B}$$

B.2 Useful Indentity for Inverson of a Complex Matrix with Complex Conjugated Columns

Let

$$A = \begin{bmatrix} a_{11} + b_{11}j & a_{11} - b_{11}j & c_{11} \\ a_{21} + b_{21}j & a_{21} - b_{21}j & c_{21} \\ a_{31} + b_{31}j & a_{31} - b_{31}j & c_{31} \end{bmatrix} \tag{6.B}$$

If one finds

$$\begin{bmatrix} a_{11} & b_{11} & c_{11} \\ a_{21} & b_{21} & c_{21} \\ a_{31} & b_{31} & c_{31} \end{bmatrix}^{-1} = \begin{bmatrix} \alpha_{11} & \alpha_{12} & \alpha_{13} \\ \beta_{11} & \beta_{12} & \beta_{13} \\ \gamma_{11} & \gamma_{12} & \gamma_{13} \end{bmatrix} \tag{7.B}$$

Then

$$A^{-1} = \begin{bmatrix} \frac{\alpha_{11}}{2} - \frac{\beta_{11}}{2} j & \frac{\alpha_{12}}{2} - \frac{\beta_{12}}{2} j & \frac{\alpha_{13}}{2} - \frac{\beta_{13}}{2} j \\ \frac{\alpha_{11}}{2} - \frac{\beta_{11}}{2} j & \frac{\alpha_{12}}{2} - \frac{\beta_{12}}{2} j & \frac{\alpha_{13}}{2} - \frac{\beta_{13}}{2} j \\ \gamma_{11} & \gamma_{12} & \gamma_{13} \end{bmatrix}$$

# APPENDIX C

## NONDIMENSIONALIZED PARAMETERS OF EXAMPLES 1 AND 2

Procedure for nondimensionalization

1 - Determine parameters for nondimensionalization described in Table 4.1

2 - Determine ratios $k_{r1}$ and $k_{r2}$ using equations (4.5) and (4.6)

3 - If $EI_1 \neq EI_2$ determine system coefficient c.s from equation (4.22) and find the diameters using $k_{r1}$, $k_{r2}$ and equations (4.23) and (4.7.2)

4 - Equations (4.11) and (4.12) determine the nondimensionalized parameters $\bar{\mu}_1$ and $\bar{\mu}_2$

Tables C.1 and C.2 present the nondimensionalized parameters for Examples 1 and 2.

| | |
|---|---|
| $k_{r1}=k_{r2}=0.978$ | $\bar{J}_{xxp} = 0.0$ |
| $\bar{EI}_1 = 1.0$ | $\bar{l}_p = 0.0$ |
| $\bar{EI}_2 = 1.0$ | $\bar{l}_1 = 0.5$ |
| $\bar{\mu}_1 = 1.0$ | $\bar{l}_2 = 0.5$ |
| $\bar{\mu}_2 = 1.0$ | $\bar{d}_{e1} = 0.0136$ |
| $\bar{m}_p = 0.0$ | $\bar{d}_{e2} = 0.0136$ |
| $\bar{m}_j = 0.0$ | |

Table C.1 - Nondimensionalized parameters of Example 1

| | |
|---|---|
| $k_{r1} = 0.842$ | $\bar{m}_j = 0.0$ |
| $k_{r2} = 0.850$ | $\bar{T}_p = 0.0$ |
| $\overline{EI}_1 = 1.0$ | $\bar{T}_1 = 0.5$ |
| $\overline{EI}_2 = 0.166$ | $\bar{T}_2 = 0.5$ |
| $\bar{\mu}_1 = 1.448$ | $\bar{d}_{e1} = 0.1039$ |
| $\bar{\mu}_2 = 0.551$ | $\bar{d}_{e2} = 0.0656$ |
| $\bar{m}_p = 0.0$ | $\bar{J}xxp = 0.0$ |

Table C.2 - Nondimensionalized parameters for Example 2

# BIBLIOGRAPHY

[B1] Bishop, R.E.D., and Johnson, D.C., Mechanics of Vibration, Cambridge at the University Press, 1960.

[B2] Book, W.J., Modeling,"Design and Control of Flexible Manipulator Arms", PhD thesis, MIT, Department of Mechanical Engineering, April 1974.

[C1] Crandall, S.H., Engineering Analysis, McGraw-Hill Book Co., 1956.

[C2] Crandall, S.H., Karnopp, D.C., Kurtz, E. and Brown, D.C., Dynamics of Mechanical and Electromechanical Systems, McGraw-Hill Book Co., 1968.

[C3] Crossley, T.R., Porter, B., "Properties of the Mode-Controllability Matrix", Int. J Control, 1970, Vol. 12, No. 2, pp. 289-295.

[E1] Ellis, J.K. and White, G.W.T., "An Introduction to Modal Analysis and Control", Control pp. 193-197, 262-266, 317-321, 1965.

[G1] Gould, L.A. and Prado, G., "Approximate Eigenvalue Relocation Method for Systems w h Constraints on the Dimensions of the Control System", Proceedings o. the JACC, 1974.

[G2] Gould, L., Chemical Process Control: Theory and Applications, Addison Wesley, 1969.

[G3] Gould, L., Murphy, A.T., Berkman, E.F., "On the Simon-Mitter Pole Allocation Algorithm - Explicit Gains for Repeated Eigenvalues", IEEE T.A.C. Vol. AC-15, No. 2, April 1970.

[K1] Kahn, M.E., "The Near-Minimum-Time Control of Open-Loop Articulated Kinematic Chains", PhD thesis, Computer Science Department, Stanford University, December 1969.

[L1] Lapidus, L. and Seinfeld, J.H., Numerical Solution of Ordinary Differential Equations, Academic Press 1971.

[M1] Meirovitch, L., Analytical Methods in Vibrations, The MacMillan Co., 1967.

[M2] Mirro, J., "Automatic Feedback Control of a Vibrating Flexible Beam," Master's thesis, MIT, Department of Mechanical Engineering, August 1972; also C.S. Draper Lab Report T-571.

[N1] "A Shuttle and Space Station Manipulator System for Assembly, Docking, Maintenance, Cargo Handling and Spacecraft Retreival, NASA CR-115482 numbers N72-22386, N72-22387, N72-22888, N72-22889, January 1972.

[N2] Nevins, J.L., "Teleoperator Technology Past, Present, and Future," Charles Stark Draper Lab Report E-2640, February 1972

[P1] Porter, B. and Mickelthwaite, D.A., "Design of Multi-Loop Modal Control Systems," Trans. S.I.T. Vol. 19, pp. 143-152, 1967

[P2] Porter, B. and Carter, J.D., "Design of Multi-Loop Modal Control Systems for Plants having Complex Eigenvalues," Measurement and Control, Vol. 1, March 1968.

[R1] Rosenbrock, H.H., "Distinctive Problems of Process Control," Chem. Eng. Progress, Vol. 58, pp. 43-50, 1962.

[R2] "Report on Advanced Automation," The Charles Stark Draper Lab Report #R-764, Cambridge, Mass. November 1973.

[S1] Simon, J.D., "Theory and Application of Modal Control," PhD thesis 1967, Case Institute of Technology.

[S2] Simon, J.D. and Mitter, S.K., "A Theory of Modal Control," Information and Control, Vol. 13, pp. 316-353, October 1968.

[T1] Townsend, A.L., "Linear Control Theory Applied to a Mechanical Manipulator," Charles Stark Draper Lab, Cambridge, Mass., Report T-558; MIT Mech. Eng. SM thesis, January 1972.

[V1] VanNess, J.E. and Boyle, J.M., "Sensitivities of Large, Multiple-Loop Control Systems," IEEE Transactions on Automatic Control, July 1965.

[W1] Whitney, D.E., "Example Force Feedback Accommodation and Related Issues," Charles Stark Draper Lab, Internal Memo #MAT97, Cambridge, Mass., January 1973. Also in Ref. [R2], pages 39-53

[W2] Whitney, D.E., Book, W.J., Lynch, P.M., "Design and Control Coordinations for Industrial and Space Manipulators," JACC Proceedings, June 1974, pp. 591-598

## ADDITIONAL REFERENCES


1. Biggs, J.M., "Introduction to Structural Dynamics, McGraw-Hill Book Co., 1964

2. Chase, M.A., Development and Application of Vector Mathematics for Kinematic Analysis, PhD thesis, University of Michigan, 1964

3. Chubb, B.A., Modern Analytical Design of Instrument Servomechanisms, Addison-Wesley Publishing Co., 1967

4. Collatz, L., The Numerical Treatment of Differential Equations, Springer-Verlag N.Y. Inc. 1966

5. Contributions to the Theory of Non-Linear Oscillations, Volume III Edited by S. Lefschetz, Princeton University Press, 1956

6. Csaki, Frigyes, Modern Control Theories, Akademiai Kiado, Budapest 1972

7. Denavit, J., Description and Displacement Analysis of Mechanisms Based on (2x2) Dual Matrices, PhD thesis, Northwestern University 1956

8. Doebelin, Ernest O., Measurement Systems: Application and Design, McGraw-Hill Book Co., 1966

9. Gear, C.W., Numerical Initial Value Problems in Ordinary Differential Equations, Prentice-Hall Inc., N.J. 1971

10. Groome, R.C. Jr.,Force Feedback Steering of a Teleoperator System, M.S. thesis, MIT, August 1972

11. Hamming, R.W., Numerical Methods for Scientists and Engineers, McGraw-Hill Book Co., Inc. 1962

12. Hurty, W.C. and Rubinstein, M.F., Dynamics of Structures, Prentice-Hall, Inc. 1964

13. Iemenschot, J.A., Optimal Trajectory Generation for Mechanical Arms, M.S. thesis, MIT, September 1972

14. Jacobsen, L.S. and Ayre, R.S., Engineering Vibrations, McGraw-Hill Book Co., Inc., 1958

15. Jastrzebski, Z.D., Nature and Properties of Engineering Materials, John Wiley and Sons, Inc., 1959

16. Kahn, M.E., "The Near-Minimum-Time Control of Open-Loop Articulated Kinematic Chains, PhD thesis, Stanford University, December 1969

17. Koehne, Manfred, Optimal Feedback Control of Flexible Mechanical Systems, Proceedings of the IFAC Symposium on the Control of Distributed Parameter Systems, Vol. I, Banff, Canada, June 21-23, 1971

18. Komkov, Vadim, Optimal Control Theory for the Damping of Vibrations of Simple Elastic Systems, Springer-Verlag, N.Y., 1972.

19. Lanczos, Cornelius, The Variational Principles of Mechanics, University of Toronto Press, Toronto, 1949

20. Lanczos, Cornelius, Applied Analysis, Prentice Hall, Inc., 1956

21. Matsumoto, J. and Ito, K., Feedback Control of Distributed Parameter Systems with Spacially Concentrated Controls, Int. J. Control, 1970, Vol. 12, #3, pp. 401-410

22. Meirovitch, L., Liapunov Stability Analysis of Hybrid Dynamical Systems with Multi-elastic Domains, Intl. Journal of Non-Linear Mechanics, August 1972, Vol. 7, #4

23. Meirovitch, L., Stability of a Spinning Body Containing Elastic Parts via Liapunov's Direct Method, AIAA J. 8(7), 1193-1200 (1970).

24. Meirovitch, L. and Nelson, H.D., "High-Spin Motion of a Satellite Containing Elastic Parts, Journal of Spacecraft and Rockets, Vol. 3, #11, November 1966, pp. 1597-1602

25. Minorsky, N., Non-Linear Oscillations, D. VanNostrand Co., Inc., Princeton, New Jersey, 1962

26. Mullen, D.P., An Evaluation of Resolved Motion Rate Control for Remote Manipulators, M.S. thesis, MIT, January 1973

27. Paynter, H.M., Analysis and Design of Engineering Systems, The MIT Press, 1960

28. Pestel, E.C. and Leckie, F.A., Matrix Methods in Elasto Mechanics, McGraw-Hill Book Co., Inc. 1963

29. Pinney, E., Non-Linear Differential Equations Systems Contributions to the Theory of Non-Linear Oscillations, Vol. III, Edited by S. Lefschetz

30. Pontriagin, L.S., A Course in Ordinary Differential Equations, Hindustan Publishing Corporation, India, 1967

31. Pringle, R., Jr., "On the Stability of a Body with Connected Moving Parts," AIAA Journal, Vol. 4, #8, August 1966, pp. 1395-1404

32. Ralston, A. and Wilf, H.S., Mathematical Methods for Digital Computers, John Wiley & Sons, Inc. 1964

33. Robe, T.R. and Kane, T.R., Dynamics of an Elastic Satellite - Parts I, II and III, International Journal of Solids and Structures, Vol. 3, 1967, pp. 333-352, 691-703, 1031-1051

34. Selection and Performance of Vibration Tests, The Shock and Vibration Information Center, United States Department of Defense, SVM-8, 1971

35. Skudrzyk, E., Simple and Complex Vibratory Systems, The Pennsylvania State University Press, 1968

36. Synthesis of Vibrating Systems, Shock and Vibration Committee of the Applied Mechanics Division ASME November 30, 1971, Winter Annual Meeting, Washington, D.

37. Timoshenko, S. and Young [illegible], Advanced Dynamics, McGraw-Hill Book Co., Inc. 1948

38. Timoshenko, S.P., The Collected Papers, McGraw-Hill Book Co., Inc., 1953

39. Timoshenko, S., and Young, D.H., Vibration Problems in Engineering, D. VanNostrand Co., Inc. 1955

40. Tong, K.N., Theory of Mechanical Vibration, John Wiley & Sons, Inc., 1963.

41. Todd, J., Survey of Numerical Analysis, McGraw-Hill Book Co., Inc., 1962

42. Traub, J.F., Iterative Methods for the Solution of Equations, Prentice Hall, Inc., 1964

43. Vicker, J.J. Jr., On the Dynamic Analysis of Spatial Linkages Using 4x4 Matrices, PhD thesis, Northwestern University, August 1965

44. Vierck, R.K., Vibration Analysis, International Textbook Co., Scranton, Penn. 1967

45. Volterra, E., Zachmanoglou, E.C., Dynamics of Vibrations, Charles E, Merril Books, Inc., Columbus, Ohio, 1965

46. Whitney, D.E., "The Mathematics of Coordinate Control of Prosthetic Arms and Manipulators, Transactions of ASME, Journal of Dynamic Systems, Measurements and Control

47. Yastrebov, V.S., Investigation of the Dynamics of a Manipulator's Working Organ, NASA-TT-F-14335-Mechanics of Machines No. 7/8, October 1972.